Current Signal Processing-Based Techniques for Transformer Protection

Adel Etumi

A thesis submitted to the Cardiff University in candidature for the degree of Doctor of Philosophy

Wolfson Centre for Magnetics
Cardiff School of Engineering
Cardiff University
Wales, United Kingdom

May 2016

DECLARATION

This work has not previously been accepted in substance for any degree and is not concurrently submitted in candidature for any degree.

Signed: ……... (candidate) Date: **19-05-2016**

STATEMENT 1

This thesis is being submitted in partial fulfilment of the requirements for the degree of PhD.

Signed: ……... (candidate) Date: **19-05-2016**

STATEMENT 2

This thesis is the result of my own independent work/investigation, except where otherwise stated. Other sources are acknowledged by explicit references.

Signed: ……... (candidate) Date: **19-05-2016**

STATEMENT 3

I hereby give consent for my thesis, if accepted, to be available for photocopying and for inter-library loan, and for the title and summary to be made available to outside organisations.

Signed: ……... (candidate) Date: **19-05-2016**

ACKNOWLEDGEMENTS

This work was carried out at the Wolfson Centre for Magnetics, Cardiff School of Engineering, Cardiff University. I am really grateful to Cardiff University for providing the opportunity and resources required for my study to complete this project.

First and foremost, I thank **ALLAH** for helping me to complete this thesis.

I would like to express my deepest gratitude to my academic supervisor, Dr Fatih Anayi for his excellent guidance, encouragement, caring, patience, and providing me with an excellent atmosphere during this project. I appreciate his vast knowledge and skill in many areas, and his advice during my study, in writing papers and this thesis.

I would also like to acknowledge Mrs Aderyn Reid, Ms Jeanette C Whyte, Mrs Christine Lee, Sandra Chelmis and Ms Chiara Singh in research office and Sandra Chapman in teaching office and Mr Denley Slade in electronic workshop and Mr Andrew Rankmore and Mr Hary in mechanical and civil workshops for taking time out from their busy schedule to help and support my project during my study in Cardiff University.

My greatest thanks are reserved to my family, especially my mother and father, for their unconditional love, support and encouragement in whole of my life.

ABSTRACT

Transformer is an expensive device and one of the most important parts in a power system. Internal faults can cause a transformer to fail and thus, it is necessary for it to be protected from these faults. Protection doesn't mean that it prevents damage to the protected transformer but it is to minimize the damage to the transformer as much as possible, which consequently minimizes the subsequent outage time and repair cost. Therefore, fast and reliable protection system should be used for limiting damages to the transformer by rapidly disconnecting the faulty transformer from the network, which also leads to the elimination of the stresses on the system itself and preventing damage to adjacent equipment.

The main aim of this thesis is to propose transformer protection technique that is fast and highly sensitive to internal faults that occur inside the transformer, to overcome the problems of current transformer saturation and inrush current, and to make it immune to the external faults (through faults) that occur outside of the transformer protection zone.

The current transformer saturation and inrush current are significant problems since they cause malfunction of the protection system, which consequently will disconnect the transformer because they are considered faults. This improper disconnection of transformer is not desirable as it shortens its life time. So the proposed protection technique was designed to be fast and to avoid maloperation caused by saturation and inrush current.

The proposed protection technique was based on current signal processing. Three methods, namely the application of correlation coefficients, current change ratio (CCR) and percentage area difference (PAD) were proposed based on practical and simulation tests. These techniques were successfully proved by carrying out tests on Simulink models using MATLAB/SIMULINK program and on a practical laboratory model.

In transformer transient state, the response time for the methods that were used to address the problem of inrush condition, was 10 ms for CCR when transformer was on no-load and 5 ms for PAD when the transformer was on-load. This response time

is faster than the most popular method relying on second harmonic, which needs at least one cycle (20ms in 50 Hz systems) to recognize the condition. In transformer steady state, it was proved that the proposed correlation method was capable of detecting the internal faults successfully within a very short time, ranging from 0.8 to 2.5 ms according to the type and severity of the fault and in addition was able to overcome the problem of current transformer (CT) saturation.

The contribution of this research is the development of a transformer protection technique, which is simple in design, fast and reliable in fault detection and at the same time capable of overcoming the problems of current transformer saturation and inrush current.

LIST OF ABBREVIATIONS AND NOMENCLATURES

Abbreviations

AC	Alternating Current
DC	Direct Current
DCR	Ratio of DC
emf	electromagnetic force
rms	root mean square
mmf	magnetomotive force
Pri	Primary
Sec	Secondary
CT	Current Transformer
OLTC	On-load Tap Changer
IEEE	Institute of Electrical and Electronics Engineers
Max	Maximum
Min	Minimum
Amp	Ampere
sw	switch
ms	millisecond
EMTP	Electro Magnetic Transient Program
ATP	Alternative Transient Program
RIFL	Ratio of Increment of Flux Linkages
RIV	Ratio of Induced Voltage
ANN	Artificial Neural Network
DWT	Discrete Wavelet Transform
PCA	Principle Component Analysis
WT	Wavelet Transform
Hz	Hertz
Cov	Covariance
CCR	Current Change Ratio
PAD	Percentage Area Difference
ARP	Area in primary

ARS	Area in secondary
TMR	Timer
D2PK	Difference between two successive peaks of cycles
DP2P	Difference between upper & lower peaks of one cycle
Diffmax	Difference between primary & secondary peaks in every half-cycle
DM	Decision Making
DAQ	Data Acquisition
USB	Universal Serial Bus
PC	Personal Computer
kg	Kilogram
W	Watt
VA	Volt Ampere
kVA	kilo Volt Ampere
MVA	Mega Volt Ampere

Nomenclatures

$Ø$	Magnetic flux
$Ø_{max}$	Maximum flux value
$Ø_l$	Leakage flux
$Ø_r$	Residual flux
λ	Flux linkage
N	Number of turns
i	Current
v	Voltage
V	Volt
a	Transformer turns ratio
P	Power
P_{ave}	Average power
P_{max}	Maximum of average power
P_c	Core power loss
P_{Pri}	Power loss on primary side
P_{Sec}	Power loss on secondary side

P_{cu}	Copper power loss
B	Flux density
B_{max}	Maximum flux density
ω	Angular frequency
f	Frequency
t	Time
A	Cross-sectional area
I_0	Exciting current or no-load current
I_m	Magnetizing current
I_c	Core loss current
e	Induced voltage
y	Exciting admittance
g_c	Conductance
b_m	Susceptance
j	imaginary part
x_l	Leakage reactance
x	Coil reactance
L	Coil inductance
l	Length of wire
ρ	Resistivity of material
R	Resistance
R_{Load}	Load resistance
R_f	Fault or protection resistor
R_m	Magnetization resistance
z	Impedance
Ω	Ohm
Ω·m	Ohm·meter
I_{Ln}	Line current
I_{Ph}	Phase current
V_{Ln}	Line votlage
V_{Ph}	Phase votlage
H	Magnetic field strength
v_m	Maximum voltage

pu	Per unit
I_{OP}	Operating or differential current
I_{RT}	Restraint current
I_{PU}	Pickup current
K_2	Constant coefficient of second harmonic
K_3	Constant coefficient of third harmonic
K_4	Constant coefficient of fourth harmonic
K_5	Constant coefficient of fifth harmonic
Th	Threshold value
I_{d1}	Fundamental component of the differential current
I_{d2}	Second harmonic component of the differential current
n	Number of samples
I_{D2}	Value of normalized second harmonic component
R_{3rd}	Ratio of third harmonic
Kh_3	Threshold restraint ratio of third harmonic
δ_{dw}	Dwell-time (dead angle) angle
ρ_{ps}	Correlation technique index
δ_{ER}	Energy difference
PI	Power index
T	Sampling interval
m	Number of samples per window
r	Pearson's correlation coefficient
r^2	Determination coefficient
r_{set}	Set value of r
r_{xy}	Cross-correlation coefficient between variables x and y
σ	Standard deviation
r^2	Determination coefficient
r_{11}	Auto-correlation of input (primary) current on one phase
r_{22}	Auto-correlation of output (secondary) current on one phase
r_{12}	Cross-correlation between input and output currents on one phase
N.m	Newton meter
K_b	Building factor (inter lamination coat)
K_c	Compensation factor

TABLE OF CONTENTS

CHAPTER 3 LITERATURE REVIEW

CHAPTER 4 PROPOSED METHODS FOR TRANSFORMER PROTECTION

CHAPTER 5 TRANSFORMER MODEL SIMULATION AND EVALUATION OF PROPOSED PROTECTION TECHNIQUES

LIST OF TABLE CAPTIONS

CHAPTER 2

CHAPTER 3

CHAPTER 6

LIST OF FIGURE CAPTIONS

CHAPTER 2

CHAPTER 3

CHAPTER 4

CHAPTER 5

CHAPTER 6

CHAPTER 7

CHAPTER 8

CHAPTER 1

Introduction and Objectives of the Thesis

1.1. Principles of transformer protection

The main task of transformer protection is to limit as much damage as possible to faulty transformers because of the long time that is taken to repair and replace the faulty transformer. Transformer is an expensive device and one of the most important parts in the power system. Therefore, fast and reliable protective relays should be used for preventing further damages to the transformer in consequence of internal faults by disconnecting the faulty transformer from the network system which also leads up to eliminate the stress on the network system itself and preventing damage to adjacent equipment. Power systems are designed to be strong enough to hold out when faulty equipment or several elements are removed from the system, without causing an inappropriate stressing on the overall system. Closely monitoring the behaviour of transformers is very necessary because sometimes, transformer failures are catastrophic and usually result in irreversible internal

damage [1, 2]. Protection doesn't mean that it prevents damage to the protected system but it is to minimize the damage to the system as much as possible, which consequently minimizes the subsequent outage time and repair cost.

The type of transformer protection varies depending on the application and the importance of the transformer. However, any type used for such protection should minimise the disconnection time due to faults occurring in transformer as well as minimise the risk of catastrophic failure in order to eventually reduce the cost of repair. The more time of transformer operation under abnormal conditions such as faults, the less life time of transformer. Therefore, an appropriate protection should be provided for quicker isolation of the faulty transformer in order to prevent it from running longer under such conditions [3].

1.2. Faults in transformer

Transformer failure caused by internal and external short circuit faults is one of major concerns in manufacturing. The internal faults occur inside the transformer protected zone such as turn-turn fault and turn-ground fault whereas external faults occur outside this zone. It is reported that internal winding short-circuited faults are the reason for approximately 70%-80% of transformer failures [4].

It is necessary to detect internal faults in case they occur in transformer as fast as possible in order to protect the overall power system as well as reduce the damage to transformer and adjacent equipment, thus reduce repair cost [5].

The earth or short circuit faults may cause a serious damage to the winding and the core of transformer. Furthermore, the high fault currents may enormously increase the gas pressure in the tank which leads to explosion of the transformer [6].

The challenge of modern transformer protection is how accurately and fast the internal faults are detected. It can be concluded that the essential objective of transformer protection system is to be highly sensitive to internal faults that occur in the transformer, concurrently is to be immune to the external faults (through faults) that occur outside of transformer protected zone [2].

1.3. Differential protection

Differential protection has been considered the best protection scheme for more than 50 years. It is usually chosen as the primary protection for transformers [7].

The inrush current which occurs when a transformer is initially energised is considered a major problem to differential protection, because it creates unbalance between entering and leaving currents to the transformer, which will be considered a fault. As a result, the differential protective relay will operate while actually, it is a normal transient phenomenon in which this relay must not operate, i.e. the inrush condition causes maloperation of the differential protective relay. Hence the discrimination between this condition and the real internal faults has been recognized as a big challenge in transformer protection system. This is the key issue and fundamental problem in the literature of transformer protection. It is normal that the relay should trip when internal faults occur but not in cases of inrush condition or external fault [1, 8].

In practical operation, inrush current, system operation mode and saturation of current transformer contribute to the malfunction of protection systems and at most, they reduce the operation precision rate of these systems to 75% which is far from satisfaction [9].

In general, three types of protection depending on purpose are used to protect transformers, overcurrent, pressure and differential protection. For the latter, which is aimed at detecting internal faults in transformer windings, the differential current (the difference between primary and secondary currents) is relatively small in case of normal operation or external fault thus the relay should not operate [10]. However, there are factors, which can cause maloperation to differential protection. To avoid that, it is necessary to distinguish between internal fault, inrush condition and external fault [10-12].

1.4. Objectives and outline of the thesis

The differential protection systems that depend on the second harmonic ratios in the current signal to overcome the maloperation may recently be maloperated due to the development in building transformers with low core power loss using new materials such as amorphous which produces low harmonic contents. This means that the development is at the cost of the methods that based on harmonics particularly the second harmonic. Although the second harmonic method has other disadvantages as it will be explained in details in literature, it is still widely used in this field, since there is no agreement to fully accept an alternative one.

The transformer protection issue is of very concern to researchers due to the importance of transformers in the power system. The researches in this field are competing with each other based on cost, complexity and response speed. The methods suggested in these researches have disadvantages as it will be explained in the literature.

This research work was oriented to achieve the following objectives:

1. To model transformers, faults and current transformer saturation using MATLAB/SIMULINK program
2. To process the data that obtained by simulating models in the same program
3. To simulate all possible faults when transformer operation is in steady state and then to test the capability of the proposed technique in detecting these faults
4. To simulate the problem of current transformer saturation and then to check how it can be overcome by the proposed technique
5. To simulate the inrush problem that occurs at the time of transformer's energization and then to see how the proposed technique is able to safely discriminate between inrush condition and real internal faults.

6. To carry out all tests in the previous points 3, 4 and 5 in the laboratory, which means that the real data are used in these tests.

7. The aim is also to make the proposed methods able to detect the internal faults within a very short time particularly the minor internal faults such as turn-turn fault, which is too difficult to detect when it starts with very few turns. This is a challenge for the proposed techniques as IEEE Standard C37.91-2000 indicates that at least 10% of the turns in transformer winding have to be short-circuited in order to cause a detectable change in the terminal current. Therefore, an undetectable value of current will be resulted if only few turns are short-circuited [31].

The research is aimed to develop new methods that:

- ✓ Are simple in algorithm design
- ✓ Do not need much computation
- ✓ Depend on a current signal only
- ✓ Are faster than the currently used methods

The current transformer saturation and inrush current are considered to be two significant problems as they cause maloperation to transformer protection systems. Therefore, they are aimed to be solved by the proposed transformer protection methods. The success of these methods in achieving their goals is to be proved by simulation in MATLAB/SIMULINK program as well as through practical experiments.

The thesis was structured as follows:

Chapter 1. *Introduction and Objectives of the Project.* It presents the objectives of the research and the outline of the thesis.

Chapter 2. *Transformer and Related Issues.* Since the transformer is aimed to study in this research, this chapter introduces background information about the transformer such as transformer theory, equivalent circuit, connections and core material. It also introduces how the inrush phenomenon and current transformer saturation occur as well as the transformer faults, because they are the problems that

are aimed to be sovled. It then presents an introduction to relays and how thay are used for transformer protection particularly, the differential protective relay which according to its impotance is introduced in details.

Chapter 3. *Literature Review.* The previous related work is presented in this chapter.

Chapter 4. *Proposed Methods for Transformer Protection.* In this chapter, all the methods that were proposed for transformer protection are shown in detailes.

Chapter 5. *Transformer Model Simulation and Evaluation of Proposed Protection Techniques.* In this chapter, the transformer models are simulated in steady and transient states using MATLAB/SIMULINK program. In each state, the problems of inrush current, current transformer saturation and all possible faults are simulated and tested by the proposed methods.

Chapter 6. *Measurements and Experiment Setup.* The practical work of the research starts in this chapter. It shows how the transformer was built, current transformer saturation was created and the faults were generated in the transformer model at the laboratory. It also shows what equipment were used in experments, the procesudre of the experiments, how the required measurements were taken and how the acquired data were stored in order to be proceesed in the next chapters.

Chapter 7. *Results and Discussions on Transformer in Steady-state condition and CT Saturation.* In this chapter, the practical data that were obtained for the faults and the CT saturation when the transformer is in stead-state operation are processed using the MATLAB program and then the results of testing the proposed correlation technique on each case of faults and current transformer saturation are shown.

Chapter 8. *Results and Discussions on Inrush Problem in Transformer Transient State.* The second part of the practical test on the propsed techinques is discussed in this chapter. The practical data that were obtained for the inrush condition when the transformer is in transient-state operation are processed using the MATLAB program and then the results of testing the proposed techniques on each case of inrush current are shown.

Chapter 9. *Conclusion and Future Work.* All the discussions about the results of testing the proposed techniques in both simulation and practical work are concluded in this chapter. It also introduces some recommendations for the future work.

CHAPTER 2

Transformer and Related Issues

2.1. Transformer

Transformer is a static electric device. It magnetically transforms AC voltage from level to level at the same frequency. The basic structure of the transformer is shown in Fig 2-1-a. It comprises of two windings wound around a ferromagnetic core, one winding is usually referred to as primary winding connected to the AC voltage source and the other one is known as secondary winding connected to load. The two windings are interlinked together by mutual magnetic flux Ø [13].

In 1831, Joseph Henry and Michael Faraday discovered the electromagnetic induction but the latter was the first one who published his work. Faraday discovered that a voltage is induced in one winding if linked by time-varying magnetic field. This voltage is proportional to the number of turns in the winding, so if two windings are linked together by common time-varying magnetic field and each winding has different number of turns, the induced voltage will be different in the two windings [13]. The basic model of transformer in Fig 2-1-a shows the

electromagnetic induction principle. The magnetic flux Ø is generated in primary winding by AC power source connected to the winding. The flux lines then cut across the turns of secondary winding inducing voltage in this winding. The original model of Faraday's transformer consists of two coils of copper insulated by cotton and wounded around iron core as shown in Fig 2-1-b [14]. All transformers that have seen today are operated based on this principle.

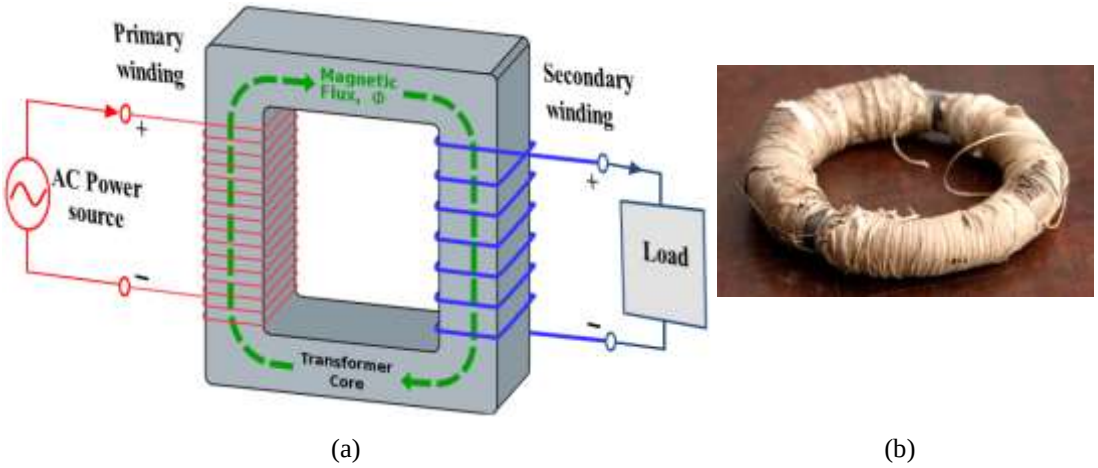

(a) (b)

Fig 2-1(a) Basic model of transformer (b) Original model of Faraday's transformer [14]

Transformer is now one of the most important units in the power systems. The major application of transformer in power system is to transform voltages from level to level in electrical networks. It has now become an integral part of modern life and available with many sizes and capacities. The transformer can be categorised into two parts according to application needed. The first one is step-up transformer which used to transform a voltage from low level to higher level as needed while the second category do the opposite and known as step-down transformer. Simply, the transformer can be either step-up or step-down transformer by setting a proper turn ratio which is defined as a number of turns in primary winding divided by number of turns in secondary winding. This turn ratio specifies in which category the transformer is.

2.1.1. Transformer core construction [15]

The core is commonly built by thin laminations of some ferromagnetic material. These laminations are stacked over each other to form the core. This way of structure is to reduce the losses which caused by eddy currents in the core [15].

In order to improve magnetic coupling between primary and secondary windings as well as minimize leakage of flux, two common designs of core and winding configuration have been accepted, core type transformer and shell type transformer [15]. In the core type, both primary and secondary windings are wrapped around the periphery of the core while in shell type, the two windings are wound around one common limb inside the core surrounded by other core limbs as shown in Fig 2-2.

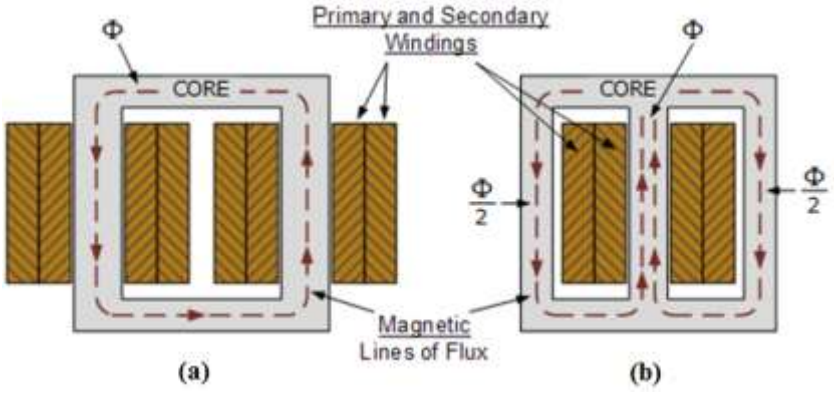

Fig 2-2 (a) Core-type transformer (b) Shell-type transformer [15]

2.1.2. Transformer theory

In order to study the theory of transformer, the ideal transformer that shown in Fig 2-3 is chosen. It is a transformer that has no loss and no leakage flux with a core of infinite of both magnetic permeability and electrical resistivity. It means that entire fluxes are seized in the core linking both windings. In fact, this is impossible to happen in real transformer because all previous assumptions are actually not correct and the neglected parts or quantities really exist. But the ideal transformer is usually taken in order for transformer theory to be simply and easily understood.

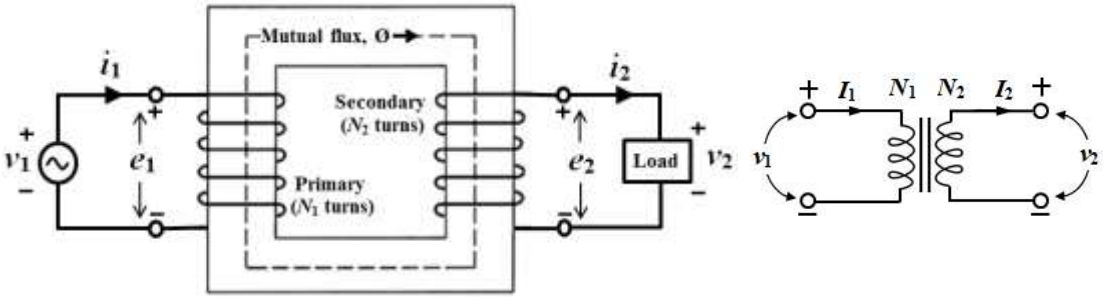

(a) (b)

Fig 2-3 Ideal transformer (a) model and (b) Schematic

In Fig 2-3, when the primary winding is supplied by AC voltage v_1 (assuming there is no resistance), the primary current i_1 flows through the primary winding in which a magnetic flux Ø is generated and then a counter electromagnetic force (emf) e_1 is induced. According to Faraday's induction principle, the emf e_1 can be given as follows [16, 17].

$$v_1 = e_1 = \frac{d\lambda_1}{dt} = N_1 \frac{d\emptyset}{dt} \tag{2-1}$$

Where λ_1 is flux linkage ($\lambda_1=N_1\emptyset$) and N_1 is the number of turns in primary winding.

As assumed that there is no leakage flux, the flux Ø entirely links all turns of winding on secondary side N_2 inducing emf e_2 in this side.

$$v_2 = e_2 = \frac{d\lambda_2}{dt} = N_2 \frac{d\emptyset}{dt} \tag{2-2}$$

Where λ_2 is flux linkage with the secondary N_2-turn winding.

When the load is connected to the secondary winding terminals, the secondary current i_2 flows in the circuit and v_2 equals e_2 as the winding resistance is neglected as shown in Fig 2-3.

Dividing equation (2-1) by equation (2-2) results:

$$\frac{v_1}{v_2} = \frac{N_1}{N_2} = \frac{e_1}{e_2} = a \tag{2-3}$$

Where a is transformer turns ratio. By applying Ampere's law in the closed loop of magnetic flux Ø, equation (2-4) can be obtained.

$$N_1 i_1 - N_2 i_2 = 0 \tag{2-4}$$

Equation (2-4) can be rewritten as:

$$\frac{i_1}{i_2} = \frac{N_2}{N_1} = \frac{1}{a} \tag{2-5}$$

As there is no power loss in the ideal transformer, the instantaneous input power P_1 is equal to the instantaneous input power P_2, i.e.

$$P_1 = P_2 \ \ or \ \ v_1 i_1 = v_2 i_2 \tag{2-6}$$

Let applied voltage v_1 and flux Ø are sinusoidal. The function of flux can be given as:

$$Ø = Ø_{max} \sin \omega t \tag{2-7}$$

And the maximum flux density B_{max} can be given by

$$B_{max} = \frac{Ø_{max}}{A} \tag{2-8}$$

Where $Ø_{max}$ is maximum flux value, ω is angular frequency ($\omega = 2\pi f$, f is frequency), A is cross-sectional area of the core. By substituting Ø from (2-7) into (2-1), the emf e_1 can be expressed as

$$e_1 = N_1 \frac{dØ}{dt} = \omega N_1 Ø_{max} \cos \omega t \tag{2-9}$$

The rms value of emf e_{rms} is then given by

$$e_{rms} = \frac{2\pi}{\sqrt{2}} f N_1 Ø_{max} = 4.44 f N_1 Ø_{max} \tag{2-10}$$

By substituting B_{max} from (2-8) into (2-10), e_{rms} can be rewritten as

$$e_{rms} = 4.44 f N_1 B_{max} A \quad (2\text{-}11)$$

Equation (2-11) is very important equation that is used for obtaining the maximum flux or flux density in transformer cores when excited by sinusoidal voltage.

2.1.3. Transformer on no-load

When there is no secondary current, i.e. there is no load connected to secondary winding, the transformer is known as no-load. But even when the transformer is on this case, there is a current called exciting current I_0 flows on the primary side due to the core losses and finite permeability of the core. This current has two components, magnetizing current I_m and core loss current I_c as shown in Fig 2-4-a which illustrates the equivalent circuit of ideal transformer with exciting circuit [16].

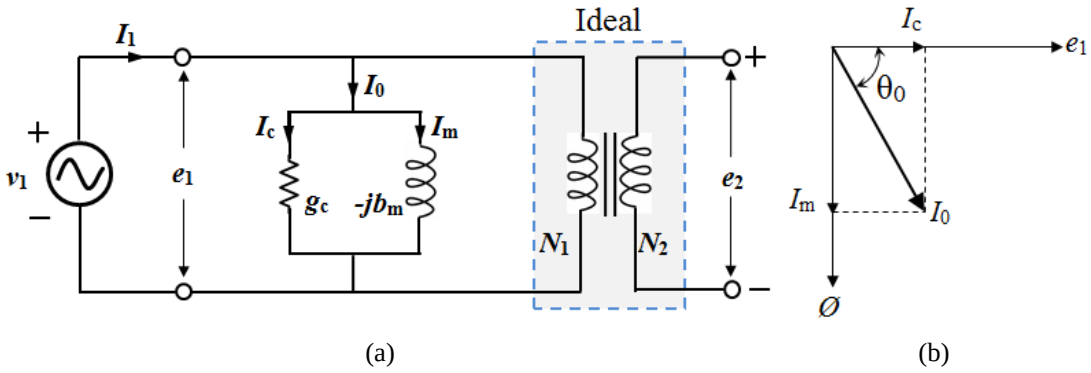

(a) (b)

Fig 2-4 (a) Equivalent circuit of transformer on no-load (b) Phasor diagram

Both induced voltage e_1 and core loss current I_c are in the same phase as shown in phasor diagram in Fig 2-4-b. the core loss current I_c can be given by

$$I_c = \frac{P_c}{e_1} \quad (2\text{-}12)$$

Where P_c is the core power loss which includes both hysteresis and eddy current losses. The magnetizing current I_m is in phase with flux Ø while the induced voltage e_1 is leading both of them by 90^o as shown in Fig 4-2-b. Core loss and magnetization can be modelled by exciting circuit which is a resistance connected in parallel with inductor. So the no load current can be given by

$$I_0 = \sqrt{I_c^2 + I_m^2} \tag{2-13}$$

And the power factor can be calculated by

$$\cos\theta_0 = \frac{I_c}{I_0} \tag{2-13}$$

The exciting admittance y_0 can be expressed as

$$y_0 = g_c - jb_m = \frac{I_0}{e_1} \tag{2-14}$$

Where g_c ($g_c = \frac{I_c}{e_1}$) and b_m ($b_m = \frac{I_m}{e_1}$) are conductance and susceptance of the exciting circuit respectively. j is the imaginary part of impedance due to inductor's reactance ($j = \sqrt{-1}$).

The waveform of exciting current is naturally Non-sinusoidal waveform. This Non-sinusoidal nature is due to nonlinearity of magnetic properties of ferromagnetic circuits that are used in transformers. But the exciting current is symmetrical and then can be represented by fundamental and odd harmonics which are predominant particularly the third harmonic which usually reaches to 40% of exciting current in typical transformers.

2.1.4. Transformer equivalent circuit and leakage impedance

For simplicity in 2.1.2, the ideal transformer has been used, i.e. it is assumed that both magnetic permeability and electrical resistivity of the core are infinity. Also winding resistances, exciting current, core losses, and leakage fluxes have been assumed to be neglected quantities. However, these assumptions and neglected quantities should be considered in order to accurately model the real transformer.

Since the core of real transformer has finite magnetic permeability, some of flux Ø around each winding leaves the core and form another path outside the core. The mutual flux Ø links the two windings, while the leakage fluxes in primary $Ø_{l1}$ and secondary $Ø_{l2}$ link only the primary and secondary winding respectively as shown in

Fig 2-5. Practically, the real paths of leakage fluxes are more complex than what is shown in the Fig 2-5 but the basic feature is still the same.

When the load is connected to secondary winding, the magnetomotive force mmf generated by secondary winding counteract the mmf that generated by primary winding. Primary mmf must be higher than secondary mmf in order to create the resultant mutual flux Ø. Thus, the primary current has two components, load current and exciting (no-load) current [16-18].

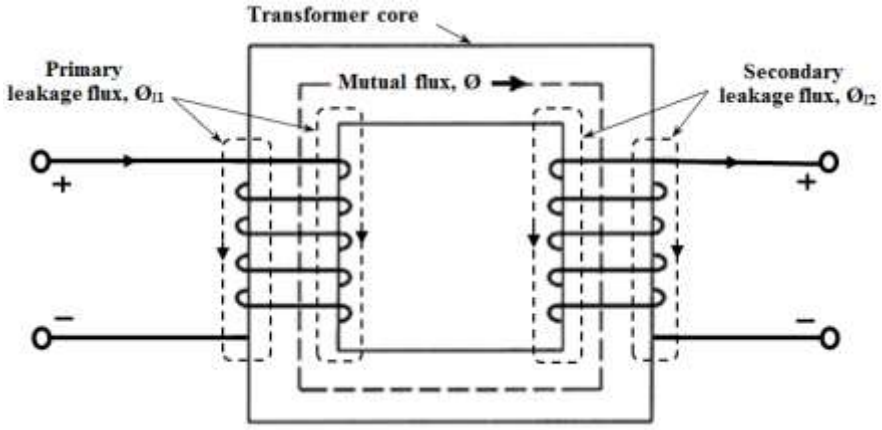

Fig 2-5 Mutual and leakage flux in real transformer

The equivalent circuit, which represents the real transformer, can now be made after taking into account the winding resistances, exciting current and leakage fluxes. In order to consider the leakage fluxes, each winding is assigned by leakage inductance and then the corresponding leakage reactances x_{l1} and x_{l2} for primary and secondary windings respectively (coil reactance $x=\omega L$, $\omega=2\pi f$, L is coil inductance) are introduced in the equivalent circuit. R_1 and R_2 represent primary and secondary winding resistances respectively. The ideal transformer is assumed to carry the resultant mutual flux only, so the equivalent circuit, which includes winding resistances, exciting circuit and leakage fluxes is shown in fig 2-6.

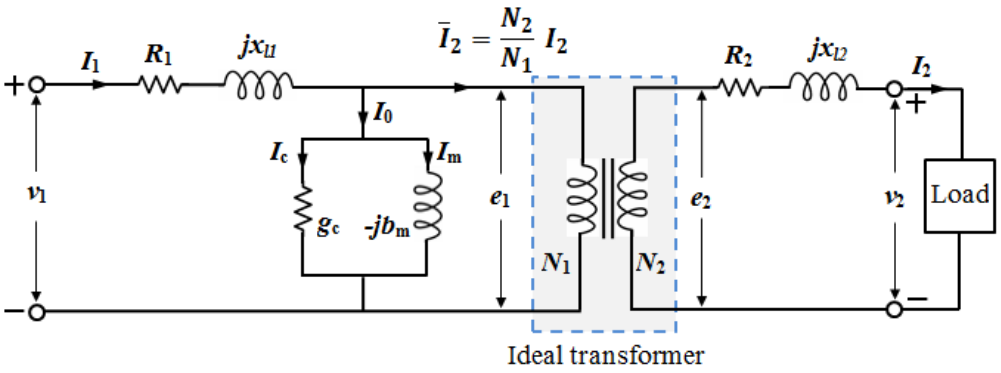

Fig 2-6 Equivalent circuit of real transformer

The primary current I_1 consists of two components, exciting current I_0 and load component $\bar{I}_2$ which equals to the secondary current I_2 referred to the primary current.

$$I_1 = \bar{I}_2 + I_0 = \frac{I_2}{a} + I_0 \tag{2-15}$$

On the primary side, the voltage source v_1 and induced voltage e_1 are now different because of impedance drop z_{l1} which consists of quantities connected in series, resistance R_1 plus leakage reactance x_{l1}. The relationship between can be derived as

$$v_1 = e_1 + I_1 z_{l1} = e_1 + I_1(R_1 + X_{l1}) \tag{2-16}$$

Similarly on the secondary side

$$v_2 = e_2 - I_2 z_{l2} = e_2 - I_2(R_2 + X_{l2}) \tag{2-17}$$

The relationship between turns ratio a and both voltages e_1 and e_2 which are induced by resultant mutual flux Ø, can be given by

$$\frac{e_1}{e_2} = \frac{N_1}{N_2} = a \tag{2-18}$$

In conclusion, the actual transformer can be modelled by ideal transformer added to external impedances and exciting shunt circuit as shown Fig 2-6.

For simplicity, all quantities are usually referred to either secondary side, i.e. the ideal transformer is moved to left or to primary side where the ideal transformer is moved to right. In order to explain how, let considering quantities referred to primary side as shown in Fig 2-7.

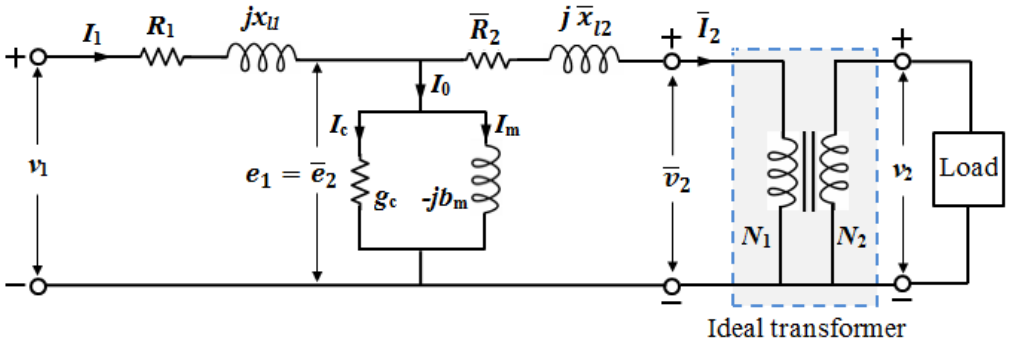

Fig 2-7 Transformer equivalent circuit referred to primary side

The secondary current I_2 can be inversely transformed to the primary side by multiplying it by inverse turns ratio of ideal transformer $1/a$ ($a=N_1/N_2$), i.e. $\bar{I}_2 = \frac{N_2}{N_1} I_2 = \frac{1}{a} I_2$ While secondary resistance R_2 and leakage reactance x_{l2} are multiplied by a^2, i.e. $\bar{R}_2 = a^2 R_2$, $j\,\bar{x}_{l2} = j\,a^2 x_{l2}$, and both secondary voltage v_2 and induced voltage e_2 are multiplied by a, such that $\bar{v}_2 = a v_2$, $\bar{e}_2 = a e_2 = e_1$.

Similarly when quantities are referred to secondary side, but the multiplier of turns ratio will be inversed, so the primary quantities are referred to secondary as follows:

Currents and voltages are multiplied by a and $1/a$ respectively, i.e.

$\bar{I}_1 = a\,I_1$, $\bar{I}_0 = a\,I_0$, $\bar{I}_c = a\,I_c$, $\bar{I}_m = a\,I_m$, $\bar{v}_1 = \frac{1}{a} v_1$, $\bar{e}_1 = \frac{1}{a} e_1 = e_2$

While resistances and impedances are multiplied by $1/a^2$ as follows:

$\bar{R}_1 = \frac{1}{a^2} R_1$, $j\,\bar{x}_{l1} = \frac{1}{a^2} j\,x_{l1}$ and admittance of exciting shunt branch is multiplied by a^2 as follows: $\bar{g}_c = a^2 g_c$, $-j\,\bar{b}_m = -j\,a^2\,b_m$.

2.1.5. Three-phase transformer

In electrical energy, three-phase system, which includes three-phase transformers is mostly used. Three-phase transformers mean that there are three alternating currents

and voltages distributed in three phases. One current and voltage at each phase and the phase shift time between these phases is 120^{o}. Three-phase transformer may be a bank of three separate and identical single-phase transformers or three-phase transformer with one core as shown in Figs 2-8-a and 2-8-b. The three phases are usually denoted by capital letters A, B and C on primary side and small letters a, b and c on secondary side. Under balanced load and voltages, the three single-phase transformers equally carry the three-phase load, i.e. each single-phase transformer will carry 1/3 of total load [16]. The one three-phase transformer has advantages over three single-phase transformers; it is lighter, cheaper and needs less space. In addition, it has 6 external connections rather than 12 as in three single-phase transformers. However, if one phase of one three-phase transformer breaks down, the whole transformer must be disconnected and taken out for repair, so it is required to be replaced with a spare one which costs much more than a spare of single-phase transformer.

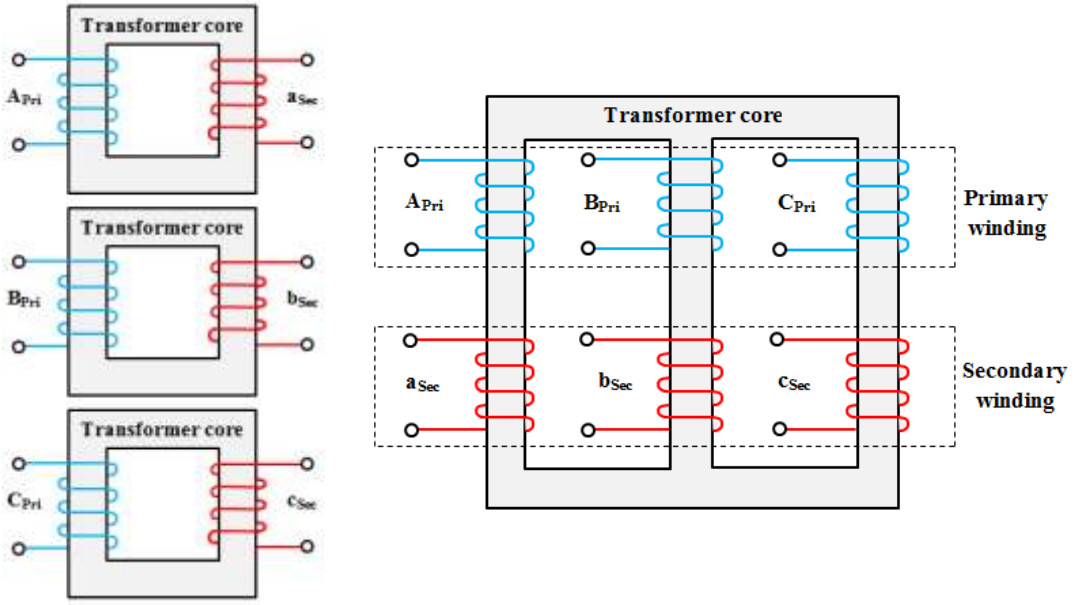

Fig 2-8 (a) Three single-phase transformer bank (b) Single three-phase transformer

2.1.6. Transformer connection

It is needed to connect transformer windings in a way to form a three-phase configuration that is compatible with three-phase power supply. The windings of three-phase transformer can be connected in either Star (Y) or Delta (Δ). Connections can be combined in three-phase two-winding transformer as Y-Δ, Δ-Y, Δ-Δ and Y-Y [16]. Fig 2-9 shows only two possible connections Y-Y and Δ-Δ as the other connections can easily be made by swapping between these two connections. In Star or why (Y) connection, the common point where the three winding end terminals are connected together is called neutral point and usually denoted with N. This point remains either float or connected to ground (earth).

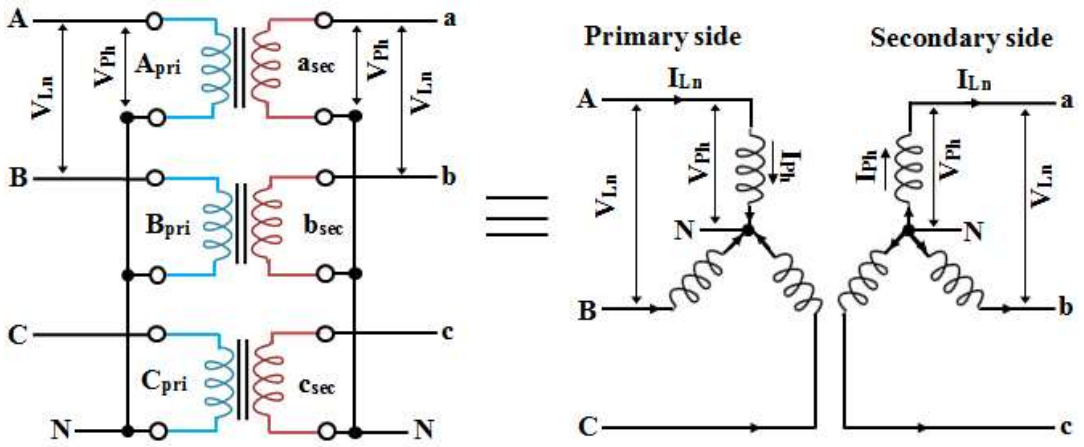

(a)

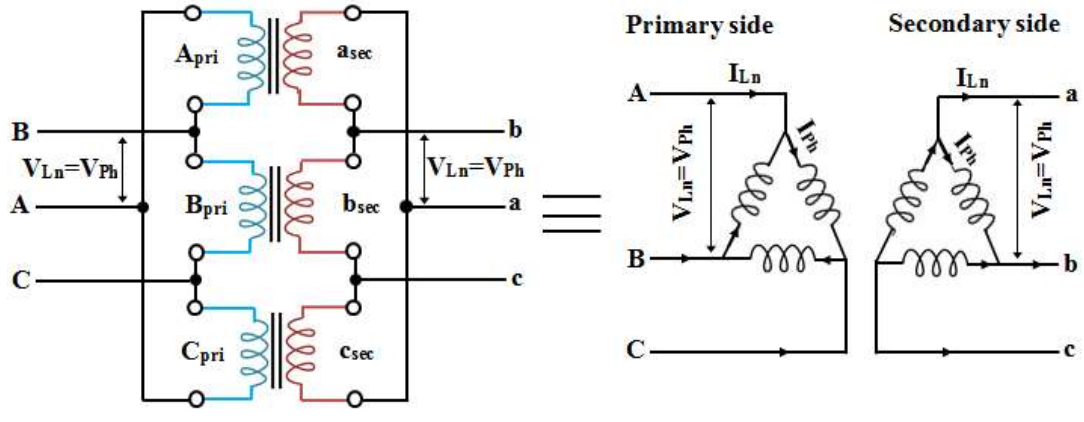

(b)

Fig 2-9 Transformer winding connections (a) Y-Y connection (b) Δ-Δ connection

The three primary windings of three phases are labelled with A, B and C while a, b and c for the three secondary windings. Table 2-1 summarizes the relationship between line to line voltage V_{Ln} or line current I_{Ln} and phase voltage V_{Ph} or phase current I_{Ph} in Delta (Δ) and Star (Y) connection of three-phase system [19].

Table 2-1 Relationship of line-line and phase-neutral voltages and currents [19]

Connection type	Phase voltage V_{Ph}	Line voltage V_{Ln}	Phase current I_{Ph}	Line current I_{Ln}
Star	$V_{Ph} = \frac{1}{\sqrt{3}} V_{Ln}$	$V_{Ln} = \sqrt{3}\, V_{Ph}$	$I_{Ph} = I_{Ln}$	$I_{Ln} = I_{Ph}$
Delta	$V_{Ph} = V_{Ln}$	$V_{Ln} = V_{Ph}$	$I_{Ph} = \frac{1}{\sqrt{3}} I_{Ln}$	$I_{Ln} = \sqrt{3}\, I_{Ph}$

2.2. B-H curve and magnetic hysteresis loop

The magnetization or B-H curve is a curve shows the characteristics of core material, which are different from material to material, thus every type of core material has own curve. The curve illustrates the relationship between flux density B and magnetic field strength H (B-H). Fig 2-10 shows B-H curve for steel, Iron and air [20]. It can be noticed that the position of saturation point (also called knee point) on the curve is different for each material. The Saturation point is the point on B-H curve where the flux density B after this point stays nearly constant and doesn't increase any further whereas the magnetic field strength H continues to increase. It can be seen that it is the highest in steel material which means if the flux density is greater than 0.6 and less than 1.5 Tesla, the core made of steel material will not be saturated while it will be saturated in case if there is no core (air) or the core made of iron, i.e. no more flux density will be increased with the increase of magnetic field strength H.

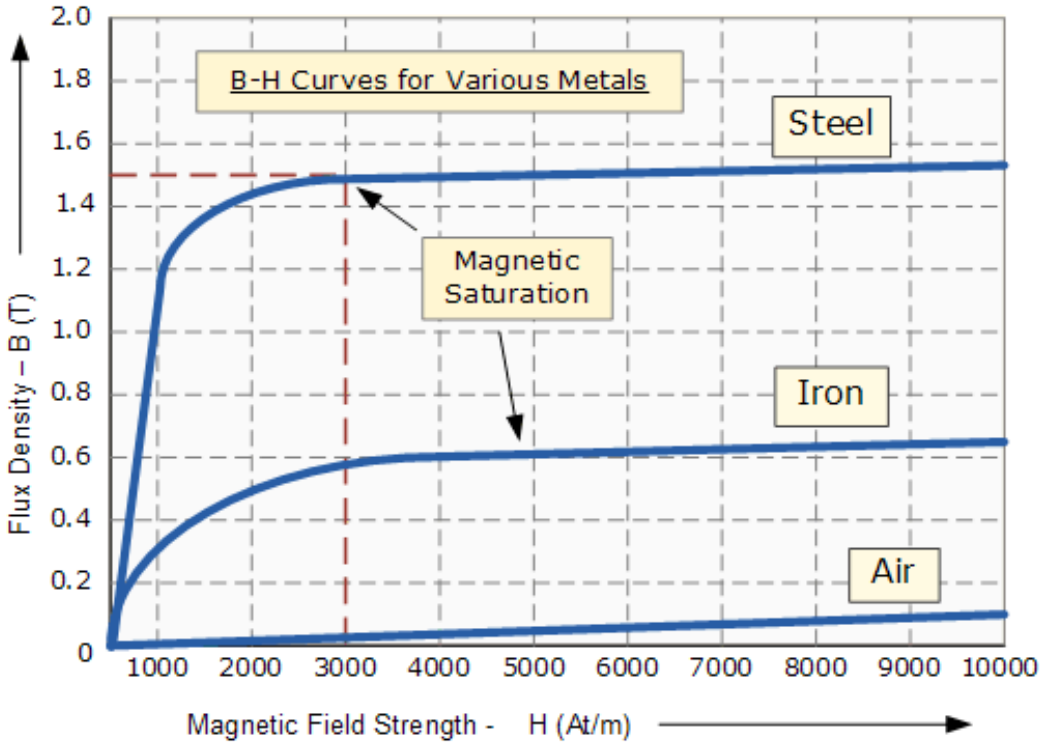

Fig 2-10 B-H curve [20]

The nonlinear relationship between B and H reflects the behaviour of ferromagnetic core as shown in Fig 2-11. Starting from zero point where B and H are zero and also the core supposes to be unmagnetised. If the magnetic field linearly increases with increase of magnetizing current, the flux density also increases till reaches to saturation point a (path 0-a). Now if the magnetising current is reduced to zero which makes also the magnetic field to be zero, the flux will not be decreased to zero due the residual flux that will remains in the core even if there is no magnetic field (it is a characteristic of ferromagnetic material), so the flux will be decreased to residual flux point b when H is reduced to zero (path a-b). By applying a reverse current, the flux can be reduced to zero at point c (path b-c). The magnetizing force that is applied to force the residual flux reducing to zero (demagnetization) is called coercive force. It reverses the magnetic field re-arranging the magnet till the core loses all residual flux and becomes clear of magnet at point c. Then the core will be negatively magnetised because the flux increases again but with negative values as the magnetizing current increases with negative values. They continue to negatively

increase until they reach the saturation point d in the opposite direction (path c-d). Similarly, the flux goes to negative residual flux at point e when magnetizing current goes back to zero (path d-e). Increase of magnetising current makes the coercive force to demagnetise the core again at point f (path e-f). The flux then increases with increase of magnetising current till they reach the saturation point again at point a (path f-a) where the path is ended. The complete path a-b-c-d-e-f-a which forms a closed loop is called magnetic hysteresis loop. This path will be followed in every cycle of AC magnetising current which alternates in the coil between positive and negative values. It means that the flux will follow the path, i.e. the core will be magnetised and demagnetized in every cycle of applied AC voltage. The form of magnetic hysteresis loop may wide or narrow i.e. coercive forces and residual fluxes point positions may be higher or lower depending on the ferromagnetic materials whether soft or hard [20].

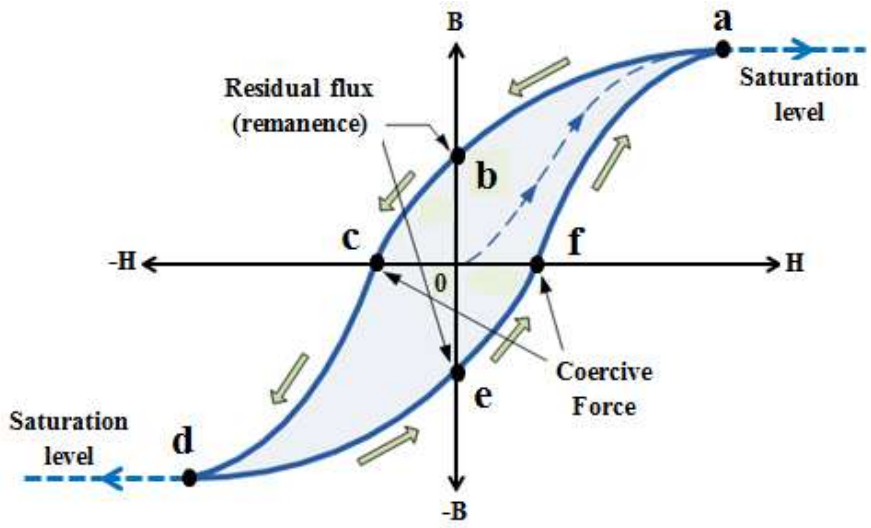

Fig 2-11 Magnetic hysteresis loop

2.3. Inrush phenomenon

When unloaded transformer is switched on, it acts as inductor. In normal condition, the flux Ø that is generated in the core follows but lagging the applied voltage by 90^0 as shown in Fig. 2-12-a. It means that the maximum flux value $Ø_m$ will be reached

when voltage wave v_1 accomplish the first half-cycle. Hence, when voltage increases from zero, the corresponding flux is in negative maximum value. This is only during steady state or supposing that the core is not magnetized and the transformer energized at a voltage peak where flux is zero. In this case, if core loss and primary winding resistance are neglected, the flux and voltage satisfy equation (2-1). Hence, the corresponding value of magnetizing current to the flux can be found by using B-H curve of the transformer core [16, 21].

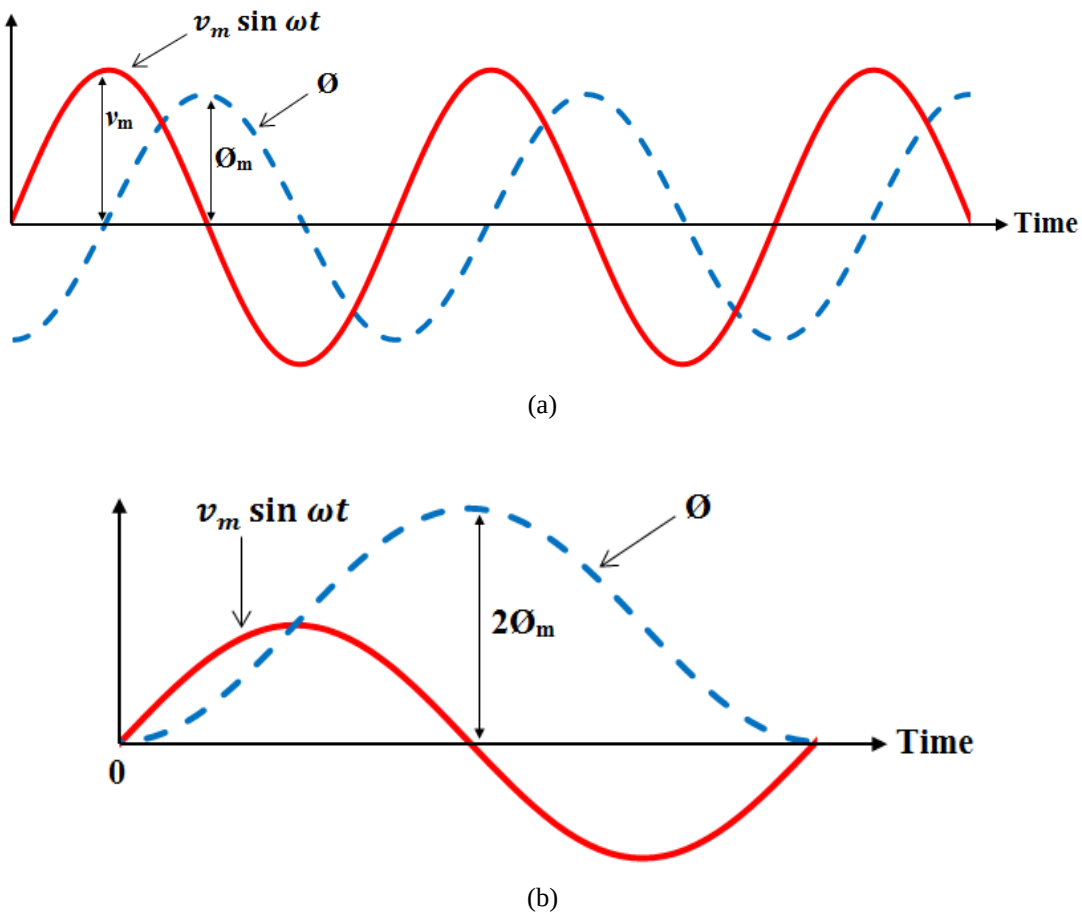

Fig 2-12 Flux and voltage (a) in steady state (b) at instant of transformer switching on

In practice, it is impossible at the instant of transformer energisation to have a negative value of flux at zero voltage as the core is clear of magnet. So the flux will

start building up from zero same as voltage. According to faraday's law, equation (2-1) can be applied here as follows

$$v_1 = v_m \sin \omega t = N_1 \frac{d\emptyset}{dt} \tag{2-19}$$

Integration of (2-19), the flux can be determined

$$\emptyset = \frac{v_m}{N_1} \int_0^t \sin \omega t \, dt = \frac{v_m}{\omega N_1} (1 - \cos \omega t)$$

Or

$$\emptyset = \emptyset_m (1 - \cos \omega t) \tag{2-20}$$

Integration of half-cycle voltage wave i.e. t from 0 to π is substituted in equation (2-20) will produce double of maximum steady state value of flux, $\emptyset = 2\emptyset_m$ as shown in Fig 2-12-b.

Now there is a double of $\emptyset_m$ which is related to the current. So, a very high current is required to produce this extra flux. Therefore, a very high peaky current (about 8-10 times higher than normal rated transformer current) will be drawn from the source by the primary winding of transformer. This current is so called magnetizing inrush current or just can be said inrush current.

The worst case occurs during energization when there is a residual flux $\emptyset_r$ in the core at the same direction (positive polarity) where the flux increases. As a result, the inrush current will be in its highest value because the required flux will be $\emptyset = 2\emptyset_m + \emptyset_r$ as shown in Fig 2-13 while it will be less than that if the remanent flux in the core $\emptyset_r$ is in negative value as the maximum required flux will be $\emptyset = 2\emptyset_m - \emptyset_r$ [16].

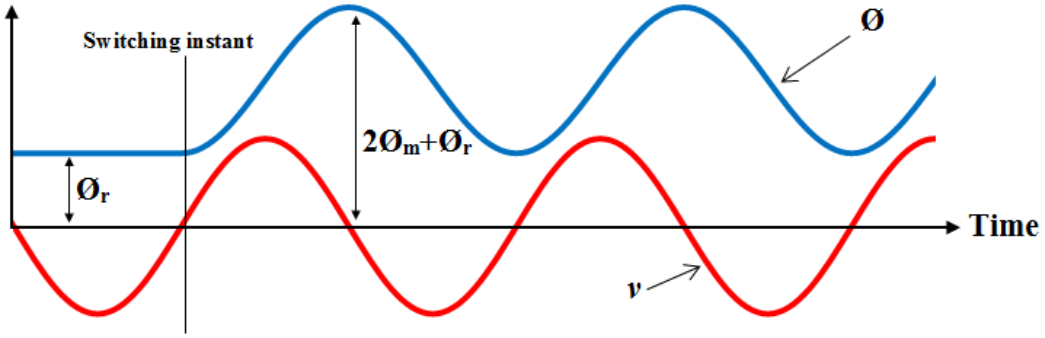

Fig 2-13 Effect of residual flux

In general, the transformer core is saturated slightly after the maximum value of steady state flux $Ø_m$ which is around the saturation point (knee point). So a flux of twice the maximum steady state flux $Ø_m$ or more with residual flux $Ø_r$ may require an exciting current hundreds times higher than the normal rated current because the core becomes supersaturated. Fig 2-14-a shows how this current is formed due to the extra required flux using B-H curve of transformer core. This current depends on the change that occurs in path of flux as well as on the time constant of the transformer which is few milliseconds and seconds for small and large transformer size respectively. This inrush current is drawn by transformer at the instant of energization and it is transient in nature as it remains just few milliseconds or seconds depending on transformer's size and then disappeared. Typical inrush current waveform is shown in Fig 2-14-b.

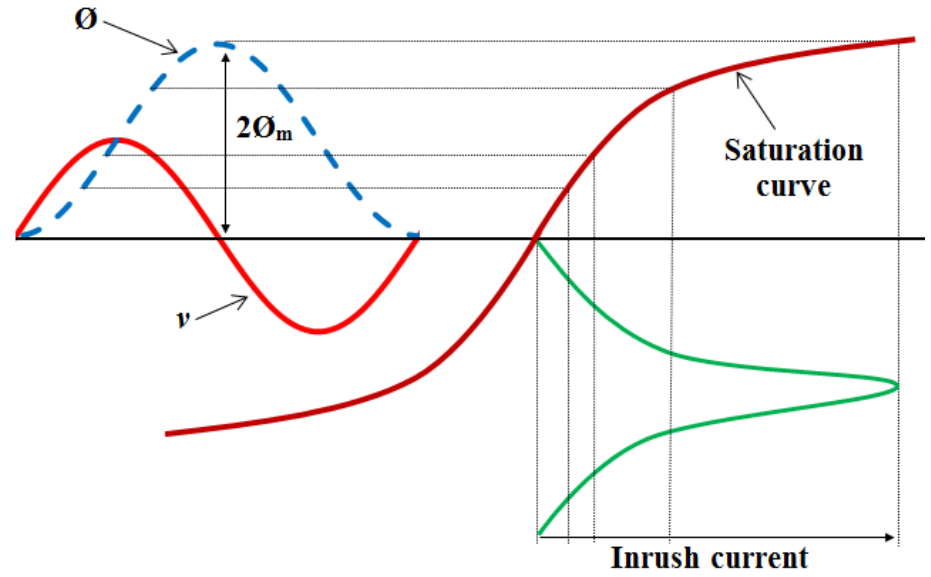

(a)

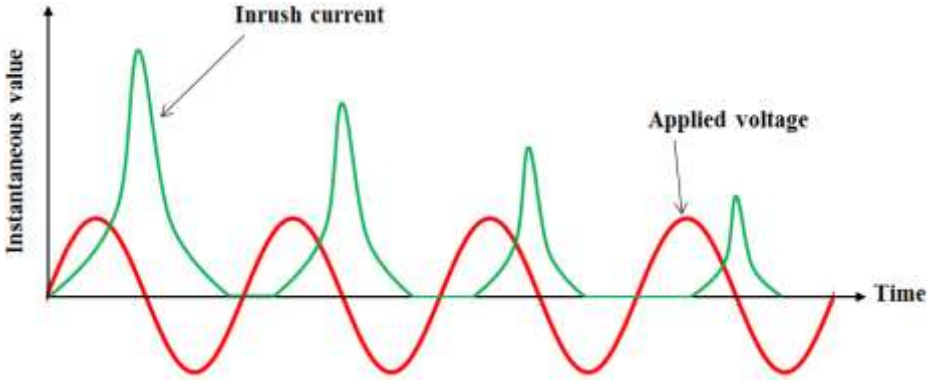

(b)

Fig 2-14 (a) Formation of inrush current (b) Typical inrush waveform

2.3.1. The main characteristics of inrush current

The inrush current has own behaviour and characteristics, which are different from those that exist in normal and fault currents. The characteristics of inrush current can be summarised as follows [22, 23]:

1- The even and odd harmonics as well as DC offset generally exist in the inrush current signal.

2- Its waveform typically consists of either unipolar or bipolar cycles, which are separated from each other by interval of time in which the current is almost zero or very low. This interval is called dwell time or dead angle.

3- Its peak values of unipolar waveform take long time to decrease, i.e. exponential decay of DC component is very slow due to large time constant which is typically much higher than that time constant of decaying DC component created by fault currents.

4- Typically, the second harmonic content is the highest in the signal.

Generally, the odd and even harmonics are predominant harmonics in symmetrical non-sinusoidal and asymmetrical waveforms respectively.

2.3.2. Problems in transformer Caused by inrush current

Inrush current may also be occurred due to any sudden change in magnetizing voltage. Transformer energization is usually considered the main cause of the inrush phenomenon [24, 25].

The magnitude of inrush current is very high but it is considered a normal phenomenon not as a fault because it is transient not permanent as it rapidly disappears. But it can stress the windings of transformer which then leads to malfunction of protective relays that will trip out circuit breakers each time the inrush current occurs to disconnect the transformer. From transformers point of view, this improper disconnection of transformer is not desirable as it shortens the life time of transformer. It may also jeopardize the insulation of windings wherefore it can be indirectly responsible for occurrence of internal fault. The other effects of high inrush current include nuisance fuse or interruption of breakers which as a result require being oversized, arcing and failure of switches and source of distortion and noise that return to mains.

The inrush current appears only on the side of transformer energization. Therefore, it will make unbalance between the primary and secondary currents. This will certainly affect the operation of relays that based on this currents balance such as

differential relay because it will be considered a fault and consequently it will cause a maloperation to this relay which must be blocked during inrush condition.

The inrush case can only be avoided if the transformer is switched off at the instant of peak value of voltage where the residual flux will be in negative value. Thus, when the transformer is switched on again, the flux is built up from the negative value of the residual flux that remained in the core in the last switching off. Therefore, the voltage wave completes the positive half-cycle whilst flux will not exceed the knee point of the core. So there is no more current (inrush) to be produced as there is no extra flux. But practically, this scenario is impossible to occur particularly in three phase transformers.

2.4. Current transformer saturation problem

The current transformer (CT) has same principal of operation as ordinary transformer. It is a type of instrument transformer which is designed to produce a current in its secondary winding which is proportional to the current that is required to be measured in its primary. By changing turn ratio, CT reduces high current to a much lower value that is convenient and can be safely used by either measuring instruments or protection devices.

Current transformers (CTs) that are used in protecting power systems, particularly in differential protection, suffer from magnetic saturation, which is considered one of the most significant problems in these systems.

The CT saturation can be defined as a case in which CT is not able to reproduce the primary current or the CT's secondary current is not a replica of the primary one. The wave shape of CT output is distorted due to CT core saturation caused by faults. As a consequence of this CT saturation, protection relay may be delayed or mis-operated. To solve this problem, relays use algorithms that are not affected by saturation, or the CT's core size is enlarged to increase the flux density thus preventing the saturation from occurring. The requirements normally lead to an impractical, large CT. In practical terms there is a limitation on spaces and also cost, so saturation can't be avoided [26]. The operating point of current transformers normally exists at the lower part of the linear region of the V-I curve. This

arrangement is to provide assurance that the transformer's core will not be subject to saturation status in the event of faults, though in severe fault conditions there is a chance that CTs will be driven into saturation [27]. ANSI/IEEE Standard C-57.13-1993 provides full information on how CTs perform specifications of their characteristics and their behaviour under steady state and symmetrical fault conditions [28]. Practically, when a short-circuit fault exists in a power system, fault currents might contain a high level of DC offset as well as high magnetic remanence in the core. These two elements force the CT cores to enter into magnetic saturation status. Hence, it's important to collect wide knowledge on how CTs perform under fault conditions by implementing simulation/modelling [27].

2.5. Transformer failure

Transformer is electrical device and most critical and expensive device in power system. Like all electrical devices, failures caused by faults can also be occurred in transformer. Many problems can be caused by just one failure. Transformer failures result in outage of power, hazards to personnel and environment, and high cost of repair and replacement.

2.5.1. General transformer failures

In general, Failures or faults of transformers are classified as: [3, 29]

1. Winding failures caused by short circuit of internal faults such as interturn, phase-phase, phase to ground or Turn-ground faults.
2. Faults occur in the core such as failure of core insulation or laminations are short circuited.
3. Terminal faults such as open leads or connections are not firmly fixed.
4. On-load tap changer faults, OLTC.
5. Tank faults and other accessories of transformer
6. Occurrence of abnormal operating cases such as over-flux, overload, or overvoltage.

7. Sustained or uncleared external faults.

Fig 2-15 shows an approximate ratio of the faults mentioned above [29].

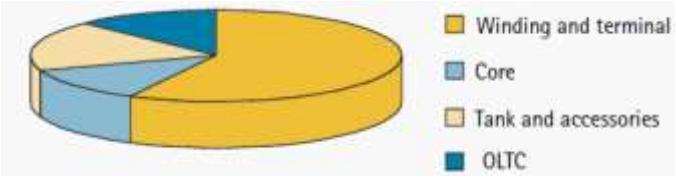

Fig 2-15 Fault statistics in transformer [29]

The percentage ratios of possible faults occurrence in three-phase system are summarized in table 2-2. It can be seen that the single-phase (or line) to ground fault is most likely to occur as it has the highest ratio. The two-phase (double line) to ground or not to ground fault may evolve to three-phase (3-lines) fault [7, 30].

Table 2-2 Percentage of fault occurrence in three-phase system [7]

Fault type	Single phase-to-ground	Phase-to-phase-to ground	Phase-phase	Three-phase
Percentage of fault occurrence	70%-80%	10%-17%	8%-10%	2%-3%

According to statistics of transformer failures given by IEEE Standard [31], the winding faults represent more than 50% of all possible failures. The effect of electromagnetic and mechanical forces on the winding causes a breakdown of insulation in the turns of coil which is considered the main reason of winding faults occurrence.

2.5.2. Internal and external faults

Winding stresses cause damages to transformer and these stresses are results of overheating, open circuits and short circuits. The short circuits either internal or external have more attention by transformer protection than open circuits because the

latter don't resent a significant hazard. The external faults are the faults that occur outside the transformer protected zone while the internal faults occur inside the transformer protected zone [32].

The internal faults can be classified into two categories [4, 6, 32-35]:

a. Incipient faults

These faults are naturally slow to develop but if the reason has not been detected and solved, they may be evolved to be a serious faults such as single-phase to ground or 3-phase faults.

b. Active faults

The breakdown of insulation which results in a sudden stress on windings is considered the main reason behind the occurrence of such faults. The insulation breakdown between winding coil turns or between core and windings may be caused by the following factors:

- Ageing or deterioration of insulation because of frequent exposure to over-temperature. The part of winding that is exposed to highest temperature (hot spot) will deteriorate much faster and therefore its life time will be shorter than the other parts.
- When the oil that is used for insulation is contaminated by water or other impurities that will reduce the oil dielectric strength or cause oil leakage from the tank.
- When partial discharges occur in the insulation.
- Frequent occurrence of transient overvoltage condition.
- When windings are frequently stressed by current forces.

The insulation between winding of low voltage and ground is usually broken-down due to the flashover between low and high voltage windings.

The active fault will be occurred when the current flows through a conductor between either two phases (phase-phase fault) or phase and ground (phase-to-

ground fault). A fast response protective relay is required to detect these faults as they may suddenly be occurred. The active faults are:

1. Earth faults

These are faults occur between windings and earth such as phase-to-ground or turn-ground faults, where windings contact either directly and metallically or by flashover to the earth through the tank or core which are earthed.

2. Short Circuits

Significant current fault occurs when there is short-circuited between phases. Its magnitude basically depends on leakage reactance of transformer and also the impedance of the source.

3. Turn-turn faults

Turn-turn (interturn) fault is one of the most important transformer failures as it may seriously shorten the life time of transformer. Since it is minor internal fault, it is very difficult to be detected.

According to the IEEE Standard documents, there is no one standard way to protect all power transformers against minor internal faults and at the same time to satisfy basic protection requirements: sensitivity, selectivity, and speed. It is too difficult to provide a power transformer protection when only few turns are shorted. As known, the changes in magnitude of terminal currents of transformer are very small when a limited number of turns are shorted in transformer windings. The IEEE Standard C37.91-2000 indicates that at least 10% of the turns in transformer winding have to be short-circuited in order to cause a detectable change in the terminal current. Therefore, when only few turns are short-circuited, it will result in an undetectable increase of current. There is no limit to the maximum internal fault that can flow, other than the protection system capability [31, 36].

It appears when there is a flashover or direct metallic contact between turns of the same winding. The main reason of this fault is the insulation breakdown of the winding and conductors which caused by vibration that generated by

electromechanical forces that originated by over currents and high external fault currents which they flow through the winding of transformer. This fault leads to over current in winding turns which results in serious damages such as hot-spots, heat to oil, deformation of winding and core, clamping and voltage sag or interruption in power system.

Small solid copper particles will be created by melting of winding turns due to the resultant heat. These particles will contaminate the oil that circulates in the transformer. So the damaged transformer should be removed to be repaired and cleaned from these copper particles and soot which means long outage time.

4. Core faults

When short-circuited occurs between laminations, the eddy currents can flow through them causing a serious overheating which may reach to a degree that can damage the winding.

5. Tank faults

The oil is used for cooling and insulation in oil-immersed transformer type. So the quality of the oil is important and should be checked whether it is contaminated by water or other impurities such as solid copper particles mentioned earlier which will reduce the oil dielectric strength. The level of the oil should also be checked as it may leak from the tank which means that the insulation in winding has reduced.

2.6. Relays

Relays are devices connected to the power system in order to protect this system from faults or unwanted conditions inside the area that aimed to be protected. These devices may be digital, analogue or numerical apparatuses. Relays are designed to limit damage to power system equipment and also to ensure high stability and continuity of power service [7, 37].

2.6.1. Relays classification

The relays can be classified into six categories based on their functions [37]:

1. **Protective relay.** Detecting faults in power lines and devices or abnormal operating conditions that may result in serious danger to power system equipment. This relay disconnects the defective apparatus from the system network by tripping one or more circuit breaker.

2. **Monitoring relay.** Verification of conditions on power system or protective devices e.g. it verifies that whether the protective relay works during faults or not.
3. **Reclosing relay.** Arrange the sequence of circuit breaker closing that following trip signals issued by protective relays.

4. **Regulating relay.** It will be activated when the parameter of operation exceeds pre-set limits.

5. **Auxiliary relay.** It is support or supplement to another relays. Timer, isolating relay and trip relay are examples of such relay.

6. **Synchronizing relay.** Insurance of appropriate interconnection condition between two parts of power system.

Since the scope of this research is transformer protection, only the protective relay will be concerned.

2.6.2. Relay design criteria

In order to well design any effective protective relay, four common criteria should be considered. Unfortunately, it is not possible to practically satisfy all these criteria simultaneously. Therefore, it is necessary to find a balance or compromise between these criteria. This compromise must be assessed based on comparative risks [7, 37].

1. **Reliability**

The reliability can be divided into two aspects, security and dependability. Security is a measure of certainty that the relay will not incorrectly operate against any fault whereas dependability is a measure of certainty that the relay will correctly operate in response to all faults that the relay is designed for. Unfortunately, the two aspects

tend to contradict each other, i.e. increasing dependability will be at the cost of lower security and vice versa. Hence, it is necessary to find a compromise between them. However, the reliability of modern relays is high and these relay provide a practical compromise between the two aspects of reliability. Dependability can easily be checked by practical or simulation tests while checking the security is more difficult and is only confirmed in the system to be protected as well as its environment.

2. Operation speed

Operation speed of relay means how fast it is in detecting faults. The faster relay, the less duration of fault which means minimising fault consequences such as damage and instability of system. Generally, the faster relay operation, the higher possibility of incorrect operation, therefore the development of relay speed must be measured based on how high the probability of unwanted case is really required a trip-out. Time is a great criterion for discrimination between real and dummy troubles.

3. Performance and Economics

The basic aim is how to obtain high protection at low total cost. The cost of protection is a major factor. High performance relays offer a great protection but generally have higher cost whereas lower-cost protective relays may not be highly reliable and may also have difficulties during operation or installation, furthermore their maintenance cost will be high. Therefore cost of relays should be assessed based on the cost of the system that are protecting, cost of outage and cost of the protected part if it is lost due to inadequate protection.

4. Simplicity

It is desirable to achieve all protection objectives with minimum equipment and circuit breakers. The relay should be as simple as possible providing that it doesn’t at the expense of relay’s performance.

2.7. Transformer protective relays

Why there is a need to protect transformers? The answer can be summarized in the following reasons [38]:

1- Detect the faulty unit and then isolate it from the other parts of network system.

2- Ensure the stability of system.

3- Minimize the damage to the equipment.

4- Reduce the risk of fire which also causes damage to the adjacent equipment.

5- Reduce the danger to personnel.

The protection of transformer is affected by the following factors:

1- Repair and maintenance cost.

2- Outage cost.

3- Impact on the other parts of system.

4- Possibility of damage to the neighbouring equipment.

5- Time period of repair or replacement of transformers.

Transformer faults i.e. short circuits are the result of internal electrical faults, the most common one being the phase to ground fault (or turn to ground). Somewhat less common are the turn to turn (interturn) faults. Since the interturn fault is minor fault at beginning, it cannot be rapidly detected and cleared. But this fault can develop to become more serious fault such as turn-ground fault. Generally, the transformer is protected from internal faults by using fuses, overcurrent, pressure and differential protection [1, 5, 36].

2.7.1. Sudden pressure protection

As mentioned in 2.5.2, the breakdown of insulation results in turn-turn fault, which in turn will generate heat in winding turns. Since the resultant heat will decompose

the oil and then gas will be released, protection systems such as Buchholz and rate-of-rise pressure which have been designed based on gas detection may be used for detecting this fault. However, they are not satisfactory relays particularly when these faults are at incipient stage [6].

Relays based on sudden pressure do not operate due to changes in pressure or static pressure, which are caused by normal condition of transformer operation. But they operate when the rising rate of gas in the transformer exceeds a predefined limit [7, 36, 39].

2.7.2. Over current protection

Transformers are protected by over-current protection devices in case that the cost of differential protection cannot be justified. However, differential relay may be supported by over-current relay in order to deal with through faults.

Over-current relay is rarely to be used in protection because they are vulnerable to misoperation which may occur due to CTs saturation or inrush current.

The principle of relay's operation is simple. When the input current magnitude exceeds the threshold level (pickup current), the relay operates and the relay's contacts will be closed in order to trip the circuit breaker. The relay's contacts are always open unless the input current magnitude exceeds pickup current. The over-current protection will be the primary protection in case that differential protection cannot be used, but if the latter is used, the over-current protection will be used as a backup protection.

Typically, transformers rated below 10MVA are primarily protected by fuses while those rated above 10MVA are primarily protected by differential protection and over-current as backup protection [1, 7, 36, 39].

2.7.3. Transformer differential protection

Sleeper [40] and Cordray [41-42] were the first who presented the percentage differential protection, which was a modified version of the basic differential protection. It has been used in transformer protection for many years. Fig 2-16 shows the basic differential protection diagram [43]. The main idea of this technique is that

the measured currents by current transformers (CTs) I_1 and I_2 entering and leaving respectively the element that needed to be protected are equals in normal condition i.e. $I_1=I_2$ or $I_1-I_2=0$, but if there is any significant difference, it means that there is a fault in the element and $I_1-I_2 > 0$. This difference is called operating or differential current I_{OP} and this current will operate the relay if it doesn't equal zero (ideally) or it is not very small. Hence that is so called a differential protection. I_{OP} can be calculated as the phasor sum of the two currents I_1 and I_2 [44]:

$$I_{OP} = |I_1+I_2| \tag{2-21}$$

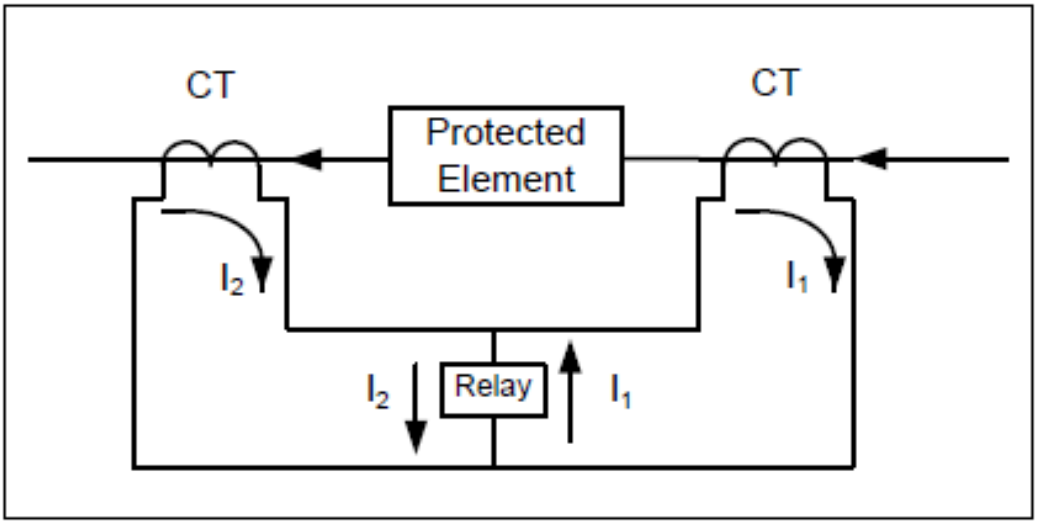

Fig 2-16 Principle of differential protection

In fact, a significant difference between the two currents also occurs in normal condition due to stray capacitance in the protected unit, current transformers are not identical or saturation of current transformer due to external fault. This problem has addressed by modifying the former simple idea of differential protection.

A restraining coil has been added to generate another current called restraint current I_{RT} or mean through current as shown in Fig 2-17. This current passes through the restraining coil and can be calculated as follows:

$$I_{RT} = \left(\frac{I_1 + I_2}{2}\right) \quad (2\text{-}22)$$

It can also be obtained by the most popular three following equations:

$$I_{RT} = k_c * |I_1 - I_2| \quad (2\text{-}23)$$

$$I_{RT} = k_c * (|I_1| - |I_2|) \quad (2\text{-}24)$$

$$I_{RT} = \text{Max}\,(|I_1|, |I_2|) \quad (2\text{-}25)$$

Where, k_c is a compensation factor, usually set to 0.5 or 1.

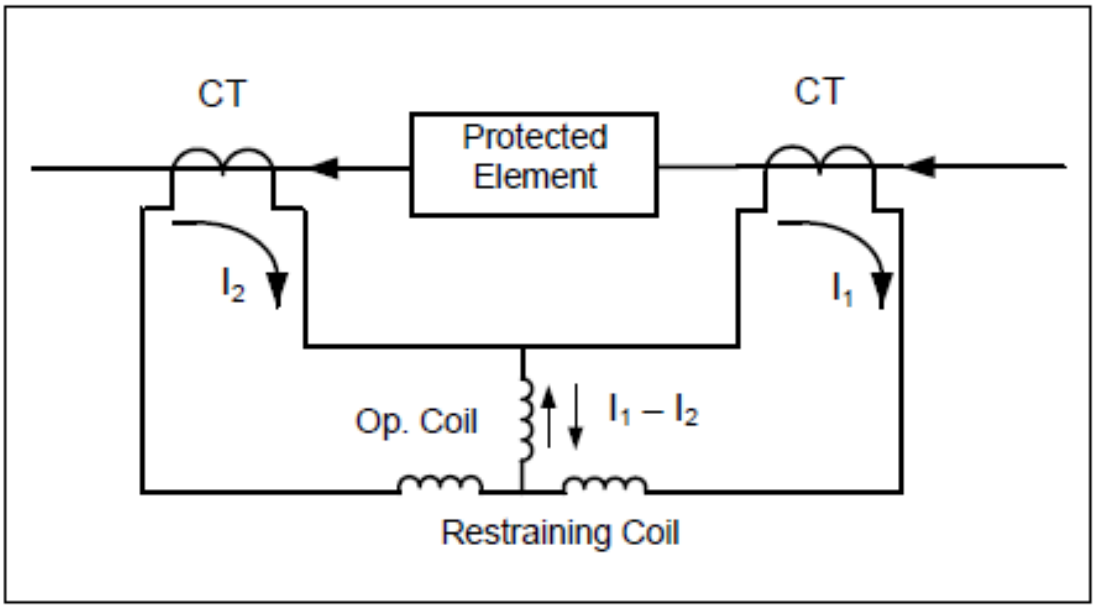

Fig 2-17 Modified differential protection

Each current generates a torque proportional to it in the coil it passes. The operating current I_{OP} passes through operating coil generating a torque (operating torque) opposite to the torque that generated by restraint current I_{RT} in the restraining coil (restraining torque). The relay will operate only if the operating torque is greater than restraining torque i.e. $I_{OP} > I_{RT}$. So if there is a small difference between I_1 and I_2 due to the reasons mentioned earlier, the relay will not operate. After this modification has been added to the basic differential protection relay, it so called a percentage differential relay or biased differential relay. But what is the value of difference

between I_{OP} and I_{RT} that makes the relay to operate or not? For this issue, different slopes 0%, 20% and 40% have been set in order to specify the difference range between these currents that is needed to either operate or restrain the relay as shown in Fig 2-18. These percentage ratios take into account the error ratio caused by non-identical values of both currents I_1 and I_2.

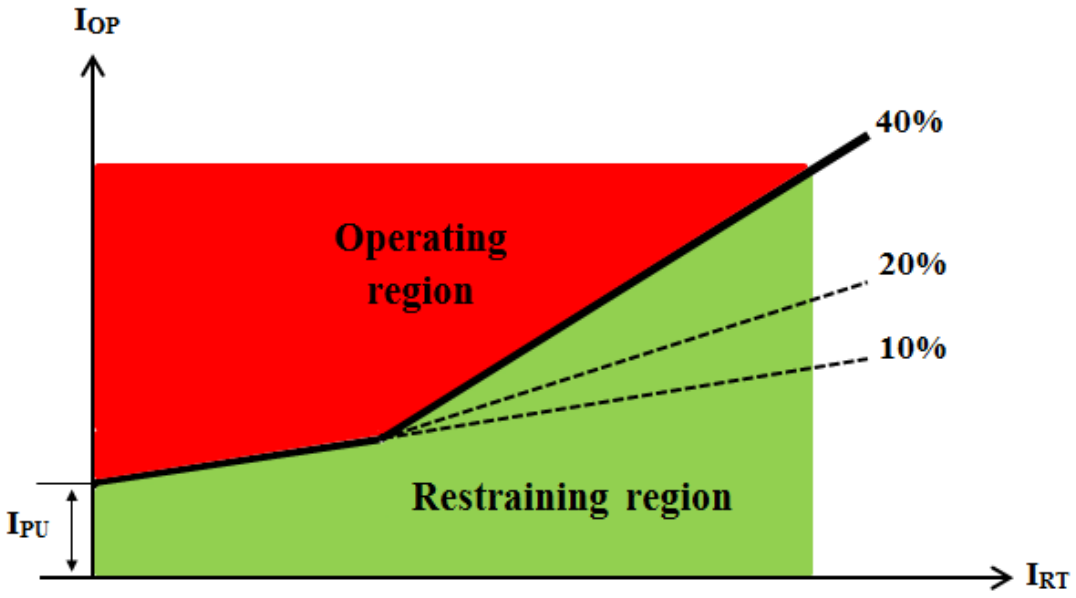

Fig 2-18 Different slopes to specify the relay operating zone

So the I_{OP} value must exceeds one of these ratios of the I_{RT} value to make the relay start to operate i.e. the condition is:

$$I_{OP} > \text{slope } I_{RT} \tag{2-26}$$

For example, I_{OP} > 20% I_{RT} if slope of 20% has been selected. The slopes characteristics increase the security for external faults with CT saturation. It can be noticed in Fig 2-18 that the differential current I_{OP} doesn't start from zero value but starts from a specific value usually set to 0.25 Amp. It is for a safety space to prevent relays from maloperation as well as the friction in traditional relays. This value is so called a minimum pickup current and usually written as $I_{PU.}$

CHAPTER 3

Literature review

3.1. Introduction

For several decades, a prime protection of most power transformers is performed by implementing differential protection systems. In the literature of transformer protection, the key issue is how to discriminate between the internal fault, which occurs inside the protected zone of the transformer and the other disturbances such as inrush condition, which is a normal phenomenon occurring during transformer energization and the external fault which occurs outside of transformer protected zone. This is to avoid the relay from maloperation since the relay should only trip in the case of internal fault while it should be blocked in the other two cases. This is the main base to develop any differential protection.

3.2. Differential relay problem

The inrush current which normally occurs during transformer energization is considered a major problem in differential relay as it appears only in the side of energization, i.e. it makes a big difference between the measured currents in both

sides of transformer. Consequently, the relay will operate because this difference will be considered a fault. This undesirable operation is so called maloperation or misoperation of relay. The early attempts to address this problem and preventing this current from tripping the differential relay were:

1- The operation of relay was delayed for a time that expected to take by inrush current to be faded out [41, 45].

2- The relay was desensitized for a specific time [41, 42].

3- The relay was supported by using a voltage signal for relay restraining [45] or relay blocking [46].

The first attempt is considered high risk because the transformer may be energized with existence of an internal fault. However, using relay desensitization or delaying is not desirable as the transformer will not be protected for a long time. The third attempt minimizes the time of operation (speeds up the operation of relay) at the expense of higher complexity.

3.3. Use of harmonics to restrain or block the relay

In order to avoid any mal-function of protecting relays, it was found that harmonic contents particularly the second harmonic are different during inrush condition and internal fault. Hence, it can be used to discriminate between them. It is very common practice to use second harmonic restraint in protection techniques to stop the operation of differential relays in the events of inrush current or external fault. A ratio of 15% was traditionally selected as a threshold of second harmonic ratio [62,67,71], where the second harmonic ratio is higher than 15% in inrush, while in internal fault it is lower than 15%. As it is still widely used, it is discussed in detail in the literature. Here are the authors whose methods were set based on harmonics:

1. Kennedy and Hayward [47]

They designed a relay circuit based on a method that only used a harmonic current restraint to prevent mal-operation of differential protection relays when there are disturbance in currents due to magnetizing inrush, external fault and internal fault.

This method was called the principle of harmonic current restraint. It took advantage of the difference in ratios of harmonic current components in both magnetizing inrush currents and internal fault. According to these ratios, threshold values were set to restrain the relay in case of inrush and to work in case of internal fault. Table 3-1 shows these ratios in various cases they were tested.

Table 3-1 Harmonic wave analysis of typical currents appearing in differential relay circuits due to various cases [47]

Wave component	Internal fault	Magnetising inrush
Fundamental	100%	100%
Direct current	38%	58%
Second harmonic	9%	63%
Third harmonic	4%	22%
Fourth harmonic	7%	5%
Fifth harmonic	4%	34%
Sixth harmonic	6%	4%
Seventh harmonic	2%	3%

It can be noticed the big difference in second harmonic between inrush and internal fault. This was the reason why it was used later for discrimination between inrush and internal fault.

2. Hayward [48]

He developed the former method by introducing the idea of percentage differential protection. He designed a percentage-differential relay based on harmonic-current restraint for protection of two-winding transformer. It was so called Hayward-differential relay. The percentage differential relays were accepted as a protection scheme for large transformer. Fig 3-1 illustrates the principle of percentage differential protection.

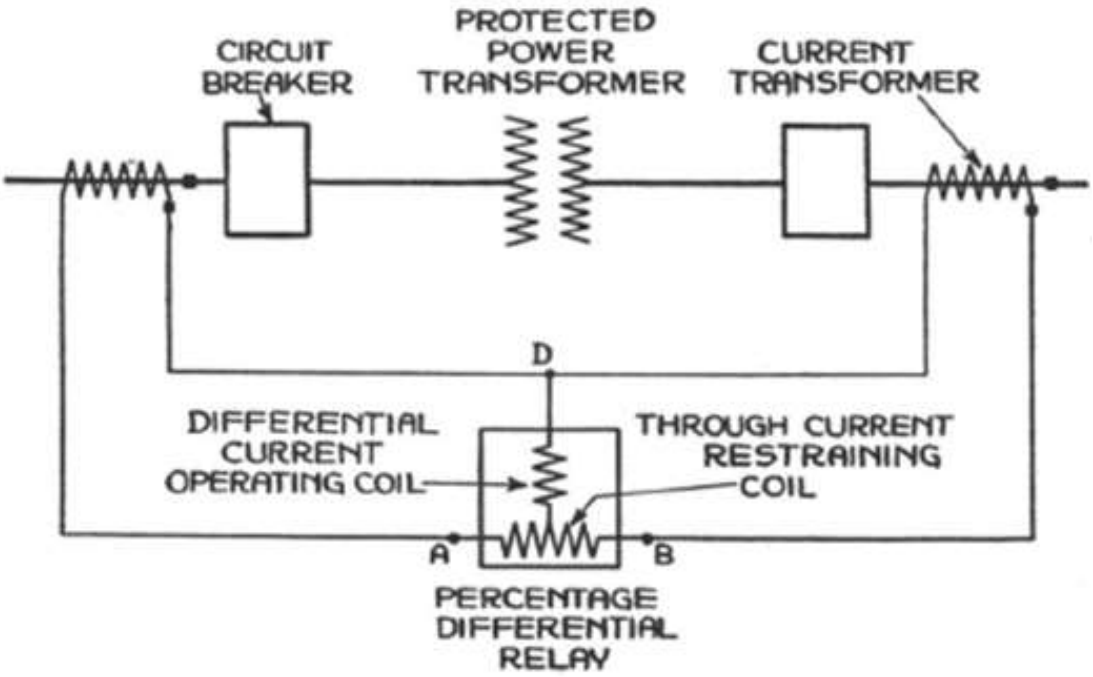

Fig 3-1 Schematic diagram of percentage differential relay [48]

The percentage differential scheme added to harmonic restraint because when transformer is on normal load and the through fault current is low, this current will be in sinusoidal form. So, the harmonic restraint will fail to discriminate it from a small internal fault.

3. Mathews [49]

He designed a relay based on the same idea of the former scheme, but this relay was more sensitive and fast. It also solved the problem of false tripping caused by magnetizing inrush. It completely operates from CTs and doesn't need any additional means for desensitizing. Then, the design of relay was improved to be in smaller size, lower burden and used for more applications.

Since one or more of the main current transformers can be saturated due to external faults to such a level that a false differential current passes through the operating coil of relay, this high speed differential protection relay may maloperate if was not able to distinguish between a false differential current and the differential current caused by internal fault. In addition, when transformer is energized or after clearance of

external fault, the inrush current which appears in one side of transformer, it is seen by relay as an internal fault. So the relay operates if was desensitized or restrained during inrush condition. Also the connection between transformer and current transformers makes the relay is more complicated, because the characteristics as well as the ratio of these current transformers differ from one CT to another. Consequently, one of the CTs may produce a secondary current different from another CT. This difference may operate the relay if it is not correctly compensated.

4. Sharp and Glassburn [50]

Unlike the previous schemes which restrain the relay using all harmonics, Sharp and Glassburn developed the former high-speed variable percentage relay but they retained its simple design and principle. The development in the relay is that it will be blocked during inrush condition or only tripping in the case of internal fault. The design doesn't depend on all harmonics but only uses second harmonic to block the relay during inrush condition as the second harmonic will always present and its ratio is high while it will be low and not predominant. The relay consists of two units, differential and harmonic blockings. Its action requires a unified operation of these two units together. In harmonic blocking unit of the relay, firstly, all harmonics of the operating current will be filtered out, and then the operating current is added to its third and higher order harmonics. This summation is compared with the second harmonic of operating current which is used as blocking signal. So the operating condition in this unit looks like this:

$$I_{OP} + K_3 I_3 + K_4 I_4 + \ldots > K_2 I_2 \qquad (3\text{-}1)$$

Where, I_2, I_3 and I_4 are magnitudes of second, third and fourth harmonics in the differential current respectively. K_2, K_3 and K_4 are constant coefficients of second, third and fourth harmonics respectively.

In the differential unit, the operating current I_{OP} which is applied to operating coil of polarized relay unit is obtained using equation (2-21) and the restraint current I_{RT} using equation (2-25). The I_{RT} which is applied to restraint coil of polarized relay unit is compared to the operating current using equation (2-26) where there are a

resistance and additional saturating transformer provide a variable slope characteristic to adjust the differential current.

They are the first who proposed a protection scheme use two slopes characteristics together to be one scheme with variable-percentage or dual slope characteristic as shown in Fig 3-2. This increases the security of the relay for heavy CT saturation.

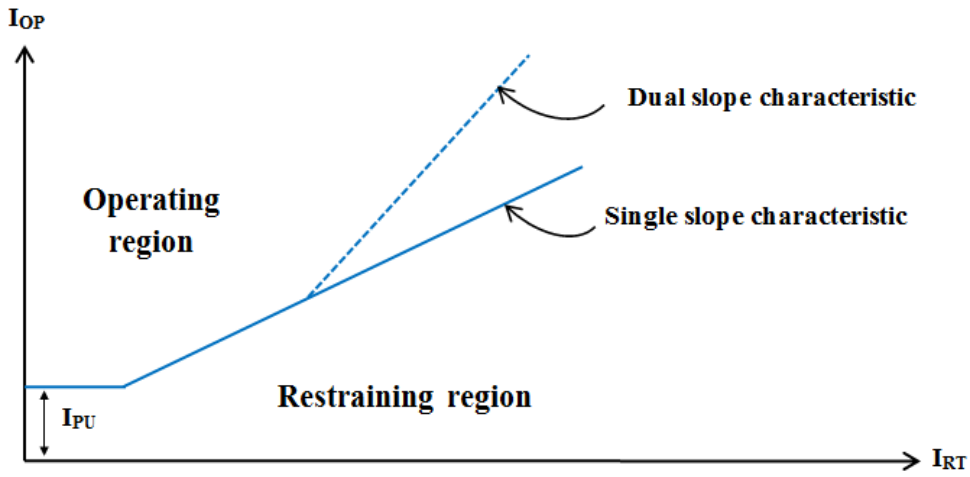

Fig 3-2 Percentage differential relay with dual slope characteristic

However, the harmonic restraint or blocking methods that used by modern transformer differential will not work in all cases especially with the inrush current (on one or two phases) which has very low harmonic content. The complexity of this relay has increased by including two auxiliary relays, time-delay relay to address misoperation caused by inrush current with low second harmonic ratio, and instantaneous overcurrent relay to rapidly trip against heavy internal fault.

5. Einval and Linders [51]

They presented a high speed three-phase differential relay based on two harmonic contents. The relay contained additional air-gap CTs used for filtering out the DC offset of the input currents as well as producing voltage signals which are checked by maximum voltage detector to obtain the restraint current I_{RT} using equation (2-25). They are the first who used the second and Fifth harmonics together as common

harmonic restraint in the relay. The relay will operate if the following condition for one phase is realised:

$$I_{OP} > \text{slope } I_{RT} + K_2 I_2 + K_5 I_5 \quad (3\text{-}2)$$

Where, I_2 and I_5 are magnitudes of second and fifth harmonics in the differential current respectively. K_2 and K_5 are constant coefficients of second and fifth harmonics respectively.

This relay is improved version of harmonic restraint differential relays. The improvements include sensitivity, simplification of circuits and rapid determination to the harmonic contents which leads to improve the response speed to transformer internal faults. It was further improved to be immune to spikes of noise, this resulting in increases the ability of the relay in discrimination between internal fault and inrush condition. So the new design of relay increases relay security for inrush condition. But it is at the cost of dependability, and its operation may be delayed for the case when the internal fault is submerged to inrush current in non-faulty phases. Also its operation time is quite long as its response to the internal winding faults takes around two cycles.

6. Guzman [52]

He presented different algorithms based on harmonic blocking and harmonic restraint methods. His new idea was to use these two methods together in one scheme. But the problem was that the selection of the coefficients which were used for detecting faults has significant effect on the algorithm's performance as well as they were experimentally selected in usual. In addition, there are no balance between harmonic restraint methods and harmonic blocking methods because the harmonic restraint in case of inrush is more secure than the harmonic blocking whereas the latter has less delay than the harmonic restraint in case of internal faults.

7. Guzman et al. [44, 53]

Some methods mentioned earlier which they are based on independent restraint or blocking, may not secure in some cases of inrush, and that method which based on

common harmonic principle for restraint or blocking is not satisfactory method in case of internal fault submerged to inrush current. Therefore Guzman et al. [44, 53] combined the methods, restraint and blocking together to be one independent method. This new approach uses even harmonics for restraint whereas both the DC component (wave shape recognition technique) and Fifth harmonic content are used for relay blocking. Assumptions of this suggestion can be written as follows:

$$\text{If } I_{OP} > \text{slope } I_{RT} + K_2 I_2 + K_4 I_4, \text{ restraint trip signal issues} \quad (3\text{-}3)$$

$$\text{If DCR} < \text{Th, blocking signal issues} \quad (3\text{-}4)$$

$$\text{If } I_{OP} < K_5 I_5, \text{ blocking relay from tripping} \quad (3\text{-}5)$$

Where DCR is ratio of DC component and Th is a threshold value which was selected to be 0.1 as a compromise value between speed and security. The first assumption used second and fourth harmonics as they are significantly exist in inrush current. So they were used to obtain a better distinguishability between inrush current and internal faults in particular to ensure the security for inrush current that has low ratio of second harmonic content, without losing dependability for internal faults with CT saturation. The second assumption ensures this dependability and at the same time maintains this security. The last assumption is to assure an effective response to over excitation.

Realizing of these three assumptions will give a full protection. In addition, realizing a condition of $I_{OP} > I_{PU}$ will enable the restraint signal.

It can be said that this new approach presented a compromise between security and dependability for the cases of internal fault and inrush.

There are two main disadvantages in this method. The first one is that the internal fault may generate harmonics causing long delay for the relay to operate. The second is that any internal fault that is submerged to inrush current during energization cannot rapidly be cleared completely until this current subsides, i.e. the relay remains unblocking in this case.

8. Liu et al. [54]

They carried out practical tests to study harmonic restraint. They found that the harmonic restraint percentage for internal faults takes shorter time to be attenuated than the time taken for inrush current. Based on these observations, the second harmonic restraint signal can still be used for discrimination between internal fault and inrush current after it is improved and modified.

There might be a long time delay in the response of the differential protection systems caused by capacitance exist in long transmission line. The capacitance and inductance of the long transmission line form a resonant circuit and as a result, harmonic of the short-circuit current is increased. They solved this problem, by using a phase voltage as a control signal in order to eliminate second harmonic component for internal fault. The main drawbacks of this solution are that is valid only in case of severe internal faults and it has a slow response.

9. Kulidjian et al. [55]

Their method is extension to the traditional second harmonic restraint method. They changed the way that traditionally followed to define the second harmonic ratio which is used as a restraint signal, to be a complex second harmonic ratio which can be used for the same purpose. As known, the classic second harmonic ratio can be calculated by dividing the magnitude of second harmonic by the magnitude of fundamental component of the differential current. Here, they used the ratio of the phase angle of second harmonic to the phase angle of fundamental frequency component of the differential current. They increased the relays' performance for internal faults since they also found a difference in this ratio during internal fault and inrush condition.

10. Al-Othman and El-Naggar [56]

They presented a new scheme for discrimination between inrush and internal fault cases. Instead of using one criterion of traditional second harmonic, this scheme depends on three factors to decide which one of these cases is occurred, traditional second harmonic content, decaying time constant of DC offset and a ratio calculated

by dividing the magnitude of fundamental component by the magnitude of first peak of the current signal. A discrete time-dynamic filter was used for estimating the current signal contents within very short time. Digital Samples of distorted current waveforms during inrush and internal faults were used by the proposed algorithm to extract the features of these current signals. The three factors were then evaluated by a simple expert system to discriminate between the cases. In addition to use the second harmonic as one of criterions in this technique, the ratio between fundamental component and the first peak magnitude was based on estimation i.e. it cannot be trusted to use as a differentiate criterion.

11. Golshan et al. [57]

The main idea of their method is to observe how second harmonic components of differential current behave during a conditions of both inrush and fault. So, the internal faults can be distinguished from inrush current by evaluating the sign of the criterion function in three phases, this function is defined in terms of time variation of second harmonic for differential current.

The normalized second harmonic components can be calculated as the second harmonic component of differential current (I_{d2}) is divided by fundamental component of the current (I_{d1}). The behaviour of normalized second harmonic components can be compared under both conditions, switching ($(I_{d2}/I_{d1})_{sw}$) and fault ($(I_{d2}/I_{d1})_{f}$). From the observation of the behaviour of normalized second harmonic under the two conditions, its time variation will be used as a good indicator to distinguish internal faults from inrush condition.

X (n) is a function in n^{th} sample indicates the variation of second harmonic and defined as:

$$X(n) = I_{D2}(n) - I_{D2}(n-1) \tag{3-6}$$

Where, $I_{D2}(n)$ and $I_{D2}(n-1)$ are values of normalized second harmonic components in n^{th} and $(n-1)^{th}$ samples respectively.

In each sample n, F(n) defined as a function of area under curve X(n), so F(n) is computed for three phases F_a, F_b and F_c, and then F_d function defined as:

$$F_d = \frac{(F_a + F_b + F_c)}{3} \quad (3\text{-}6)$$

If at least the signs of two functions of F_a, F_b, F_c and F_d are positive, the condition is internal fault, while if either all of functions are negative or at least the sign of one of these functions is positive, the condition is inrush.

The disadvantage of this method is that more computations are needed to extract the components of both fundamental and second harmonic from the operating current. This extraction process carried out by a filter which some parameters of the method depend on. These parameters were set by trial and error. Also, the method addressed cases of fault instants after instant of energization. So when the energization is accompanied by fault, this method will fail to detect this fault. In addition, it was mentioned in the paper that the method doesn't depend on the selection of thresholds although it used the difference function method to convert samples of continuous current signal in cases of inrush and internal into pulses that can be easily used for discrimination between the two cases. But the selection of thresholds is needed in this method.

12. Verma and Kakoti [58]

They proposed a method to distinguish between inrush and internal fault. This method also uses fundamental component for operating signal, second and fifth harmonics as a restraint signals. The new of their proposal that they used a digital filters based on discrete Hartley transform to extract these components. The average values of these components are compared to thresholds to decide whether the case is inrush or internal fault. The threshold values have been selected based on the effect of different parameters of transformer as well as work conditions on these values. In addition to complexity and design cost of this method, the relay based on this method takes 17.5 ms to either trip in case of internal fault or restrain in case of inrush. Dependability and security have been developed here, but a considerable ratio of second harmonic has been reported that also exists during some internal faults.

13. Sykes and Morrison [59]

They used the same basis of second harmonic restraint to distinguish between inrush and internal fault that used by other old methods such as Sharp and Glassburn [50]. The techniques of filtering that used for extracting the second harmonic and fundamental components from differential current have been developed to be fast digital techniques and provide more accurate outputs than the old techniques. Hence, they devised digital filtering schemes for the extraction process which was slow and sometimes provides inaccurate outputs. It can be said that their method is the digital version of harmonic restraint schemes. The components extraction process was also paid attention by other authors, Malik et al. [60] used the correlation of differential current with respect to pair of perpendicular wave in order to extract the components while Schweitzer et a1. [61] proposed a new design of filters called a Finite Impulse Response (FIR) filters for the same objective.

14. Yufeng et al. [62]

They suggested what so called a virtual third harmonic restraint to distinguish between inrush and internal fault. They carried out a simulation as well as a dynamic test on the novel scheme and proved that it is better in reliability and the operation speed is faster than the conventional second harmonic restraint principle, so it can be considered the important component of differential relay. It can overcome some shortcomings of traditional methods such as second harmonic restraint and dead angle which are widely used in this field. Their idea was to assume that the inrush first and second half-cycles are the same if the second half-cycle is reversed. So the inrush waveform can be reconstructed by moving the spiry pulse of inrush backward for half-cycle and reversed to form an intact signal in the whole cycle period as shown in Fig 3-2.

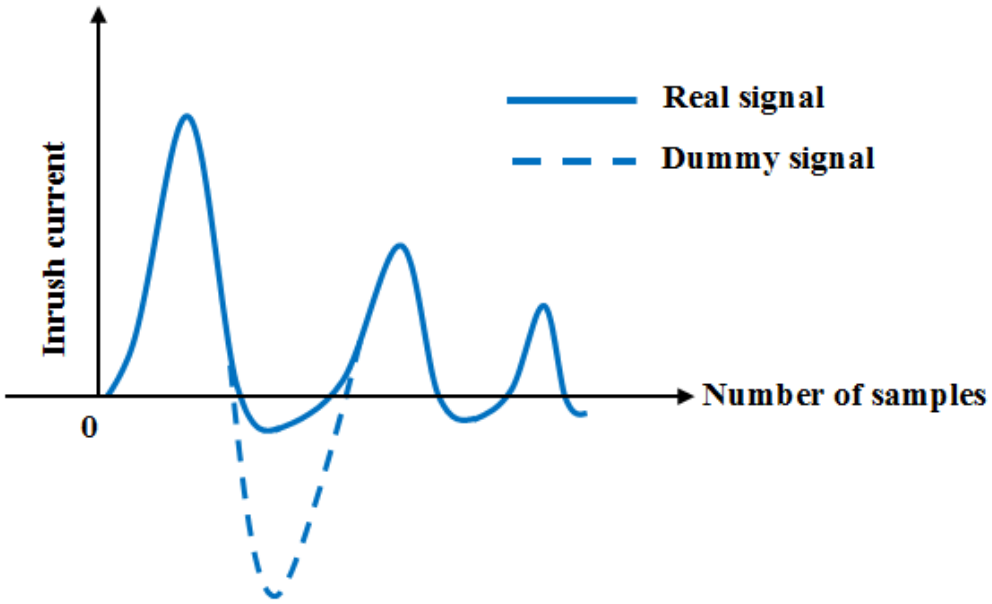

Fig 3-3 Reconstruction of inrush current waveform

This virtual waveform will be having the characteristics of odd symmetry and according to the nonlinearity of transformer's magnetism characteristics, this wave contains high odd harmonics especially the third harmonic contents (virtual third harmonics) which will be used here for restraint unlike what it was traditionally used for operating based on fact that it was low in inrush and higher in internal fault. The condition for restraint scheme is:

$$I_3 \geq K_3 I_{OP} \text{ or } R_{3rd} \geq Kh_3 \tag{3-7}$$

Where, I_3 and I_{OP} are the magnitudes of third harmonic and fundamental component of the operating current in virtual current signal respectively. R_{3rd} is the ratio of third harmonic to the fundamental component i.e. $R_{3rd}= I_3/I_{OP}$. Kh_3 is the threshold restraint ratio which was selected as 16% based on practical tests and taking into account both reliability and speed.

The data window which contains samples of half-cycle current signal will be analysed by half-cycle Fourier principle to get the harmonics. The analysis results may vary in accordance with variation in position taken for this window. The best position should be taken where spiry pulse and symmetrical axis are in the same

position. So the scheme carries out calculations many times where this window is moved back to sampling point every time. By comparing these calculations, the best window is selected. Also the harmonic analysis is affected by DC component, so it should be removed before this analysis is performed. But the main disadvantage of this method is that it depends on the information of first half cycle only while it fully ignores the second half-cycle. It means that the unit to be protected by this scheme remains unprotected until the first half-cycle appears again. Therefore, the use of this scheme should be incorporated with another principle which is able to operate after cycle and a half in order to work in the unprotected duration.

15. Madzikanda and Negnevitsky [63]

They added extra indicator to the second harmonic blocking scheme in order to prevent the scheme from blocking the relay when the current transformer is saturated due to the fault. When this saturation occurs, the rate of second harmonic is also high which will make the scheme block the relay although that is fault. Since the rate of third harmonic is low during inrush and high during CT saturation caused fault, they used it to prevent the second harmonic from restrain the relay when CT is saturated due to the fault. They proposed to measure the rate of change of the third harmonic. If it exceeds a predefined threshold, the second and/or fourth harmonic signal will be prevented from restrain/blocking the differential protection scheme, otherwise the restraint signals are permitted to pass as shown in the block diagram in Fig 3-4.

Regardless to the drawbacks of using harmonics which will be discussed in the next section, they supposed that CT saturation occurs only due to the internal fault in most cases. In fact the CTs are most likely to being saturated due to external faults in which case the relay should not operate against. This case was not considered in the proposed additional indicator.

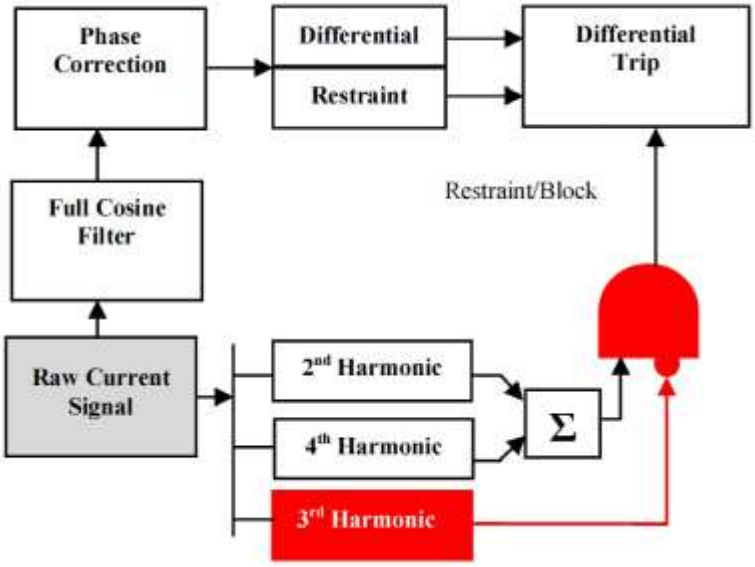

Fig 3-4 Numerical transformer differential protection with third harmonic bias [63]

3.4. The main drawbacks of using harmonics based methods

The protection schemes based on harmonic restraint or blocking particularly the second harmonic have been considerably discussed in the literature because the second harmonic based method has widely been used and it is still used as a main scheme in differential protection as there are no reliable alternative schemes. So many proposals have been presented to overcome the shortcomings in second harmonic based method and to improve it, but they are not enough. In addition, the selection of second harmonic threshold ratio is the main drawback that has not been addressed yet. It is not easy to select the threshold ratio that is required for restraint or blocking. Because the ratio of harmonic contents in the inrush current is changeable and cannot exactly be specified as it is influenced by so many factors such as core structure, hysteresis loop of core material, remanence of core, winding connection, supply voltage of the system as well as its impedance and the instant of transformer switch on/off. So it is a complex way and not reliable to specify exactly the ratio of harmonics as it is produced from different sources with different ratios. In addition, as transmission lines become now longer, it is noticeable that a significant ratio of second harmonic has also been produced during internal fault.

This will make the second harmonic based method confused in deciding whether this high ratio is for inrush current or internal fault.

The second harmonic based methods are unable to detect small faults such as interturn fault and also there are some cases where using this method cannot be relied on. These include internal faults occurring on transformer windings and in power transformers having their cores built using amorphous materials that exhibit low core power loss. The latter introduces low second harmonic components on the supply voltage as around 7% of the fundamental during the inrush condition. Consequently, the second harmonic restraint might not be the best candidate in preventing differential relays from false tripping. Supposing that a threshold for the second harmonic component is reduced below a conventional value of 15%, this give rise to a chance that differential protective relay might not work adequately in case of severe internal faults that introduce second harmonic component above 15% of the fundamental. Furthermore, current transformers may be saturated during internal faults and this will lead to generate a significant amount of the second harmonic.

3.5. Use of wave shape recognition

Methods were presented as protection schemes do not depend on the use of harmonics but depend on the wave shape of current signal. The current signal behaviour changes according to the conditions either inrush or fault. In the inrush case, the current signal takes a unique shape different from the shape that current signal takes during faults. Thus, the discrimination between inrush and faults can be made by recognizing this shape difference. The researches based on this idea are:

1. Dmitrenko [64], Giuliante and Clough [65]

The dwell time approach is a traditional method was used for distinguishing inrush from internal fault. One characteristic of inrush waveform is that its shape becomes flat in the second half-cycle and the value of the current is close to zero. This duration of discontinuity in current is so called dwell time or dead angle. Based on this feature, approaches were proposed. Their idea was that the dwell time during inrush t_A is longer than dwell time during internal fault t_B as shown in Fig 3-5.

Positive and negative threshold values are set to be compared with the differential current in order to determine the duration of dwell time.

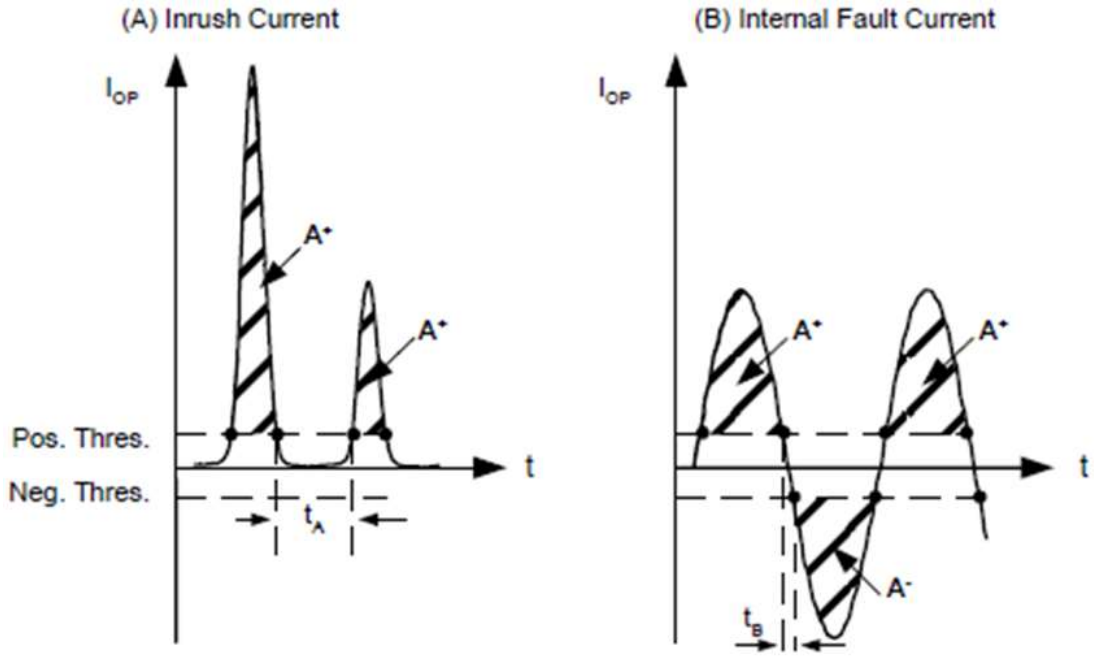

Fig 3-5 Dwell time during (A) inrush and (B) internal fault [44]

One-quarter cycle was used as a threshold time to be compared with the dwell time that is obtained. If the dwell time of the differential current is greater than threshold time, it is inrush case and the relay will be blocked while if it is less than the threshold time, it is internal fault and the relay will be operated.

2. Zhuguang [66] and Lin et al. [67]

Also, dead angle (dwell-time) approach was used here as a restraint scheme. The flat shape occurs in the second half cycle of inrush was utilized to identify the inrush condition by measuring the corresponding angle δ_{dw} to the differential current in this zone (non-current) in one cycle (360^o). This angle and its magnitude are much greater in inrush than in internal fault, because the latter is close to sinusoid. So it can be used to discriminate between inrush and internal fault. Although the cross-blocking schemes were used with it, the tests proved that the threshold of $\delta_{dw} = 60^o$ may cause a maloperation during sever inrush current due the effect of CT saturation

on the shape of the current signal. The reverse charge of current transformer will make the dead angle to disappear, so the schemes that depend on the dead angle will no longer work. In addition, the operation time of this approach is long and takes about one cycle and a half in some fault cases.

3. Rockefeller [68]

He suggested a method to distinguish between inrush and internal fault based on the wave shape of inrush current. His idea was to determine the time between two successive peaks of the current signal as this time is longer in case of inrush than that of internal fault case. So this can be used to identify inrush condition. Once the time at the first peak of current signal is recorded, the scheme waits between 7.5-10 ms (15 to 20 samples) since that time, if the following peak is not detected, the case will be considered inrush and the relay will be blocked. The following peak should be between 75% and 125 % of the previous peak in consideration of peak value sign.

In addition to long delay, the disadvantage will be appeared when cases are occurred such as transformer energization with internal fault. Moreover, how to distinguish between internal and external faults which also have a sinusoidal shape.

4. Hamouda et al. [69]

They proposed a numerical algorithm to identify inrush condition. They utilized the fact that the first peak of inrush current is the highest one then successive peaks decrease until inrush fades out, while the peak of current during internal fault will be higher than the previous one that is the peak pre fault. The algorithm based on this fact will subtract the Root Mean Square (RMS) value of differential current in one cycle from the RMS value of differential current in the previous cycle. If the result of subtraction is positive (greater than zero), it is internal case, but when it is negative, it means that is inrush case. This method is not satisfied at all. Its operation time is so long as it needs information of two successive cycles to decide whether the case is internal fault or inrush. In addition, it will fail to detect the internal fault that originally exists during transformer energisation. It will also fail to distinguish between internal fault and the external fault if the latter applies.

5. Kasztenny et al. [70, 71]

They used the principle of dwell time with assistance of bidirectional instantaneous differential overcurrent which was used for accelerating detection of internal faults versus inrush condition.

In addition to the problem of dead angle disappearance due to the reverse current of current transformers, the proposed method was not able to detect minor faults such as turn-turn during inrush condition. The dwell time occurs in the last part of the current cycle, so it works by the end of the cycle which means that there will be long delay if the transformer energized with a fault.

6. Hooshyar et al. [72]

They presented an algorithm combined two wave shape recognition techniques, correlation and energy difference which in turn they provide two indices. A window of half-cycle length contained samples of voltage and current signal was selected for calculating those indices. The first index (ρ_{ps}) was using correlation technique to evaluate the similarity between the average power (P_{ave}) using equation (3-8) and a sinusoidal signal (S) generated using equation (3-9).

$$P_{ave} = \frac{1}{N}\sum_{k=1}^{N} v_k \; i_k \tag{3-8}$$

$$S = P_{max} \sin\left(\frac{\pi}{2} \pm \frac{\pi k}{N}\right), \qquad k = 0 \sim \frac{N}{2} \tag{3-9}$$

Where v_k and i_k are k^{th} samples of voltage and current signals respectively. *N* is the number of samples in the window. P_{max} is the maximum of average power among the *N* samples inside the window.

During inrush condition, the average power signal had a sinusoidal-like shape which made the similarity was very high while in fault condition, this signal had no sinusoidal-like shape but straight forward increasing trend which made the similarity is very low. So the index based on this fact can be used for differentiating between inrush and fault conditions.

The second index was the difference between the energy of odd and even parts of the power signal in the window. The power signal was broken into the sum of two parts odd and even. The origin was shifted to the centre of the window then the power calculated by subtracting the power at the centre of the window from the power at the end of the window. After that, the odd and even parts of the calculated power signal in new coordinates were extracted. In inrush condition, the odd part was near zero whereas the even part was nearly the same as the power signal. In fault condition, the even part was near zero whereas the odd part was very close to the power signal. This feature was used as a discriminative indicator in the second index. This index (δ_{ER}) was calculated as the difference between the energy of odd and even parts of the power signal.

The final power wave shape index (PI) which combined the two indices ρ_{ps} and δ_{ER} was calculated as:

$$PI = (\rho_{ps} - 0.5) + (\delta_{ER} - 0.2) \quad (3\text{-}10)$$

Where, 0.5 and 0.2 were threshold values of ρ_{ps} and δ_{ER} respectively. The threshold value of PI was chosen a zero. If PI was a positive number, the case was classified as an inrush case, otherwise, it was a fault case.

The window was selected when the peak value of average power should be in the center of the window which starts when inrush current starts to increase after quarter cycle time approximately. It means that the algorithm needs half cycle time and the time from energization till the beginning of window plus the short time for required calculations, i.e. the algorithm takes long response time. Only heavy faults such as single phase-ground were discriminated from inrush condition by the proposed method, while it was not able to do so with minor faults such as turn-turn.

3.6. Use of transformer electro-magnetic equations

Here are methods were produced as an alternative protection schemes. These schemes were built based on the equations that derived from transformer circuit model.

1. Phadke and Thorp [11]

They used the relationship between the flux and current to find a restraint function. The flux is obtained by integration of terminal voltage. According to their algorithm, the flux in the case of internal fault is much smaller than in inrush condition, so the flux change ratio with respect to the differential current can be used to discriminate between these two cases. The flux depends on the voltage signal and should be calculated correctly.

2. Inagaki et al. [73]

They used the equivalent circuits with inverse inductance matrix to represent the transformer. They found that there is a significant difference between values of the inverse inductance which introduced here as the reciprocal of inductance in case of inrush and these values in case of internal fault. So it can be used to discriminate between the two cases. The algorithm firstly calculates the value of what it so called transfer inverse inductance, from leakage inductance and then set into relay. Secondly, value of shunt inverse inductance is determined by sampling both current and voltage at each terminal. Finally this value will be compared with the previous one to decide whether the case is inrush, no fault or internal fault. The former two methods need all transformers' winding currents for decision making, so it is necessary to be measured in all windings. But these currents are difficult to measure when transformer is connected in Delta in which the terminals of transformer usually are not taken out of the tank. Either the parameters of equivalent circuits or data of B-H curve are also needed. However sometimes these requirements are unavailable and it is difficult to be experimentally obtained. The difficulty will be more when the transformer is loaded at the time of inrush occurrence.

3. Kawady et al. [74]

They used the electromagnetic equations of transformer equivalent circuit to detect the internal fault. They selected Brandwajn and Dmmel model to derive these equations. The standard tests of open & short circuits are used to represent the transformer in R and L matrices. From these matrices, two equations of voltage for

each phase of the transformer, primary and secondary can be obtained, i.e. there will be six equations of voltage in three phase transformer. The idea is that in cases of normal operation, inrush and external fault, the calculated voltages using these equations are equal to the measured voltages. In other words, these equations are valid in these cases only, while they are not valid in case of internal fault. According to this assumption, there are six tripping detectors and each one looks like this:

Tripping detector voltage = Voltage (measured) – Voltage (calculated by equations)

In case of internal fault, tripping detector will sense the mismatching between calculated voltage and the measured one. The required parameters for equations are experimentally obtained or using the "BCTRAN" routine in Electro Magnetic Transient Program (EMTP). The circulating currents in Delta winding connection which are needed for the equations are practically not available and it is difficult to obtain them.

4. Kang et al. [75, 76]

They used the electro-magnetic equations to derive the ratio of increment of flux linkages (RIFL) in windings primary and secondary. This ratio was used to distinguish the inrush from internal fault. To illustrate how to get this ratio, a two winding single-phase transformer shown in Fig 3-6 can be taken as an example:

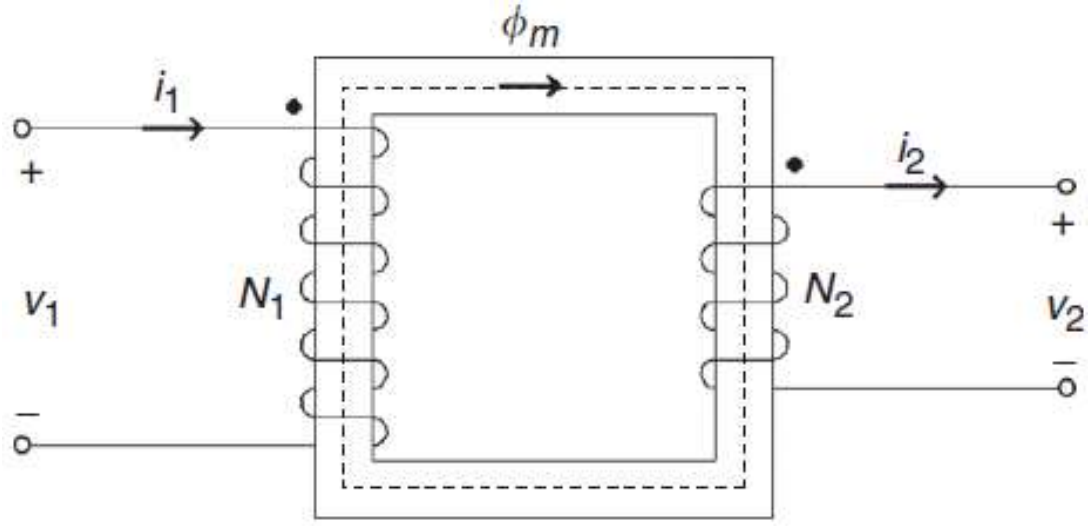

Fig 3-6 Two winding single-phase transformer [75]

Voltages on primary side v_1 and secondary side v_2 can be determined as follows:

$$V_1 = R_1 i_1 + L_1 \frac{di_1}{dt} + \frac{d\lambda_1}{dt} \quad (3\text{-}11)$$

$$V_2 = -R_2 i_2 + L_2 \frac{di_2}{dt} + \frac{d\lambda_2}{dt} \quad (3\text{-}12)$$

Where R_1, i_1, L_1 and λ_1 are wire resistance, current, inductance and flux linkage on primary side respectively, and R_2, i_2, L_2 and λ_2 are the same as previous ones but on secondary side.

The flux linkage can be written as:

$$\frac{d\lambda_1}{dt} = V_1 - R_1 i_1 - L_1 \frac{di_1}{dt} \quad (3\text{-}13)$$

$$\frac{d\lambda_2}{dt} = V_2 + R_2 i_2 + L_2 \frac{di_2}{dt} \quad (3\text{-}14)$$

By integration of (3-13) and (3-14), the increment of flux linkage can be estimated for primary and secondary windings $\Delta\lambda_1$ and $\Delta\lambda_2$, so the RIFL can be defined as:

$$\text{RIFL} = \frac{\Delta\lambda_1}{\Delta\lambda_2} \quad (3\text{-}15)$$

In case of inrush, The RIFL is equal to the turn ratio between primary and secondary (N_1/N_2), while they are not equal to each other in case of internal fault. However, they are also not equal in normal case. Therefore the following detector will be used:

$$Detector = \frac{\Delta\lambda_1 - \frac{N_1}{N_2}\Delta\lambda_2}{\sqrt{2}\,V_1.T}.100(\%) \quad (3\text{-}16)$$

Where, T is sampling interval. The detector in (3-16) is for one phase, thus in three-phase transformer, this detector will be for each phase, i.e. three detectors for phases A, B and C. The detector is compared with the threshold ratio which set to 5%. They used a counter to count how many times the sample value exceeds the threshold ratio. It increased by 1 every time the value exceeds threshold, otherwise decreased

by 1. If it goes below zero, it will be reset to zero. According to this scheme, the relay will operate if the counter exceeds 4, which indicates that an internal fault has occurred.

5. Kang et al. [77]

They used exactly the same principle and procedure as the previous one, except that they used the ratio of induced voltage (RIV) for the cases discrimination rather than using the RIFL. So, the equations (3-15) and (3-16) will be based on induced voltages e_1 and e_2 ($e = \frac{d\lambda}{dt}$) on primary and secondary sides respectively as follows:

$$\mathrm{RIV} = \frac{e_1}{e_2} \tag{3-17}$$

$$Detector = \frac{e_1 - \frac{N_1}{N_2} e_2}{\sqrt{2}\, V_1} . 100(\%) \tag{3-18}$$

The two former techniques are not able to directly specify the type of fault. Also, under some conditions, there is such numerical oscillation caused by using the backward Euler principle which was used for estimating voltages or flux linkages in the equations. In addition, the suggested methods didn't specify which side of windings primary or secondary experiences the fault.

6. Sachdev et al. [78]

They also used the same idea as the previous two methods. But here, they only used the linear elements in the electro-magnetic equations. It also used the currents of Delta winding which are practically not available as mentioned earlier in 3.6(3). In addition, if the windings of transformer are connected in Delta-Delta, each winding has circulating current which has own components and hence the factors in the equations to obtain these currents will be more complicated because all reference phase parameters as well as other phases should be included in these factors.

In general, in methods based on electromagnetic equations, the transformer equivalent circuit in case of core saturation should be accurate. However it is difficult to confirm this accuracy.

3.7. Use of Pattern recognition

The pattern recognition can be defined as a way that is used for either comparing two items to find out the similar properties between them or feature detection where any unique feature of any item can be identified. The current signal is processed under inrush and fault conditions to extract any pattern that is different in the two conditions. Once the unique pattern for each condition is recognized, it can be used for discrimination between inrush condition and faults. Pattern recognition has many applications in signal processing. The relative techniques that are applied in pattern recognition are:

3.7.1. Cross-correlation technique

This technique is used as a measure of similarity of two waveforms or variables. It indicates to which dgree these two signals or variables are similar. It is recently used for transformer protection and here are the works that were done based on this technique:

1. Zhang et al [79]

They suggested a method to discriminate inrush current from internal fault by utilizing the characteristics that only exist in inrush current such as asymmetry of two consecutive half cycles and the dead angle. These characteristics are extracted by using the short-time correlation function. The operation time of this scheme is no less than a cycle. As mentioned in 3.5(2), the dead angle may disappear due to the reverse charge of current transformer.

2. Lin et al [67]

They proposed a blocking scheme based on improved correlation algorithm and wave comparison. It has been implemented for fault detection by the use of correlation coefficients between the first and following half cycles. In this scheme, one cycle of the current is measured at each phase, and then finds out the similarity by calculating the correlation coefficients between first half and latter half of this current cycle. Through sampling one-cycle and extend the sampling process into

next cycle, sample observing window to be correlated is created as shown in the box in Fig 3-7 for inrush case and Fig 3-8 for internal fault case. This window of samples is equally divided into two parts x(t) and y(t) represent first and latter half cycles respectively (the two small windows in Figs 3-7-a and 3-8-a). x(t) is then correlated with reversed y(t) as shown in the box in Figs 3-7-b and 3-8-b. According to the comparison between the value of correlation coefficient and the threshold value, the algorithm specifies whether it is internal fault or inrush current. It is clear that correlation coefficient is close to one in case of internal fault as the two half-cycles are more similar than in the case of inrush in which the correlation coefficient will be far from one as there is no high similarity between the two halves x(t) and y(t).

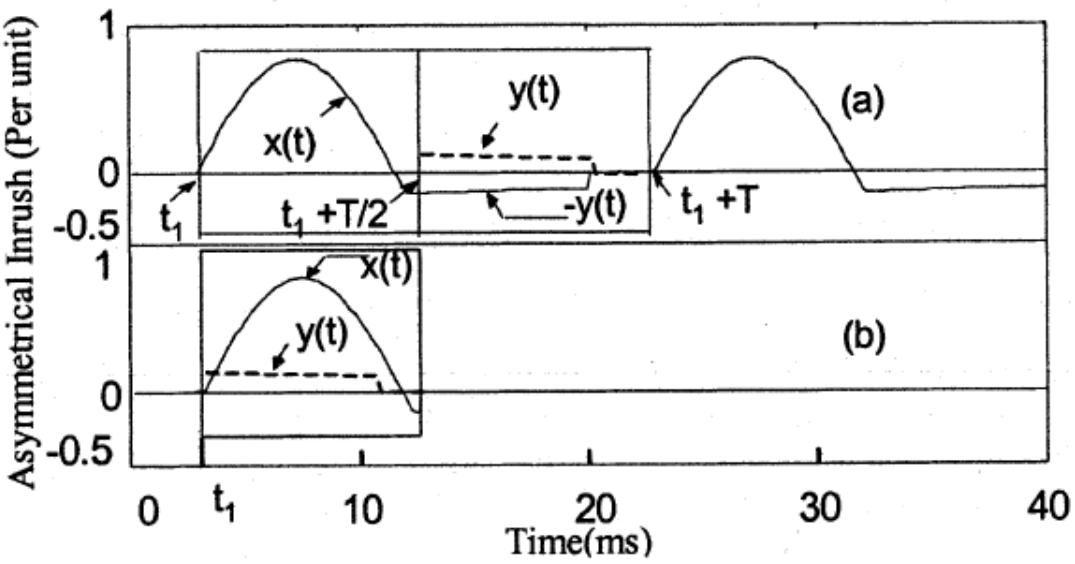

Fig 3-7 Observing window in inrush case (a) first and latter half cycles in the window (b) the two halves to be correlated [67]

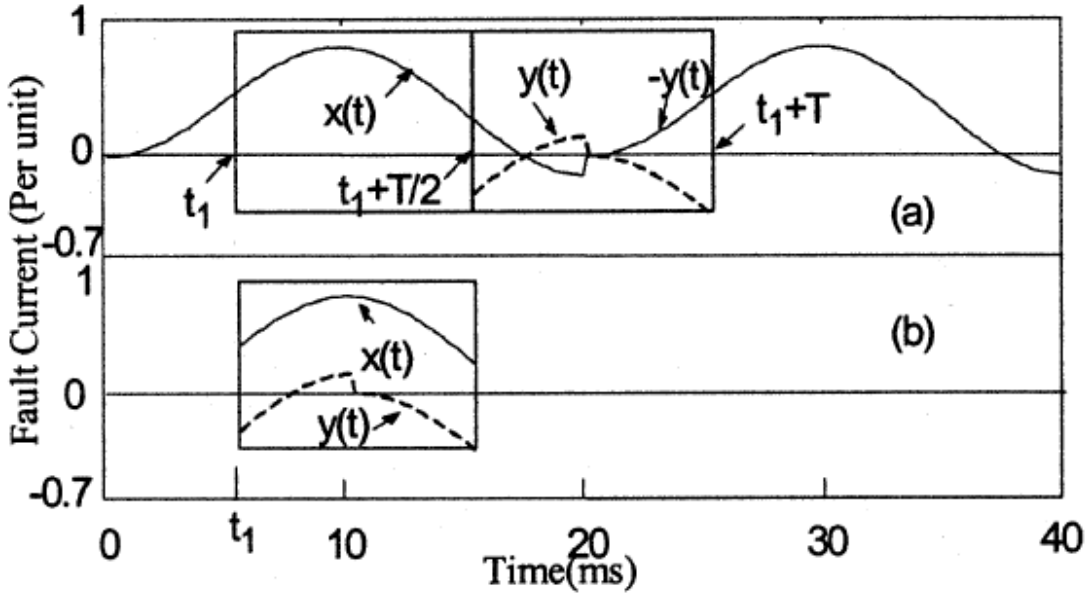

Fig 3-8 Observing window in internal fault case (a) first and latter half cycles in the window (b) the two halves to be correlated [67]

The problems associated with this approach are prolong time taken for processing and weakness of symmetry between the first and the latter half-cycle that are caused by fading of components. In addition, when the transformer is energized with a small turn-turn fault and the fault phase is submerged in the inrush current, the similarity between the first half-cycle and the latter half-cycle of differential current is so bad that the present algorithm will not be able to detect the fault until the inrush fades out.

3. Bi et al [80]

Their method also uses a correlation analysis. It is based on the analysis of the waveform in non-saturation zone of the waveform (dead angle or dwell time) to distinguish between inrush condition and internal fault. One cycle is sampled to obtain observing window. In this window, smaller size of window called local window is created to find the dead angle zone through the sample sequences of observing window. Once the local window specifies the zone, its samples sequence x will then be used to construct two sinusoidal signals y_1 and y_2 as shown in Figs 3-9 and 3-10 for inrush and internal fault cases respectively.

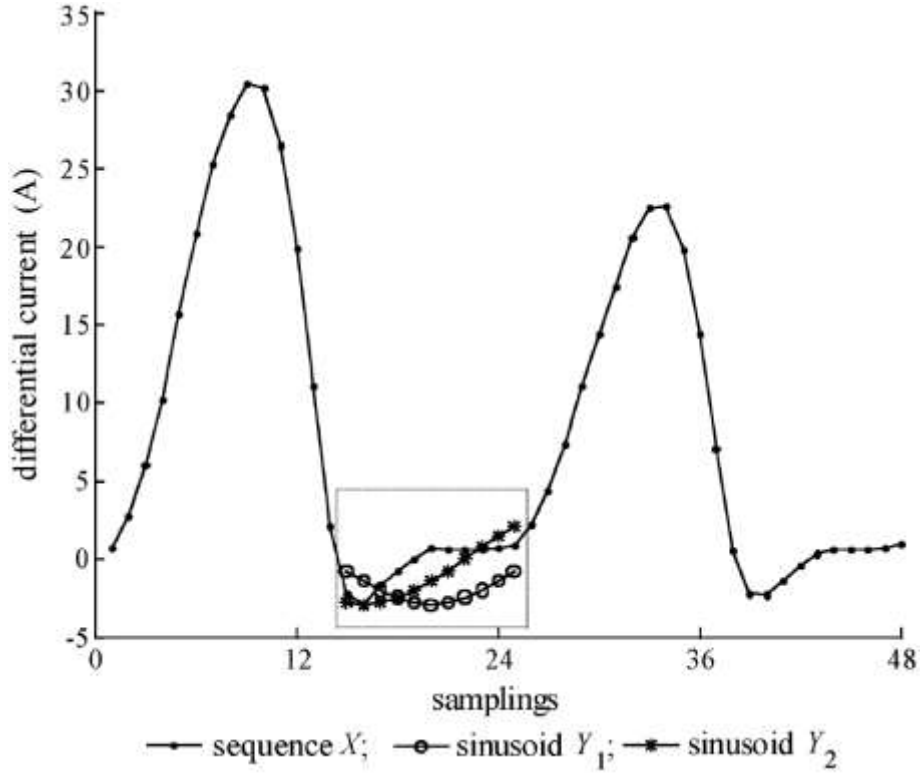

Fig 3-9 Inrush case [80]

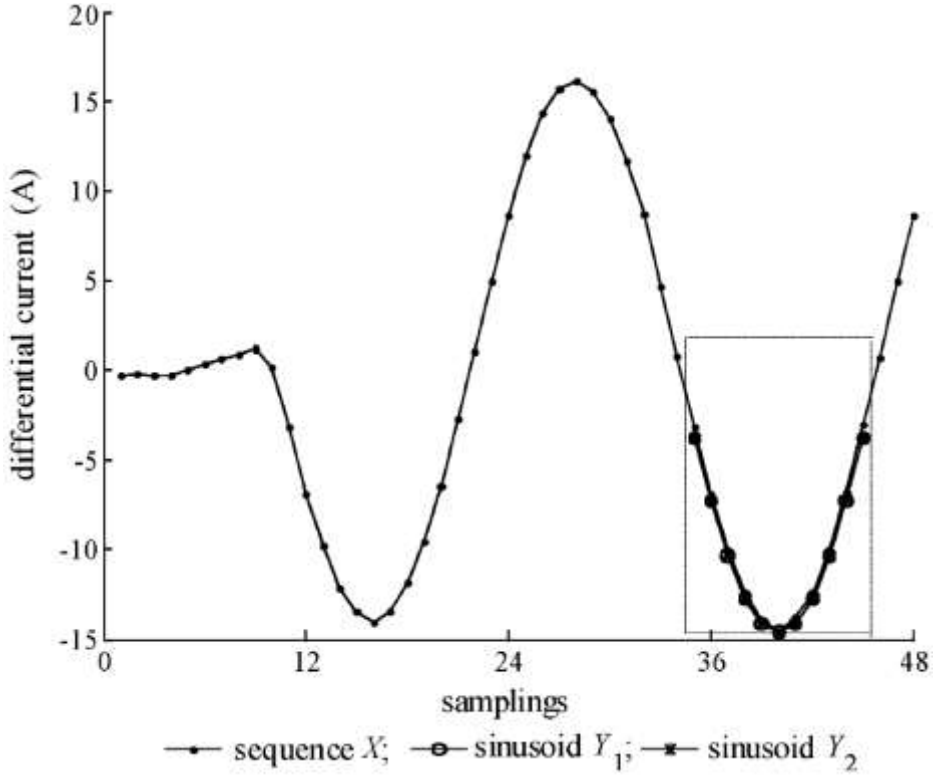

Fig 3-10 Internal fault case [80]

The algorithm then finds out the similarity between the original samples sequence x and the two constructed signals y_1 and y_2 by calculating the cross-correlation coefficients *r* between x and both y_1 (r_{xy1}) and y_2 (r_{xy2}) using the following equation:

$$r_{xy_1} = \frac{\sum_{k=1}^{m}(x(k)-\bar{x})(y_1(k)-\bar{y}_1)}{\sqrt{\sum_{k=1}^{m}(x(k)-\bar{x})^2 - \sum_{k=1}^{m}(y_1(k)-\bar{y}_1)^2}} \quad (3\text{-}19)$$

Where $\bar{x}$ and $\bar{y}_1$ are means of sequences x and y_1 respectively. m is a number of samples per window to be correlated (11 samples was selected), x(k) and $y_1(k)$ are sampled current values at instant k for original and constructed signals respectively. Similarly, r_{xy2} can be obtained by setting y_2 in place of y_1 in equation (3-19). There are two criteria to choose *r***:**

Criterion 1: $r = \min(|r_{xy1}|, |r_{xy2}|)$

Criterion 2: $r = (|r_{xy1}| + |r_{xy2}|) / 2$

Comparison between criterion 1 and 2 using a large number of experimental results, verified that criterion 2 obtained a good compromise between stability and speed. Accordingliy, criterion 2 was chosen and also, setting of threshold r_{set} to 0.8 showed a good performance. If $r \geq r_{set}$ means that the case is internal fault, so the differential protection relay operates. Otherwise, it means that it is inrush current, so the differential protection relay should be blocked.

The disadvantage of this method is that it depends on the information of non-saturation zone or dead angle. However, when a high inrush current occurs, the current transformer (CT) produces a distorted current on its secondary winding called a reverse current or reverse charge of CT, which causes the dead angle to disappear from the inrush current waveform [55, 62, 67]. In addition, it needs the information of the whole cycle, which means that it takes a long time to detect the fault.

3.7.2. Artificial neural network ANN

Recently, the methods of artificial intelligence have been widely used for the protection of power systems as the pattern can be learned. Artificial neural networks (ANNs) are the most common implementation of artificial intelligence. Since ANN has largely been used in fields such as pattern recognition, image processing and power quality analysis, it can be used for transformer protection. Hence, some works in [81-88] have checked the feasibility of applying such a technique while others have used further principles in combination with ANN such as the following two methods. In [89], a method was introduced for detecting winding faults was based on ANN using principle component analysis (PCA). In [90], the scheme used ANN as a pattern classifier whilst the inputs of ANN were the symmetrical components of current waveform. However, the main drawbacks of ANNs are that the parameters of neural networks cannot be set by accurate rules, and the process of pattern learning takes a very long time. In addition, the topology is most likely to be changed in real large power systems. These changes will not be reflected in the huge number of neural networks, which represent the power system. The real problem is that the neural networks cannot be used to protect different power systems, i.e. if it is designed to protect a specific power system, this design cannot be used to protect another one. Furthermore, when the ANN method is used for detecting the turn-turn fault, data of a large number of fault cases are required to train the neurons. This requires more computation and large memory, and hence the method requires a large number of instruments and processors.

3.7.3. Fuzzy logic

Fuzzy logic which is also an application of artificial intelligence was used for transformer protection. Wiszniewski and Kasztenny [91] proposed a scheme to distinguish the internal fault from inrush and external fault. The scheme uses 14 different criteria based on Fuzzy sets to make decision whether there is internal fault or not. M.C. Shin et al. [92] proposed an algorithm using Fuzzy logic principle to increase the fault detection sensitivity of the relays that were designed based on traditional approaches such as harmonic restraint. However, disadvantage of

methods based on ANN and Fuzzy logic is that the design of neural networks or Fuzzy laws is needed. So, different cases will be simulated in order to produce a large number of learning pattern that is required to this design. The primary Fuzzy systems are not able to deal with the noise or any distorted input. Also, it is difficult and not easy to be adapted in protection system. In addition, the decision on any case is accessed after searching through a huge number of rules, therefore from transformer protection point of view, the Fuzzy system can be considered slow technique compared with other protection systems.

3.7.4. Wavelet transform WT

Wavelet transform (WT) is also used for discrimination between internal faults and other disturbances such as inrush conditions and external faults. Transformer protection methods based on this approach are suggested in [93-102]. Also, there are methods based on combining ANN and WT such as the methods in [103-105].

WT is a mathematical mean used for analyzing a signal when its frequency varies with respect to time. It is an extension of Fourier analysis and is applied in order to extract the most important feature of the signal by decomposing it to low and high frequency band over iterative execution. But the coefficients of wavelet in this frequency band will not only be affected by specific harmonics and fundamentals of the desired signal, but also by other signals in the same frequency band. In addition, the coefficients of WT are severely influenced by noise when they are in high-level details. So, the features of the signal that are extracted by WT are not reliable in the case that there is noise around the signal. Besides its sensitivity to noise and unexpected disturbance, it needs a long data window. However, in some methods such as in [102, 105], wavelet transform needs at least ¼ cycle of the current waveform (5ms in system of 50 Hz) following the instant of the fault in cases of internal and external faults, then the decision of the algorithm can be built using software techniques based on data obtained by several trial and error processes.

3.8. Other methods

K. Yabe [106] proposed a new method based on the calculation of active power or average power at two sides of the transformer. Accordingly, the average power which can be calculated by the sum of power flowing in and out of transformer is very small in normal operation and energization. While large power is consumed during internal fault. So it can be used to discriminate between inrush current and internal fault. However, the average power during inrush is also high at the first cycle and then will be low. A threshold value is set to be compared with the calculated average power value within one period of time (20ms in system of 50Hz). If the average power exceeds the threshold means that is an internal fault has occurred, otherwise the case is either inrush or normal operation. The selection of the threshold depends on how power is consumed during inrush. The scheme started from the second period as the power consumption is high during the first period of inrush. In addition to one cycle delay, using both current and voltage signals in this scheme increases complexity and cost.

Sidhu and Sachdev [12] proposed an algorithm uses a transformer model and the modal transformation which converts instantaneous voltage of phases A, B and C to be represented as modal voltages. Using this transformation, three equations represent modal components of voltage as a function of modal components of current, can be obtained. The voltage drop at each phase is computed using these equations and then compared with measured voltage drop. If the difference between calculated and measured voltage drops exceeds the pre-specified threshold value, it means that is internal fault case, otherwise, the case is normal, inrush or external fault. Also, this algorithm uses two signals voltages and currents, i.e. more complexity and more cost. In addition, time of 10-20ms is needed to detect the fault according to the type of fault and how sever it is.

He et al. [107] presented a new scheme to distinguish internal faults from other normal conditions such as inrush depending on error estimation. It utilizes the dead angle feature that only exists in the inrush current. The differential current is extracted from dead angle, and then two estimation errors are determined by

estimating this current under two different frequencies. The difference between two estimation errors decides whether the case is inrush or internal fault. The algorithm takes long time as 18 ms for the width of data observation window in which 10 ms is aimed to obtain the estimation error. Also, it is unsatisfactory scheme as it depends on the dead angle feature which may be disappeared as mentioned in 3.5.2.

Mahmoud et al. [108] proposed a new technique for distinguishing external fault from internal fault. It is based on transient current components of three phases that extracted from both primary and secondary sides of transformer. These components are converted to modal transient components by using Clark's transformation matrix, and then an equation of fault detection is derived as a function of new transient modal components. The output sign of this equation is considered a detector. It is negative for internal fault and positive for external fault. However, the method takes more than one cycle to identify the case.

Eissa et al. [109, 110] proposed a technique based on positive sequence of admittances to distinguish between cases of internal fault and external fault as well as inrush condition. The positive sequence admittance is computed by dividing the positive sequence current over positive sequence voltage. The instantaneous voltages and currents are measured at both sides of transformer, and then, the instantaneous admittances in primary and secondary sides are computed at each samples of voltage and current are taken. Afterwards, the instantaneous admittance values are accumulated sample after sample until one cycle finishes. It results in two accumulated values of positive sequence admittance, one for primary side and one for secondary side. According to location of the contour of these accumulated values, the algorithm decides which one of the cases is. While Sidhu et al. [111] proposed a technique was a slightly different from previous one. It is based on the positive and negative sequence of impedance which is calculated by division of the measured voltage and current values every one cycle. Firstly the fault occurrence is detected by comparing window of 25 samples of voltage and current in one cycle with the previous one and then the difference is checked with threshold value. If it is met, the voltage and current sequences are computed and also compared with a threshold and then used to calculate the positive and negative impedance. Two trip-counters for

positive and negative sequence impedances are incremented or decremented by one if the calculated impedance is located in a proper quadrant. The algorithm will then decide that the case is internal fault if both trip-counters reach the negative value of a threshold, while it will be considered external fault if one of the trip-counters reaches the positive value of the threshold. In addition to the long delay in detecting faults of the former two techniques, they have to find a way to overcome the problem of error in calculating those results when numerator of equations that calculate the admittance or impedance divided by zero.

Babiy et al. [112] presented a new method to be used for discrimination between internal and external faults. It depends on negative sequence currents. The idea is that when external fault occurs, the negative sequence current enters the transformer from the faulty side while negative sequence current on the other side leaves the transformer, i.e. they are in opposite direction which means that the phase shift between them is 180^{o}. But in case of internal fault, both negative sequence currents leave the transformer, i.e. they are in the same direction which means the phase shift between them is zero. Hence the algorithm was built to discriminate between external and internal faults. However, the algorithm cannot detect faults in less than one cycle.

3.9. Summary

Based on what was mentioned in details about the methods that were used in transformer protection, their main disadvantages can be summarized as follows:

1. The use of harmonics to restrain or block the relay

The ratio of harmonic contents in the inrush current is changeable and cannot exactly be specified as it is influenced by so many factors. The second harmonic based methods are unable to detect small faults such as interturn fault. Also, power transformers having their cores built using amorphous materials which produce low second harmonic components of around 7% during the inrush condition. Consequently, the second harmonic restraint might not be the best candidate in preventing differential relays from false tripping. Furthermore, current transformers

may be saturated during internal faults and this will lead to a significant amount of the second harmonic being generated. This will confuse the second harmonic based method in deciding whether this high ratio is from inrush current or internal fault. In addition, the information of current signal that are needed by harmonic based methods are no less than one cycle.

2. Use of wave shape recognition

The reverse charge of current transformer will make the dead angle to disappear, so the schemes that depend on the dead angle will no longer work. In addition, the operation time of this approach is long and takes about one cycle and a half in some fault cases.

3. Use of transformer electro-magnetic equations

The methods need all transformers' winding currents for decision making, so it is necessary to be measured in all windings. However, these currents are difficult to measure when transformer is connected in Delta in which the terminals of transformer usually are not taken out of the tank. Either the parameters of equivalent circuits or data of B-H curve are also needed. However, sometimes these requirements are unavailable and it is difficult to be experimentally obtained. The difficulty will be more when the transformer is loaded at the time of inrush occurrence.

4. Use of Pattern recognition

- **Correlation technique**

The disadvantages of these methods are that they depend on the information of non-saturation zone or dead angle and need the information of the whole cycle, which means that they take a long time to detect the fault.

- **Artificial neural network ANN**

The main drawbacks of ANNs are that the parameters of neural networks cannot be set by accurate rules, and the process of pattern learning takes a very long time. In

addition, it is not general protection scheme, i.e. it is designed to protect a specific power system, and this design cannot be used to protect another one. Furthermore, when the ANN method is used for detecting the turn-turn fault, data of a large number of fault cases are required to train the neurons. This requires more computation and large memory, and hence the method requires a large number of instruments and processors.

- **Fuzzy logic**

Disadvantage of methods based on Fuzzy logic is that the design requires Fuzzy laws. So, different cases will be simulated in order to produce a large number of learning patterns. The primary Fuzzy systems are not able to deal with the noise or any distorted input. Also, it is difficult and not easy to be adapted in protection system. In addition, the decision on any case is accessed after searching through a huge number of rules, therefore from transformer protection point of view, the Fuzzy system can be considered a slow technique compared with other protection systems.

- **Wavelet transform WT**

The coefficients of wavelet in a frequency band will not only be affected by specific harmonics and fundamentals of the desired signal, but also by other signals in the same frequency band. In addition, these coefficients are severely influenced by noise when they are in high-level details. So, the features of the signal that are extracted by WT are not reliable in the case when there is noise around the signal.

Considering the aforementioned shortcomings of the methods that were used in transformer protections, this research is aimed to address these disadvantages by presenting methods that are simple in algorithm design, do not need much computations, need a current signal only, need a current information window, which takes no more than half a cycle time and are not affected by current transformer saturation problem.

CHAPTER 4

Proposed Methods for Transformer Protection

4.1. Correlation coefficient concept

In modern digital protection systems, a correlation technique has recently been used for study and analysis. The technique is developed for fault detection, classification and condition discrimination.

The correlation coefficient which is usually denoted by *r* is a number measuring the degree to which two variables are linearly related. It is a measure of the strength of the linear relationship between two variables. The linear correlation coefficient is referred to as the Pearson product-moment correlation coefficient in honor of the person who developed it: Karl Pearson [113]. The Pearson correlation coefficient *r* between two variables x and y is defined as the covariance of the two variables divided by the product of their standard deviations and can be calculated by

$$r_{x,y} = \frac{\mathrm{Cov}(x, y)}{\sigma_x \, \sigma_y} \tag{4-1}$$

Where, $\mathrm{Cov}(x, y)$ is covariance of x and y. σ_x and σ_y are standard deviation of x and y respectively.

r is a dimensionless quantity and doesn't depend on the units used and its value only ranges from -1 to +1 i.e. $-1 \leq r \leq +1$.

The value of *r* within this range can be interpreted by the following guidelines:

1. 0 means that the relationship between two variables is not linear
2. +1 means that the relationship is perfect positive linear, i.e. both variables simultaneously increase or decrease in their values
3. -1 means that the relationship is perfect negative linear, i.e. one variable values increase whereas the other variable values decrease or vice versa
4. $0 < r \leq 0.3$ and $0 > r \geq -0.3$ indicate that the relationship is a weak positive and negative linear respectively
5. $0.3 < r \leq 0.7$ and $-0.3 > r \geq -0.7$ indicate that the relationship is moderate positive and negative linear respectively
6. $0.7 < r < 1$ and $-0.7 > r > -1$ indicate that the relationship is strong positive and negative linear respectively

The correlation coefficient requires that the two variables under consideration are fundamentally linearly related. The correlation coefficient provides a reliable measure for linear relationship strength if the relationship between the two variables is known to be linear or the observed pattern between them seems to be linear.

Correlation coefficient is zero when the variables are independent but it is not vice versa because Pearson's correlation coefficient only detects the linear dependencies between the variables to be correlated, e.g. supposing a random variable x is related to another variable y where $y=x^2$. Then values of y completely depend on x i.e. x and y are perfectly dependent, but they are uncorrelated, i.e. the correlation coefficient between them is zero.

The correlation coefficient contains much useful knowledge such as:

- The Correlation coefficient *r* measures the degree and direction (sign) of the correlation between any two variables
- The squared correlation coefficient r^2 defines the proportion of covariation between these variables
- The Correlation coefficient is the cosine of the angle between the two variables as vectors of mean-deviation data. Positive correlation means an acute angle, negative correlation means an obtuse angle. Uncorrelated means orthogonal.

Since the correlation coefficient value is dimensionless quantity, it does not affect the scales or units of measurement when they are calculated for similar or non-similar signals. Therefore, the correlation coefficient is powerful expression compared to graphical depiction in determining the strength of the association between two variables.

4.1.1. Calculation of correlation coefficient r

Given series of n measurements (samples) of x and y written as (x_1, y_1), (x_2, y_2)….. (x_n, y_n), Pearson's correlation coefficient *r* between x and y can be estimated by rewriting equation (4-1) [114] as

$$r = \frac{\sum_{k=1}^{n} x_k y_k - n\,\bar{x}\,\bar{y}}{(n-1)\sigma_x\,\sigma_y} \tag{4-2}$$

Where, n is a number of samples used to be correlated during a certain time interval. x_k are values of sampled signal x at instant k and y_k are values of sampled signal y at instant k.

$\bar{x}$ is mean value of sampled signal x. and $\bar{y}$ is mean value of sampled signal y. they can be calculated as follows

$$\bar{x} = \left(\frac{1}{n}\right)\left(\sum_{k=1}^{n} x_k\right) \tag{4-3}$$

$$\bar{y} = (\frac{1}{n})(\sum_{k=1}^{n} y_k) \tag{4-4}$$

σ_x and σ_y can be calculated as

$$\sigma_x = \sqrt{(\frac{1}{n-1})\sum_{k=1}^{n}(x_k - \bar{x})^2} \tag{4-5}$$

$$\sigma_y = \sqrt{(\frac{1}{n-1})\sum_{k=1}^{n}(y_k - \bar{y})^2} \tag{4-6}$$

Substituting the values of (4-3), (4-4), (4-5), (4-6) in equation (4-2), a new description for *r* is given by

$$r = \frac{\sum_{k=1}^{n} x_k y_k - \frac{1}{n}\sum_{k=1}^{n} x_k \sum_{k=1}^{n} y_k}{\left(\sqrt{\sum_{k=1}^{n}(x_k)^2 - \frac{1}{n}(\sum_{k=1}^{n} x_k)^2}\right) \times \left(\sqrt{\sum_{k=1}^{n}(y_k)^2 - \frac{1}{n}(\sum_{k=1}^{n} y_k)^2}\right)} \tag{4-7}$$

The correlation coefficient is also directly related to the simple linear regression line equation y = a + bx for any two variables, where a is intercept and the slope b can be calculated by

$$b = r\,\frac{\sigma_y}{\sigma_x} \tag{4-8}$$

As the least-squares regression line will always pass through the means of x and y, the regression line may be entirely described by the means, standard deviations, and correlation of the two variables under consideration. The covariance determines whether units of variables increase or decrease and has no upper and lower limits. But it is impossible to measure the degree to which these variables moved together because the covariance does not use one standard unit of measurement, while it is possible to do so using the correlation [113-122].

4.1.2. Determination coefficient, r^2

The squared correlation coefficient r^2 is called the coefficient of determination and it is a key output of regression analysis. r^2 generally measures the degree of linearity between any two variables [119]. r^2 can be described as follows:

a. It indicates the proportion of the variance (fluctuation) in one dependent variable which is predictable from another independent variable

b. It is the ratio of the explained variation to the total variation

c. It is such that $0 < r^2 < 1$, and denotes the strength of the linear association between x and y

d. It represents the percent of data that is being closer to the line of best fit. For example, if $r = 0.922$, then $r^2 = 0.850$, which means that 85% of the total variation in y can be explained by the linear relationship between x and y, while the rest 15% of the total variation in y stays unexplained

4.1.3. Correlation Functions

The theory of correlation is described by two types of correlation functions, auto and cross correlations.

1. Cross-correlation function

The cross-correlation coefficient function is a measure of similarity between two waveform signals as a function of time. It is widely used for signal processing such as applications in pattern recognition. The cross-correlation coefficient can be used to measure the similarity between two signals such as voltage or current signals in transformer that are obtained from two transducers [122]. The signals are simultaneously sampled and divided into windows and each window contains a certain number of samples. Then using equation (4-7), cross-correlation coefficient is computed between window of signal (x) and the opposite window of the other signal (y).

2. Auto-correlation function

The auto-correlation is the cross-correlation of a signal with itself. It is the similarity between observations as a function of the time separation between them (time shift). It is used for finding repetitive patterns.

The auto-correlation coefficient is computed between a window with a certain number of samples n in a signal (x) and another window with the same number of samples in the same signal but shifted from each other by a time interval of hΔt, where h is the number of samples between the two windows and Δt is the sampling interval time [122]. Thus, equation (4-7) can be rewritten for calculating the auto-correlation coefficient as follows

$$r = \frac{\sum_{k=1}^{n} x_k \, x_{k+h\Delta t} - \frac{1}{n}\sum_{k=1}^{n} x_k \sum_{k=1}^{n} x_{k+h\Delta t}}{\left(\sqrt{\sum_{k=1}^{n}(x_k)^2 - \frac{1}{n}(\sum_{k=1}^{n} x_k)^2}\right) \times \left(\sqrt{\sum_{k=1}^{n}(x_{k+h\Delta t})^2 - \frac{1}{n}(\sum_{k=1}^{n} x_{k+h\Delta t})^2}\right)} \quad (4\text{-}9)$$

When there is no time shift i.e. hΔt = 0, the two windows to be correlated in the signal will be the same, so the auto-correlation coefficient between them is 1.

4.2. The proposed method in steady state

The new proposed method is based on the calculation of correlation coefficients. It is suggested to protect the transformer from internal faults while the transformer is in operation i.e. in steady state. It uses the principle of differential protection as it compares between currents entering and leaving the transformer. It is based on correlation coefficients analysis of current signals which are obtained by current transformers (CTs) that are set on both sides of transformer.

The new in the technique is that using auto-correlation coefficient together with cross-correlation coefficient in order to obtain a better fault discrimination and to increase speed in detecting the fault within a very short time. So there are three correlation coefficients, two auto-correlations for primary and secondary current signals and one cross-correlation between primary and secondary current signals.

The values of these coefficients will be compared with threshold values to decide whether there is a fault or not. Fig 4-1 shows the block diagram of the proposed protection scheme applied on single-phase transformer.

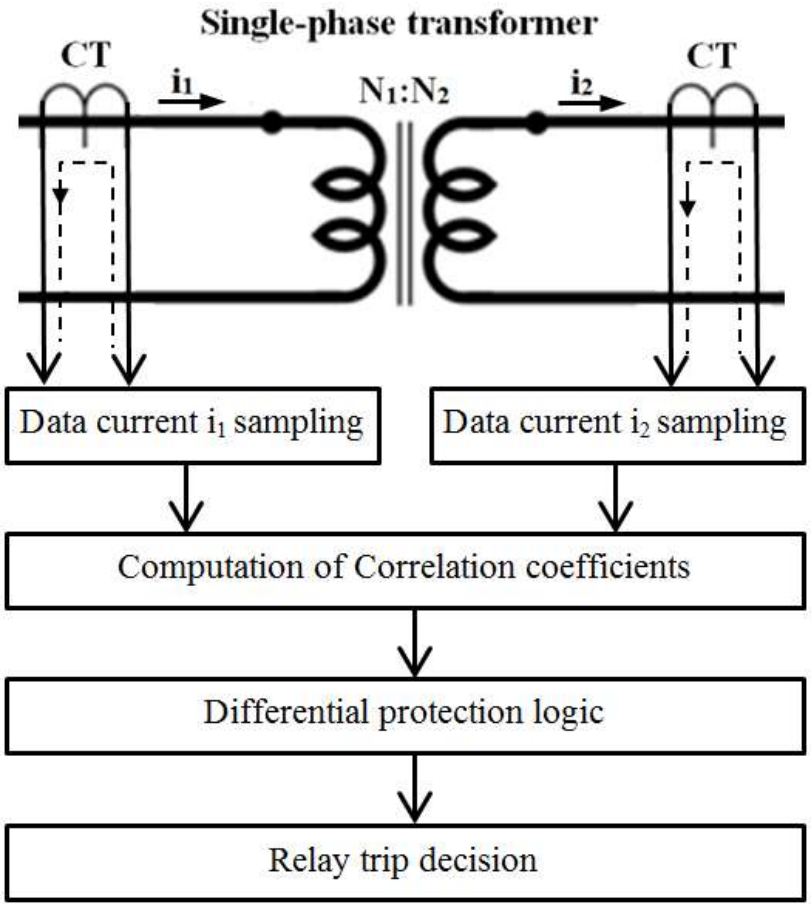

Fig 4-1 Block diagram of the proposed protection scheme

In three-phase transformer, auto/cross-correlation coefficients are estimated for each phase as if it were the single-phase transformer shown above. In phase A, r_{A11} is auto-correlation of input (primary) current i_1, r_{A22} is auto-correlation of output (secondary) current i_2 and r_{A12} is cross-correlation between i_1 and i_2. Using current signals, equation (4-7) can be rearranged to calculate r_{A12} as follows:

$$r_{A12} = \frac{\sum_{k=1}^{m} i_1(k) i_2(k) - \frac{1}{m}\sum_{k=1}^{m} i_1(k) \sum_{k=1}^{m} i_2(k)}{\left(\sqrt{\sum_{k=1}^{m}(i_1(k))^2 - \frac{1}{m}\left(\sum_{k=1}^{m} i_1(k)\right)^2}\right) \times \left(\sqrt{\sum_{k=1}^{m}(i_2(k))^2 - \frac{1}{m}\left(\sum_{k=1}^{m} i_2(k)\right)^2}\right)} \quad (4\text{-}10)$$

Where, r_{A12} is cross-correlation coefficient between primary current i_1 and secondary current i_2 for phase A.

m: number of current samples per window to be correlated.

i_1 (k): sampled current values at instant k on primary side.

i_2 (k): sampled current values at instant k on secondary side.

Equation (4-9) is also rearranged to calculate r_{A11} and r_{A22} such that

$$r_{A11} = \frac{\sum_{k=1}^{m} i_1(k) i_1(k - h\Delta t) - \frac{1}{m}\sum_{k=1}^{m} i_1(k) \sum_{k=1}^{m} i_1(k - h\Delta t)}{\left(\sqrt{\sum_{k=1}^{m}(i_1(k))^2 - \frac{1}{m}\left(\sum_{k=1}^{m} i_1(k)\right)^2}\right) \times \left(\sqrt{\sum_{k=1}^{m}(i_1(k - h\Delta t))^2 - \frac{1}{m}\left(\sum_{k=1}^{m} i_1(k - h\Delta t)\right)^2}\right)} \quad (4\text{-}11)$$

$$r_{A22} = \frac{\sum_{k=1}^{m} i_2(k) i_2(k - h\Delta t) - \frac{1}{m}\sum_{k=1}^{m} i_2(k) \sum_{k=1}^{m} i_2(k - h\Delta t)}{\left(\sqrt{\sum_{k=1}^{m}(i_2(k))^2 - \frac{1}{m}\left(\sum_{k=1}^{m} i_2(k)\right)^2}\right) \times \left(\sqrt{\sum_{k=1}^{m}(i_2(k - h\Delta t))^2 - \frac{1}{m}\left(\sum_{k=1}^{m} i_2(k - h\Delta t)\right)^2}\right)} \quad (4\text{-}12)$$

In the proposed algorithm, the windows in the same signal are shifted from each other by one cycle time, this means window in one cycle is auto correlated with window at the same position in the previous cycle, i.e. the time interval $h\Delta t$ = 20ms in system frequency of 50Hz.

Similarly, r_{B12}, r_{B11} and r_{B22} are calculated for phase B while r_{C12}, r_{C11} and r_{C22} for phase C. So there are three correlation coefficients for detecting faults in each phase of the transformer.

Reliability of the current value measurements and poor sampling are factors that may affect the correlation coefficient. Auto-correlation or cross-correlation detects any disturbance, change, distortion or difference in current signals due to abnormal

condition in power system which causes change to electrical signals in magnitude, frequency, shape, direction or phase shift.

The proposed differential protection scheme based correlation coefficients is used for detecting internal faults occur in the transformer, determining faulty phase and distinguishing internal faults from external ones. The technique depends on the changes in current waveform that occur during the fault.

The features of correlation algorithm can be summarised as follows:

1. Compares pre-fault current signals
2. Acts as a fault detector and faulty phase identifier
3. Sensitive to any fault type
4. Algorithm operation speed can be controlled by selecting the size of correlated window in correlation equations, i.e. to adjust the speed, window may be selected to consist of (2 or 3…..n) samples
5. Control of proposed algorithm sensitivity by selecting auto/cross-correlation coefficient settings and correlated window
6. Independent of the transformer and CT parameters
7. Simple, fast, reliable, accurate and can be implemented practically

The flow chart in Fig 4-2 shows how the proposed differential protection algorithm works. It is applied on both SIMULINK model (simulation) and practical model (built in laboratory) as it will be seen in next chapters. In normal case, coefficient values of cross-correlation r_{12} and both auto-correlation r_{11} and r_{22} on any phase are 1 or very close to 1, but in the case of faults, these values change and will be less than 1. Their values are compared with threshold values to decide whether there is an internal fault occurring in transformer, so a trip signal must be sent to the circuit breaker to switch off the transformer or external fault, so a trip signal must not be issued and the relay must be blocked. The threshold of 0.9 was selected as the best value based on monitoring the change in correlation coefficient values during fault

conditions after a large number of simulations as well as experimental tests for each case of fault were carried out.

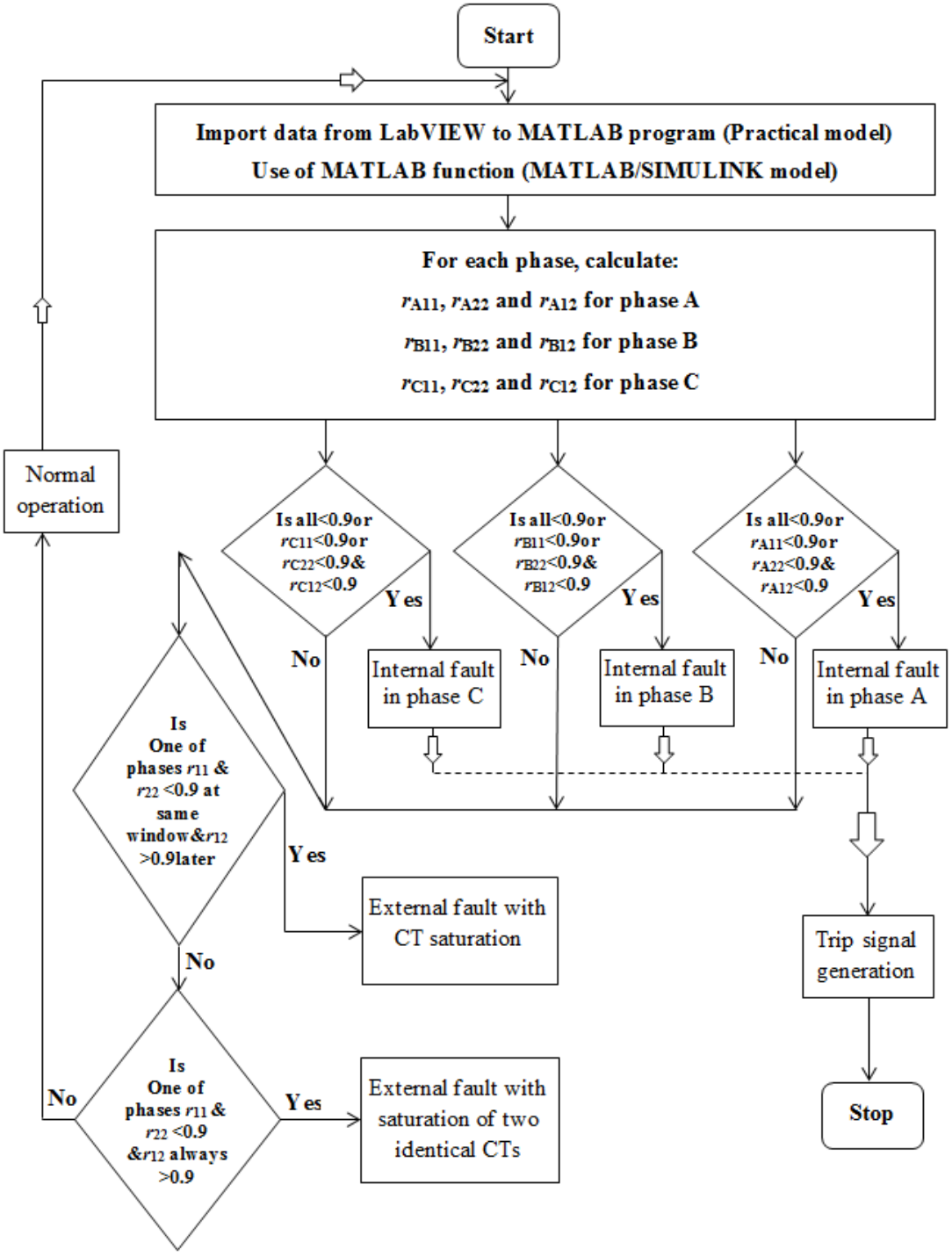

Fig 4-2 Flow chart for the MATLAB algorithm based on Auto/Cross correlation Technique

4.3. The proposed method in transient state

Two techniques for identifying transformer magnetising inrush current are suggested here, current change ratio method (CCR) and percentage area difference method (PAD). The first method is individually used only when the transformer is on no-load condition while both methods are used when the transformer is on-load condition. The methods are suggested to discriminate the inrush current from real internal faults when the transformer is energized i.e. in transient state.

4.3.1. Current Change Ratio method (CCR)

Before going ahead to explain the proposed method that is used for solving inrush phenomenon, it should be known what are the nature, shape and behavior of inrush current waveform. The waveform of internal fault is normally sinusoidal while the typical inrush waveform is not sinusoidal as shown in Figs 4-3-a and 4-3-b.

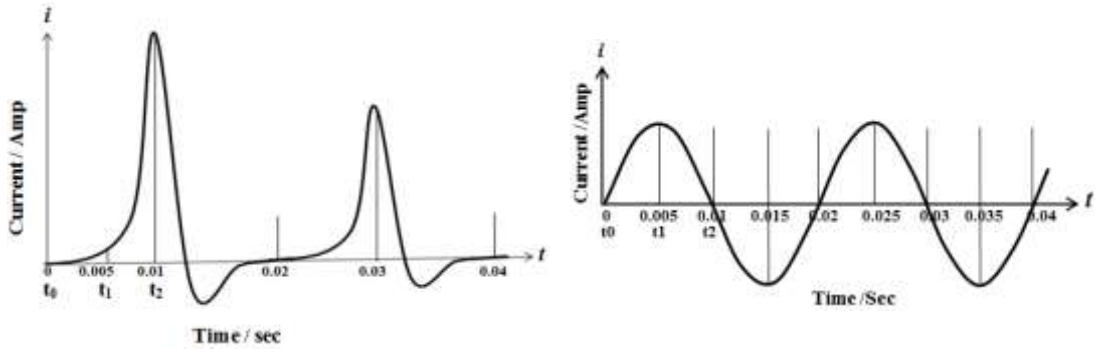

(a) (b)

Fig 4-3 (a) Typical inrush current waveform (b) Typical internal fault current waveform

Based on this difference between the two shapes, a discrimination method can be suggested to distinguish between internal faults and inrush conditions. The idea of this method is based on dividing a half-cycle of the current signal into two halves and then calculates the CCR with respect to time interval between these two halves. For a system with frequency of 50Hz, the half cycle is 0.01 second, and 0.005 second of each half t_0-t_1 and t_1-t_2 as shown in Figs 4-3-a and 4-3-b. The CCR is the

difference between values of currents that corresponds to times t_0 and t_1 divided by the difference between values that corresponds to times t_1 and t_2. The equation can be written as follows:

$$CCR = \frac{i(t_1)-i(t_0)}{i(t_1)-i(t_2)} \quad (4\text{-}13)$$

In the case of internal fault, it can be noticed that this rate is close to 1 or above, because the waveform of the internal fault current is sinusoidal and regularly increases with respect to time, and consequently the difference of current values in the numerator is very close to that in denominator in equation (4-13). But in the case of inrush condition, the rate is always less than 1, because the current in the first half of half cycle is much smaller than the second one as shown in Fig 4-3-a and hence in equation (4-13), the current difference value in numerator is much smaller than that in denominator.

4.3.2. Percentage area difference (PAD)

This method is applied when transformer is loaded as the secondary current is needed to compare with primary current. In simulation tests of transformer models, one of interesting findings was that when the transformer was switched on and before the knee-point on B-H curve i.e. before core saturation begins, the transformer was correctly transformed primary currents to secondary side in this zone. That was also realized in experimental tests. It was found that in inrush condition, the secondary current is very close to primary current (the two currents are almost identical and overlapping) in that zone as the transformer turns ratio was 1. However, if the ratio is not 1, the currents in primary and secondary sides can be equalized by adjusting the turn's ratios of the CTs that are deployed on both sides. While in fault condition, there was a difference in values between those currents. This difference depends on how high the fault current is i.e. the higher the fault current, the bigger difference and vice-versa. In order to avoid further calculations for specifying the saturation point and finding this zone, it was found that it is very good choice to select the first quarter of the current cycle as the required zone because it is very close to the zone before core saturation and shows good results as

well. So the area under the curve of the current signal in the zone is calculated for both primary and secondary currents of each phase. Then the PAD between area on primary (ARP) and area on secondary (ARS) in the zone is calculated by

$$\text{PAD} = \frac{\text{ARP}-\text{ARS}}{\text{ARP}} \times 100\ \% \tag{4-14}$$

In the zone, the PAD is low in inrush or normal conditions, while it is high in case of internal fault. This indicator is used in first quarter of the cycles to distinguish between internal fault and inrush. If PAD is low then signal checking is continued to the half cycle to calculate the current change ratio to make sure that is inrush condition. It can also be noted during inrush condition that the lower or upper peak of the second half of the primary current cycle is always equal to corresponding peak in the secondary current cycle when inrush is low or faded out while it is lower than the corresponding peak in the secondary current cycle if the first half inrush current cycle is negatively high and vice versa. But in the case there is an internal fault on primary side, the second half peak of primary current cycle is greater than the second half peak of secondary current cycle if the first half cycle is negative and vice versa. This is because that in non-saturation zone (dead angle), the fault current signal which is submerged to inrush will be appeared. So, in last quarter of cycles, PAD during inrush may be high but in negative ratio because the ARS is greater than ARP while PAD is always positive high ratio during the fault as ARP is greater than ARS. This can be used as another indicator if the fault occurs in the second half of the cycle.

The flow chart in Fig 4-4 shows how the MATLAB algorithm of the proposed method works. This algorithm was applied on both SIMULINK model and practical model as it will be seen in next chapters.

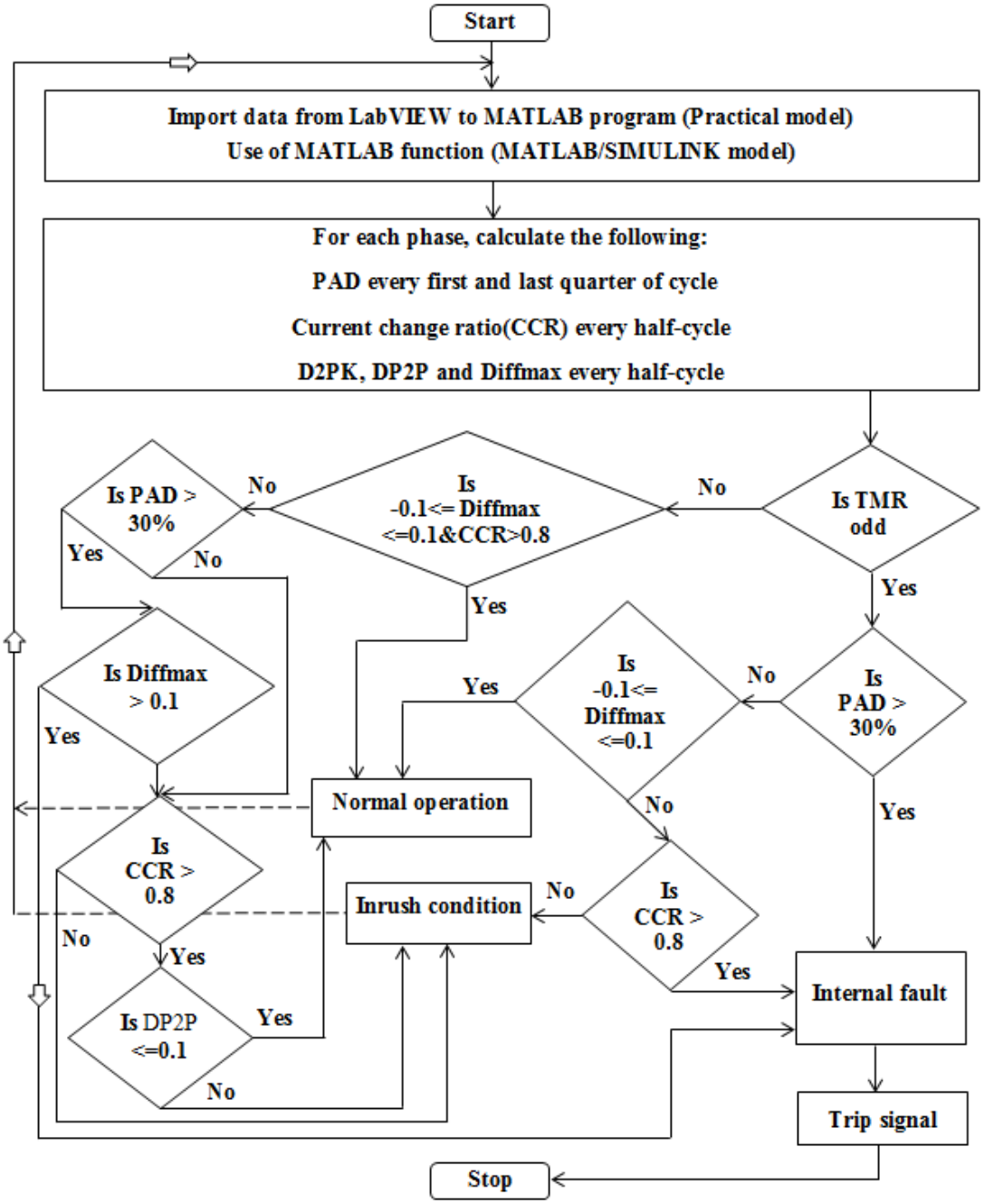

Fig 4-4 Flow chart for the MATLAB algorithm based on PAD and CCR

The percentage area difference is calculated using equation (4-14). Difference between two successive positive and negative peaks of cycles (D2PK), difference between upper & lower peaks of one cycle (DP2P) are also computed to show the

status of operation. Difference between primary and secondary peaks in every half-cycle (Diffmax) is also computed to be used as an additional indicator that supports in discrimination between normal operation and other conditions. PAD is computed every first and last quarter of cycle as they are the most important zones that should be targeted in the cycle. The idea of current change ratio (CCR) is also applied when the transformer at on-load condition. This means that both CCR and PAD are used together in this case.

After calculating the required quantities, the timer of the loop (TMR) counts every half-cycle starting with number 1 for the first half-cycle and so on. TMR is checked whether it is odd or even. If TMR is odd, it means that it is a first quarter of cycle, so PAD is checked and compared with threshold of PAD which was selected as 30% after carrying out so many simulations as well as experimental tests on the proposed algorithm. If PAD is greater than 30%, there is an internal fault has occurred, otherwise, the program continues to half-cycle and checks Diffmax. If its absolute value is equal or less than 0.1(this is ideally zero but 0.1 has been chosen as a margin of error in practical test since it is difficult practically to make primary current equal to secondary current using CTs, so there is always a small difference between them) or -0.1<= Diffmax<=0.1, it means that it is normal operation, if not, CCR is checked. In the case that CCR is greater than 0.8, there is an internal fault, otherwise, it's an inrush condition. However, when TMR is even, it represents the last quarter of the cycle, so steps of execution are followed as shown in the flowchart in Fig 4-4.

4.4. Summary

Three methods were proposed to protect the transformer; the correlation coefficients method was used to detect internal faults that occur in the transformer when it is in steady state operation while the other two methods, current change ratio (CCR) and percentage area difference (PAD) were used to discriminate the inrush current from real internal faults when the transformer is energized.

The novelty in the application of correlation coefficient method was that it uses auto-correlation coefficient together with cross-correlation coefficient in order to

obtain a better fault discrimination and to increase speed in detecting the fault within a very short time. So there were three correlation coefficients for each phase of the transformer, two auto-correlations for primary and secondary current signals and one cross-correlation between primary and secondary current signals. The values of these coefficients were compared with a threshold of 0.9 to decide whether there is a fault or not. The PAD was calculated at first and last quarter of each current cycle and compared to a threshold of 30% to check whether there is internal fault or not. If not, the algorithm continues to check the CCR which was calculated at every half cycle of the current signal and compared to a threshold of 0.8 to recognize the inrush condition.

CHAPTER 5

Transformer Model Simulation and Evaluation of Proposed Protection Techniques

5.1. Introduction

The MATLAB algorithms of proposed protection techniques were tested in order to check their speed and reliability in faults detection, inrush condition discrimination and detection of current transformer saturation. The algorithms were tested on transformer model that was built and simulated in MATLAB/SIMULINK program. The algorithm of correlation technique is applied to detect internal faults as well as CT saturation when the transformer in steady state, while the algorithms of current change ratio CCR and percentage area difference PAD are applied to detect internal faults as well as inrush identification when the transformer is in transient state.

5.2. Transformer model simulation in steady state

Fig 5-1 shows the model that was processed by MATLAB/SIMULINK program. The algorithm was programmed by MATLAB program and set into MATLAB function block of the model in order to process the data that obtained from the 6

current transformers (CT1-CT6) which were connected on both sides of the transformer. The process can be divided into two parts, modelling and simulation.

1. Modelling

The model data, description and transformer core hysteresis curve can be found in the appendix B. The data processing unit consists of data store memory used for sampling the current signal which is taken from CT, subsystem used for delaying the data by one cycle in order to be used to compute auto-correlation coefficients, and MATLAB function block in which the MATLAB code of algorithm is set to compute correlation coefficients during simulation.

2. Simulation

The simulation time for the model was 0.2 second in a system frequency of 50Hz. The sample was taken every 0.0001 second (i.e. sampling rate is 10 kHz) which means that each cycle represented by 200 samples. The samples were divided into windows, each one was selected to contain 20 samples because 200 samples per one cycle makes window to share the tops and bottoms (Peaks) of waveforms, i.e. 10 samples of window on left side before peak value and the remaining 10 samples on the right side after peak value. This arrangement leads to that any change in current will affect the peak values, so it can be easily and quickly detected. Equations (4-10), (4-11) and (4-12) were programmed in MATLAB program to process the consecutive windows for each phase to compute correlation coefficients, cross-correlation coefficients r_{12} between primary and secondary current data of the same phase at the same time, auto-correlation coefficients r_{11} between windows of primary current data for one phase with themselves but shifted by one cycle, i.e. windows of one cycle with windows of previous one and auto-correlation coefficients r_{22} is similar to r_{11} but between windows of secondary current data for the same phase. The computation results which were used to make a decision for any case assessment were obtained every 2 ms (20 samples * 0.0001 sample interval in seconds).

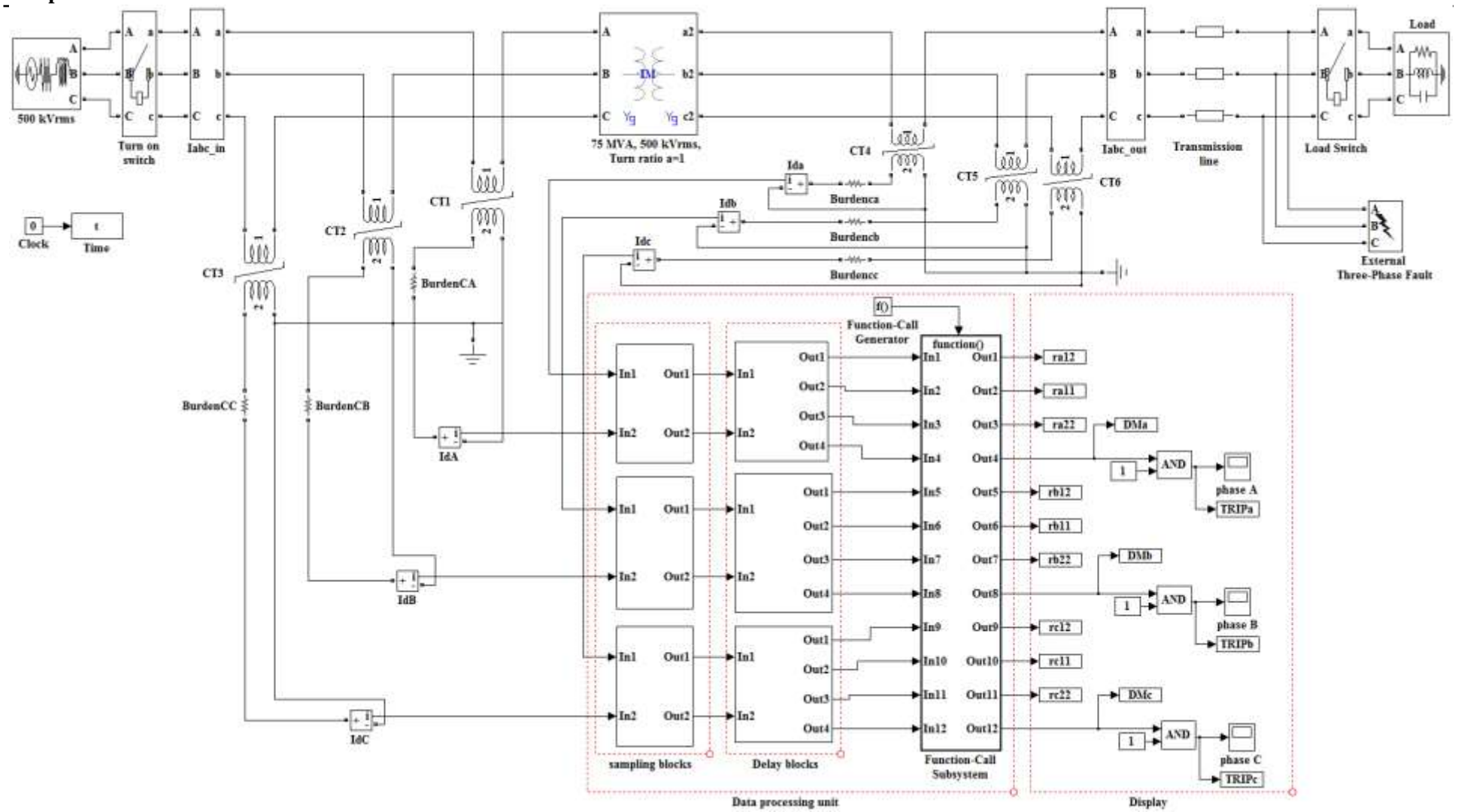

Fig 5-1 System model for the protection technique based on correlation analysis

5.2.1. Faults versus proposed correlation protection algorithm

The efficiency of the proposed algorithm was tested against the following faults. For comparison purposes between faults, all faults were generated at 0.06 second and lasted for 3 cycles by closing specified fault switches in the system model. Since the results were not different between phases as well as primary and secondary sides, only phase A on the secondary side will be shown.

1. Interturn (turn-turn) fault

2% of turns were short-circuited to be represented as a turn-turn fault. The fault was generated on secondary side of phase A. Changes in both primary and secondary currents during the duration of fault are shown in Fig 5-2.

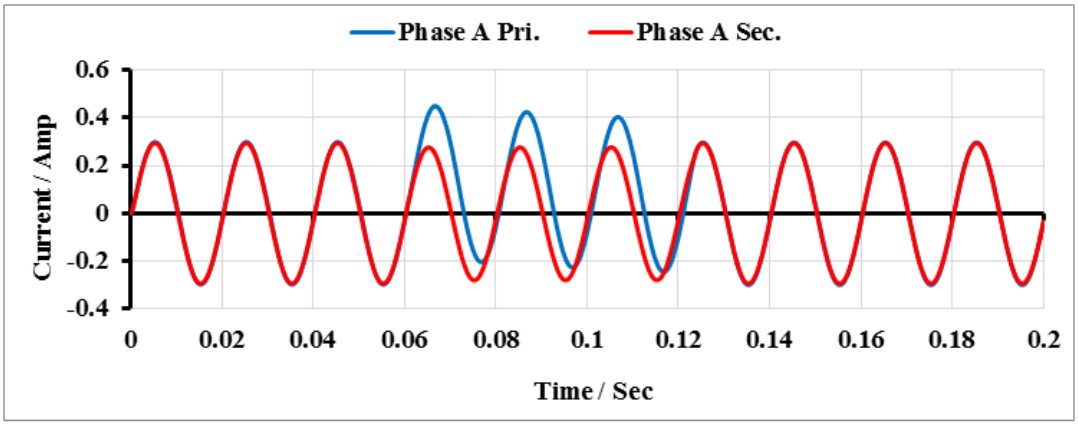

Fig 5-2 Interturn fault on secondary side of phase A

Changes in correlation coefficient values due to this fault can be seen in Fig 5-3. It can be seen that r_{A11} and r_{A12} simultaneously dropped to less than 0.9 at second 0.066 whereas r_{A22} wasn't much affected by the fault. It also can be noted that only cross-correlation r_{A12} started from the first cycle because window of samples in current cycles in both primary and secondary were simultaneously cross-correlated, while the auto-correlation coefficients r_{A11} and r_{A22} started after the first cycle because there was no cycle before zero time to be correlated with the first cycle.

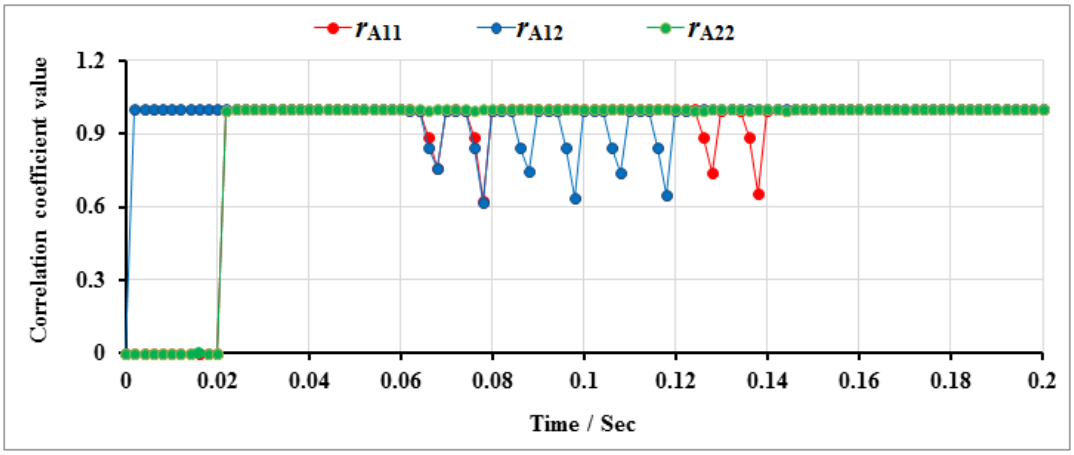

Fig 5-3 Change in correlation coefficients during interturn fault in phase A

According to the algorithm shown in Fig 4-2, the fault was detected at 0.066 second. Since the fault was generated at 0.06 second, it means that the fault was detected after 0.066 - 0.06 = 0.006 second i.e. after 6 ms from incidence of the fault. Trip signal was issued for faulted phase A as shown in Fig 5-4.

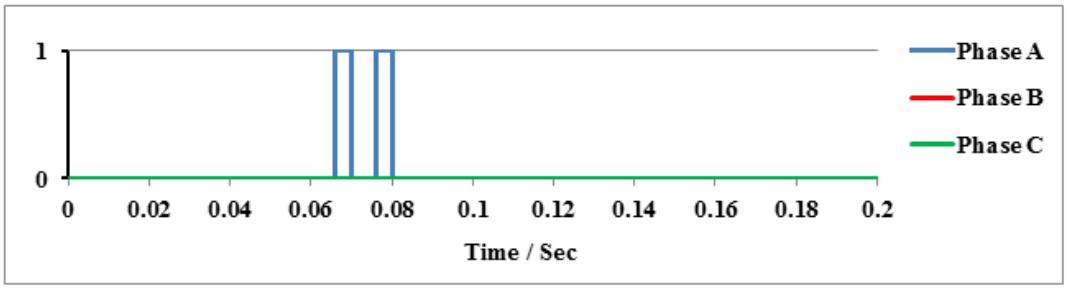

Fig 5-4 Trip signal was issued due to interturn fault in phase A

2. Turn-ground fault

Different turns along the winding of all three phases on both primary and secondary sides were grounded for testing the turn to ground fault at different positions along the winding. Since similar results were obtained, only the mid-turn of phase A on the secondary side is shown. Due to this fault, primary current largely increased as the half voltage of secondary winding was lost and low fault resistance

of 5Ω, while secondary current largely decreased as most of it passed through a low resistance of fault branch rather than through a load as shown in Fig 5-5.

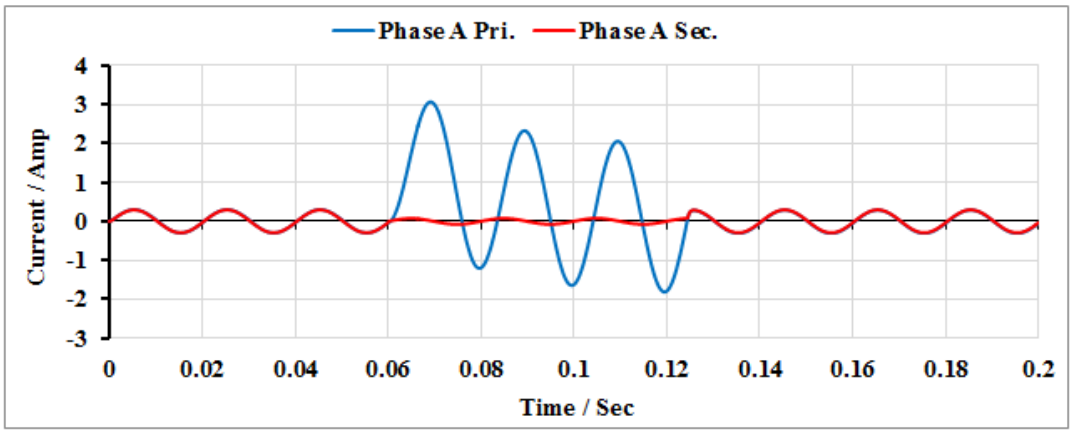

Fig 5-5 Turn-ground fault on secondary side of phase A

The fault causes correlation coefficient values r_{A11}, r_{A22} and r_{A12} to simultaneously drop to less than 0.9 at 0.066 second as shown in Fig 5-6. According to the algorithm, a trip signal was issued at 0.066 second, i.e. after 6 ms of fault occurrence as shown in Fig 5-7.

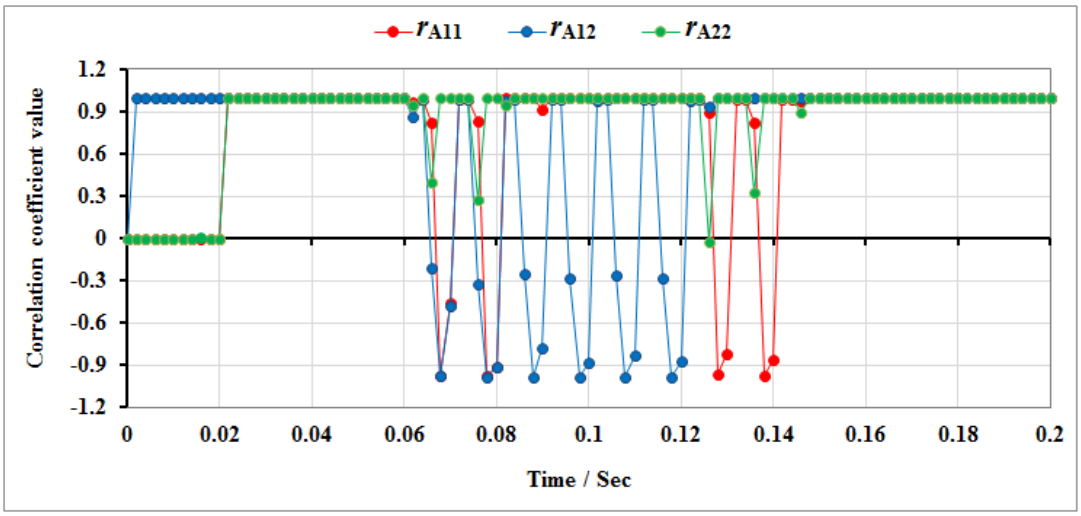

Fig 5-6 Change in correlation coefficients during turn-ground fault in phase A

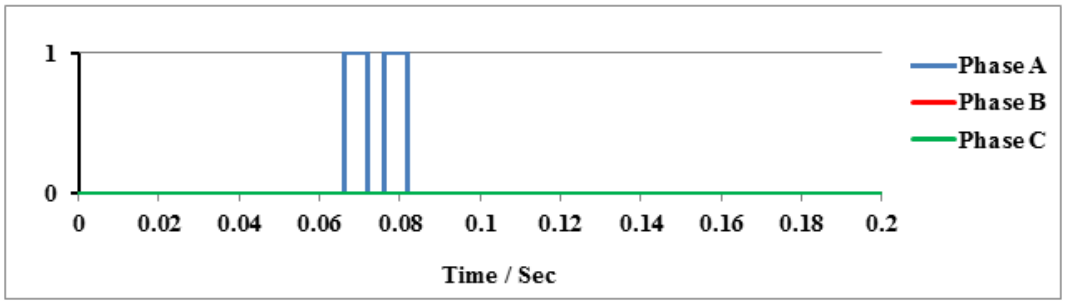

Fig 5-7 Trip signal was issued due to turn-ground fault in phase A

3. Single phase-to-ground fault

The first turn on secondary side of phase A was grounded to generate this fault. As a consequence, this phase was entirely lost. Thus, most of secondary current flowed through the fault branch while almost zero current flowed through the load as shown in Fig 5-8.

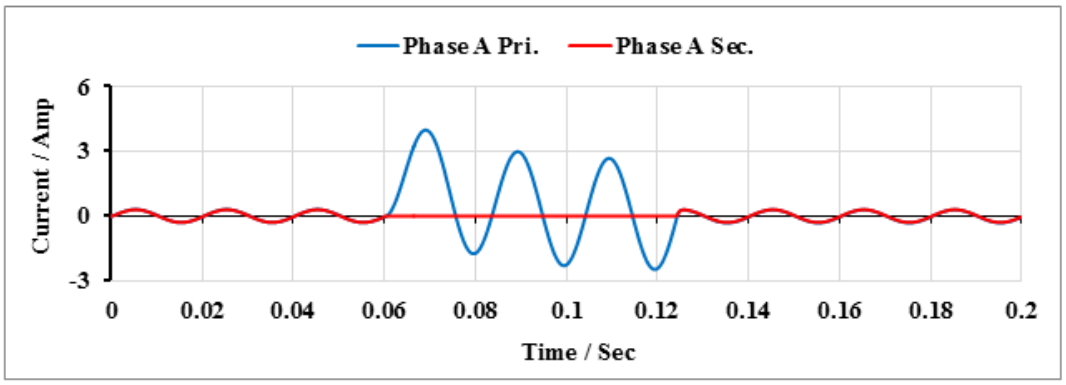

Fig 5-8 Single phase-to-ground fault in phase A

As a result of this fault, correlation coefficient values r_{A22} and r_{A12} simultaneously dropped to less than 0.9 at 0.062 second, while r_{A11} dropped later as shown in Fig 5-9. This is because the secondary current was much more affected by the fault than the primary current.

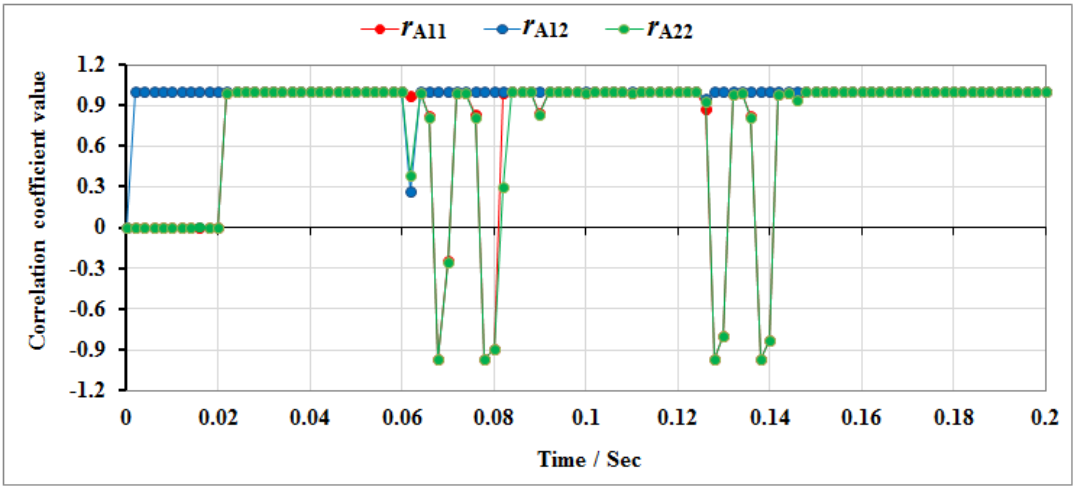

Fig 5-9 Single phase-to-ground fault in phase A

The fault was successfully detected by the algorithm, and accordingly, a trip signal was issued at 0.062 second as shown in Fig 5-10, i.e. after just 2 ms from instant of fault occurrence which means very fast action was taken against the fault.

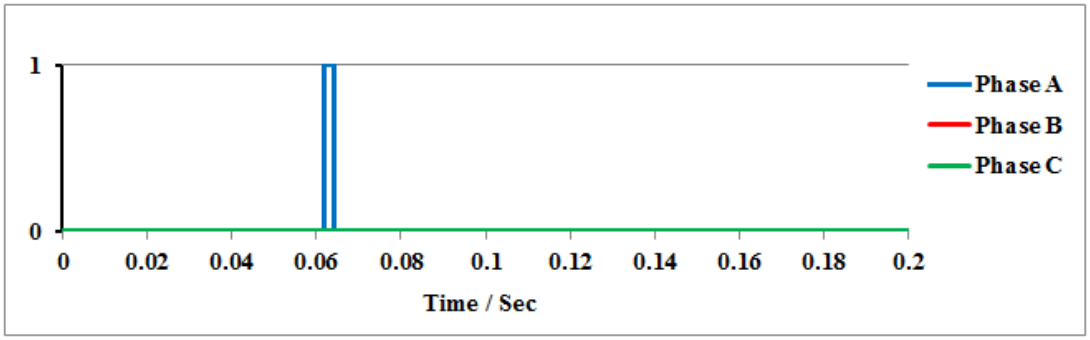

Fig 5-10 Single phase-to-ground fault in phase A

4. Phase-phase fault

Two phases A and B were connected together through a fault resistor (R_f) of 5 Ω in order to generate this type of fault. Because of this fault, primary current of phase A increased in value with same direction of secondary current whereas primary current of phase B increased in value but with opposite direction of secondary current as shown in Figs 5-11-a and 5-11-b.

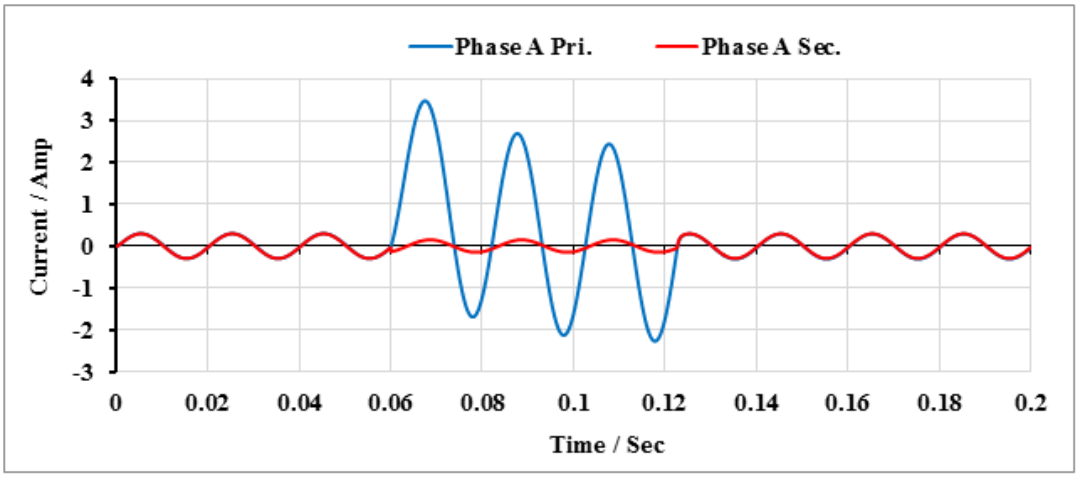

(a)

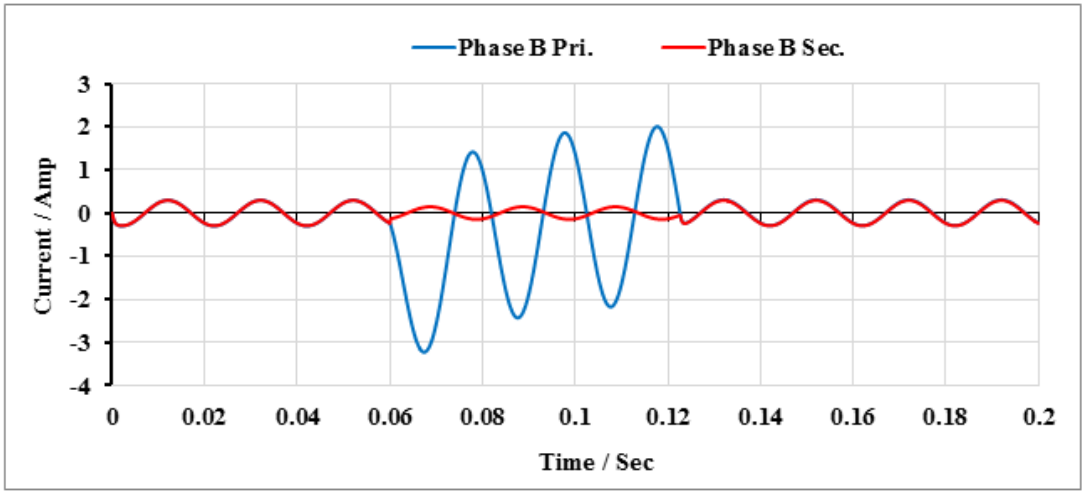

(b)

Fig 5-11 Phase-phase fault between (a) phase A and (b) phase B

The correlation coefficient values for both phases A and B, r_{A22} and r_{A12}, r_{B22} and r_{B12} directly dropped to less than 0.9 in the first windows after incidence of the fault as shown in Figs 5-12 and 5-13. This is because in phase A, the secondary current dramatically decreased while primary current largely increased in same direction. In phase B, the primary current largely increased in same direction while secondary directly dropped before completing its cycle as if it were reversed its direction as shown in Figs 5-11-a and 5-11-b.

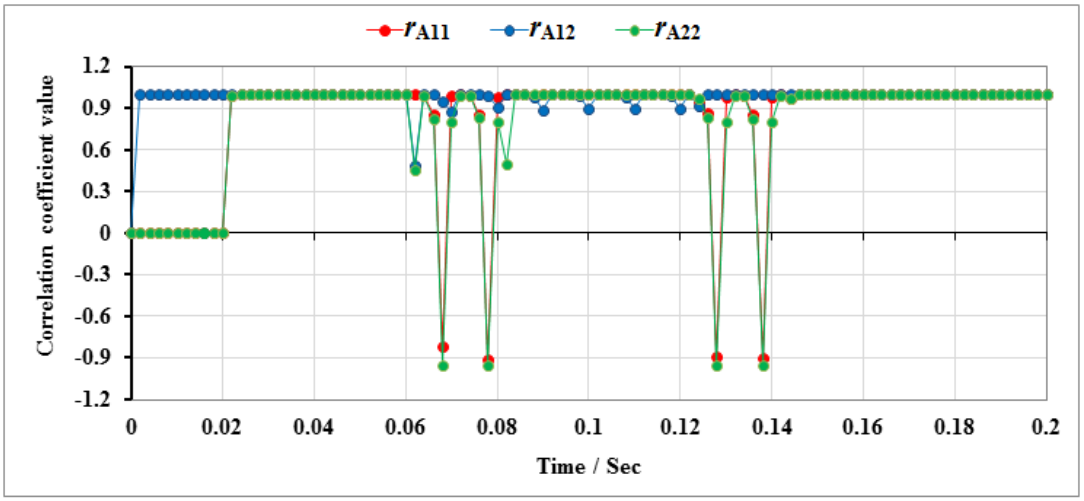

Fig 5-12 Change in correlation coefficients of phase A during phase-phase fault

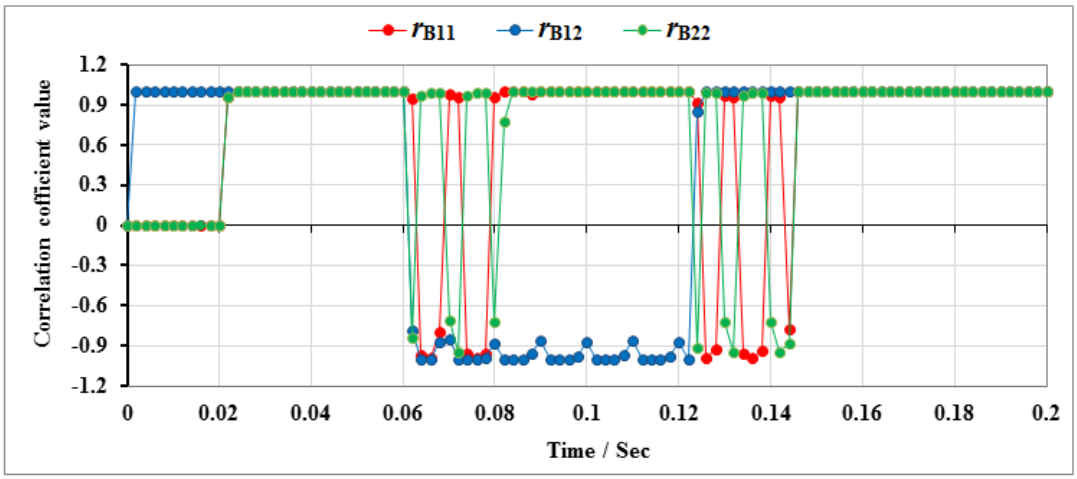

Fig 5-13 Change in correlation coefficients of phase B during phase-phase fault

According to the algorithm shown in Fig 4-2, a trip signal was issued at 0.062 second for phases A and B as shown in Fig 5-14, i.e. this fault was detected after just 2 ms from incidence of the fault. The algorithm was also tested under two fault cases, firstly under double phase to ground fault (Two phases to ground fault) and the result was as same as phase-phase fault, and secondly under both three-phase fault and three-phase-to-ground fault, where the results were as same as phase-phase fault except that trip signals were simultaneously issued for three phases A, B and C.

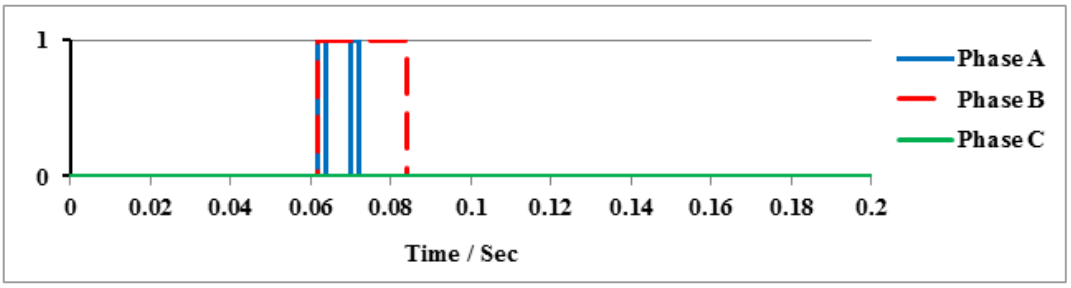

Fig 5-14 Simultaneous trip signals of phases A and B due to phase-phase fault

5. External fault

The external fault switch shown in the Simulink model in Fig 5-1 was closed to generate this type of fault in phase A outside of transformer protected zone. Since the fault occurred in location beyond the connection of CTs, both primary and secondary currents simultaneously increased and their curves overlapped as shown in Fig 5-15.

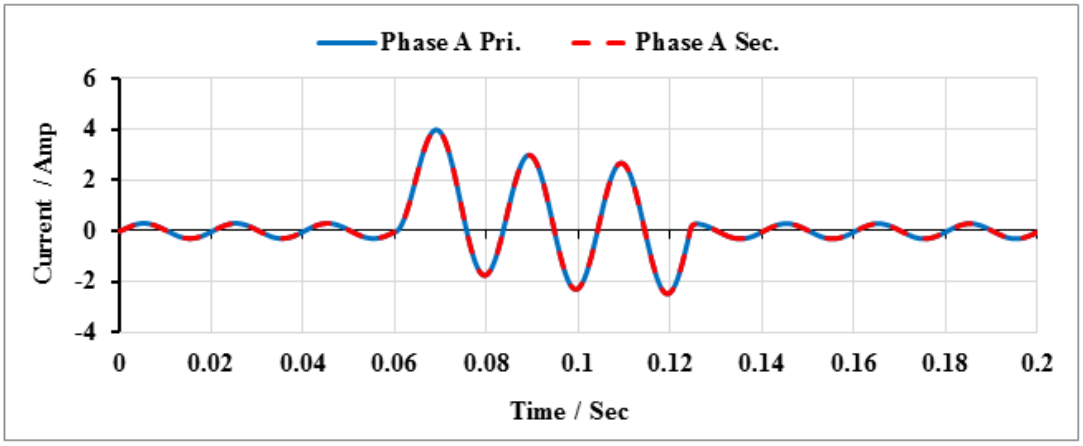

Fig 5-15 Primary and secondary currents during external fault in phase A

Due to this fault, correlation coefficient values r_{A11}, r_{A22} simultaneously dropped to less than 0.9 at 0.066 second while r_{A12} kept above 0.9 within the whole duration of fault as shown in Fig 5-16. This happened because the increase in both primary and secondary currents is the same and they are still identical to each other as shown in Fig 5-15. This demonstrates that r_{A12} was always above 0.9 and very close to 1

which also seen in other tests for this type of fault on the other phases. It was noticed that it happens only in the case of external faults. Thus the algorithm considered it an external fault and there was no trip signal for this case. The algorithm was also tested for other phases, B and C. However, the results were similar to phase A case.

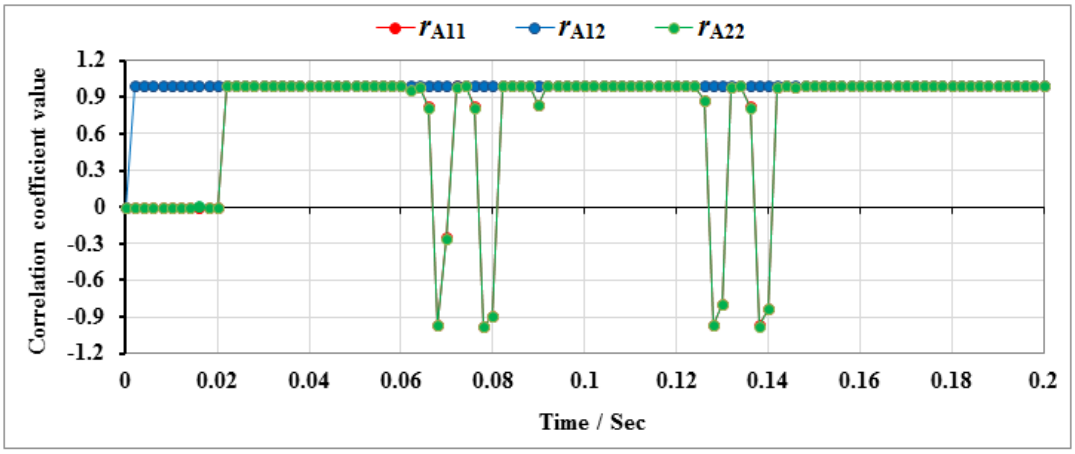

Fig 5-16 Change in correlation coefficients during external fault in phase A

5.2.2. Current Transformer saturation

The action of proposed algorithm was tested on possible cases of CT saturation problem when internal and external faults occur. The system model shown in Fig 5-1 was also used to simulate the CT saturation which is caused by the following faults:-

1. Turn-ground fault with saturation of CT

On the secondary side of phase A, 50% of turns were grounded to generate turn-ground fault. The incidence time and duration of fault are the same as the previous cases. Because of this fault, the primary current increased whereas secondary current decreased (the increase and decrease in currents depend on the intensity of fault). Therefore, the CT1 will most likely to be saturated. In order to make CT1 saturated, its burden was increased from 1Ω to 10Ω, the time to saturation can also be controlled by changing saturation characteristics. To show how this can be implemented, the burden of CT1was fixed to 10Ω, and saturation point was set to 10

pu. Fig 5-17 shows distortion on primary current when CT1 saturated due to the fault and Fig 5-18-a shows the change of flux in CT1 due to the fault.

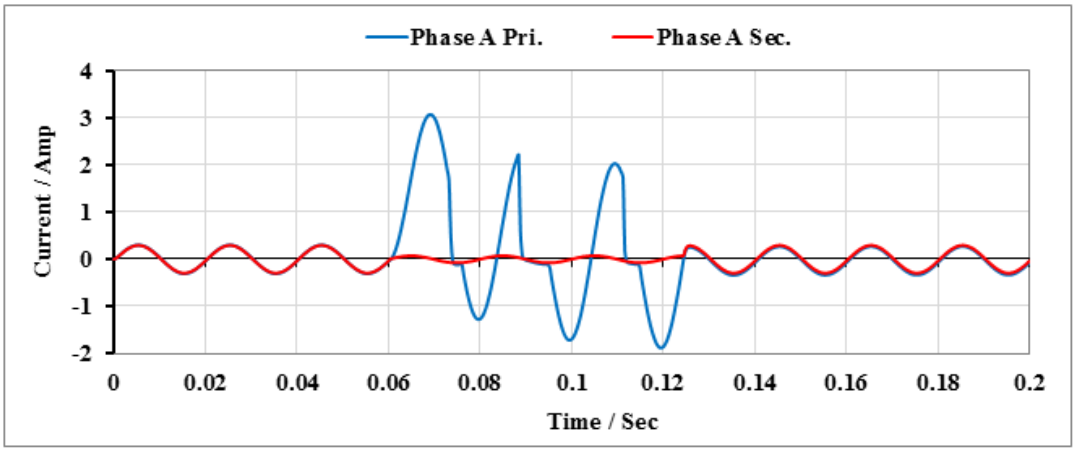

Fig 5-17 Primary current distortion when CT1 saturation point is 10 pu

It can be seen that the flux reached to saturation point at 0.0734 second i.e. after 0.0134 second (0.0734 – 0.06 = 0.0134) from incidence of the fault, since then primary current started to distort. Distortion only occurred during flux peaks that exceeded 10 pu. The flux went down below 10 pu after the fault had cleared at 0.12 second since then the primary current signal got back to normal.

When the saturation point of CT1 changed to 5 pu, the simulation result showed that CT1's flux reached to 5 pu at 0.06865 second i.e. after 0.00865 second (less than half cycle) from incidence of the fault as shown in Fig 5-18-b. Since the time to saturation became shorter, the primary current distorted faster than the previous case where it started to distort at 0.06865 second as shown in Fig 5-19.

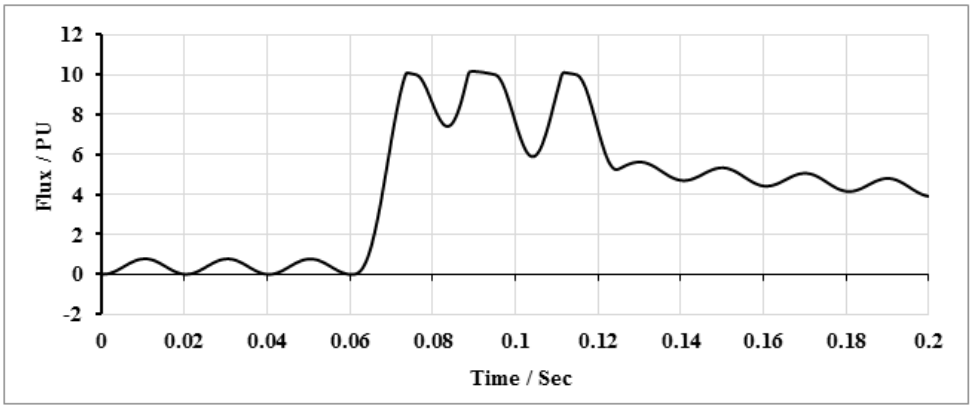

(a)

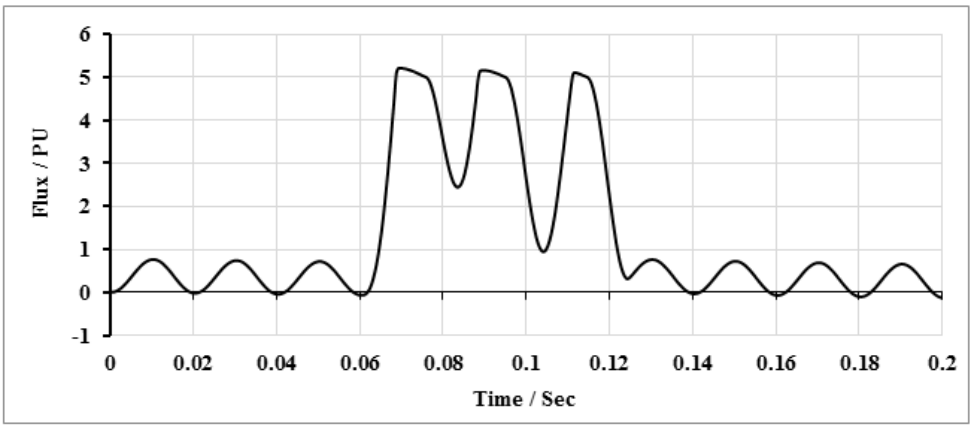

(b)

Fig 5-18 CT1 flux when saturation point is (a) 10 pu and (b) 5 pu

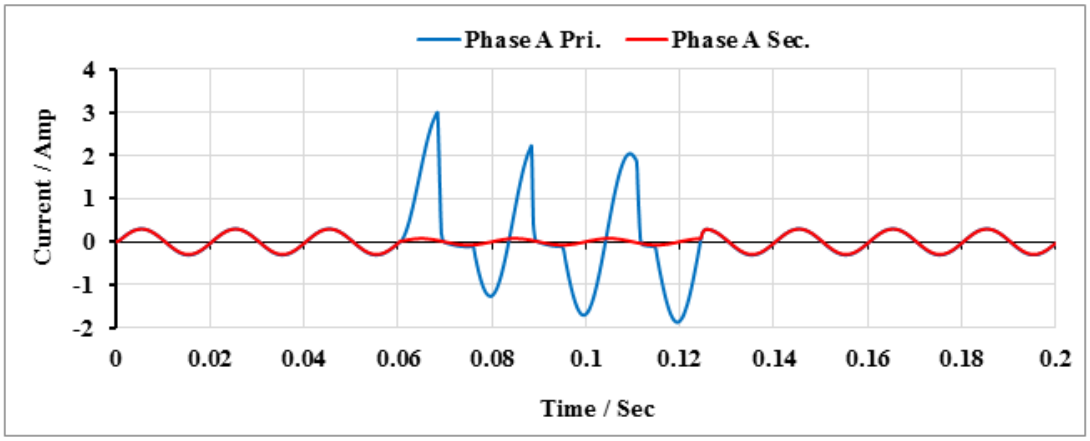

Fig 5-19 Primary current distortion when CT1 saturation point is 5 pu

The simulation result for the CT saturation caused by this fault and the changes in correlation coefficients during the zone of fault are shown in Fig 5-20. It can be seen that all coefficients r_{A11}, r_{A12} and r_{A22} went down to less than 0.9 at 0.066 second due to the fault. This indicates that the fault was detected after 6 ms from the incidence of the fault and before the CT saturation taking place. It can also be noted that the auto-correlation coefficients were still affected by this CT saturation till one more cycle after the fault ended at 0.12 second.

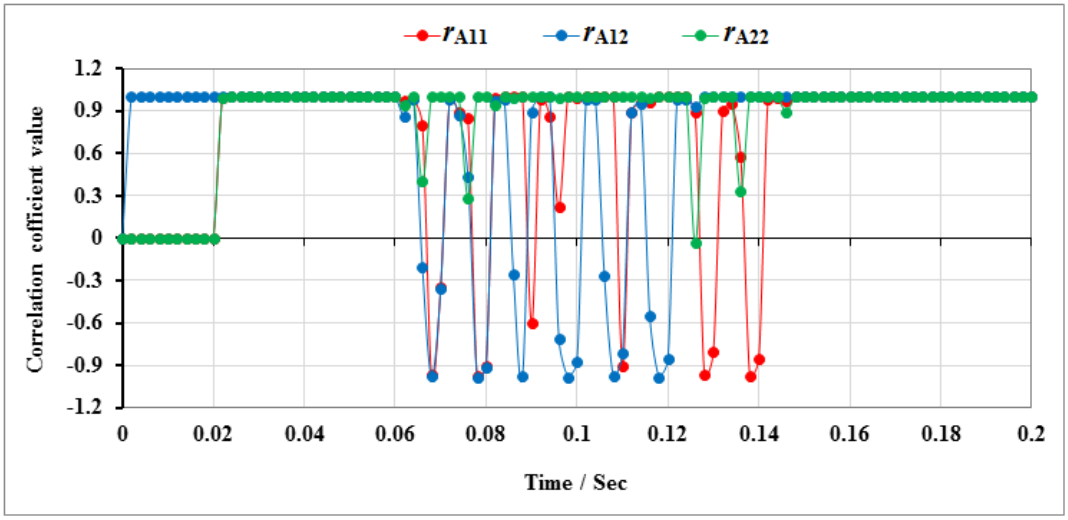

Fig 5-20 Correlation coefficient values when Turn-ground fault occurred in phase A

2. Phase to ground fault with saturation of CT

Phase-to-ground fault was generated as 100% of turns were grounded on the secondary side of phase A, i.e. the voltage in phase A was lost and the secondary current that flows normally through the load was almost zero as most of it flowed through the fault branch via low fault resistance of 5Ω. Due to this fault, CT1 flux reached to saturation point at 0.07084 second when the signal started to distort as shown in Fig 5-21.

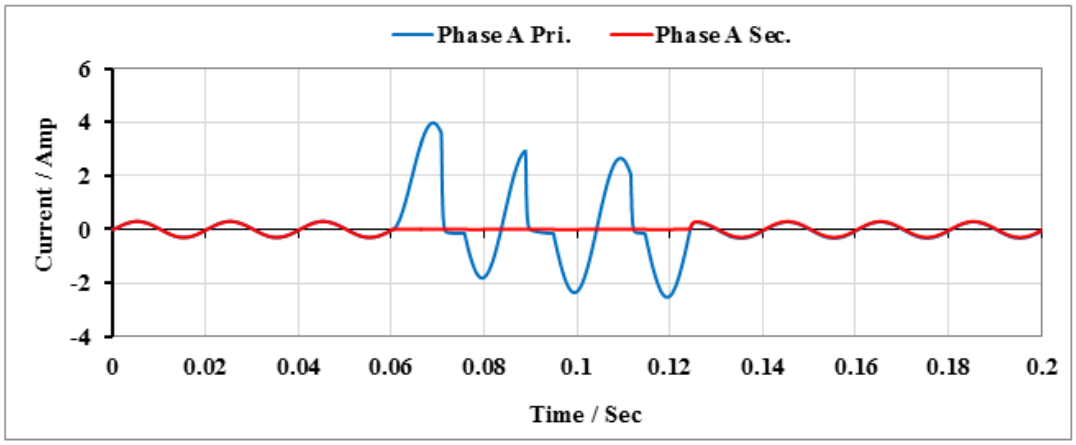

Fig 5-21 Current signals when CT1 saturated due to phase-to-ground fault

The changes in correlation coefficients due to this fault are shown in Fig 5-22. Since the secondary current decreased to approximately zero, correlation coefficients r_{A12} and r_{A22} dropped immediately to less than 0.9 at the first windows after the instant of fault occurrence, specifically at 0.062 second i.e. the fault was detected after just 2 ms from the incidence of the fault. This means that the action of the algorithm against this fault was much faster than the occurrence of CT1 saturation.

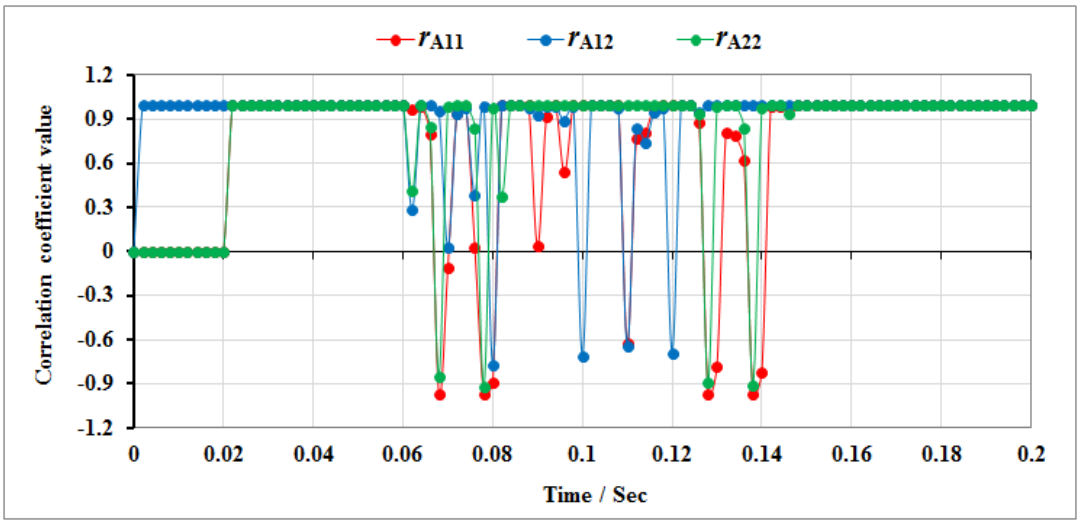

Fig 5-22 Correlation coefficient values when phase-to-ground fault occurs in phase A

3. External fault with CT saturation

An external fault was generated on the line connected to phase A. Since currents on primary and secondary sides simultaneously increased, CT1 and CT4 were likely to be simultaneously saturated if they are identical to each other. It was supposed that CT1 was not identical to CT4. Thus, CT1 didn't saturate whereas CT4 which was closer to the fault was most likely to be saturated. Due to this fault, the flux in CT4 reached to the saturation level at 0.0677 second at which the secondary current started to distort as shown in Fig 5-23.

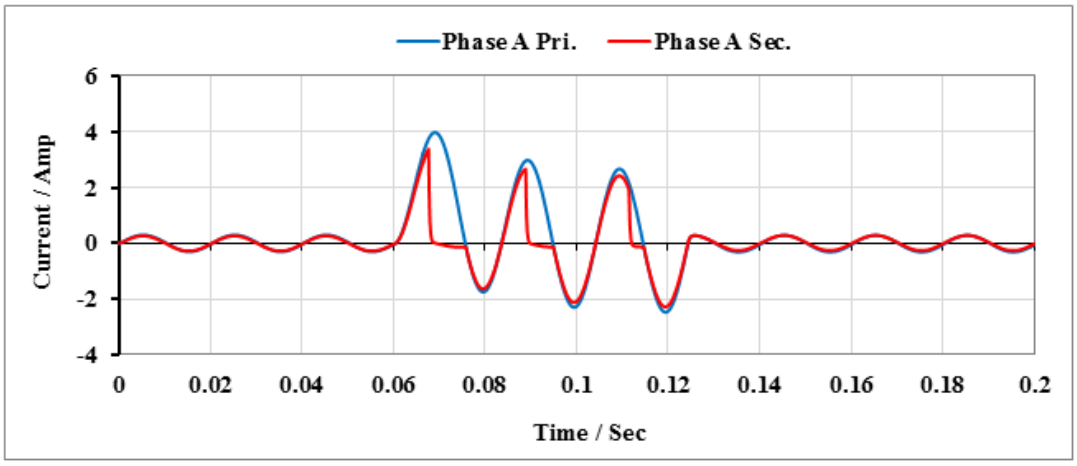

Fig 5-23 Primary and secondary currents when CT saturated due to external fault

From the incidence of external fault till prior to saturation of CTs, both CT1 and CT4 work correctly, thus the primary and secondary currents increase together and follow each other. It means that r_{A12} will be greater than 0.9 whereas r_{A11} and r_{A22} will drop to less than 0.9 due to the fault. However, r_{A12} will be dropped in following windows when the currents will have been distorted due to saturation in CTs. This was verified by simulating this case as shown in Fig 5-24. It can be seen that r_{A11} and r_{A22} firstly dropped to less than 0.9 in the same window at 0.066 second due to the fault whereas r_{A12} dropped to less than 0.9 in the next window at 0.068 second due to the saturation in CT4. This occurred only in the case of external fault. Accordingly, this case was treated by the algorithm in which if the declines in values of r_{A11} and r_{A22} have been detected firstly at same window and then r_{A12} declined in the next

windows, it will be considered an external fault with CT saturation. This was what it happened, and thus there was no trip signal for this case.

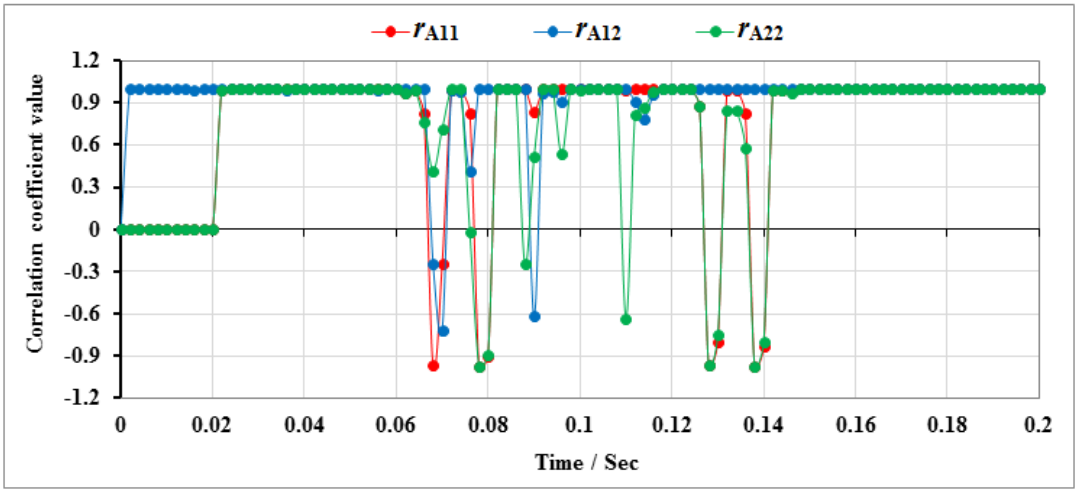

Fig 5-24 Changes in correlation coefficient values due to external fault with CT saturation

4. External fault with saturation of two identical CTs

An external fault was made similar to the previous case, but here both CT1 and CT4 were identical to each other. Therefore, they are likely to be simultaneously saturated due to this fault. Fluxes in the two CTs reached to the saturation level at 0.0677 second at which both primary and secondary currents simultaneously started to distort as shown in Fig 5-25.

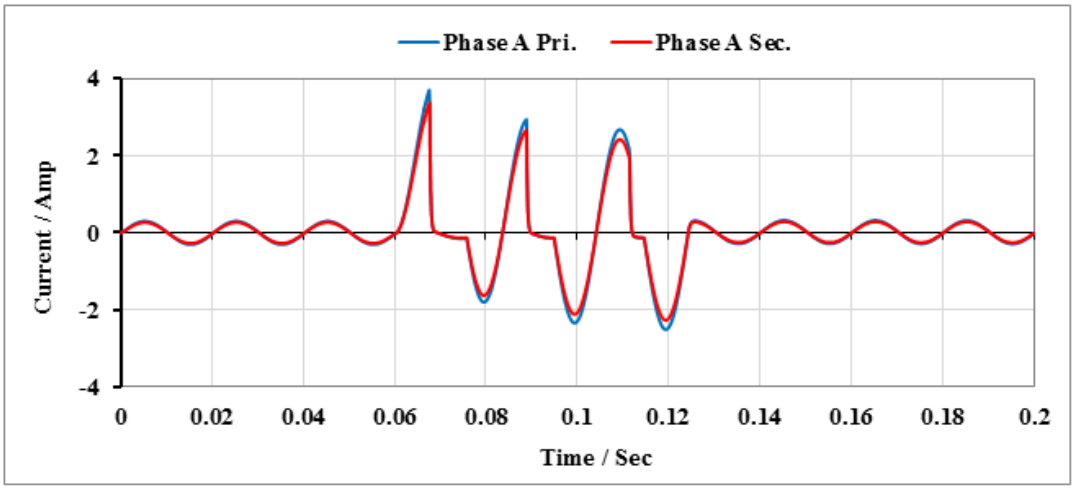

Fig 5-25 Primary and secondary currents when two identical CTs saturated due to external fault

Since CT1 and CT4 were identical CTs and simultaneously saturated due to the fault, the primary and secondary currents increased together and followed each other either before or after saturation. So, r_{A11} and r_{A22} dropped to less than 0.9 in the same window at 0.066 second due to the fault whereas r_{A12} wasn't affected and remained close to 1 during the whole duration of the fault as shown in Fig 5-26. This case was easily detected by the algorithm which considered it an external fault with saturation of two identical CTs. Accordingly, there was no action taken by the algorithm in this case.

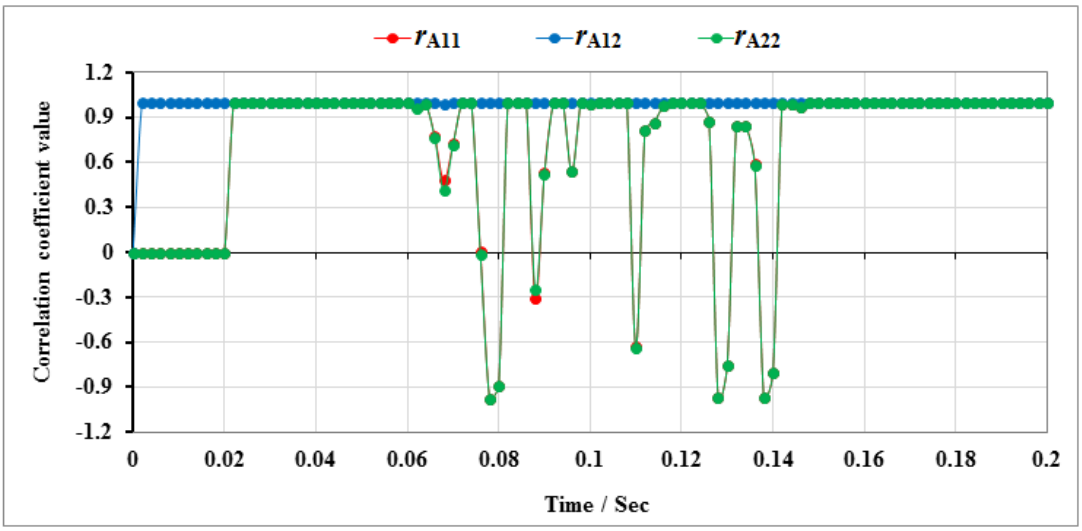

Fig 5-26 Correlation coefficient values during external fault with saturation of two identical CTs

5.3. Transformer model simulation in transient state

The MATLAB/SIMULINK model shown in Fig 5-27 was used for testing the proposed technique in identifying the inrush current and discriminate it from real internal faults when transformer is energized. The core hysteresis data of the transformer are the same as in the model shown in Fig 5-1 except for magnetization resistance R_m ($R_m = 1/g_c$, g_c was shown in Fig 2-4) which was set to 200 pu in this model.

The simulation time for the model was 0.4 second with sample rate 10 kHz, i.e. each cycle represented by 200 samples. The MATLAB function where the MATLAB code of the algorithm was set to run every half-cycle (0.01 second) to compute the current change ratio (CCR) using equation (4-13) and runs every quarter-cycle (0.005 second) to compute percentage area difference (PAD) using equation (4-14). The MATLAB function also computes the supported indicators DP2P, D2PK and Diffmax.

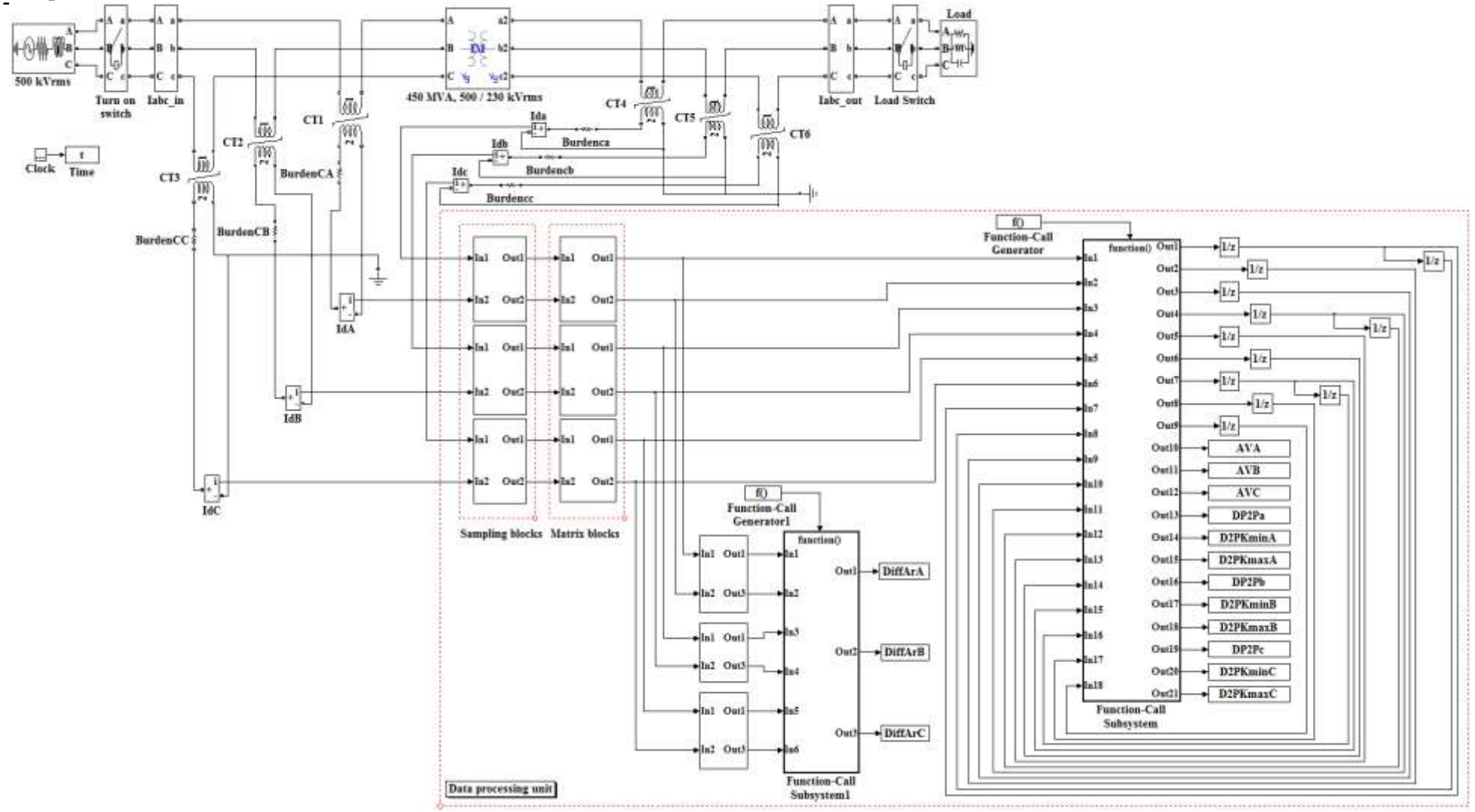

Fig 5-27 System model for the protection technique based on CCR and PAD

5.3.1. Inrush condition when transformer is energized without load

As mentioned in 4.3, there was no need to compute PAD and thus the algorithm used only a current change ratio (CCR) when no-load transformer switched on once without internal fault i.e. pure inrush condition and once with internal fault where the inrush current was submerged in internal fault.

1. Inrush condition

The no-load transformer was energized and consequently the inrush current appeared as shown in Fig 5-28. It can be seen that inrush current signal in phase A is higher than other phases. This depends on the moment of transformer switch on, the sign of voltage signal when transformer last switched off and the residual flux on the core as well as its signal sign.

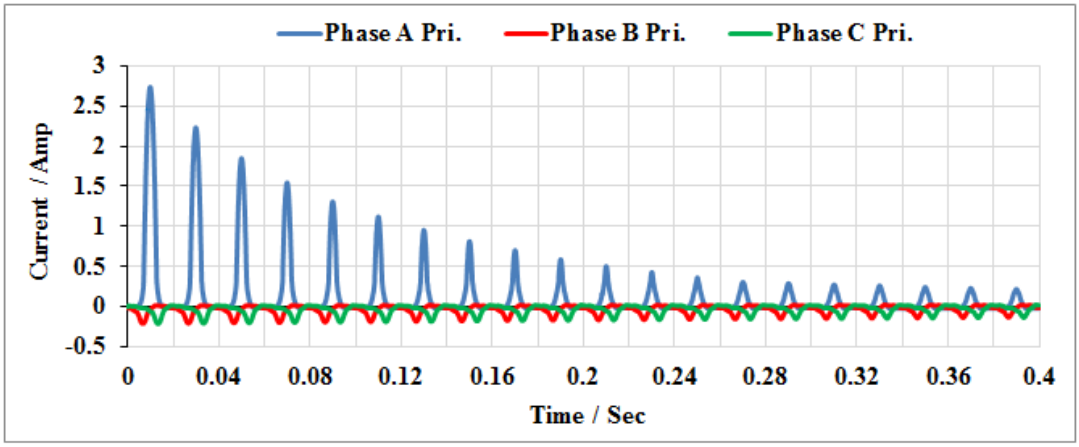

Fig 5-28 Inrush current signal when no-load transformer was energized without fault

The inrush decaying time can be checked by calculating indicators DP2P, D2PK positive and D2PK negative as shown in Fig 5-29 for phase A. It can be seen that inrush signal faded out after approximately 0.36 second and it completely faded out when indicator values reach to very small values (ideally zero), i.e. two consecutive cycles are sinusoids and they are same in size and shape.

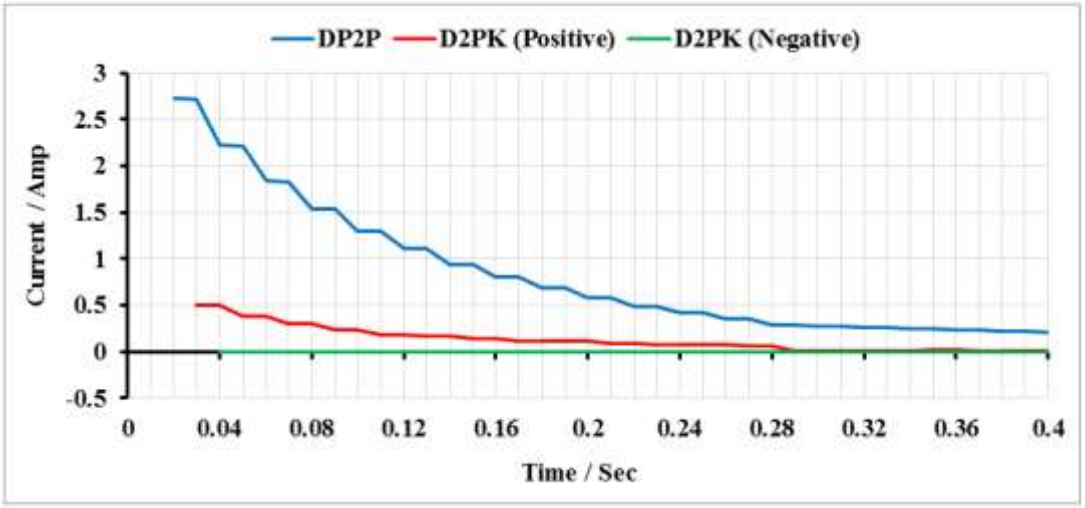

Fig 5-29 Decrease of DP2P and D2PK during Inrush condition for phase A

During inrush condition, the primary current peak was greater than no-load current peak which was checked by Diffmax (note that secondary current peak was zero in this case) but the current change ratio (CCR) was always below 0.8 as shown in Fig 5-30. According to the algorithm shown in Fig 4-4 for this case, it was considered an inrush condition.

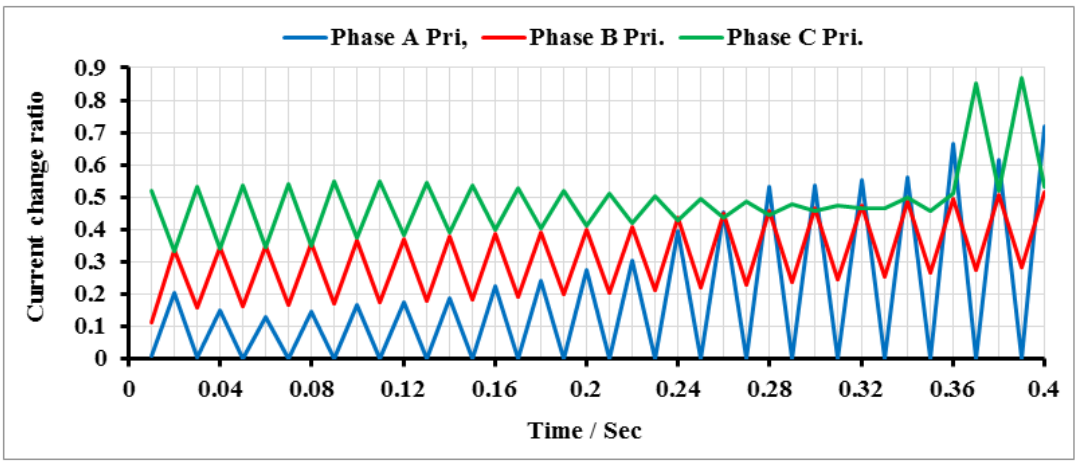

Fig 5-30 CCR when no-load transformer was energized without fault

2. Interturn fault with inrush condition

5% of turns were short-circuited to make a turn-turn fault on the primary side of transformer in phase A. Fig 5-31 shows the current signal when the transformer was switched on with this fault.

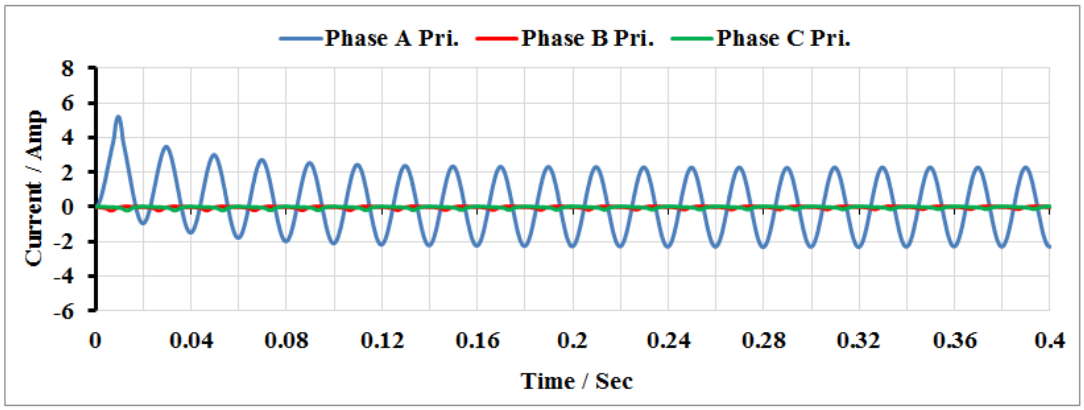

Fig 5-31 Inrush condition when no-load transformer was energized with interturn fault in phase A

It can be seen in phase A that the first few cycles were still affected by inrush current but their shape were close to sinusoids and DC offset didn't take long time to be decayed as can be noticed by the indicators that reached to zero after four cycles as shown in Fig 5-32.

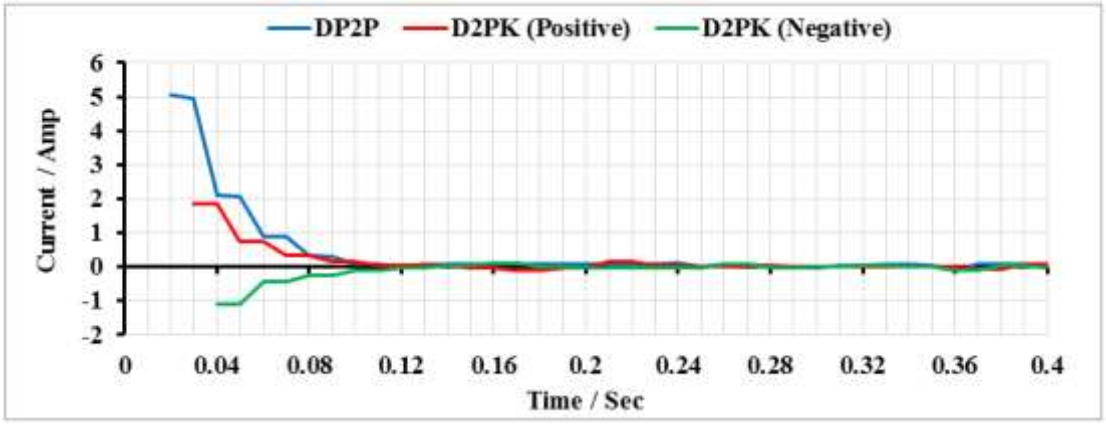

Fig 5-32 Decrease of DP2P and D2PK for phase A during Inrush current with interturn fault

Since the interturn fault was submerged to inrush signal, the shape was close to sinusoid. This is why the current change ratio was above 0.8 as shown in Fig 5-33. At the first half-cycle, the current change ratio was greater than 0.8 and the current peak value was greater than no-load current value, so the algorithm considered this case an internal fault, i.e. the fault was detected after half-cycle from the moment of transformer switch-on.

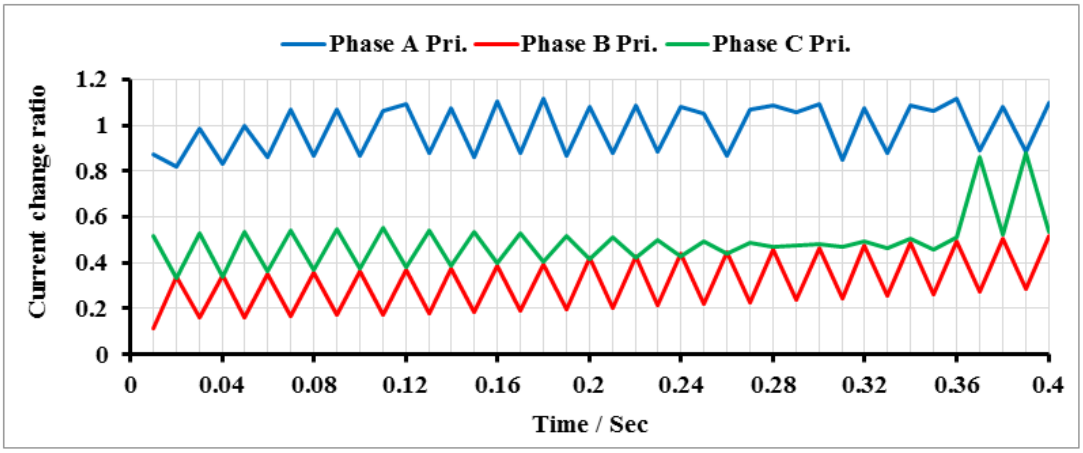

Fig 5-33 CCR when no-load transformer was energized with interturn fault in phase A

3. Turn-ground fault with inrush condition

The transformer was switched on with a turn-ground fault at the middle of winding on primary side of phase A. The shape of current waveform was very close to sinusoid as shown in Fig 5-34.

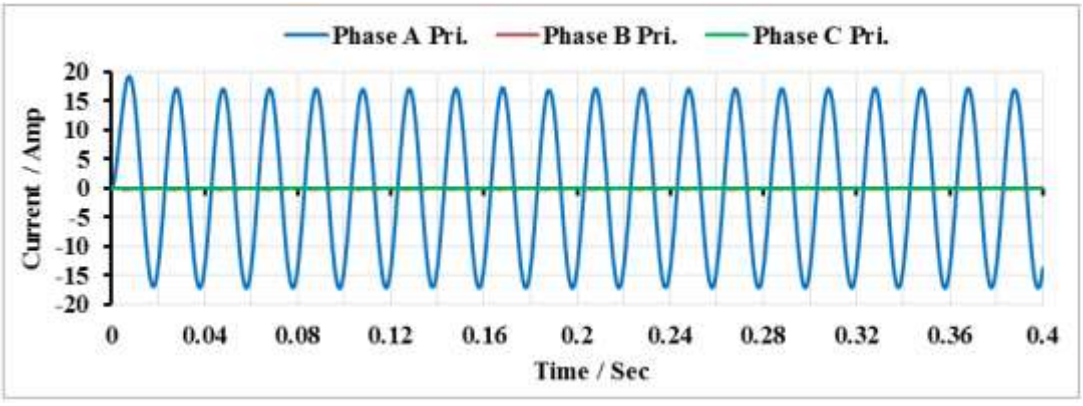

Fig 5-34 No-load transformer was energized with turn-ground fault in phase A

The simulation results for this fault indicated that the CCR was above 0.8 for the faulty phase A in the duration of fault, while it was less than 0.8 for the other phases B and C because they are as shape as inrush current signal as shown in Fig 5-35. The CCR exceeded the threshold at the first half-cycle from the instant of transformer switch-on, so the internal fault was detected and a trip signal was issued. The algorithm effectively distinguished the internal fault in phase A from inrush condition after just 10 ms.

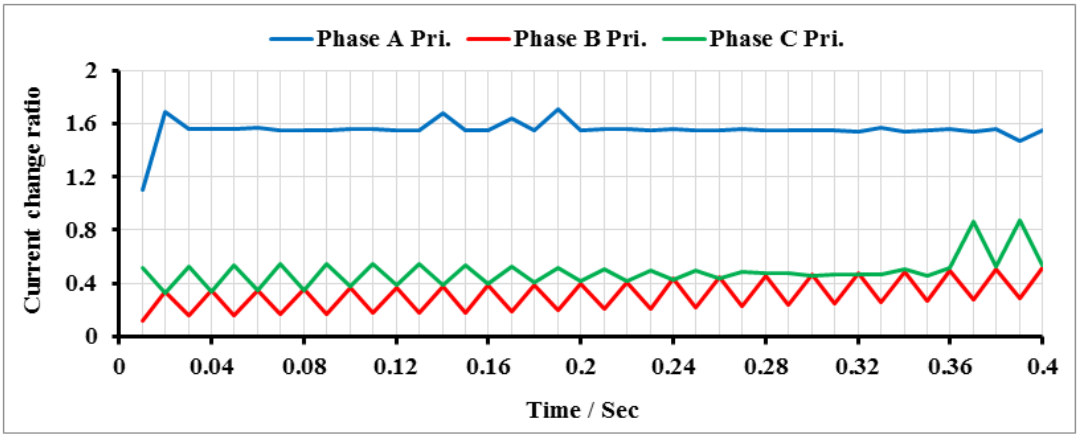

Fig 5-35 CCR when no-load transformer was energized with turn-ground fault in phase A

5.3.2. Inrush condition when transformer is energized with load

Here, the load in the model was considered in order for algorithm to be tested for the same former cases. The algorithm used both percentage area difference (PAD) and CCR when transformer was on-load.

1. Inrush condition

The loaded transformer was switched on without internal fault. Since the voltage peak location at instant of last transformer switch-off cannot be controlled, the sign of residual flux on the core limbs cannot be known. Therefore when the transformer was switched on, the inrush current appeared only in phase A as shown in Fig 5-36.

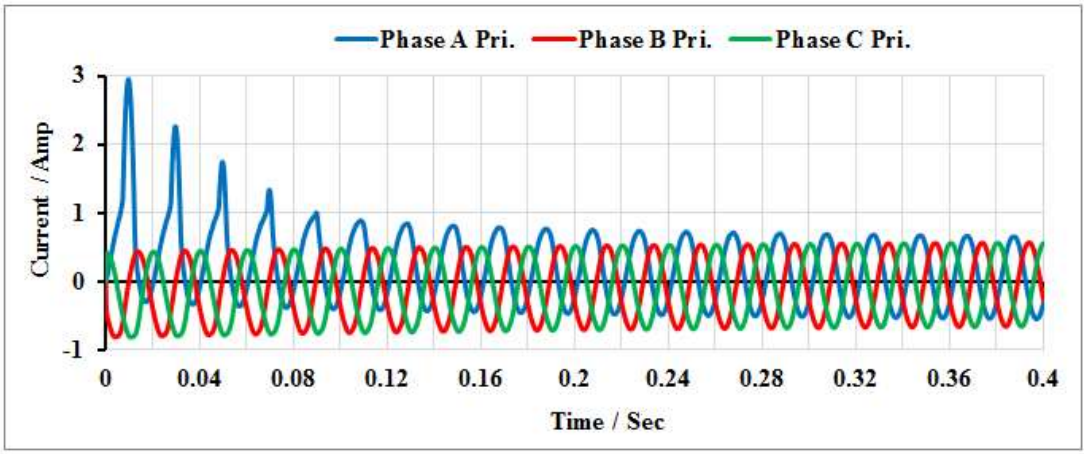

Fig 5-36 Inrush current when on-load transformer was energized

Although the load was connected, i.e. the secondary currents flow on the secondary side, there was still inrush in first four cycles of phase A as shown in Fig 5-37. As known, the inrush appears only in the energisation side. This is why that is a problem for differential protection schemes which may mal-operate in this case due to the significant difference in values between currents entering and leaving the transformer.

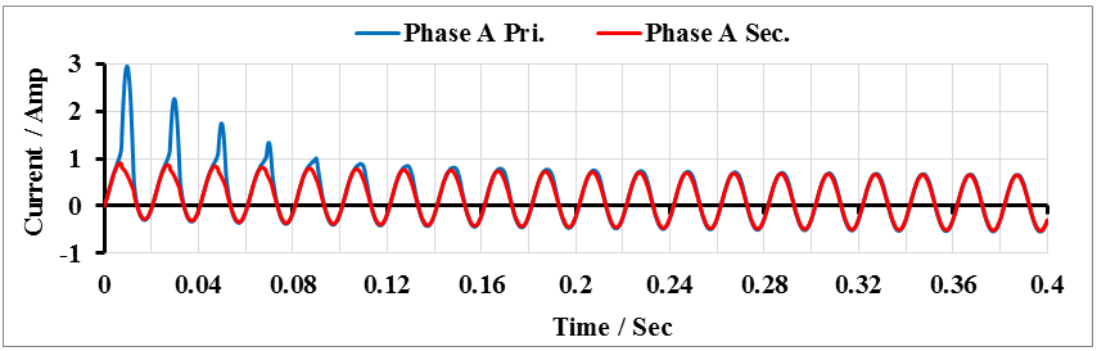

Fig 5-37 Primary and secondary currents in phase A when on-load transformer was energized

The inrush signal faded out faster than when transformer was on no-load. Fig 5-38 shows the decrease in DP2P, D2PK positive and D2PK negative.

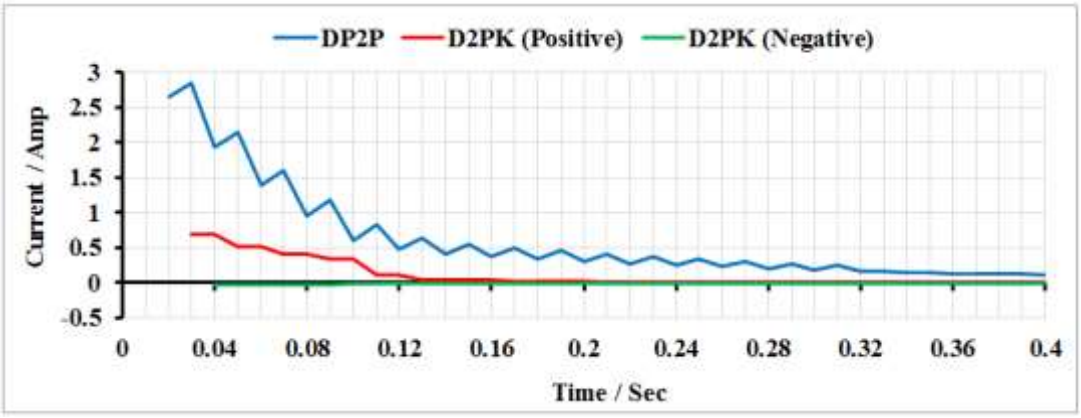

Fig 5-38 DP2P and D2PK for phase A when loaded transformer was energized without fault

Since the inrush current was the highest in phase A, primary current was much higher than secondary current in this phase i.e. Diffmax was significant, particularly in the first four cycles which were the highest inrush current values as shown in Fig 5-39

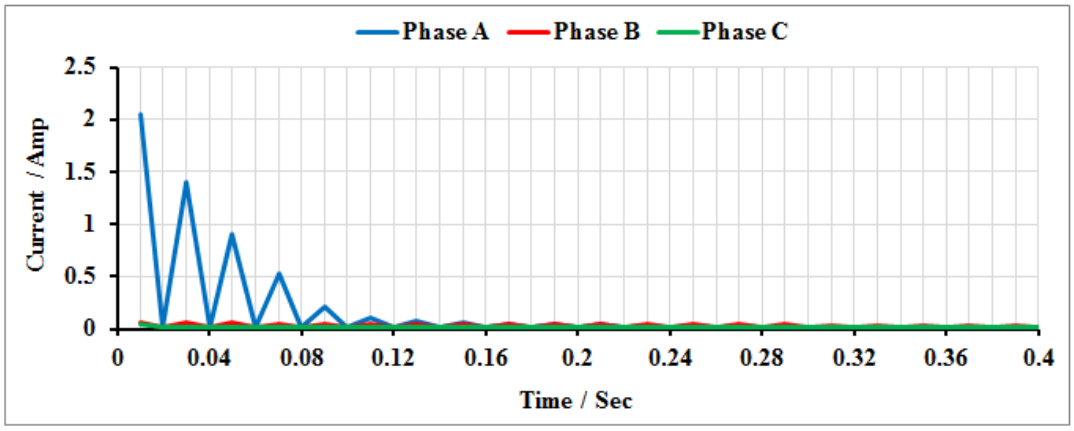

Fig 5-39 Diffmax when loaded transformer was energized without faults

The PAD was less than 30%, so there was no internal fault till first quarter-cycle (5ms) as shown in Fig 5-40. So the algorithm continued to the first half-cycle (10ms) to check Diffmax which found greater than 0.1 in phase A. So the current change ratio (CCR) checked and was less than 0.8 for first cycles as shown in Fig 5-41. Therefore the algorithm considered it an inrush condition.

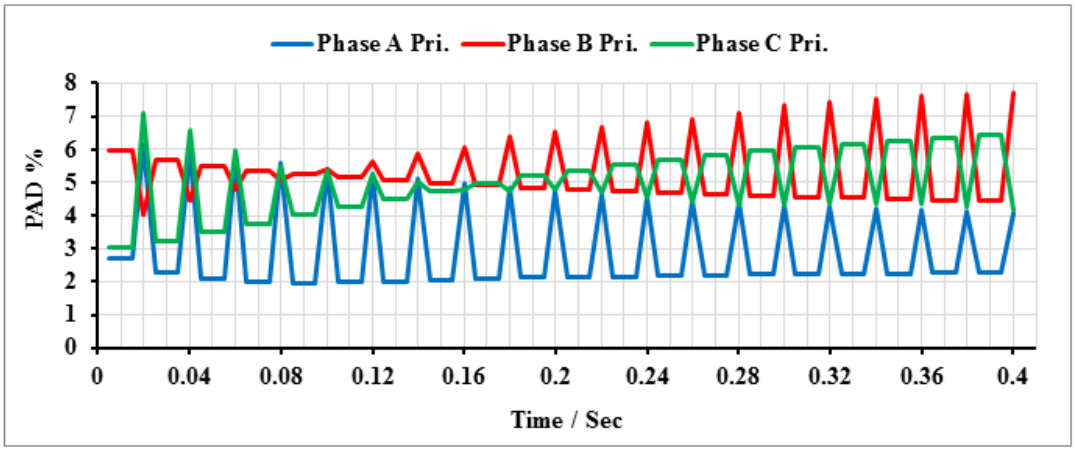

Fig 5-40 PAD when loaded transformer was energized without fault

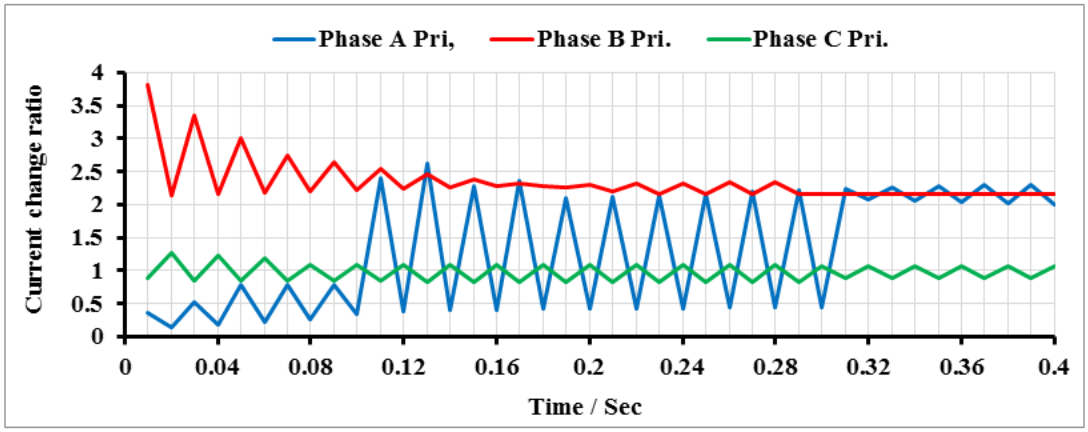

Fig 5-41 CCR when loaded transformer was energized without fault

It can be noticed that CCR in phases B and C were greater than 0.8, but they were not checked as their Diffmax was less than 0.1, so it was considered a normal condition.

2. Interturn fault with inrush condition

The transformer was energized with 2% of turns were short-circuited in the secondary winding of transformer in phase A. Fig 5-42 shows the consequence of this fault on the primary currents of the three phases. It can be seen that the influence of inrush still existed at the first two cycles of primary current.

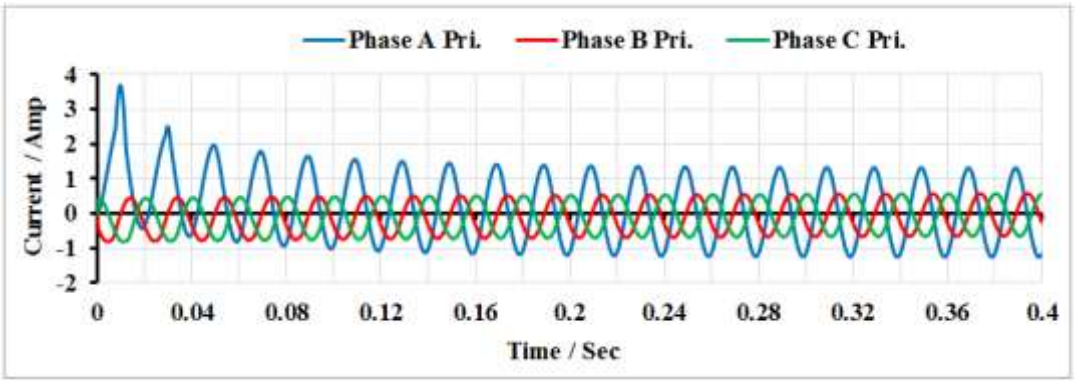

Fig 5-42 The currents when loaded transformer was energized with turn-turn fault in phase A

The fault caused a significant difference between primary and secondary currents in phase A as shown in Fig 5-43.

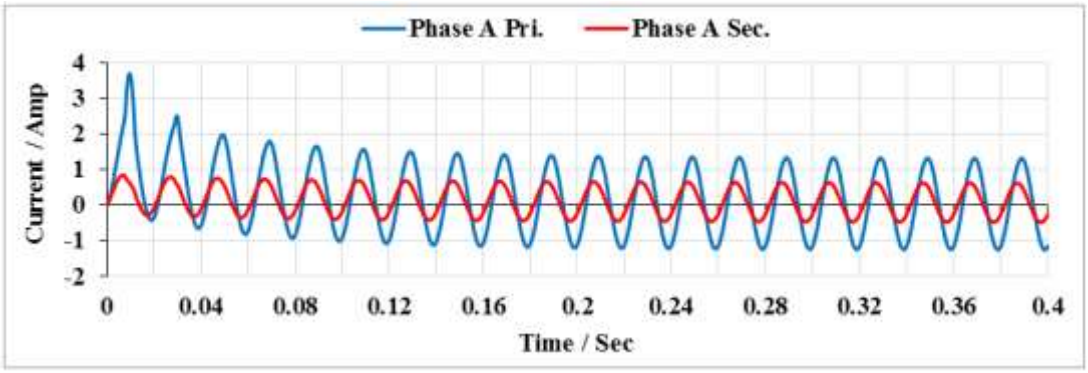

Fig 5-43 Primary and secondary currents when loaded transformer was energized with turn-turn fault in phase A

The end of inrush's effect can be seen at 0.16 seconds as DP2P, D2PK positive and D2PK negative approached to zero as shown in Fig 5-44.

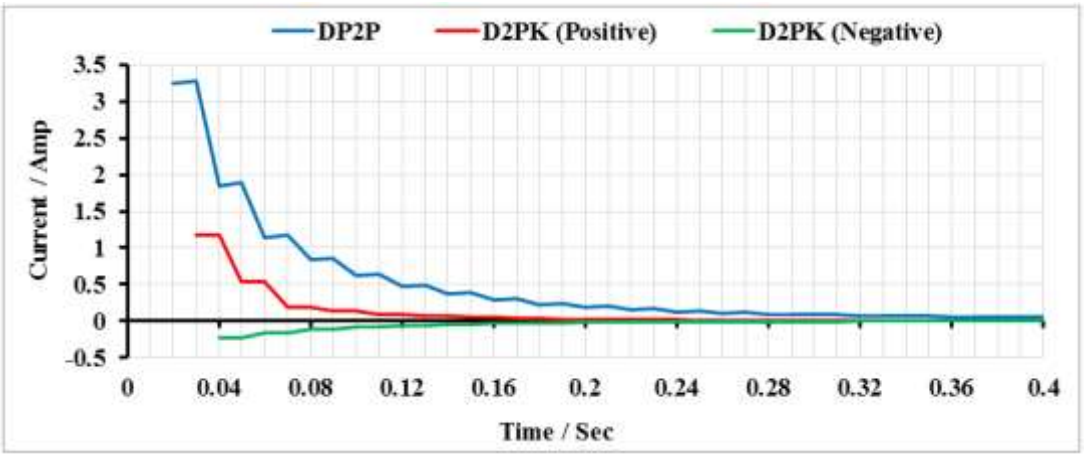

Fig 5-44 DP2P and D2PK for phase A when loaded transformer was energized with interturn fault

Because of this fault, the PAD exceeded 30% at the first quarter-cycle as shown in Fig 5-45. So the fault was effectively detected after just 5 ms from the moment when transformer was switched on and there was no need for algorithm to check CCR.

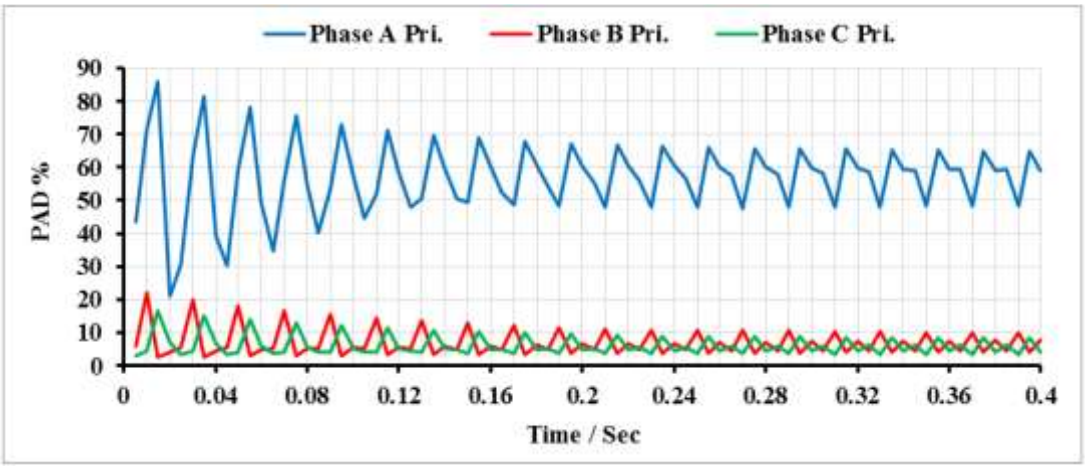

Fig 5-45 PAD when loaded transformer was energized with interturn fault in phase A

3. Turn-ground fault with inrush condition

The turn in transformer's mid-winding on the secondary side was connected to ground when transformer was switched on. The first cycle of primary current was slightly affected by inrush as shown in Fig 5-46.

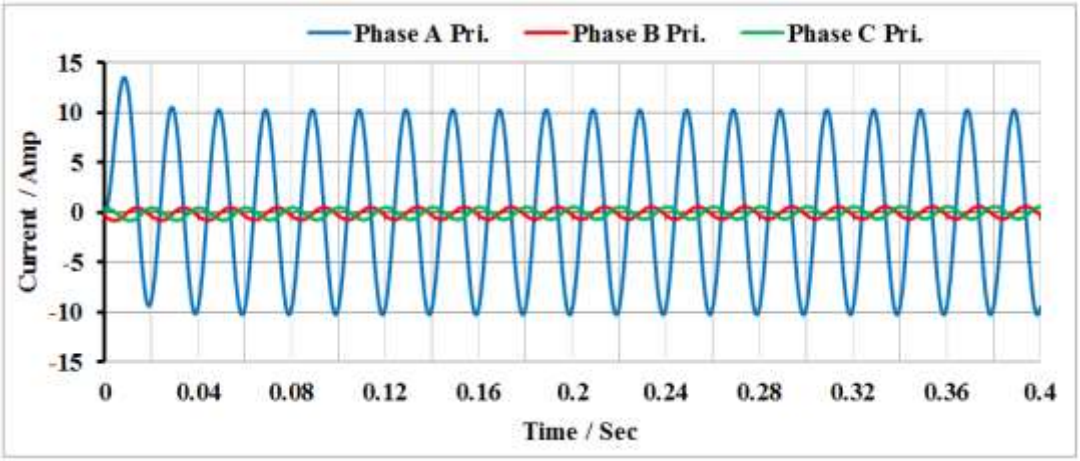

Fig 5-46 Currents when loaded transformer was energized with turn-ground fault in phase A

Big difference between primary and secondary currents in phase A was caused by this fault as shown in Fig 5-47.

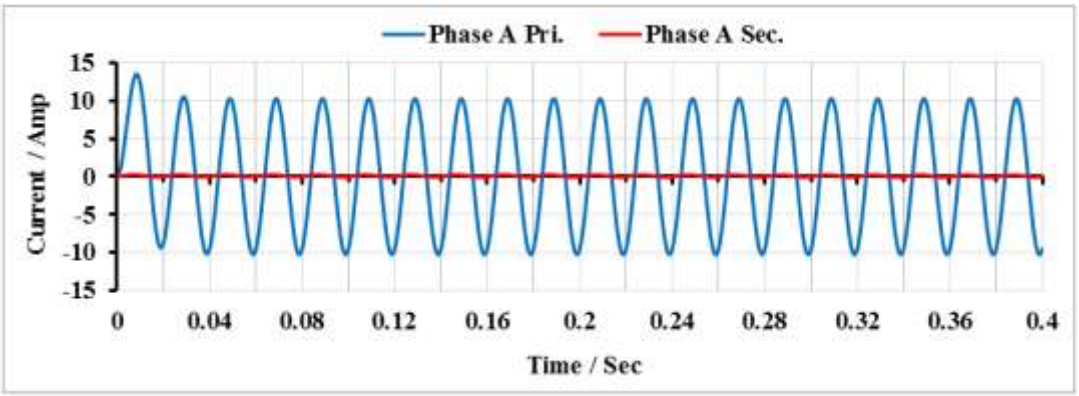

Fig 5-47 Primary and secondary currents when loaded transformer was energized with turn-ground fault in phase A

The effect of inrush current ended rapidly due to this high fault current. DP2P, positive and negative of D2PK show that the effect of inrush current significantly reduced after the first cycle as shown in Fig 5-48.

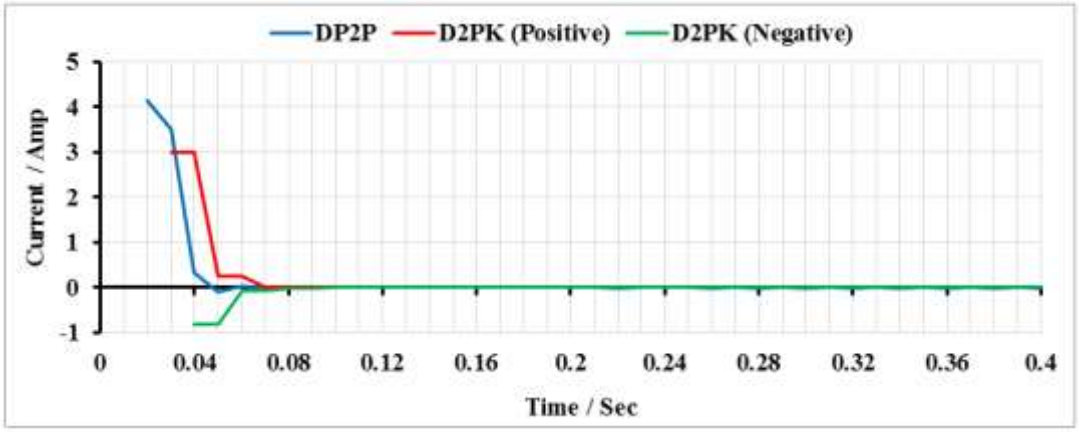

Fig 5-48 Decrease of DP2P and D2PK during turn-ground fault in phase A

PAD is very high and greater than 30% because there was a big difference in values between primary and secondary currents due to high fault current as shown in Fig 5-49. The fault was then detected after 5ms from instant of transformer's energization.

Since all primary currents in three phases had the shape of sinusoidal signals due to the fault, their current change ratios were above 0.8 as shown in Fig 5-50.

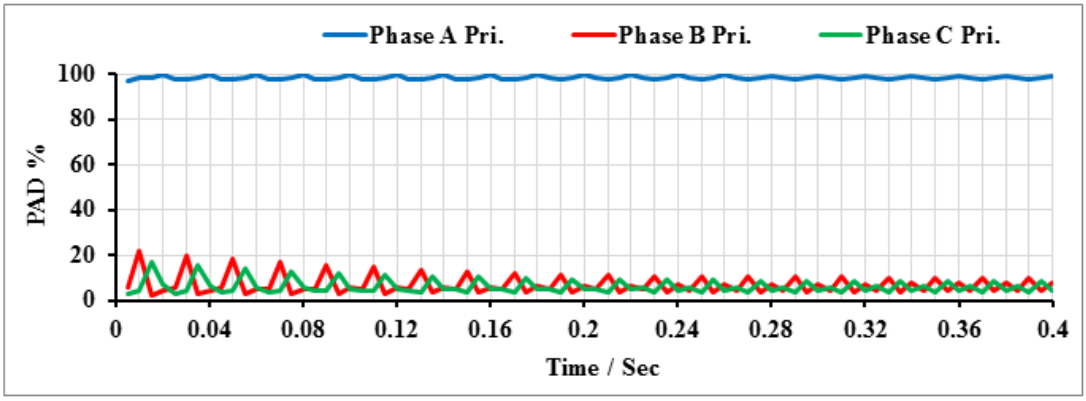

Fig 5-49 PAD when loaded transformer was energized with turn-ground fault in phase A

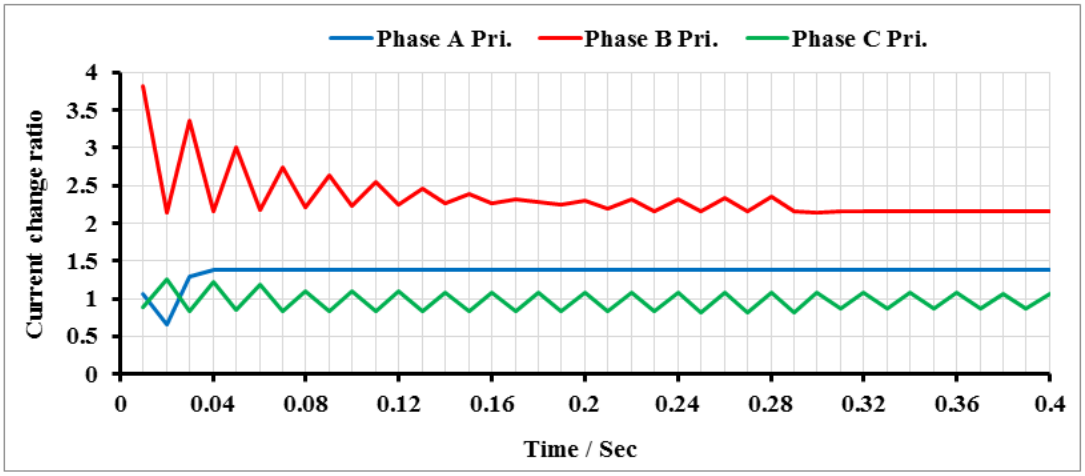

Fig 5-50 CCR when loaded transformer was energized with turn-ground fault in phase A

5.4. Summary

The proposed protection technique was tested on a transformer modelled by MATLAB/SIMULINK program. Most common faults that occur in transformer were generated to show the action of the technique against these faults.

In steady state, it was proved that the technique was efficient in detecting faults and also fast as it detected faults in 2 or 6 ms according to the type of fault and how heavy the fault was. The technique was also tested under possible cases of current transformer saturation which is considered one of the biggest problems in differential protection systems. It was proved that this problem can be overcome depending on high speed action of the technique. In transient state, the proposed technique rapidly and soundly discriminated inrush current from the internal faults which were generated simultaneously with transformer energization once without load and once with load. These faults were detected in only 10 ms and 5 ms in no-load and on-load cases respectively.

CHAPTER 6

Measurements and Experiment Setup

6.1. Transformer design

The transformer was built in Cardiff University's laboratory with core of 4.1cm height and 11 cm width as shown in Fig 6-1. This research transformer was a three-phase, three-limb laminated core transformer with a rated power of 20kVA and the core's material was grain-oriented 3% silicon electrical steel. Uniform clamping torque of 1 N.m was applied on the bolts to make uniform clamping pressure on the transformer core.

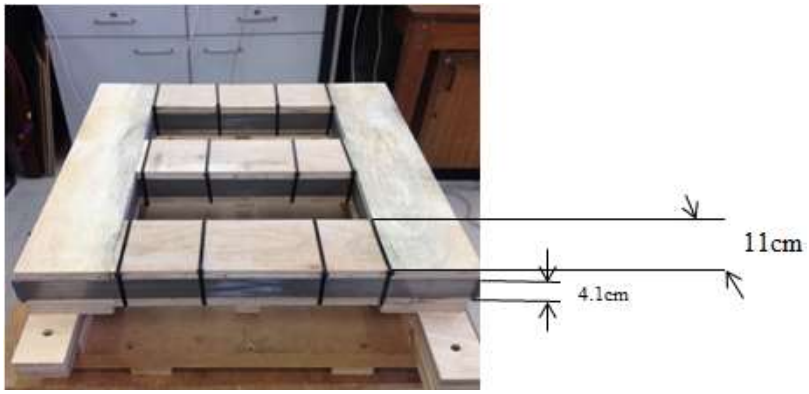

Fig 6-1 Transformer under study

6.1.1. Transformer core test

The flux density corresponding to voltage supply can be adjusted using equation (2-11) which was modified by adding another factor as follows

$$e_{rms} = 4.44 f N_1 B_{max} A \, K_b \quad (6\text{-}1)$$

Where K_b is building factor (inter lamination coat) = 0.95, 0.96 or 0.97. The cross-sectional area is not pure area because there is coat between lamination that was why the equation has to multiply by this factor.

The flux density was determined in inverse way, i.e. substitute the desired value of flux density in the equation (6-1) and find the corresponding value of voltage. For simplicity, coil of one turn was used to adjust the desired flux density. The following steps show how to do so:

1. If the desired flux density (B) was 1.3 Tesla in system frequency of 50 Hz, the corresponding e_{rms} can be found by
   e_{rms} = 4.44*50*1*1.3*0.00451*0.95=1.24 V (rms)

2. A single coil wraps around the core limb and their two terminal ends are connected to a multimeter.

3. The supplied voltage to the primary winding is increased until the multimeter reads the calculated corresponding voltage value across the turn, that time the supplied voltage is the voltage needed for the desired flux density. The table 6-1 shows the corresponding voltages for different flux densities that the transformer core was tested under.

Table 6-1 Flux density corresponding to supplied voltage

Flux density (Tesla)	Phase voltage (Vrms) phase A	Phase voltage (Vrms) phase B	Phase voltage (Vrms) phase C
0.53	30	30	30
1.05	60	60	60
1.3	75	75	75
1.5	86	86	86
1.7	98	98	98

The flux density (B) can also be determined by fluxmeter device (LakeShore 480) shown in Fig 6-2.

Fig 6-2 Fluxmeter

A Comparison was carried out between above calculated flux density and flux density measured by fluxmeter device. Fig 6-3 shows the calculated and measured flux densities corresponding to different applied voltages from 0 V to 69 V.

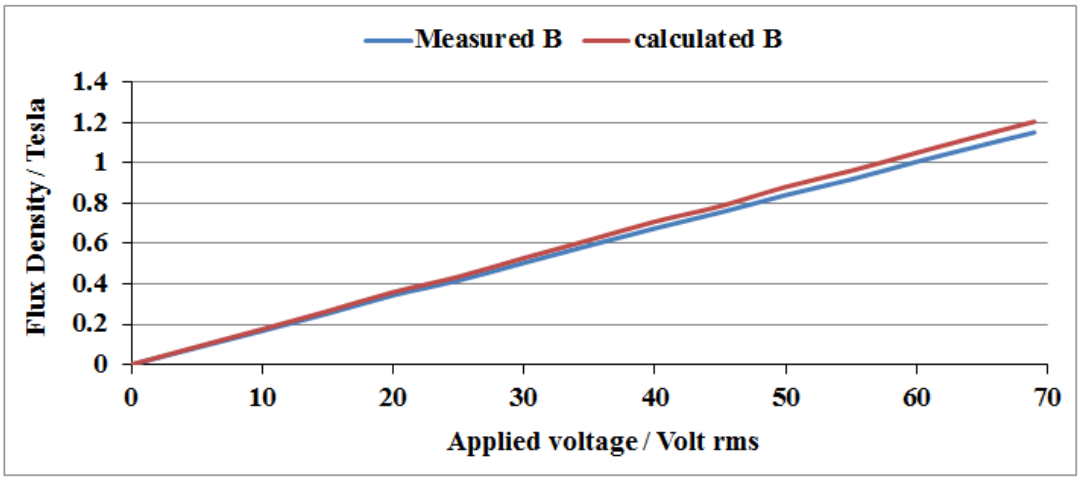

Fig 6-3 Measured and calculated flux density (B)

The two curves are approximately overlapping to each other. It is clear that they are approximately the same. So equation (6-1) was proved and can be used for measuring the flux density in the transformer core.

6.1.2. Winding taps distribution

Fig 6-4 shows how taps and winding turns were achieved around the transformer core. There were 120 turns at each phase, 60 turns for primary (red) side and the same number for secondary (black) side. There were 25 taps connected to the turns, 5 at first, middle and last of the winding while the remaining taps were in between but after every 5 turns. The taps were fixed in order to be used for generating faults on the transformer.

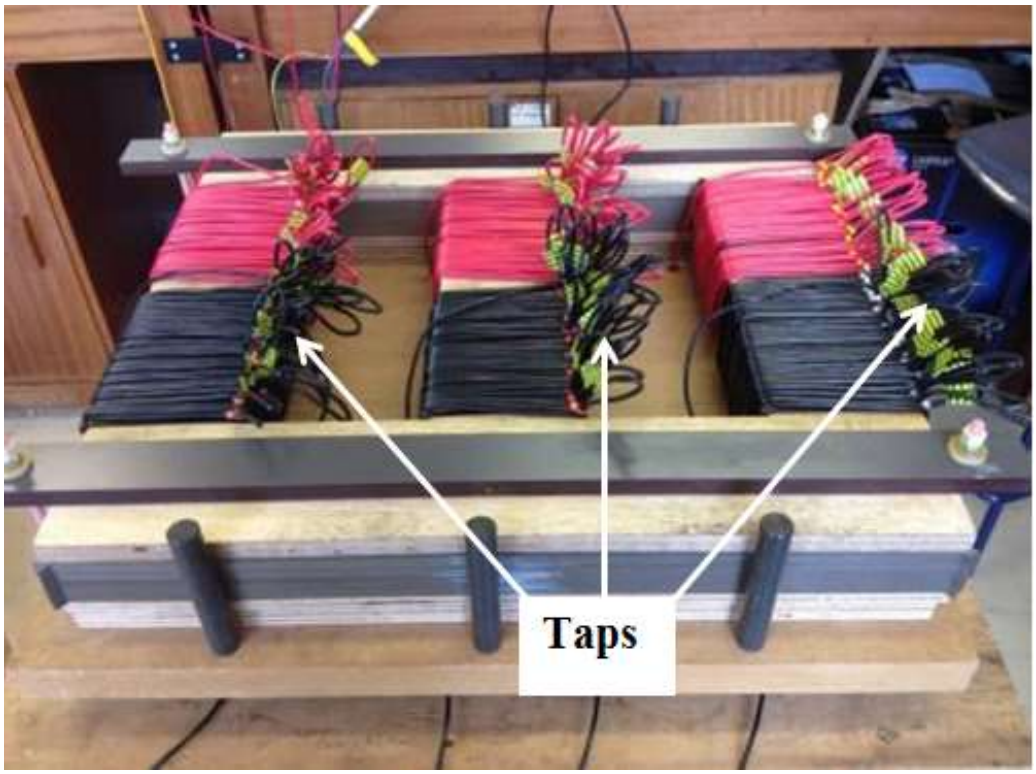

Fig 6-4 Winding turns and taps

6.2. Faults generation

Internal faults were generated by connecting a wire either between taps (interturn fault) or between tap and ground (turn-ground fault) while external faults were outside of the transformer. For laboratory safety purposes and calculation simplicity, the phase voltage was set to 60V and the number of turns was 60 for both primary and secondary windings i.e. the turn ratio was 1. Also, in order to prevent any difficulty and challenge, the use of oil/tank in the transformer was practically avoided as it does not affect the results and, furthermore, the proposed technique was capable of detecting the internal faults in the transformer regardless of the existence of the tank, oil and insulation between the winding.

6.2.1. Turn-turn fault generation

Generating the interturn fault is practically possible but unsafe, because the turns to be shorted N_x will be damaged due to very high circulating current I_f in the loop as

shown Fig 6-5. This high current is generated due to very low wire resistance, so a high precision resistor R_f of 0.1Ω was connected in the loop to limit the current that flows through the loop and hence to protect winding turns from the damage due to the high current in the loop.

If the turns are identical, each turn is supposed to has 1 V across it. So for 3 turns there will be 3 V. Since the turns were approximately identical (manually wrapped around the core limb), 3 turns measured of 2.95 V induced voltage across it and resistance of 0.1 ohm added to wire resistance of roughly 0.018 Ω which was calculated by

$$R = \frac{\rho \times l}{A} \tag{6-2}$$

Where R is the resistance of the wire in ohm (Ω), ρ is the resistivity of the material (copper was used) in Ohm·meter (Ω·m), l is the length of the wire in meters (m) and A is the cross sectional area of the wire in square meter (m^2).

Thus, the total resistance was 0.1+0.018 = 0.118 Ω. The circulating current in this case was equal 2.95/0.118 = 25 Amp which can be afforded as the manufacturing current limit of the used winding wire was 30 Amp. In order to generate the fault at any desired time, Closing or opening the switch (SW) can be controlled by LabVIEW programwhich generates a pulse signal via data acquisition card to an electro-mechanical relay that connected in series with the protection resistor R_f of the short circuit. This relay was used as a switch (SW) to make short-circuit between turns as shown in Fig 6-5.

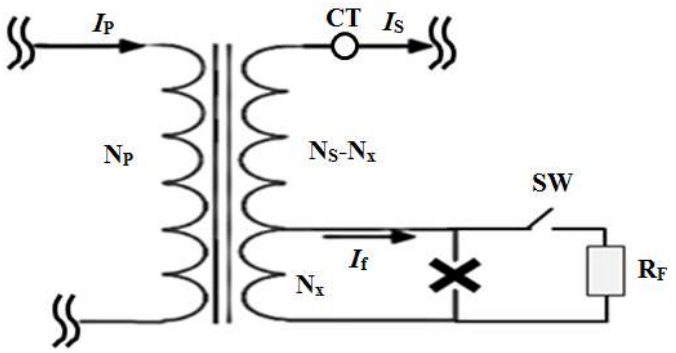

Fig 6-5 Interturn fault representation

The relay was not ideal as it took a few milliseconds time to close after triggering, and this time was specified by the manufacturer. Therefore, it was too difficult to specify exactly the moment of switch-on of the relay after triggering it, but according to the manufacturer, the maximum operating time is 15 ms so it may be switched on in less than 15 ms.

Fig 6-6 shows how this fault was generated in the laboratory. R_f was just introduced in the experimental circuit to represent the interturn fault. In a real case of interturn fault (without protection resistor R_f), there will be just the resistance of the wire which is as low as 0.018 Ω roughly, so the real current that will circulate in the loop is 2.95/0.018 = 163.9 Amp which is very high and will burn off these turns. This is what really happens when this fault occurs.

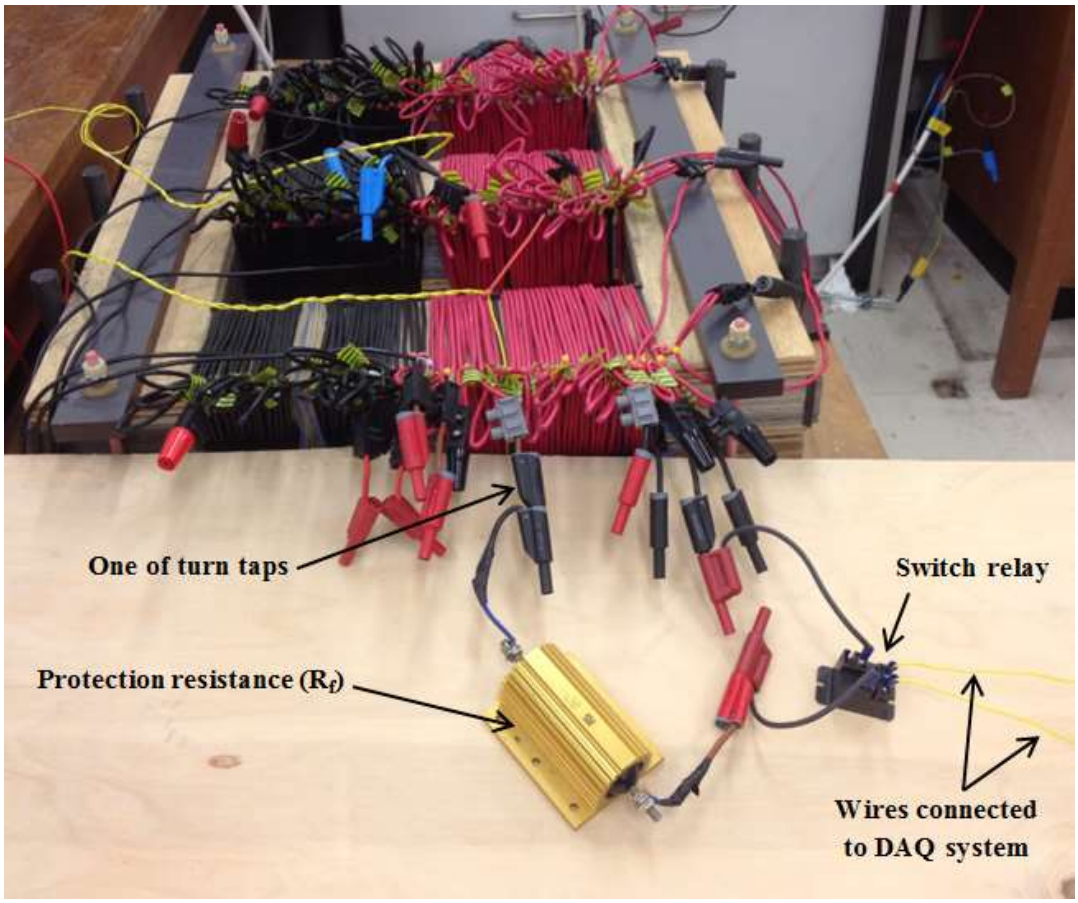

Fig 6-6 Implementation of interturn fault in the laboratory

6.2.2. Turn-ground fault generation

Different turns along the winding of all three phases on both primary and secondary side had been grounded for testing the turn-ground fault at different positions along the winding. Since similar results had been obtained, only the turn in the mid-winding of phase A on secondary side is shown. This turn, which is tap no. 30, was connected in series with a resistor of 5Ω then to ground. This resistor was used for limiting the high current that flows from the turn to the ground point. The half of the phase voltage would be lost if this resistor had not existed. It was necessary to insert this resistor in order to protect windings from this high current, which can be calculated as follows.

The phase voltage was 60V and the turns were supposed to be identical. For 30 turns, the induced voltage was measured as 29.97 V (ideally 30 V) and with a wire resistance of 0.02 Ω roughly, hence the expected current is 29.97/0.02=1498.5 Amp. This current jeopardizes the function of these windings but by using the resistor of 5Ω in series, the current was reduced to 29.97/5 = 5.99 Amp which does not cause a danger to the windings. This is when this fault occurs on the primary side, where most of it practically flows through only 30 turns to ground via wire of very low resistance so the remaining 30 turns are obsolete.

As mentioned above, the protection resistor was inserted to minimize the current to around 6 Amp, which represented the input primary current and was measured by the CT provided. But it is different in case that the fault occurs on the secondary side. However, Fig 6-7 shows how this case can be represented and Fig 6-8 shows how this fault was carried out in the laboratory.

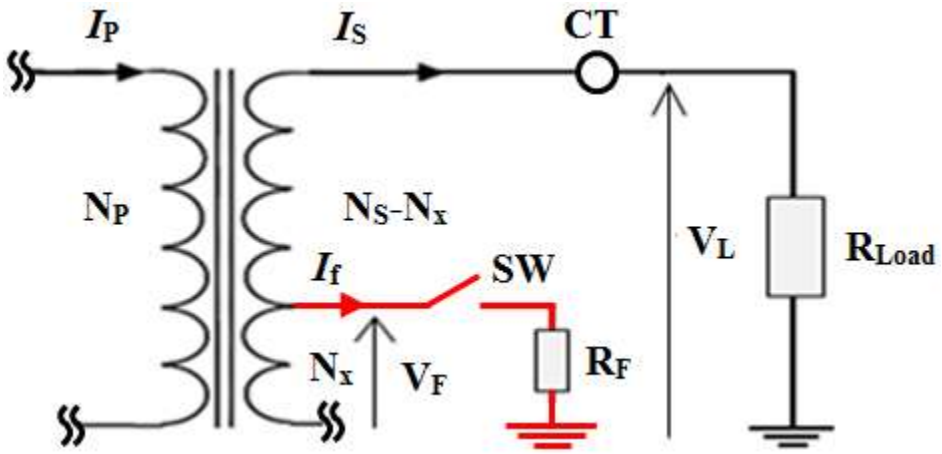

Fig 6-7 Turn-ground fault representation

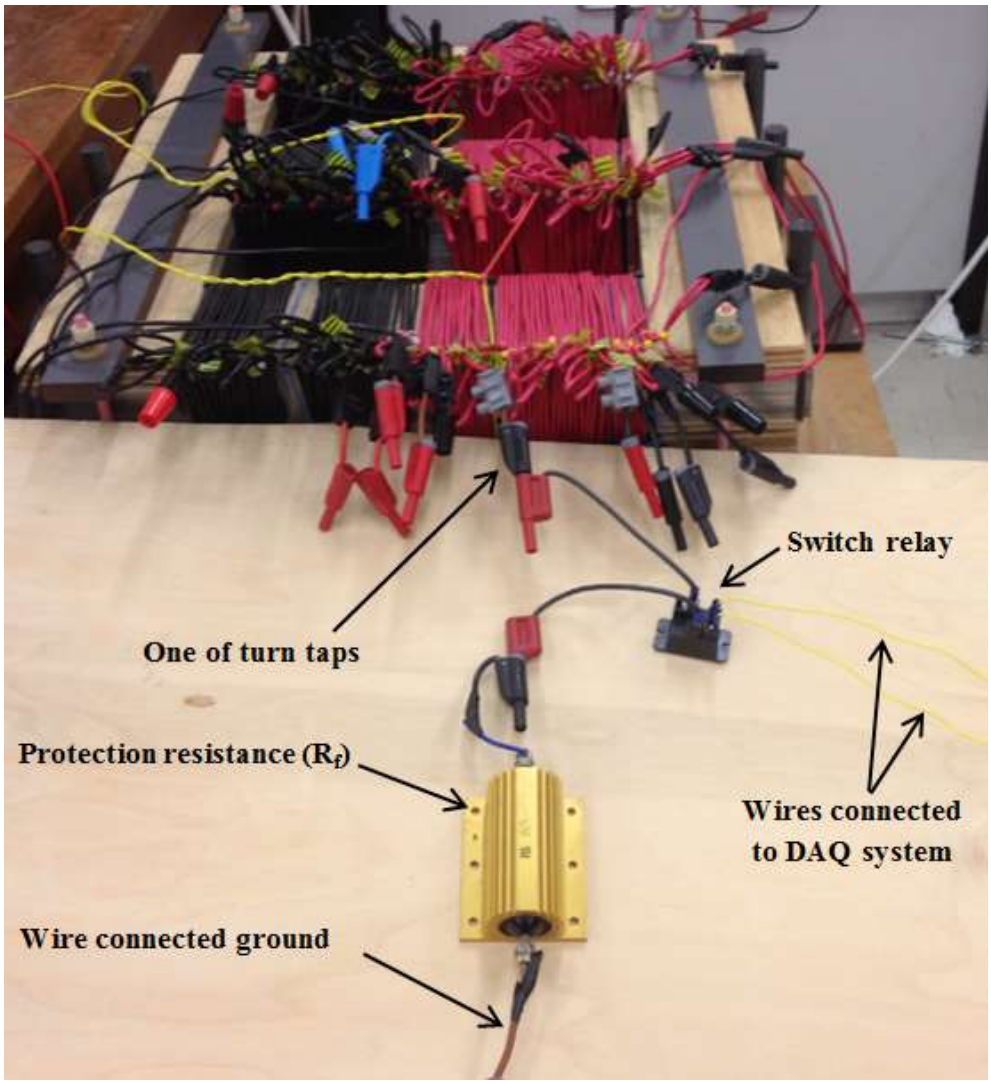

Fig 6-8 Implementation of turn-ground fault in the laboratory

When the switch of the fault (SW) was closed, a fault current I_f of 1.93 Amp measured by clamp meter, flowed through the protection resistor R_f of 5Ω. V_f in this case was 1.93*5 = 9.65 V which also measured using a voltmeter. The secondary current I_s which flowed through the load R_{Load} was measured as 1.46 Amp. I_s is the current that is measured by the CT. The summation of I_s and I_f will balance the primary current I_p. So $I_p = I_s + I_f$ = 1.46 +1.93 = 3.39 Amp which was also read by the power analyzer system (LEM NORMA D 6000 is shown in Fig 6-11). V_L was 40 V measured by the voltmeter i.e. $V_L = V_F$ + voltage across 30 turns = 9.65 + 30 = 39.65 V.

6.2.3. Single phase-ground fault generation

The fault was generated by connecting the first turn to the ground through a protection resistor R_f of 5Ω (represents a ground and fault resistance). It is similar to turn-ground fault current but it's the highest fault current as the whole phase will be lost.

When it was generated on the primary side, the phase voltage supposed to be highly reduced because most of the primary current I_p had to flow through the lower resistance of fault branch rather than the high impedance of winding in which the remaining very low current flowed through. Due to the existence of R_f, the phase voltage wasn't reduced too much but was reduced to around 44 V.

The CT on the primary side measured the primary current I_p which is the summation of fault current I_f and the winding current. Again, this current is normally high due to very low resistance of fault branch, so the protection resistor was used to minimize it to just around 12 Amp. But when the fault was generated on the secondary side, the current flowed through the load I_L was very small as most of the secondary current I_S flowed through the fault branch as shown in Fig 6-9. The CT on the secondary side measured I_L only.

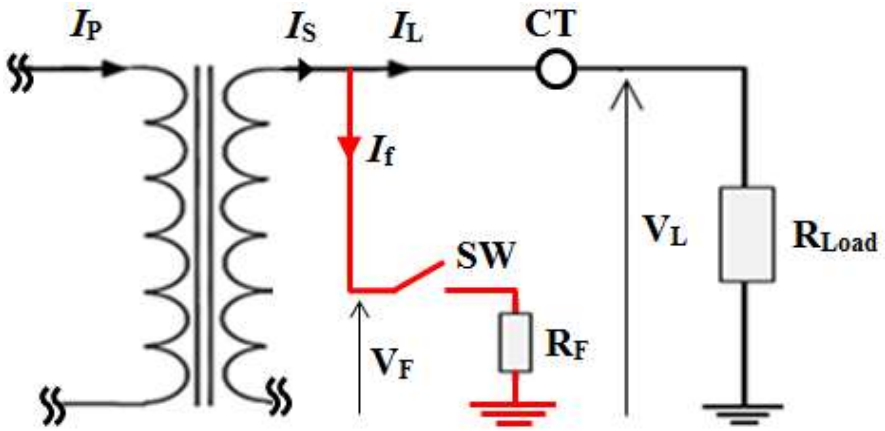

Fig 6-9 Single phase-to-ground fault representation

6.2.4. External fault generation

The external fault occurs outside of the protected zone of the transformer. It is between the load and the secondary side of the transformer. Since the CT on the secondary side is located before external fault point, it measures the secondary current I_s as shown in Fig 6-10. When the switch was closed, the phase voltage reduced from 60 V to around 20 V which was value of V_f ($V_f = V_L$) causing an increase in the secondary current I_s to around 5 Amp. I_s split into high fault current I_f of 3.98 Amp flowed through low resistance of fault resistor R_f of 5Ω and low load current I_L of 1 Amp flowed through higher resistance load R_{Load} i.e. $I_s = I_L + I_F$ =3.98+1=4.98 Amp.

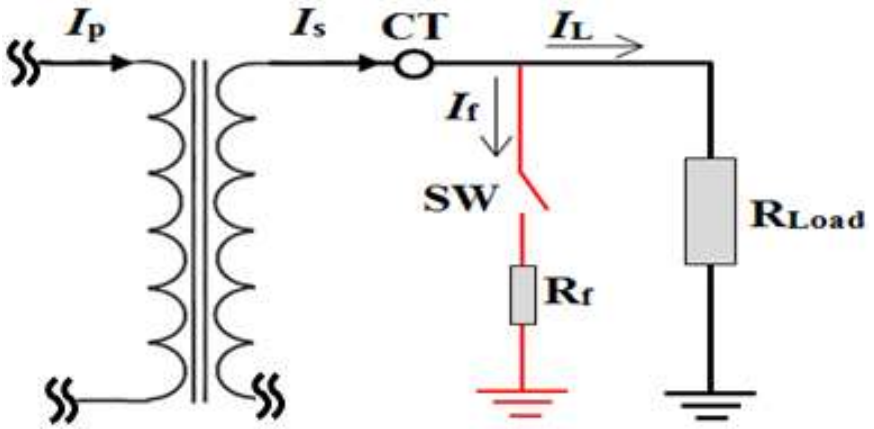

Fig 6-10 External fault representation

6.3. Flux density, power loss and interturn fault relationships

Since all equipment and needed parts were available in the laboratory, some other interesting tests were carried out to see what is the effect of internal faults such as interturn faults on flux density and power loss in the transformer core. This may be utilized by researchers who search in these relationships. The Power analyzer system shown in Fig 6-11 is multi measurement device. It was used for measuring currents and voltages of each phase applied to transformer windings. It can also be used for measuring the power loss.

Fig 6-11 Power analyzer system

6.3.1. Flux density and power loss relationship

The secondary voltages and primary currents are measured by power analyser system when it is connected to the secondary windings of no-load transformer. v_2 is

the secondary voltage in the equivalent circuit of the no-load transformer as shown in Fig 6-12. Since $I_2 = 0$, $v_2 = e_2 = e_1$. It means that the power loss (P_{Sec}) on the power analyser system is the core loss only (e_1^2/g_c). But when the power analyser system is connected to the primary winding, it measures primary voltages and currents (v_1 and I_1 in Fig 6-12). Therefore, the power loss (P_{Pri}) represents the total power loss of the system including copper loss ($I_1^2 R_1$) of primary wires i.e. $I_1^2 R_1 + e_1^2/g_c$. However, the copper loss is so small that is usually negligible in calculations as shown in tables 6-2 and 6-3.

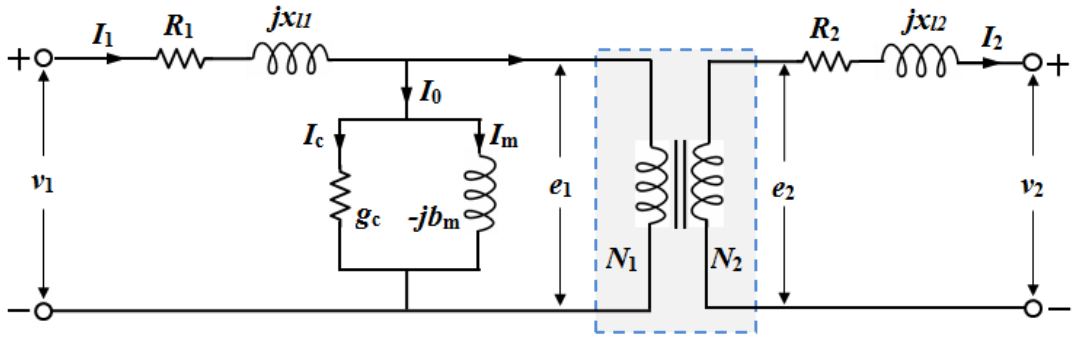

Fig 6-12 No-load transformer equivalent circuit

The voltage supply was gradually increased and consequently the flux density in the core increased. Fig 6-13 shows the core loss corresponding to different flux densities. The transformer core weight was 72.7515 kg. Normally, at flux density 1.7 Tesla in no-load transformer with such size, the core loss ranging from 1.0 W/kg to 1.2 W/kg.

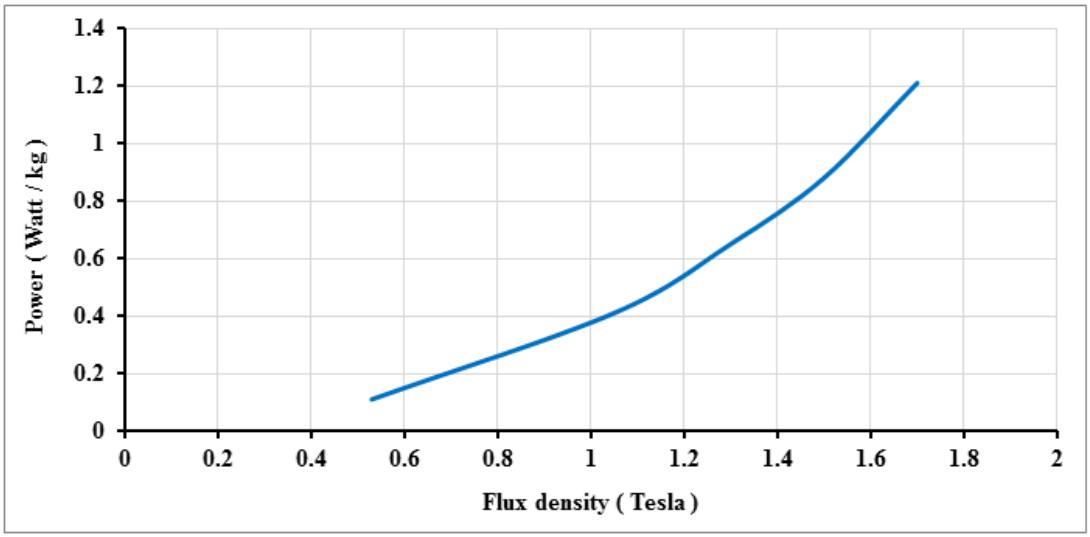

Fig 6-13 No-load transformer core loss

6.3.2. Power loss and interturn fault relationship

In no-load case, the pure copper loss (P_{cu}) can be calculated by subtracting Power loss (P_{Sec}) which represents the core loss from the total power loss (P_{Pri}) such that

$$P_{cu} = P_{Pri} - P_{Sec} \tag{6-3}$$

The voltage supply was set to two values 30V and 60V which were corresponding to flux densities 0.53 and 1.05 Tesla respectively. The number of turns that were short circuited was increased at each fixed flux density. Tables 6-2 and 6-3 show the increase of power losses in the no-load transformer due to the increase in number of short-circuited turns at the two flux densities respectively.

Table 6-2 Power losses at flux density of 0.53 Tesla

Number of short-circuited turns	P_{Pri} (Watt)	P_{Sec} (Watt)	P_{cu} (Watt)
0	8.04	7.95	0.09
1	9.99	9.68	0.31
2	15.4	14.7	0.7
3	24.4	23.7	0.7
4	35.3	33.7	1.6
5	48.2	46.5	1.7
6	66.5	63	3.5

Table 6-3 Power losses at flux density of 1.05 Tesla

Number of short-circuited turns	P_{Pri} (Watt)	P_{Sec} (Watt)	P_{cu} (Watt)
0	29.7	29.6	0.1
1	37.1	36.8	0.3
2	58.3	56.9	1.4
3	95	93.9	1.1
4	140.2	138	2.2
5	196.2	195	1.2
6	260	258	2

It can be noticed that the copper loss was very small compared with the core loss which was higher at higher flux density as shown in Fig 6-14.

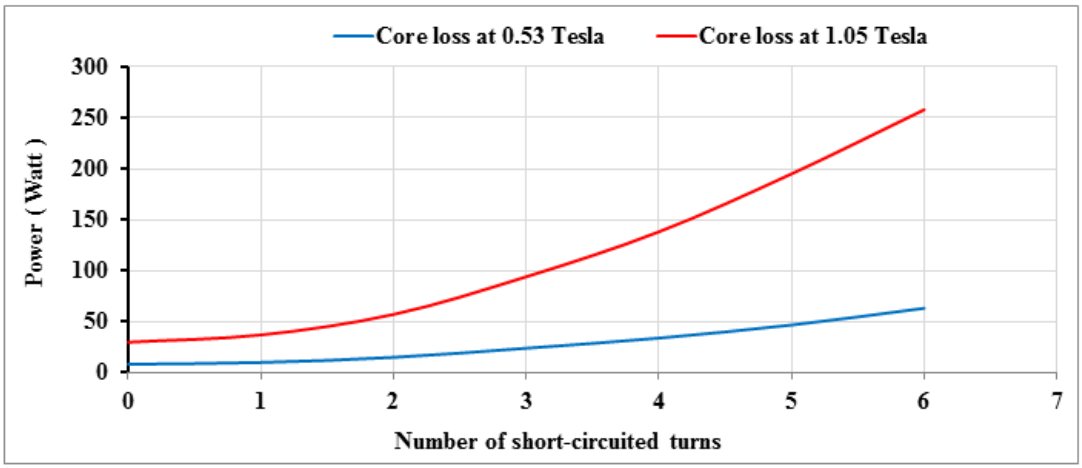

Fig 6-14 No-load transformer core loss due to short-circuited turns

It was clear that power losses proportionally increase with the increase of number of turns that short-circuited because the latter resulted in increase of primary current. Also, there was power loss in wires of winding turns due to the high circulating current in the loop of short-circuited turns. This power loss was in the form of heat in wires and smoke was seen came out from infected turns when short-circuit turns was applied in just very short time in order not to be damaged.

6.3.3. Flux density and interturn fault relationship

The effect of short-circuit turns on the distribution of flux in core limbs was tested when the transformer runs once with load and once without load.

1. The test on no-load transformer

The test was carried out under two supply voltages of 30V and 60V as a maximum value in order to make a short circuit between turns in less danger. Interturns were tested in all phases but since the result was the same, only that in phase A is shown. The flux density in the core limb of faulty phase A was affected by the increase of the turns that were short-circuited as shown in Figs 6-15-a and 6-15-b.

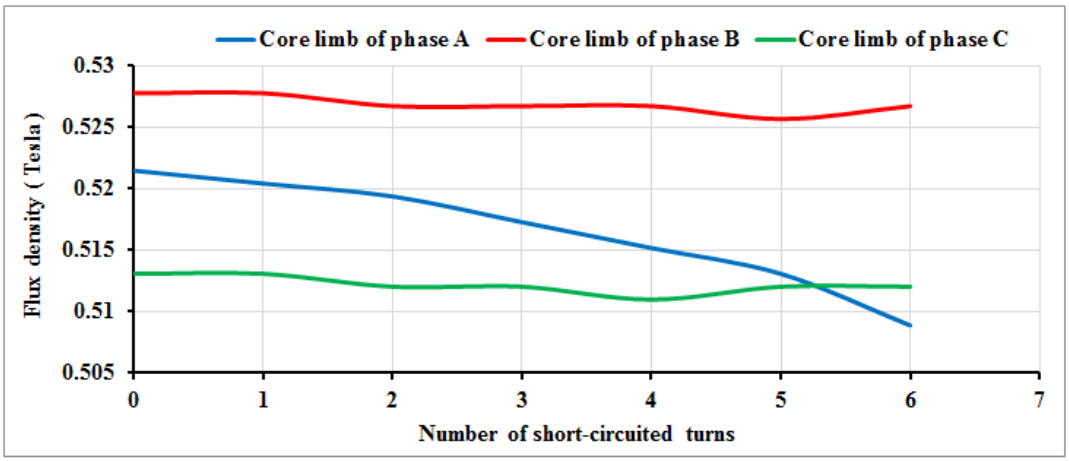

(a)

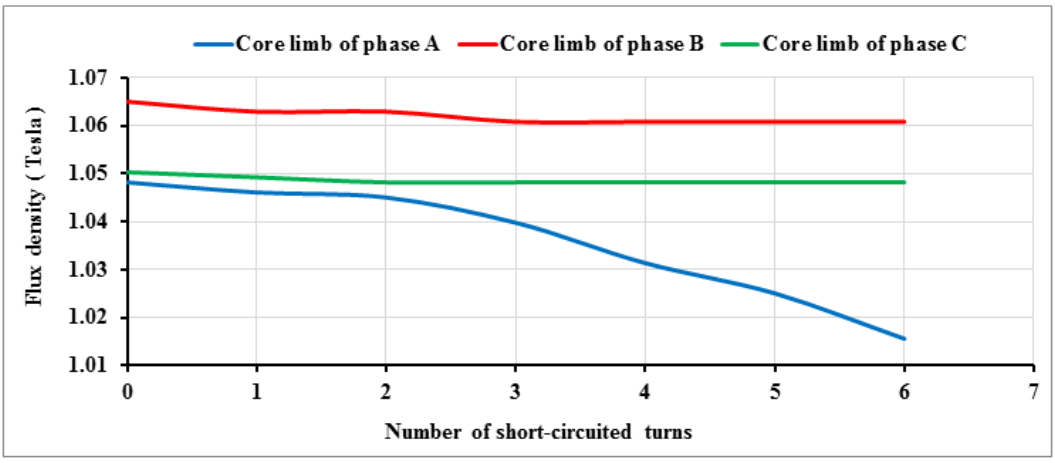

(b)

Fig 6-15 The effect of interturn fault on flux density when no-load transformer was operated at (a) 30V and (b) 60V

2. The test on on-load transformer

The same previous test was carried out when the transformer connected to the load. The effect of short-circuited turns on the flux density was the same as no-load transformer test as shown in Figs 6-16-a and 6-16-b.

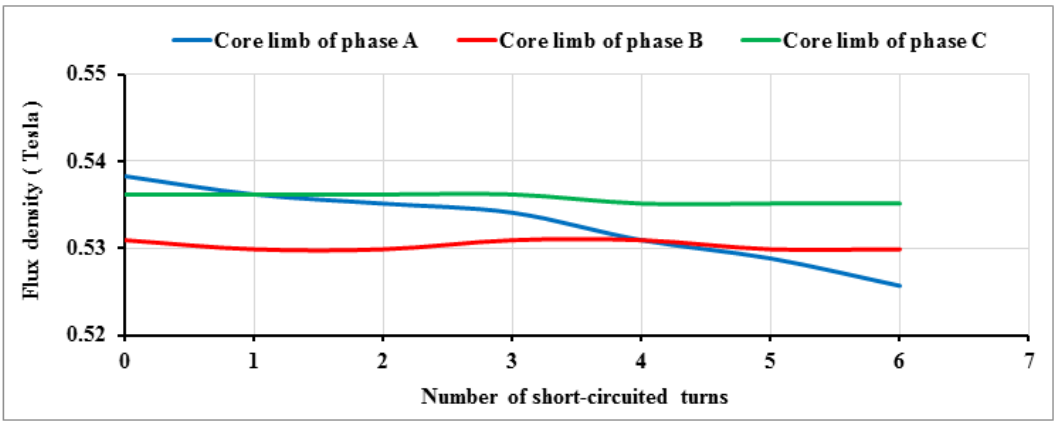

(a)

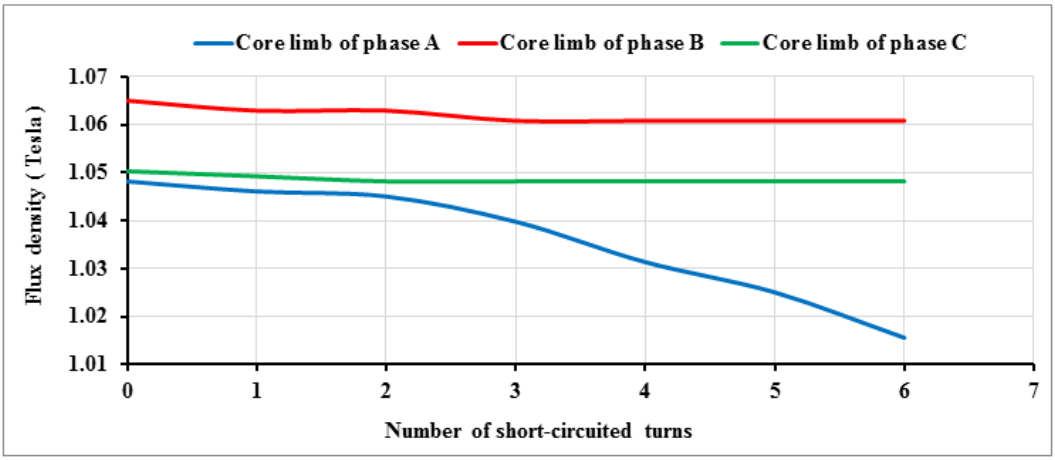

(b)

Fig 6-16 The effect of interturn fault on flux density when on-load transformer was operated at (a) 30V and (b) 60V

It can be concluded in either tests that when more turns were short-circuited, the flux density decreased in the core limb which was wrapped by the winding of phase A in which the turn were short-circuited.

But why it happened? The answer is that when an interturn fault occurs on the primary winding, a very large circulating current will flow in the loop of the short-circuited turns. This current is the source of a magnetomotive force (mmf) which opposes to the primary winding and with the same direction of the secondary winding. Thus, the turn-turn fault has an effect in decreasing the main flux, which results in increasing the primary current and decreasing the secondary current to compensate it. In a healthy transformer, the distribution of flux density has a horizontal symmetry axis that passes through the centre of the transformer core limbs and the magnetic flux in the core is much higher than the leakage flux. After occurrence of interturn fault, the leakage flux around the short-circuited turns increases significantly while the flux in the core limb that is surrounded by the short-circuited turns decreases. Thus, the distribution of the magnetic flux density has no symmetry i.e. it becomes asymmetrical [123].

When the interturn fault occurs on the secondary winding, the current and flux density distribution has similar characteristics with the occurrence on the primary. Such as the primary and secondary currents of non-faulty phase will increase, the secondary current of faulty phase will decrease and the distribution of the magnetic flux density is asymmetrical inside the faulty transformer [123].

6.4. Laboratory model description

The model that was built in laboratory consisted of the following main parts:

1. Three-phase transformer
2. Three-phase switch
3. Three-phase power supply
4. Three-phase load
5. HOTBUT, DIN Rail, CT132, IEC60044-1current transformer with turn ratio of 40/5, Class 3 FS5 and rated burden is 1VA
6. LEM NORMA D 6000 power analyzer system

7. NI USB-6259 data acquisition (DAQ) card
8. Switch relay, OMRON G8P series SPST-NO, 5VDC, 30A
9. NI LabVIEW 2013 software which has already been installed in a personal computer (PC)

The schematic diagram in Fig 6-17 shows how the system model was connected. Six current transformers (CTs) were deployed on both sides of a three-phase transformer as three CTs for phases A, B and C on the primary side CT1, CT2 and CT3 respectively and similarly on the secondary side CT4, CT5 and CT6.

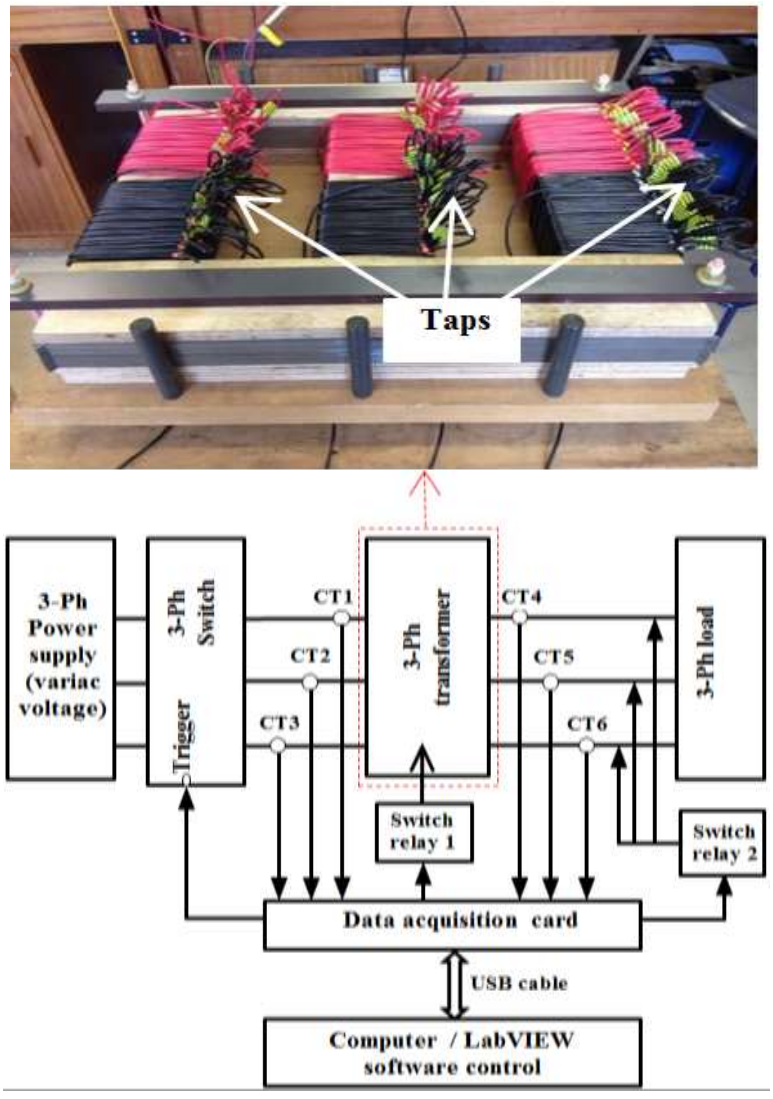

Fig 6-17 Schematic diagram for the system model

The LEM NORMA D 6000 power analyzer system was also connected to the transformer windings in order to be used for monitoring values of current and voltage of each phase and thus, adjusting voltages and currents by turning three-phase variac voltage (power supply) until it can be seen that the three voltages are balanced on the phases of the transformer. The NI USB-6259 data acquisition card was connected to a personal computer (PC) via USB cable and controlled by installed NI LabVIEW 2013 software, which has been programmed to trigger a three-phase switch for energization, switch relay 1 for generating internal faults and switch relay2 for generating external faults. The internal faults were generated via numbered tap points that were distributed along the transformer's winding.

Fig 6-18 shows the connection of data acquisition card (DAQ system) to measurement and switch relay components in the laboratory. Switch relays were received voltage trigger signals from the DAQ system to which was supplied reduced current signals by CTs. These current signals were converted into voltage signals using burden resistances of 0.1 Ω, in order to be accepted by the DAQ system. However, the voltage signals were converted back to current signals in the LabVIEW program. The LabVIEW model which was designed for controlling the practical tests is shown in appendix D.

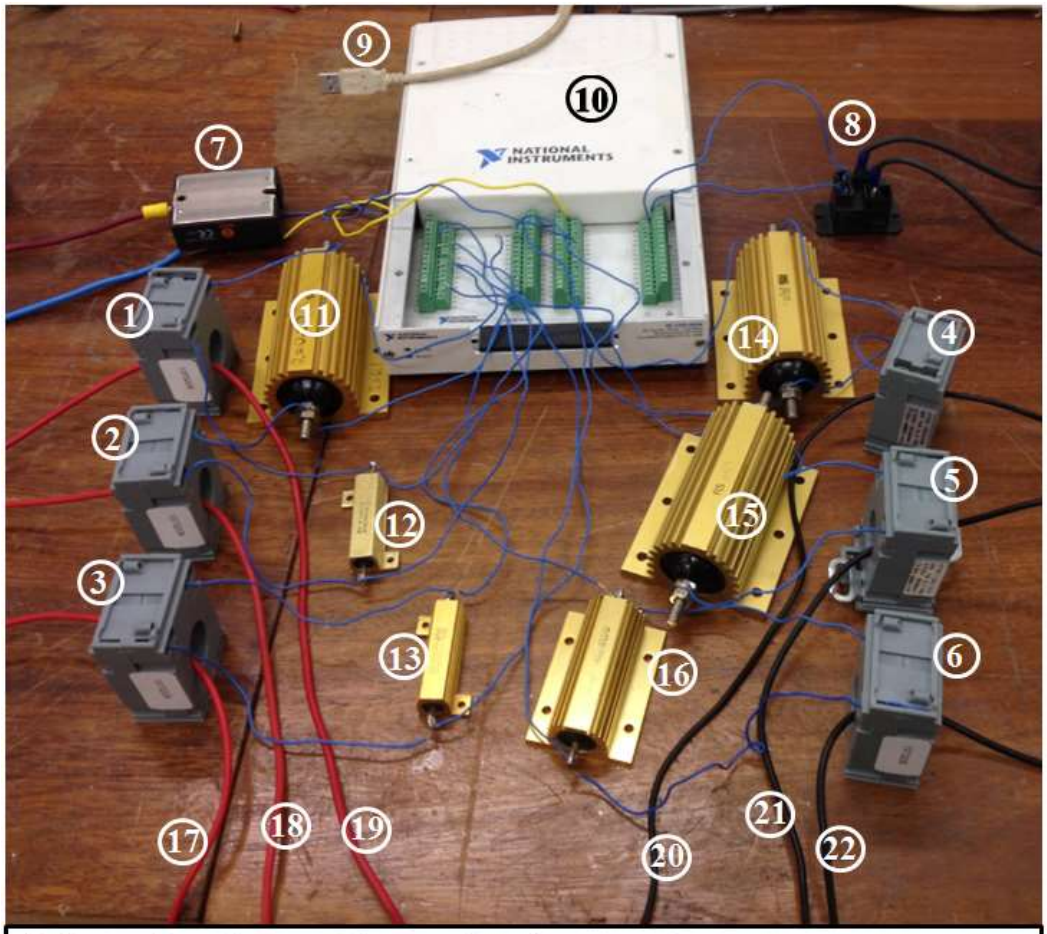

(1-3) current transformers set for measuring primary currents
(4-6) current transformers set for measuring secondary currents
(7-8) switch relays for internal and external faults
(9) USB connection cable between PC and data acquisition card
(10) Data acquisition card
(11-16) Burden resistance of 0.1Ω
(17-19) Connection cables between power supply and phases in primary side of transformer
(20-22) Connection cables between load and phases in secondary side of transformer

Fig 6-18 Data acquisition card connections

6.5. Experiment procedure in steady-state

As mentioned in 4.2, the proposed correlation protection technique is applying when the transformer is in operation. For results comparison, the experiment was carried out with the same procedure as in simulation using MATLAB/SIMULINK program.

The sample rate, which can be modified by the LabVIEW program, was selected as 10 kHz, i.e. 200 samples per cycle. The run time for the LabVIEW program to analyse the faults was 10 seconds, which means there were 100000 samples (excluding samples at zero time) collected from a Data Acquisition (DAQ) card and saved into seven columns in Excel sheet. The first column represents the sampling time, and then the next three columns represent the data that obtained from the primary side of phases A, B, and C respectively while the remaining columns represent the data that obtained from the secondary side of phases A, B and C respectively. All signals that were acquired from the data acquisition card were filtered from harmonics and noise using low pass filters with 50Hz cut-off frequency and Butterworth topology order 1 which can be done in the LabVIEW program. In consequence, the collected data were in the fundamental frequency and clear of noise and harmonics.

The data were imported to the MATLAB program for processing. Since there was a huge number of current samples in 10 seconds, only 2000 samples in 0.2 seconds were selected to be processed in the MATLAB program. These samples represent the fault zone, which was intended for processing. 200 samples for each cycle were divided into ten groups called windows consisted of 20 samples each. These windows were used for calculating correlation coefficients $r_{12,}$ r_{11} and r_{22}. So ten values of correlation coefficients were calculated in each cycle and 90 values for the whole run duration of 0.2 seconds because calculation was started from the second cycle i.e. from sample number 200. This is because the first cycle was saved to be auto-correlated with the second cycle. Therefore, 2000 samples subtracted by 200 samples is 1800 samples, i.e. 90 values of correlation coefficients in total.

6.6. Experiment procedure in transient state

The proposed CCR and PAD protection technique are applying when the transformer is energized. Also, for results comparison, the experiment was carried out with the same procedure as in simulation using MATLAB/SIMULINK program. In this experiment, the run time for the LabVIEW program to analyse faults or inrush condition was 0.4 seconds. This means that there were 4000 samples (excluding samples at zero time) collected from the data acquisition card and saved into the Excel sheet in order to be used by the MATLAB program later on.

The data in the Excel sheet were then imported to the MATLAB program for processing. In the case that the inrush condition was to be examined when the transformer was at no-load condition, the load was disconnected, which means that there were only three current signals were generated by CT1, CT2 and CT3 on the primary side of the transformer. However, in the case that the inrush condition was to be examined when the transformer was loaded, there were six current signals generated by CTs on the primary and secondary sides of three signals each.

6.7. Summary

The transformer model, construction details and how it was built in the laboratory as well as generating real internal and external faults on this model and all the equipment used were shown in this chapter. The real data that were obtained when generating different types of faults were stored in order to be used for testing the proposed alogrithims which were written as MATLAB program. The most commonly occurring fault in the transformer is the turn-to-turn shrot circuit fault, which damages the winding turns of the transformer. It was practically shown how this short circuit fault between turns generates a high circulating current which deteriorates the insulation between winding turns and hence burns them off.

Some other interesting tests were carried out to see how practically the interturn fault affects the distribution of flux in the transformer limbs where the windings are wrapped around and also, its effect on the power loss in the transformer core. This may be utilized by researchers in this field.

CHAPTER 7

Results and Discussions on Transformer in Steady-State Condition and CT Saturation

7.1. Introduction

In this chapter, the proposed correlation technique was tested practically against internal and external faults when transformer was in steady-state. Also, it was tested to see how it withstands and overcomes the problem of current transformer saturation. In order to test the technique on this problem, the Current transformer was turned into the saturation which usually caused by heavy faults particularly the external faults.

7.2. Faults versus the proposed protection technique results

The faults were generated practically as shown in the previous chapter. The data were then imported to the MATLAB program in order to be used in testing the

efficiency of the proposed protection algorithm against each fault as it will next be shown. The results of phase A either on primary or secondary sides were only shown here as the same results had been obtained from two other phases. However, the results of all phases are shown in appendix F. It should be noticed that the current values in the figures which were reduced by 1/8 (CT turns ratio) appeared slightly less than the actual current values that read by the power analyser system because they lost some of their values when treated by low pass filter in the LabVIEW program.

1. **Turn-turn fault (interturn fault)**

Two turns were short-circuited to generate an interturn fault on the primary side of phase A. The command was sent by the LabVIEW program to switch relay 1 and thus the fault occurred at approximately 4.8961second. As mentioned earlier, the large number of collected samples (100000 samples in 10 Seconds) was difficult to show or process. Also, as they were similar in steady state condition, samples can only be taken before and after the occurrence of a fault and 0.2 seconds was enough time for covering the area where the fault occurred as shown in Fig 7-1. In this fault zone, all the times at which the samples started to be taken were represented the start of simulation (zero time). So the fault zone consisted of 2000 samples started from zero time to 0.2 seconds.

In order to make it simple and easy, the MATLAB program run at the same time for all zones of phases. From the collected 100000 samples in 10 seconds, the samples for the zone of phase A started to be taken at zero-crossing from second 4.8521, then samples of phase C started from second 4.8554 as it was closer to zero-crossing than phase B in which the samples started from second 4.8587. This procedure makes the MATLAB program simply and easily compute the correlation coefficients of all phases at the same time rather than each phase separately but, the time shift between phases should be taken into account when specifying the time of the algorithm response. So only the amount of data in each zone was processed by the MATLAB program. The zone of faulty phase A can also be shown with respect to samples as in Fig 7-2.

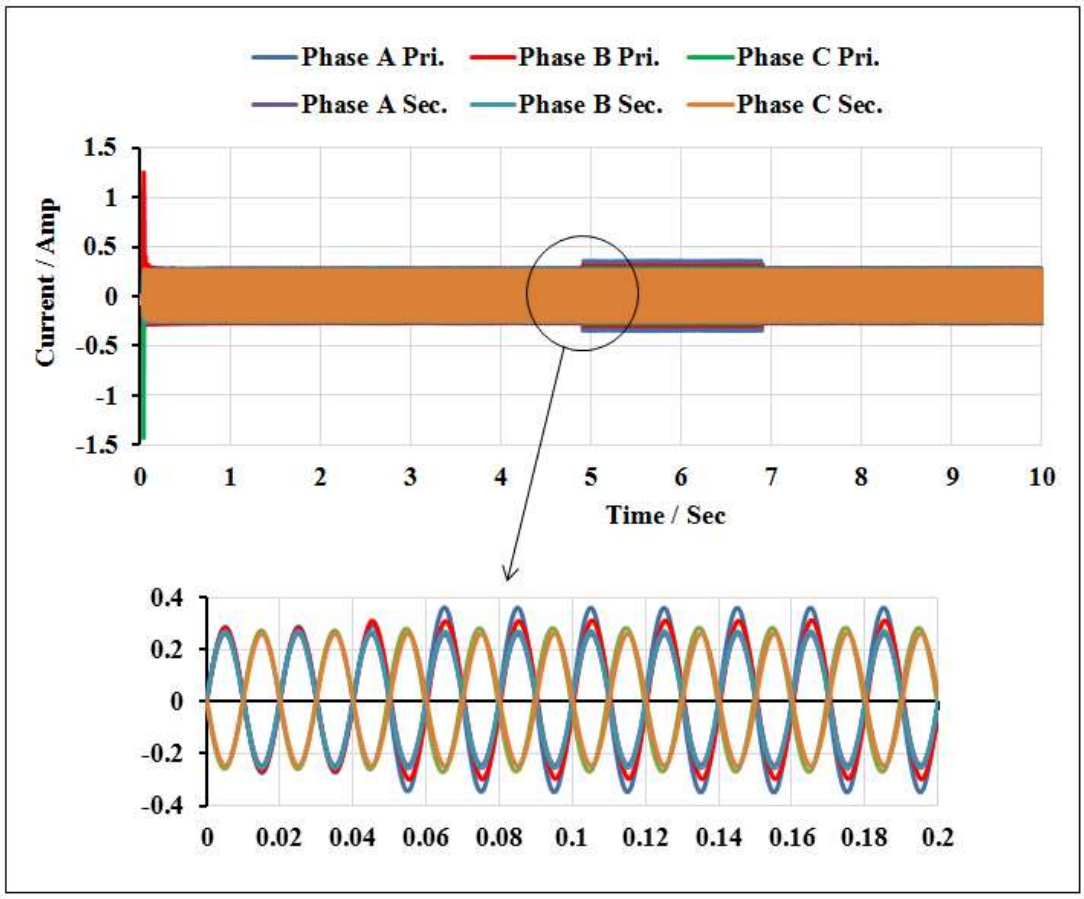

Fig 7-1 The currents of three phases during interturn fault in phase A

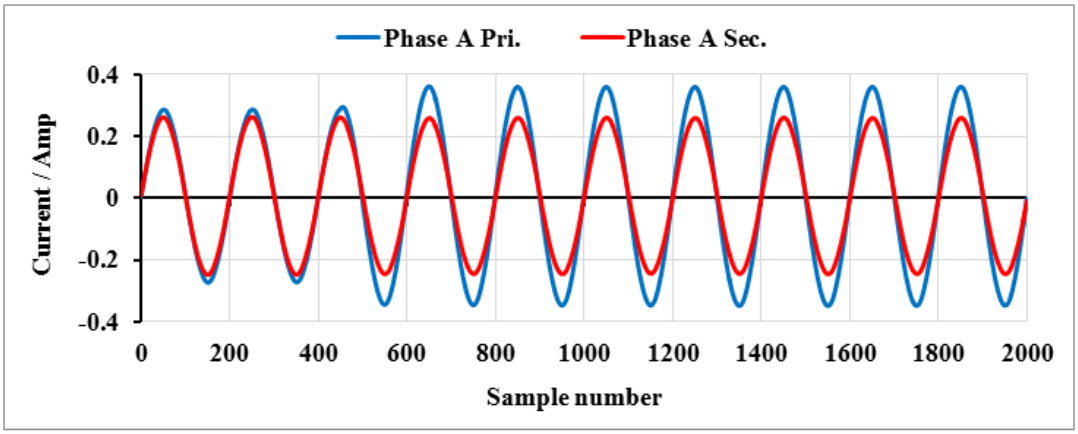

Fig 7-2 Primary and secondary currents during interturn fault in phase A

The correlation coefficients of phase A for the full duration of the fault zone are shown in Fig 7-3. Due to this fault, it can be noticed that at window 13, both r_{A11} and

r_{A12} reduced to less than 0.9 whereas r_{A22} slightly reduced to less than 1 because the fault occurred on the primary side.

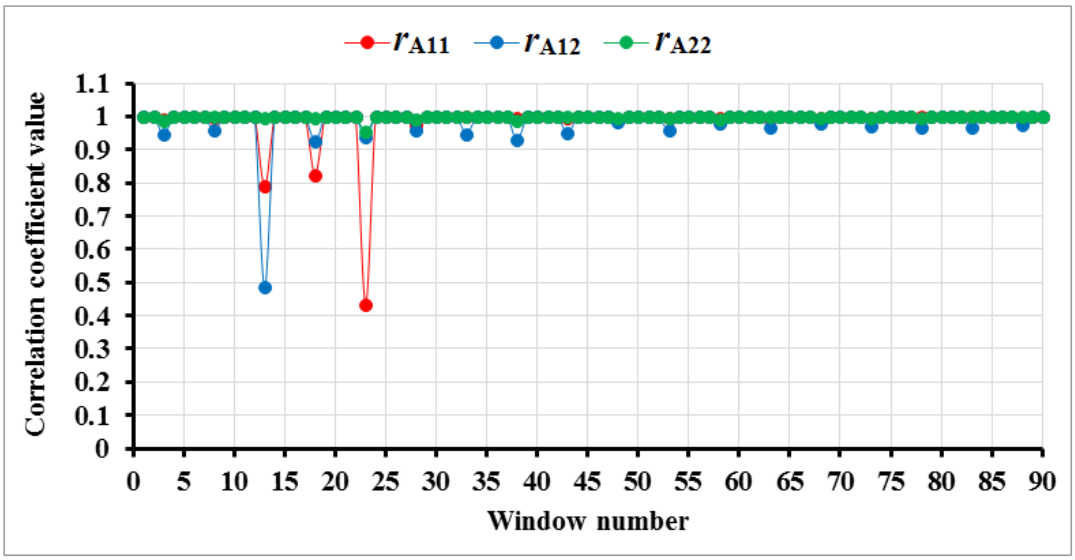

Fig 7-3 Correlation coefficients during interturn fault in phase A

By applying the algorithm of proposed technique, the fault was detected in window 13 which ended with sample number 460 (200 + 13 × 20), i.e. 460 × 0.0001 (time/sample) = 0.046 second. As explained earlier, the zero time of the samples in phase A started from second 4.8521, so the time at window 13 was 4.8521 + 0.046 = 4.8981 second. The time that was taken by algorithm to detect the fault which can then be calculated by subtracting the time of the fault detection from the time of the fault incidence. So the fault was detected after 4.8981 - 4.8961 = 0.002 second i.e. just 2 ms from incidence of the fault and consequently a trip signal was issued as shown in Fig 7-4.

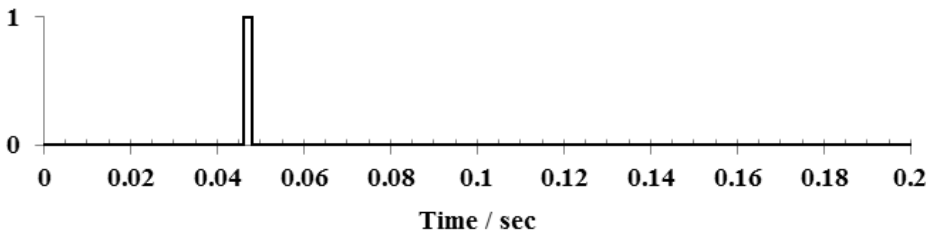

Fig 7-4 Trip signal was issued due to interturn fault in phase A

2. Turn-ground fault

The fault was generated on the secondary side of phase A when switch relay 1 was closed at approximately 4.8464 second. The current samples in the fault zone of all phases were changed due to the fault as shown in Fig 7-5-a. but the significant change occurred in the faulty phase A as shown in Fig 7-5-b. The samples of the fault zone started from seconds 4.8029, 4.8063 and 4.8097 for phases A, C and B respectively.

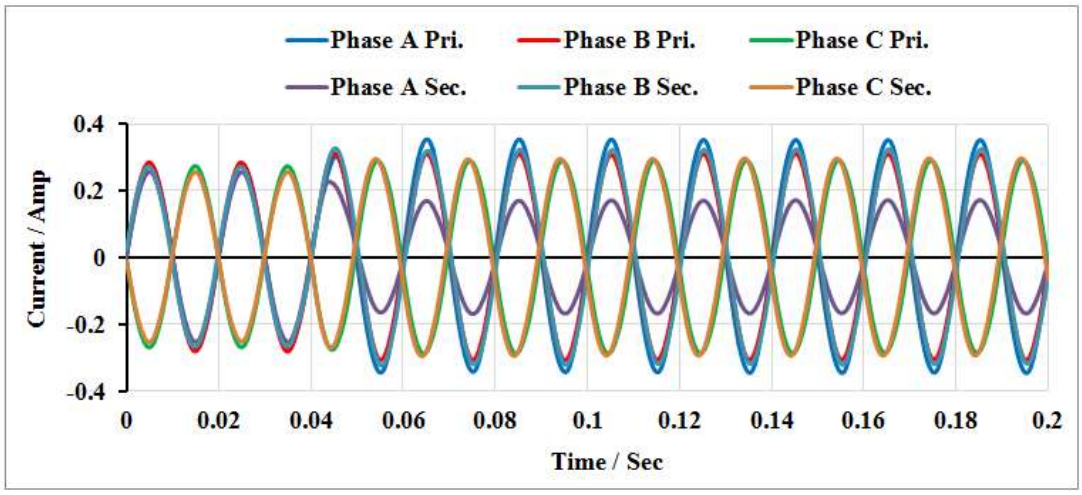

(a)

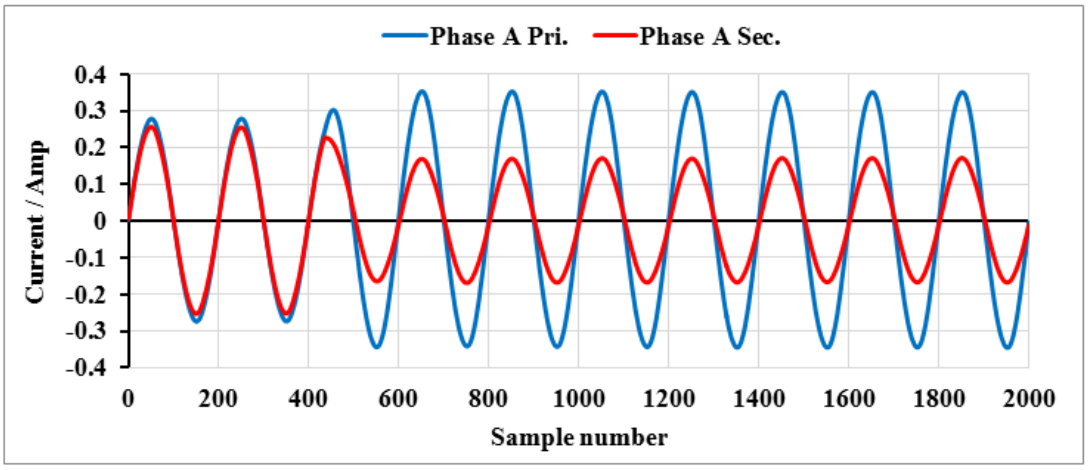

(b)

Fig 7-5 Change in currents due to turn-ground fault in phase A for (a) three phases and (b) phase A

Because of the presence of protection resistor (R_f), it can be noticed that the change in currents was not as big as it should be.

This fault has caused obvious changes in the values of correlation coefficients on the faulty phase A as shown Fig 7-6.

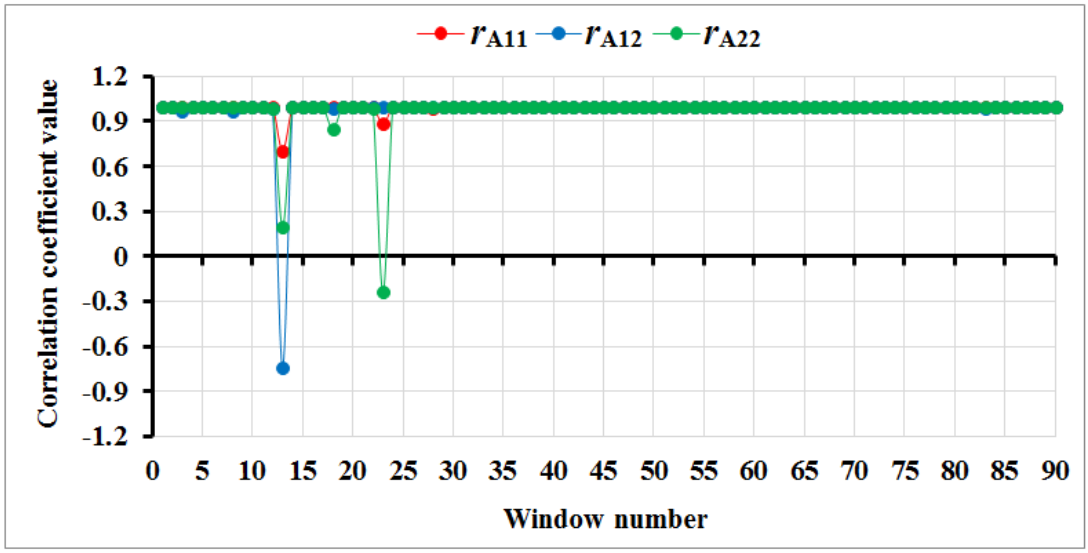

Fig 7-6 Correlation coefficients during turn-ground fault in phase A

It can be noticed that at window 13, the three coefficients r_{A11}, r_{A12} and r_{A22} simultaneously reduced to less than 0.9. This means that the fault was detected at this window which ended with sample number 460, i.e. it was 460×0.0001 (time/sample) =0.046 second in samples of the fault zone. Since the zero time of the samples started from second 4.8029, the time at window 13 can be calculated as 4.8029 + 0.046 = 4.8489 second which means that the fault was detected after 4.8489 - 4.8464 = 0.0025 second or 2.5 ms from the instant of the fault occurrence.

3. Single phase-to-ground fault

The fault was generated on the secondary side of phase A when a pulse signal sent by the LabVIEW program to close the switch relay 1 at approximately 4.8449 second. The primary and the secondary currents largely increased and decreased respectively as shown in Fig 7-7.

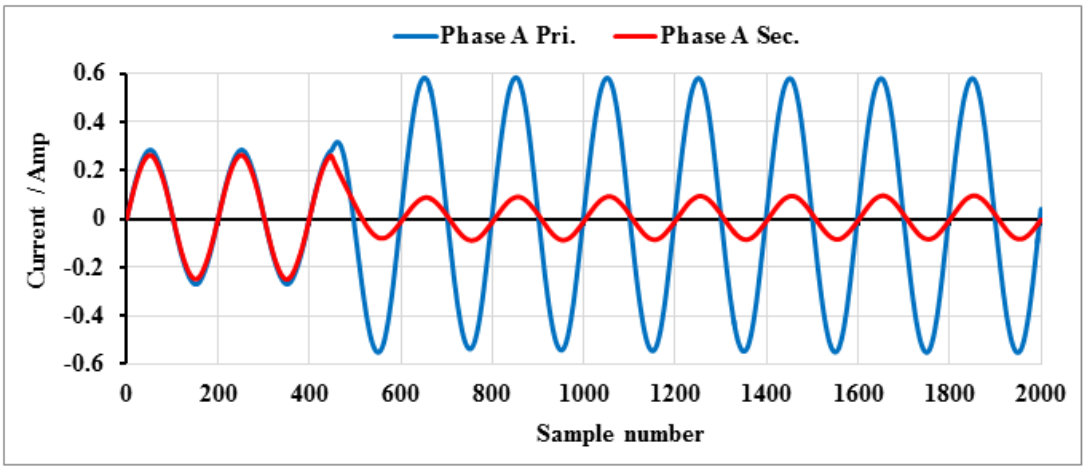

Fig 7-7 Change in currents due to single phase-to-ground fault on secondary side of phase A

In fact, when this fault occurs, the value of primary current should be higher than this value and the secondary current should be very small (almost zero) because the entire fault current almost flows through a very low resistance of fault branch to the ground. But since a protection resistor (R_f) was connected in the fault branch, the currents were reduced as shown in the last figure. The samples of the fault zone started to take from the whole duration of acquired samples at seconds 4.8002 in phase A, 4.8037 in phase C and 4.8069 in phase B.

Because of this high fault current which resulted in a big difference between primary and secondary currents, the correlation coefficients were greatly affected particularly r_{A12} which reduced to less than -0.9. The reason behind is that when the fault occurred, the primary current was still increasing whereas the secondary was decreasing as shown in Fig 7-8.

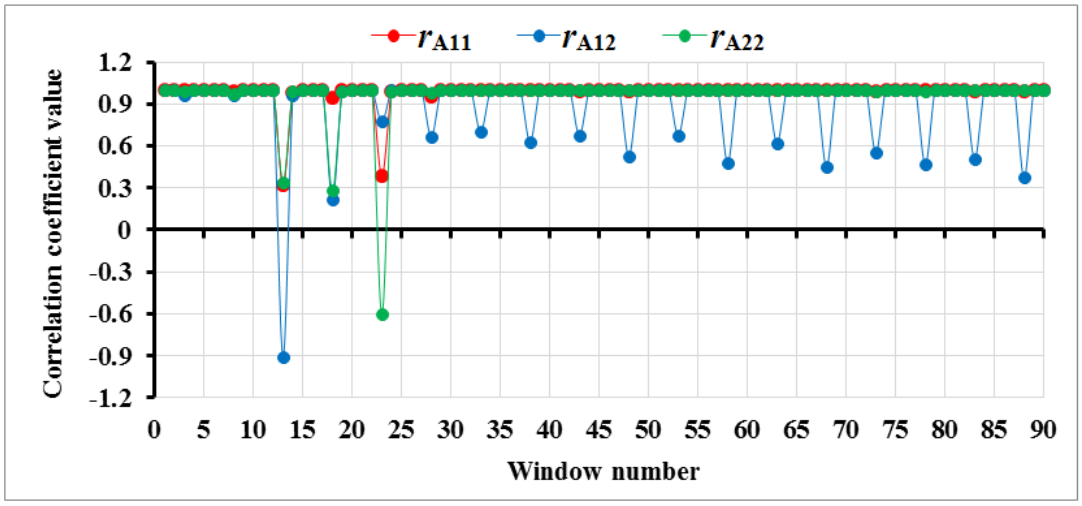

Fig 7-8 Correlation coefficients during single phase-to-ground fault on secondary side of phase A

It can be seen that at window 13, the three coefficients r_{A11}, r_{A12} and r_{A22} simultaneously reduced to much less than 0.9. This means that the fault was detected in this window which ended with sample number 460 or 460 × 0.0001 (time/sample) = 0.046 second in samples of fault zone. Since the zero time of the samples started from 4.8002 second and the fault occurred at 4.8449 second, the time that was taken by algorithm to detect the fault was (4.8002 + 0.046) - 4.8449 = 0.0013 second or 1.3 ms. This fast detection of the fault was a result of the big impact on the current signals caused by the fault which consequently led to a quick and large change in correlation coefficients values.

The fault current was very high when it was generated on the primary side of phase A as shown in Fig 7-9. However this fault current was reduced by the protection resistance (R_f) which resulted in a small amount of primary current was transferred to secondary side.

The fault occurred approximately at 4.8464 second and the samples of the fault zone started at seconds 4.7932 in phase A, 4.7966 in phase C and 4.7999 in phase B. The fault was detected at window 17 as the correlation coefficients r_{A11}, r_{A12} dropped to less than 0.9 in this window as shown in Fig 7-10.

Thus, the last sample of window 17 was 540 (200 + 17 × 20), so the fault was detected after (4.7932 + 540 × 0.0001) - 4.8464 =0.0008 second or 0.8 ms. This was very fast fault detection because the fault current was heavy and occurred close to the peak current signal at which the signal started to turn.

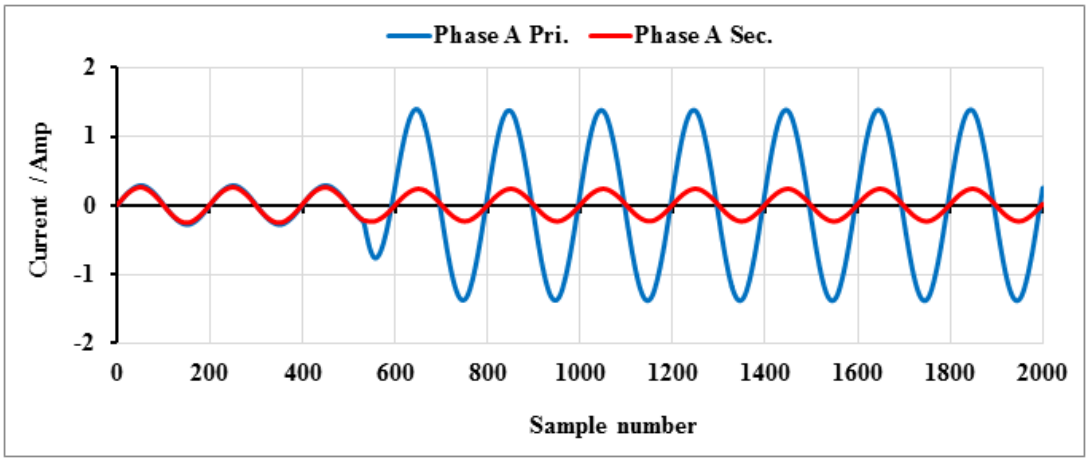

Fig 7-9 Change in currents due to single phase-to-ground fault on primary side of phase A

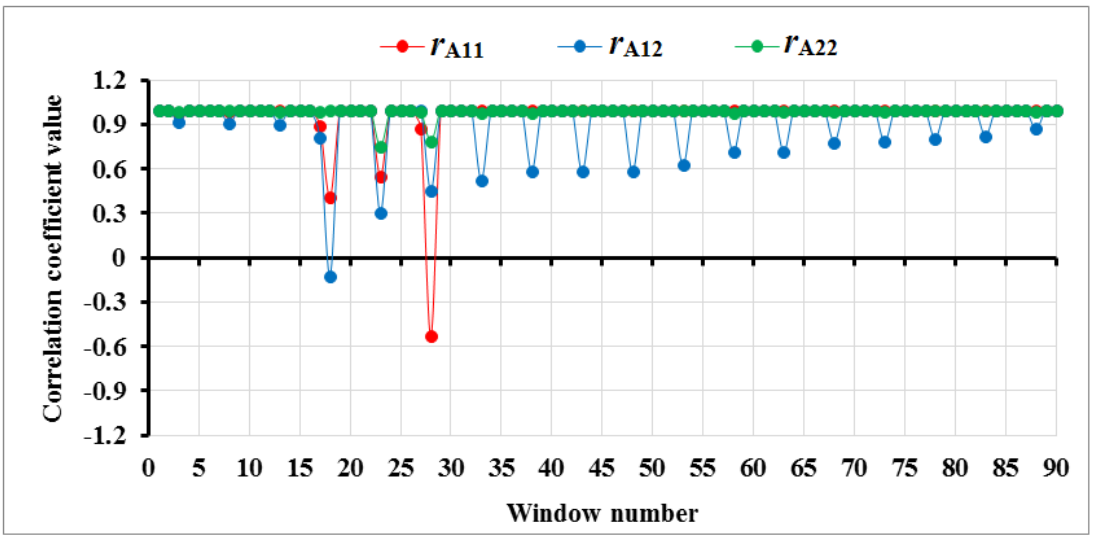

Fig 7-10 Correlation coefficients during single phase-to-ground fault on primary side of phase A

4. External fault

The fault was generated on the secondary side of phase A when switch relay 2 was closed at approximately 4.8465 second. Phase A was highly affected by the fault as shown in Fig 7-11. Since the fault occurred outside the transformer protected zone, CTs on both primary and secondary sides measured the same increase in current values, and also the waveforms had the same shape, therefore the currents remained identical to each other as shown in Fig 7-12. The samples of the fault zone started from seconds 4.796 in phase A, 4.7992 in phase C and 4.8026 in phase B.

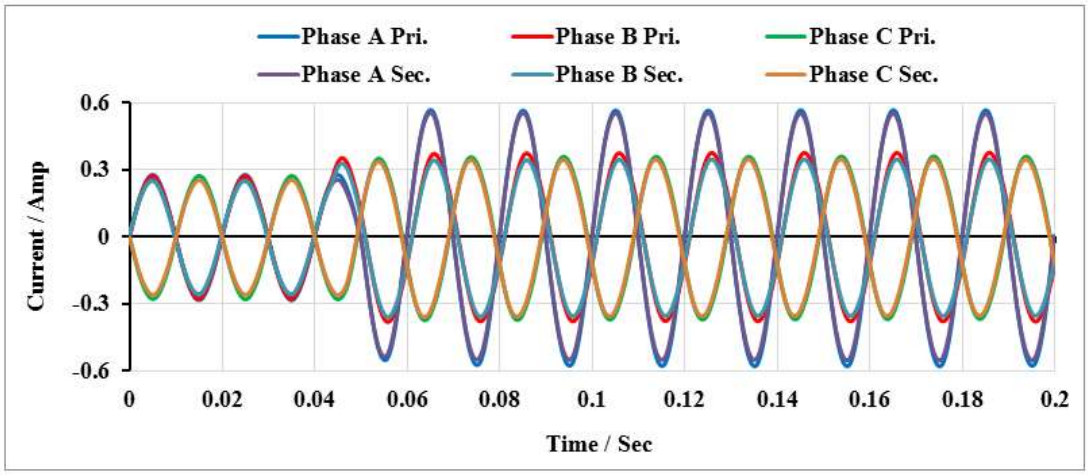

Fig 7-11 Change in currents during external fault in phase A

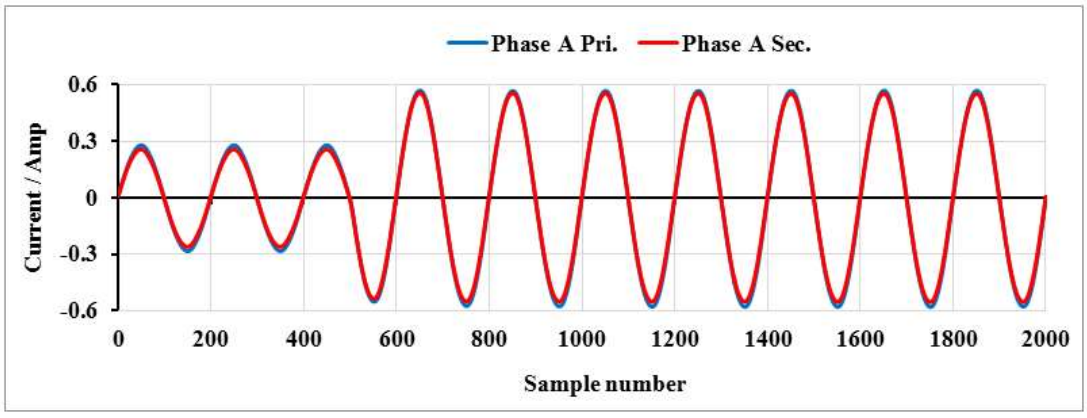

Fig 7-12 Primary and secondary currents during external fault in phase A

The correlation coefficients of phase A for the full duration of the fault are shown in Fig 7-13. It can be seen that at window 18, both r_{A11} and r_{A22} reduced to less than 0.9 as there was a change in both primary and secondary currents. But r_{A12} slightly reduced to less than 1 and remained greater than 0.9 for the whole duration of the fault, because the increase in both currents were the same and they were still identical to each other and consequently r_{A12} was not affected and remained above 0.9. This happens only in the case of external faults. According to the flowchart of the algorithm shown in Fig 4-4, the relay remained stable and didn't issue a trip signal to the circuit breaker against this fault. This is an action that needs to be taken by the relay when an external fault occurs.

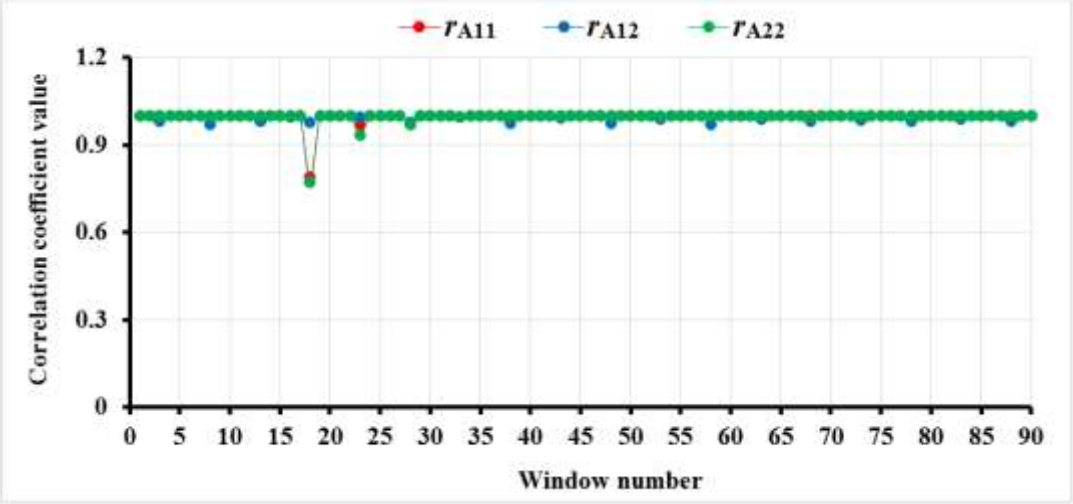

Fig 7-13 Correlation coefficients in case of external fault in phase A

7.3. CT saturation case

The current transformer that used in the experiment needs high current in order to be driven into saturation therefore, the faults were generated on the primary side as fault currents will be higher. In addition, the response of the algorithm to these faults can be shown here as they were only faults generated on the secondary side were shown in the previous section. The previous researches on this case have confirmed that even at major external faults, there is always a delay between the occurrence of such faults and initial saturation of CT.

This delay is normally in the range of 3 ~ 5 ms during which the primary current is unaffected and transformed correctly to the secondary side of the CT without any differential current [124]. In the case of internal fault occurrences, initially CT performs properly, though theoretically, differential current takes place simultaneously and instantaneously with these faults [125]. Hence, the speed response of the proposed technique was tested to make sure that is able to detect faults before CT saturation starts. The cases of possible saturation to CTs due to faults were tested by the proposed algorithm as follows.

1. CT saturation due to turn-ground fault

The 5Ω protection resistor (R_f) was replaced with 1Ω in order to increase the fault current. The fault occurred at approximately the second 4.8571 on the primary side of phase A. Thus, the current transformer CT1 was most likely to be saturated, therefore the CT burden of CT1 was increased by setting a resistance of 4Ω in order to make this CT become saturated during the fault. Consequently, the CT1 was saturated at the beginning of the third cycle and its secondary current, which is a replica of the primary current, was distorted as shown in Fig 7-14.

The execution time of the LabVIEW program to collect the samples was also 10 seconds the same as in the previous section, and thus the zone that covers the case was also 0.2 seconds and the 2000 samples to be processed in the MATLAB program started from seconds 4.8176, 4.8243 and 4.8211 for phases A, B and C respectively.

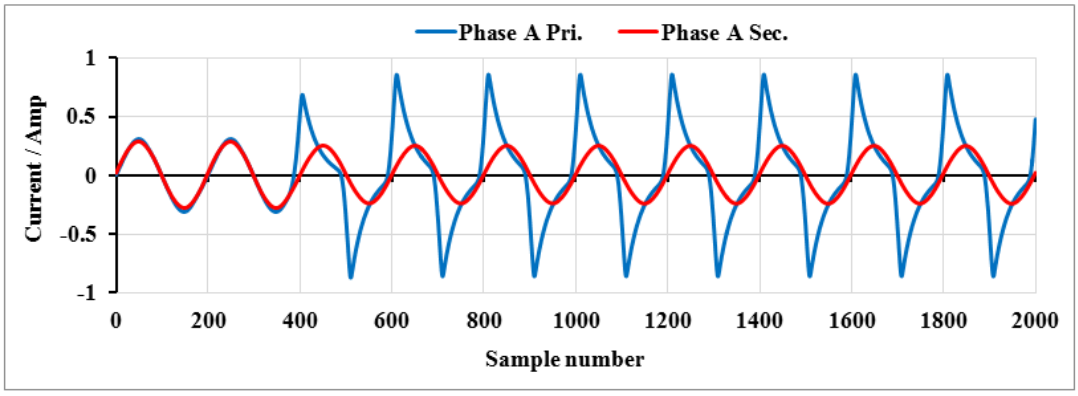

Fig 7-14 CT saturation during turn-ground fault in phase A

Unlike the MATLAB/SIMULINK program, the instant of the fault occurrence cannot practically be controlled. Therefore, this fault cannot be generated at an exact time. The fault occurred during the normal increase of the current cycle, so there was no significant auto-correlation for the first samples of the fault current.

The correlation coefficients for the whole duration of fault zone are shown in Fig 7-15. Due to this fault, it can be noticed that at window 11, both r_{A11} and r_{A12} reduced to less than 0.9 while r_{A22} was not much affected and reduced slightly to less than 1 because of the protection resistor as well as the fault occurred on primary side. As the saturation problem does not occur immediately since it takes time to start (time to saturation), there was enough time for the algorithm to respond for this fault. Accordingly, the algorithm detected the fault at window 11 which ended in sample number 420 (200 + 11 × 20) or 420 × 0.0001 (time/sample) = 0.042 seconds in the selected samples zone. Since the samples started at 4.8176 seconds, the fault was recognised after (4.8176 + 0.042) - 4.8571 = 0.0025 seconds or 2.5 ms from the incidence of the fault at which the CT1 started to saturate. This means that the algorithm was an efficient scheme and fast enough to detect the fault before the CT was saturated although it saturated quickly.

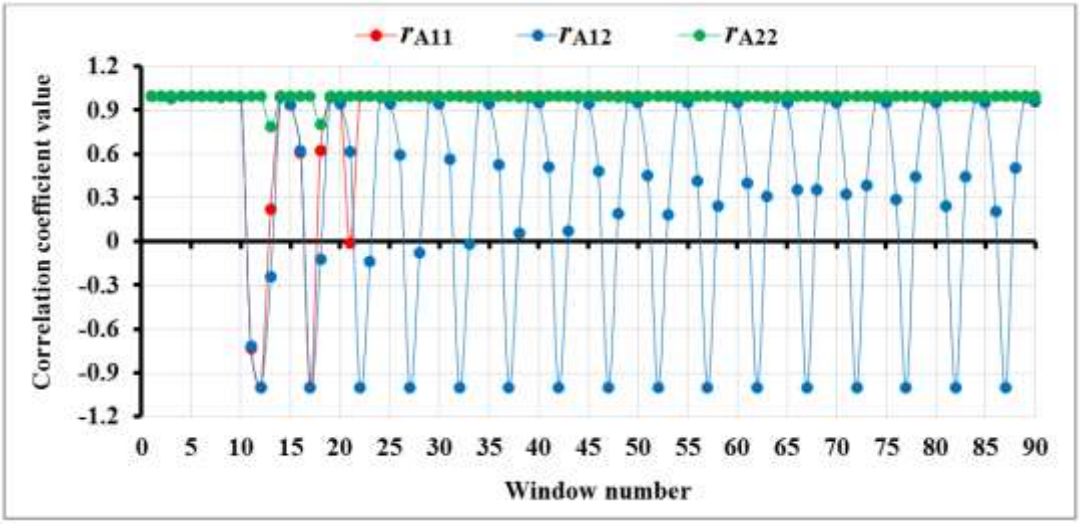

Fig 7-15 Change in correlation coefficients due to CT saturation caused by turn-ground fault

2. CT saturation due to single phase-to-ground fault

The fault was generated on the primary side of phase A in which the secondary current is supposed to be zero. But because the existence of R_f, there was some secondary current flowed through to the load. However, the response of the algorithm will be faster when there is no or almost zero current on the secondary side. This can be achieved by simulating this fault in MATLAB/SIMULINK or Alternative Transients Program (ATP) programs as there will be no risk to do so.

The fault occurred at approximately the second 4.8567 and the samples of the fault zone that were processed started from seconds 4.827, 4.8339 and 4.8305 for phases A, B and C respectively. As a result of this fault, the current transformer CT1 which is located on the primary side was saturated at the end of the second cycle and consequently, the primary current was distorted as shown in Fig 7-16. It can also be noticed here that the fault occurred during the normal decrease of the current cycle.

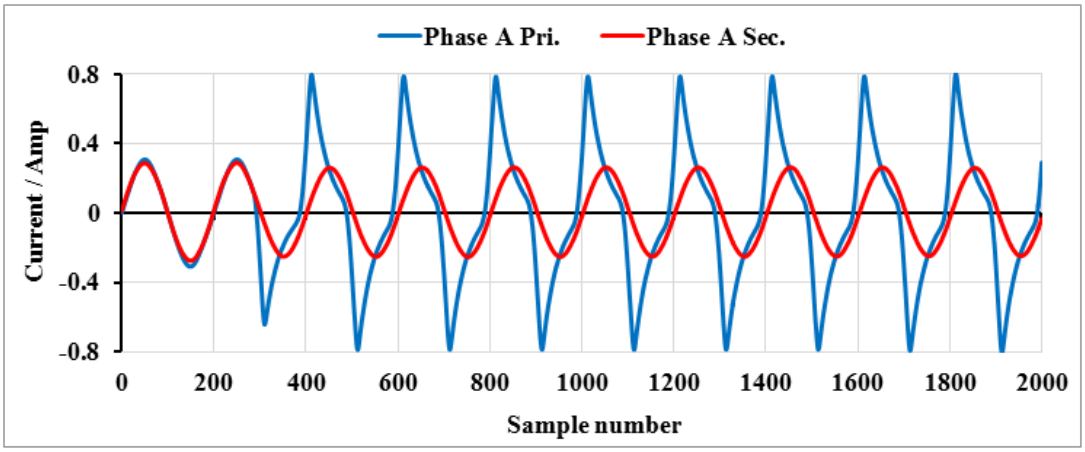

Fig 7-16 CT saturation during single phase-to-ground fault in phase A

As a consequence of this fault, both correlation coefficients r_{A11} and r_{A12} reduced to less than 0.9 at window number 6 whereas r_{A22} reduced slightly to less than 1 because the fault occurred on the primary side as shown in Fig 7-17. However r_{A22} should also be less than 0.9 at window 6 as the secondary current is supposed to become almost zero due to this fault as mentioned earlier and this can be seen when

this fault is modelled and tested by MATLAB SIMULINK or ATP programs. According to the changes in correlation coefficients, the fault was detected at window 6 which ended by a sample number 320 (200 + 6 × 20) or 320 × 0.0001 = 0.032 second in the selected samples zone. Thus, the fault was detected after (4.827 + 0.032) - 4.8567 = 0.0023 seconds or 2.3 ms from the incidence of the fault i.e. at which the saturation in CT1hadn't taken place yet. It means that the algorithm effectively responded to the fault before the CT was fully saturated.

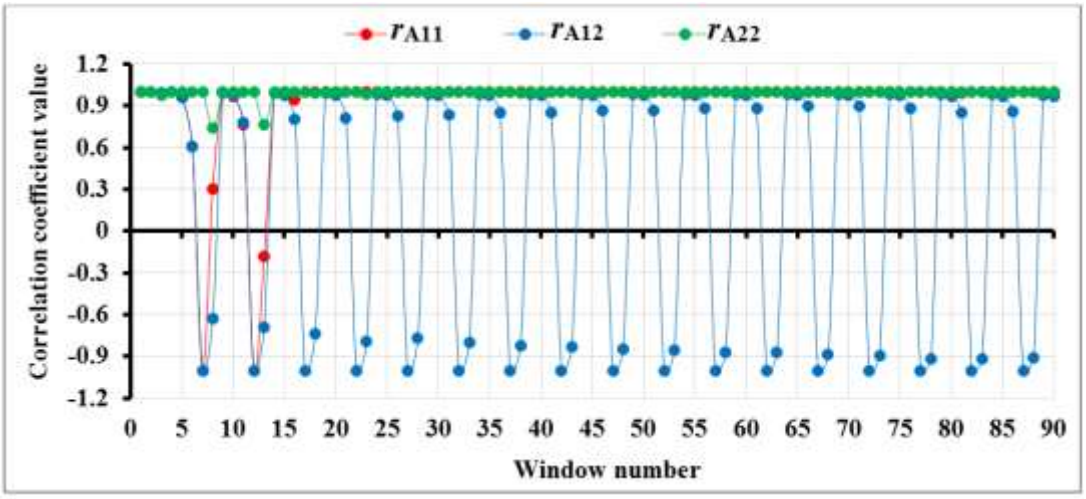

Fig 7-17 Change in correlation coefficients due to CT saturation caused by phase-to-ground fault

3. CT saturation due to external fault

For CT saturation purposes, the external fault, which was generated in phase A was also increased by decreasing the value of R_f to 2.5Ω. It was measured at approximately 26.21 Amp, and consequently CT4 will be more exposed to saturation as it is the closest to the fault point. So its burden was increased to 4Ω to make it saturated when the external fault occurred and to see how the algorithm responds in this case. The fault occurred at approximately the second 4.8437. As expected, the CT4 was deeply saturated and only the secondary current was distorted while the CT1 on the primary side was still working properly as shown in Fig 7-18. This suggests that both CTs on the primary and secondary sides are not identical and hence they do not saturate at the same time. However, the case of two identical CTs saturation was next examined.

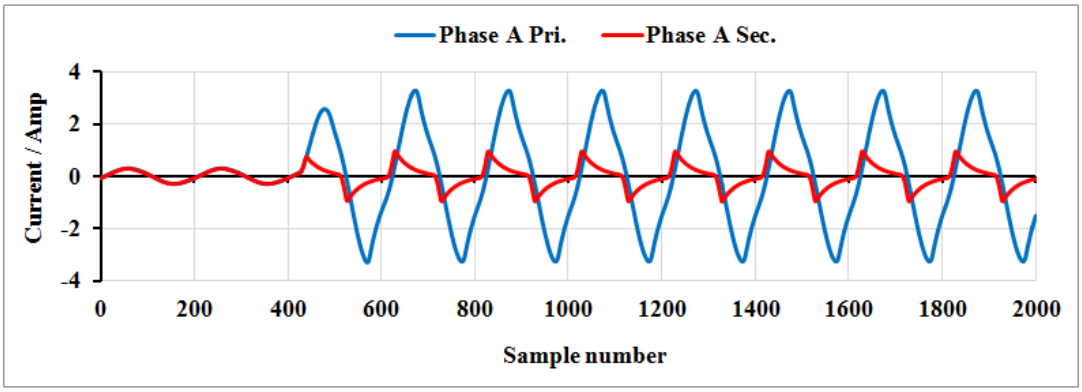

Fig 7-18 CT saturation during external fault in phase A

The selected zone of samples to be processed in the MATLAB program started from seconds 4.8017, 4.8096 and 4.8063 for phases A, B and C respectively.

The change in correlation coefficients that caused by the fault is shown in Fig 7-19. It can be seen at window 12, both r_{A11} and r_{A22} reduced to less than 0.9 at the same window whereas r_{A12} was still greater than 0.9 as CT4 had not reached to saturation level yet. But at the next window (window 13), r_{A12} and r_{A22} steeply reduced due to saturation. Although the time to saturation was very short which is so called early saturation, there was still enough time for the proposed fast algorithm to detect any changes in correlation coefficients before CT becomes fully saturated. By checking the threshold of the algorithm for this case as shown in flowchart of the proposed algorithm in Fig 4-4, reduction of both r_{A11} and r_{A22} under the threshold was detected at window 12 which ended in sample number 440 (200 + 12 × 20), i.e. at (440 × 0.0001 + 4.8017) = 4.8457 seconds, and r_{A12} reduced under threshold at window 13 which ended in sample 460 i.e. at (460 × 0.0001 + 4.8017) = 4.8477 seconds.

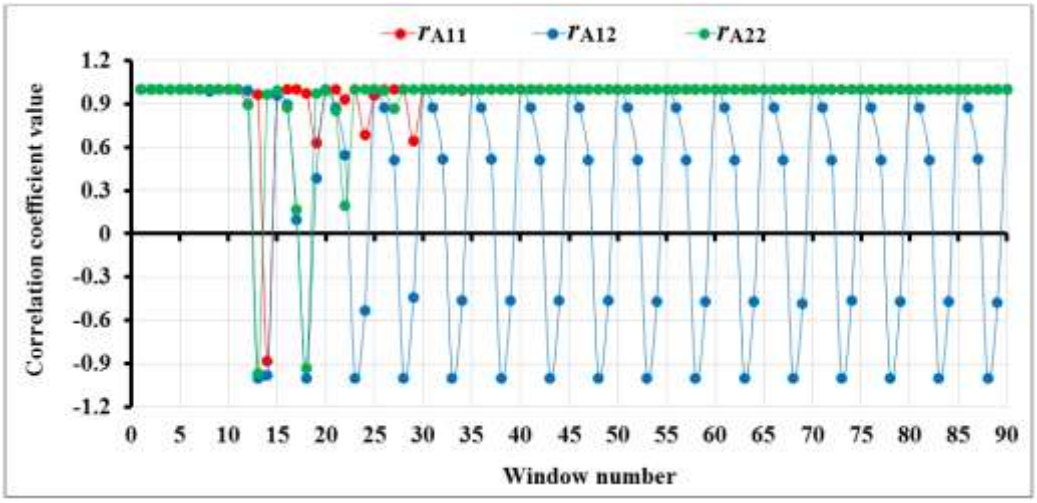

Fig 7-19 Change in correlation coefficients due to CT saturation caused by external fault in phase A

The fault occurred at close to the beginning of the current signal's cycle, which makes it more difficult for algorithms to detect any changes in terms of speed than if it occurred at or close to the peak of the signal's cycle. This was good for testing the maximum efficiency of the proposed algorithm in such cases. The algorithm properly and quickly identified this condition and considered it an external fault with saturation and there was no need for tripping.

4. Saturation of two identical current transformers due to external fault

Since all CTs that were used in this experimental work are of the same type, manufacturer and characteristics, they will be simultaneously saturated when the flux in the CT core exceeds the saturation point or the voltage on the secondary side of CT when exceeding the knee point. The flux increases, as the current increases due to the fault. When the external fault occurs, both primary and secondary currents simultaneously increase with the same values and follow each other as seen in Fig 7-12. This means that the CTs on both the primary and secondary sides are subject to saturation at the same time. In order to test this case, the burdens of the two CTs in phase A, CT1 and CT4 were increased to 4Ω. The external fault was generated in phase A at approximately the second 4.8565. As expected, CT1 and CT4 were saturated and both samples of primary and secondary currents were identically distorted as shown in Fig 7-20. These samples, which were selected to be processed, started from seconds 4.816, 4.8231 and 4.8197 for phases A, B and C respectively.

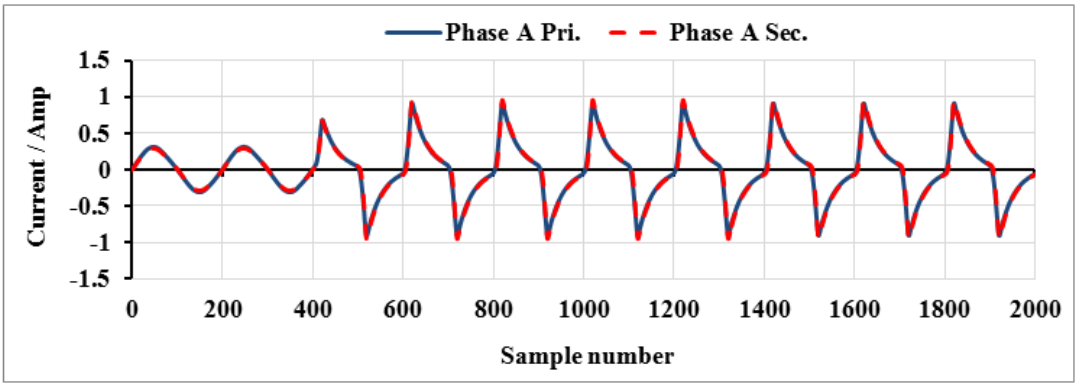

Fig 7-20 Saturation of two identical CTs due to external fault in phase A

The Correlation coefficients of phase A had only changed as the external fault occurred in phase A causing simultaneous saturation of CT1 and CT4 as shown in Fig 7-21. At window 11, both r_{A11} and r_{A22} reduced to less than 0.9 at the same window whereas r_{A12} always remained greater than 0.9 because both primary and secondary currents, even though they had been distorted, followed each other in the same behaviour during saturation. Since r_{A12} never reduced under the threshold through the whole duration of fault, this made it easier for the proposed algorithm to identify such cases. The algorithm properly and quickly considered it as an external fault with simultaneous saturation of two CTs and there was no trip signal to be issued.

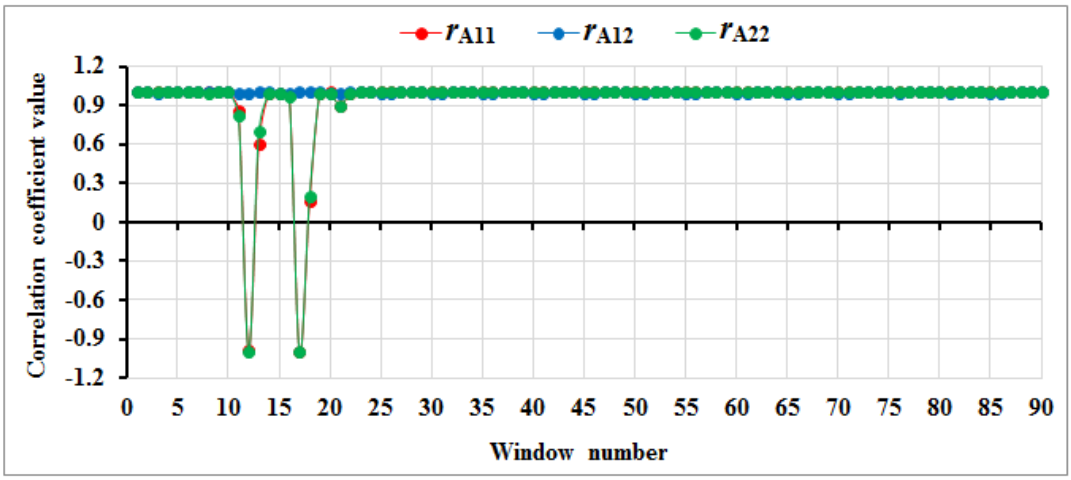

Fig 7-21 Change in correlation coefficients due to saturation of two identical CTs

7.4. Summary

The proposed technique was examined and tested under different conditions including the most prevalent internal faults that may occur when the transformer is in steady-state operation. All possible faults were safely generated in the laboratory and then the data were imported to be processed in MATLAB program where the algorithm of the proposed technique was set. It was practically proved that the technique successfully detected the internal faults and took proper action against them within a very short time ranging from 0.8~2.5ms depends on the strength of the fault current. It was effectively able to distinguish between internal and external faults. In addition, it was tested under CT saturation, which is a major problem in protection schemes. This problem was overcome by the algorithm as its response was faster than the time usually taken by CTs to reach saturation level.

The proposed technique was able to detect turn-turn faults although they were generated on a small transformer model with only two turns being short-circuited which is less than the standard that has been specified by IEEE. Certainly, the technique will be more efficient if it is implemented on larger transformer or more turns are shorted, which means that there will be a significant increase in the turn-turn fault current. Since the proposed algorithm doesn't depend on current values, but rather on the shape of the waveform, which changes during the fault, it was not tripping against the external fault current. This shows how this algorithm is better than overcurrent protection, which causes it to trip depending on the increase of the current regardless of whether it is due to internal or external faults. External faults were a good example for changing currents due to load changes, i.e. if the load has changed, the change in current will be considered as if it were an external fault, so the relay was still stable, and no tripping was issued in this case.

CHAPTER 8

Results and Discussions on Inrush Problem in Transformer Transient State

8.1. Introduction

In this chapter, the proposed technique for transient state was tested using real data obtained in the laboratory, in order to check its ability in distinguishing between internal fault and inrush condition. The inrush phenomenon was considered during two cases of transformer, the first was that when the transformer was energized under no-load case and the second when it was energized under load case.

8.2. Inrush condition when transformer is on no-load

As mentioned before, the current change ratio (CCR) was enough to identify the inrush when unloaded transformer was energized. The proposed algorithm was applied when the transformer was switched on once without internal fault i.e. pure inrush and once with internal fault as follows.

1. Inrush condition without internal fault

The transformer was switched on/off so many times i.e. different instant of sinusoidal voltage wave to obtain inrush current signals. The no-load current measured by CTs on primary side was 0.06 Amp. Since the transformer was supplied at low voltage of 60 V, it can be noticed that inrush decaying time was short as shown in Fig 8-1. However, the rate of decay depends on factors such as ratio of reactance to resistance (X/R ratio) of the system.

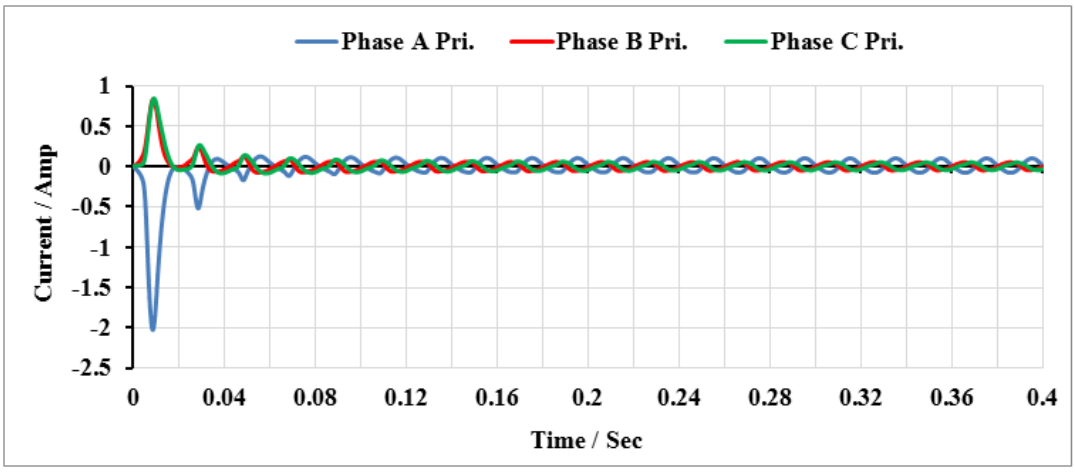

Fig 8-1 Inrush current signal when no-load transformer was energized without fault

Inrush decaying can be recognized by MATLAB algorithm through subtracting two successive positive and negative peaks of cycles (D2PK) and also the peak of half cycle is subtracted from the next one (DP2P) which indicates the decay of DC offset. When the difference approaches zero, it means that the inrush as well as DC component are faded out. In 20 cycles, there were 19 values for successive peak cycles (D2PK) and 20 values for peaks of one cycle (DP2P) as shown in Fig 8-2 for phase A.

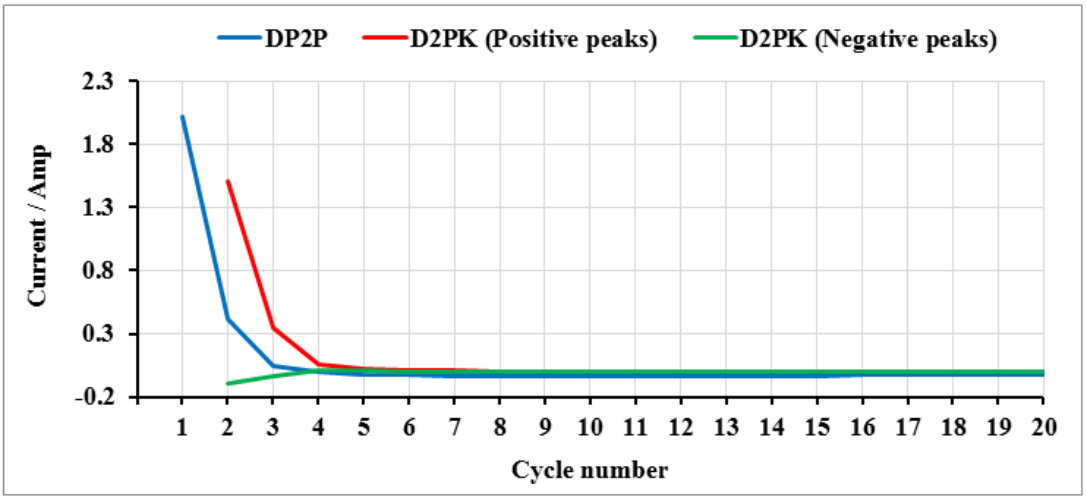

Fig 8-2 Decrease of DP2P and D2PK during Inrush condition for phase A

As inrush decayed, the half-cycle peaks of current signals decreased to the value of no-load current at half-cycle number 6 as shown in Fig 8-3. This means that the current signal returned to normal condition as inrush faded out.

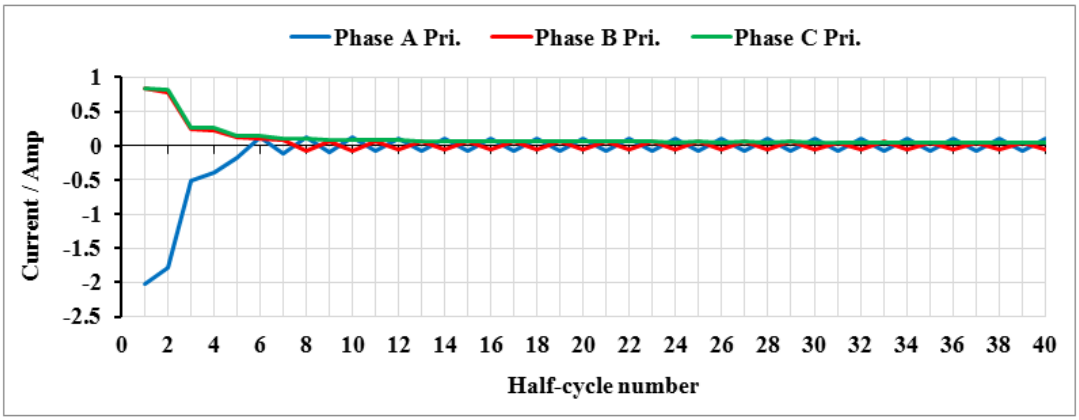

Fig 8-3 Peaks of half-cycle current signal

The simulation results for inrush condition indicated that the current change ratio (CCR) remained below 0.8 until half-cycle number 5 for phase A, 6 for phase B and 16 for phase C, then it changed to above 0.8 as the shape became close to sinusoid as shown in Fig 8-4. However, the second half-cycle of each cycle in phase C (even

numbers of half-cycle) were less than 0.8. This doesn't make any difference as these half-cycle peaks were less than half-cycle peaks of no-load current either in positive or negative values according to the sign of inrush peak as shown in Fig 8-3. It can also be noticed that the peak values of half-cycle current signals for all phases were higher than the peak value of the no-load current signal before half-cycle number 6. But at the same time, their current change ratios were less than 0.8. Therefore it was classified as inrush condition which can also be recognized by difference between two peaks of successive cycles (D2PK) and difference between upper & lower peaks of one cycle (DP2P) as shown in Fig 8-2 and the normal condition started at half-cycle number 6. The relay operation should remain stable, so there was no trip signal to be issued in either two conditions and the algorithm effectively recognized this case.

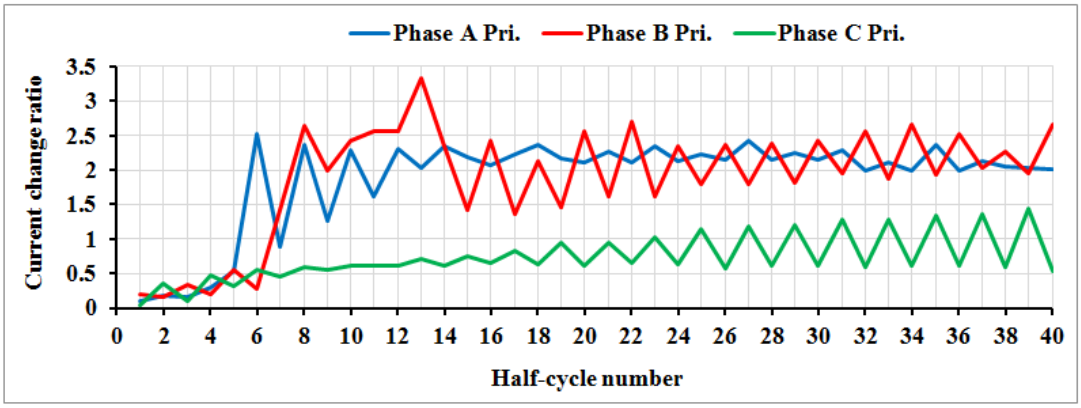

Fig 8-4 Current change ratio when no-load transformer was energized without fault

2. Interturn fault with inrush condition

The transformer was switched on with four turns were short-circuited on the primary side of transformer in phase A. The inrush waveforms in the first two cycles were clear and had the normal shape in phases B and C while in a faulty phase A, its shape was closer to sinusoid due to the effect of the fault as shown in Fig 8-5.

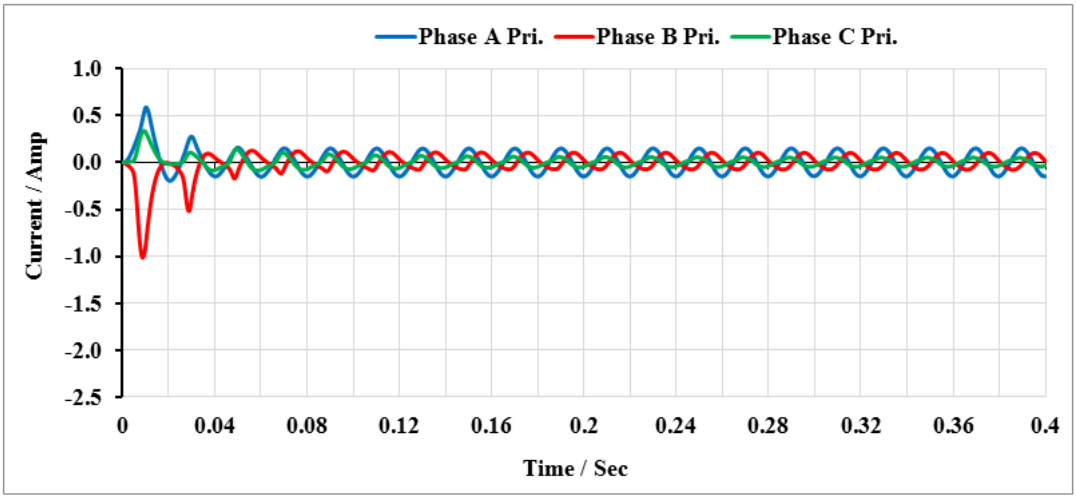

Fig 8-5 Inrush condition when no-load transformer was energized with interturn fault in phase A

DP2P and D2PK indicated that the inrush current fully faded after two cycles as shown in Fig 8-6.

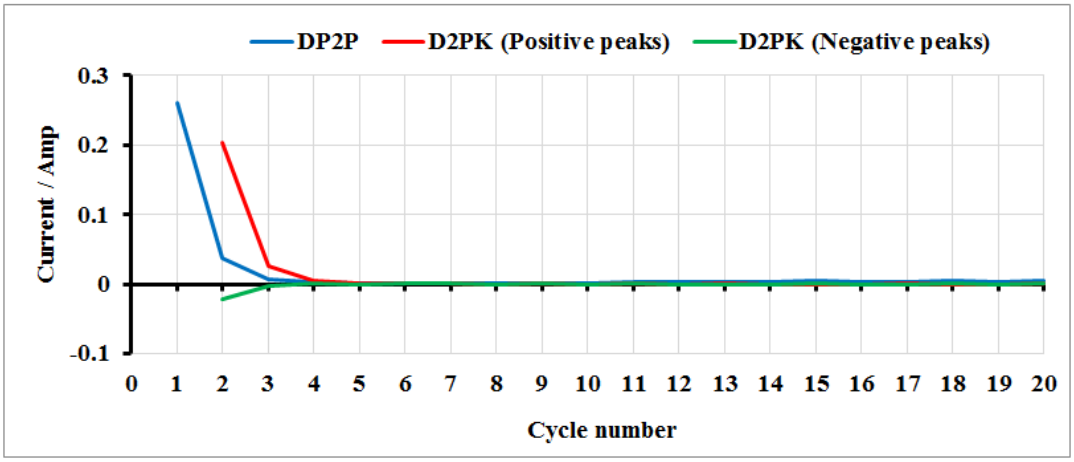

Fig 8-6 Decrease of DP2P and D2PK for phase A during Inrush current with interturn fault

The current change ratio (CCR) was checked because the peak current value at the first cycle was greater than no-load current value. But since the fault forced the inrush waveform to be closer to sinusoid, CCR was greater than 0.8 as shown in Fig 8-7. Therefore the algorithm considered this case an internal fault.

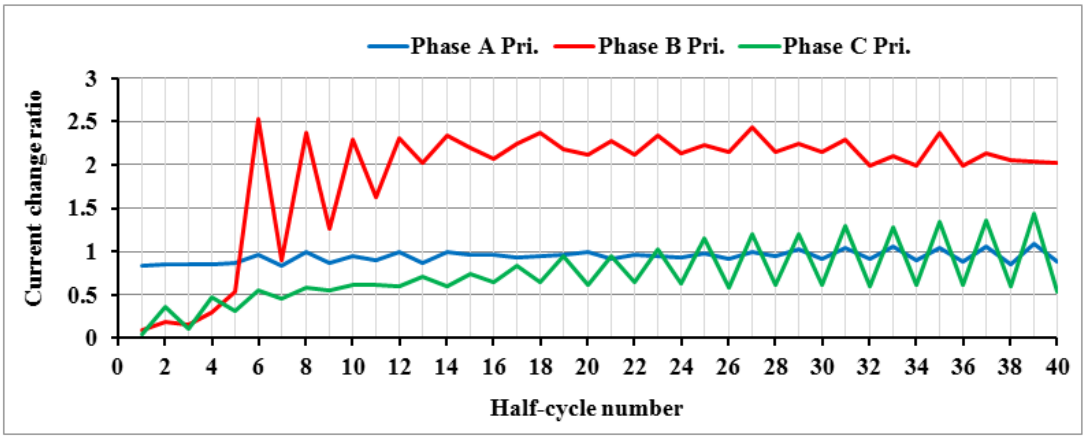

Fig 8-7 CCR when no-load transformer was energized with interturn fault in phase A

3. Turn-ground fault with inrush condition

The transformer was switched on with a Turn-ground fault in phase A. The shape of current waveform was very close to sinusoid as shown in Fig 8-8.

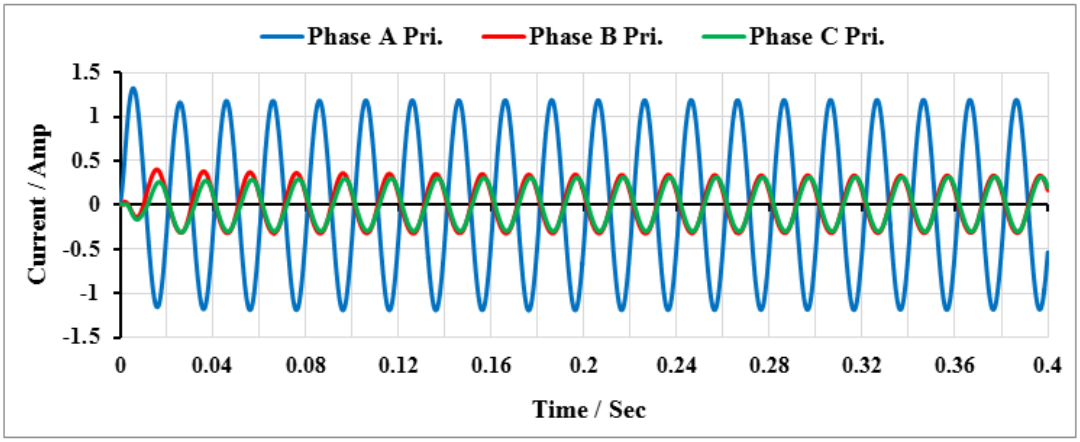

Fig 8-8 No-load transformer was energized with turn-ground fault in phase A

The simulation results for this fault indicated that the CCR was greater than 0.8 in the faulty phase A in the full duration of simulation starting from the first half-cycle, while it was less than 0.8 in the first half-cycle of both phases B and C as shown in Fig 8-9. This was because healthy phases B and C took longer time to start than

faulty phase A due to the phase shift between the three phases, so it can be seen that the shape of first half-cycles of phases B and C are similar to the shape of inrush condition as shown in Fig 8-8. It doesn't matter as long as CCR in faulty phase A was greater than 0.8. The algorithm checked CCR at the first cycle because the peak value of the half-cycle of the current signal was higher than the peak value of the no-load current signal. Accordingly, it was classified as an internal fault condition and a trip signal should be issued. The algorithm detected this internal fault in phase A and effectively distinguished it from inrush condition after half-cycle time of transformer's energization.

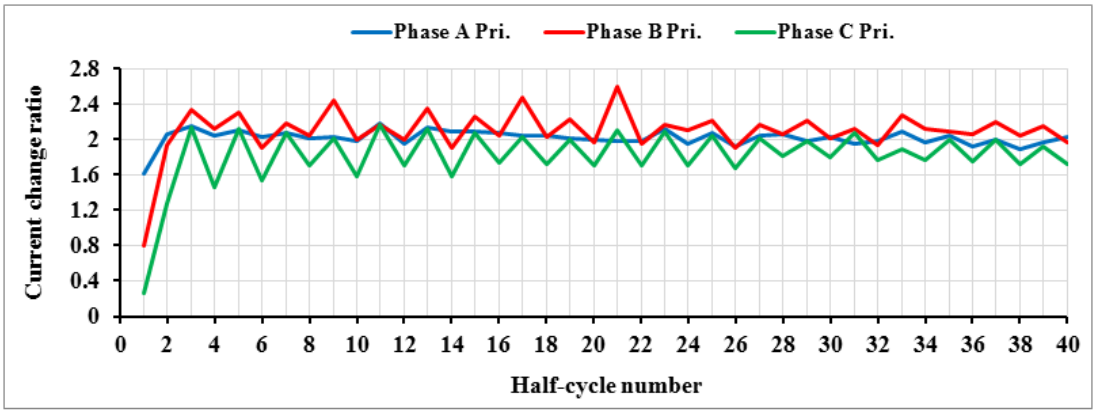

Fig 8-9 CCR when no-load transformer was energized with turn-ground fault in phase A

8.3. Inrush condition when transformer is on-load

The transformer was connected to a balanced load which means that there were six current signals to be processed, three input current signals of three phases A, B and C on the side of energization and the opposite three output current signals on the load side.

Since the transformer turns ratio was 1, the difference between primary and secondary current peak values (Diffmax) indicates the status whether it is normal when the difference is equal or less than 0.1(it is ideally zero but 0.1 has been chosen as a margin of error in practical test) or either fault or inrush when Diffmax is greater

than 0.1. Therefore, the half-cycle current peaks are not necessary to be compared with the load current unlike the case in the no-load.

The on-load transformer was switched on, once without internal fault i.e. pure inrush and once with internal fault in order to check the ability and efficiency of the MATLAB algorithm in distinguishing between internal faults and inrush condition.

1. **Inrush condition without internal fault**

It was noted that frequent switch on/off operations were needed to obtain inrush signal. That was contrary to the case when the transformer was in no-load condition in which the inrush can be obtained almost every switch on operation.

Fig 8-10 shows the inrush condition when loaded transformer was switched on without internal fault. The steady state current which was measured by CT was around 0.28 Amp.

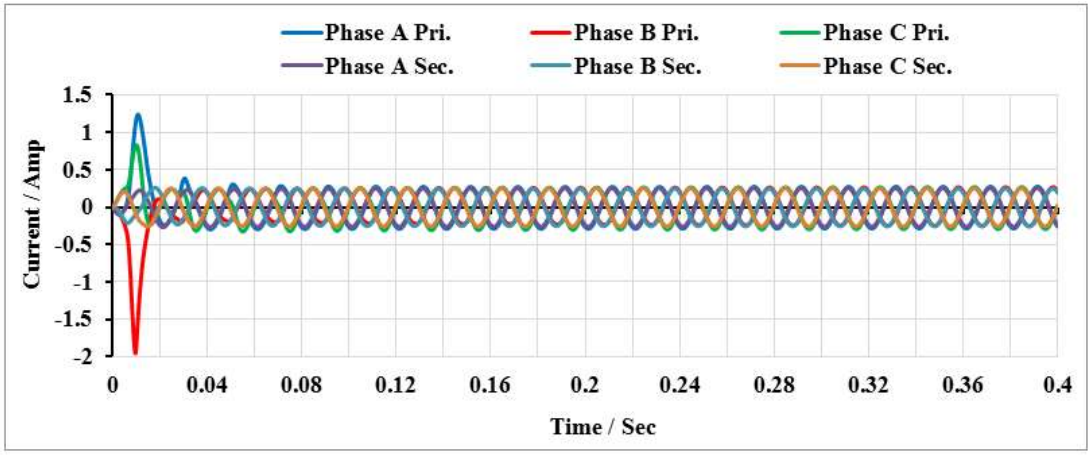

Fig 8-10 Inrush current when on-load transformer was energized

It can be seen that the first current cycles of the three phases had high inrush currents. But in the second current cycles, the inrush currents almost disappeared in phases B and C while in phase A, it was still slightly affected by inrush current as shown in Fig 8-11.

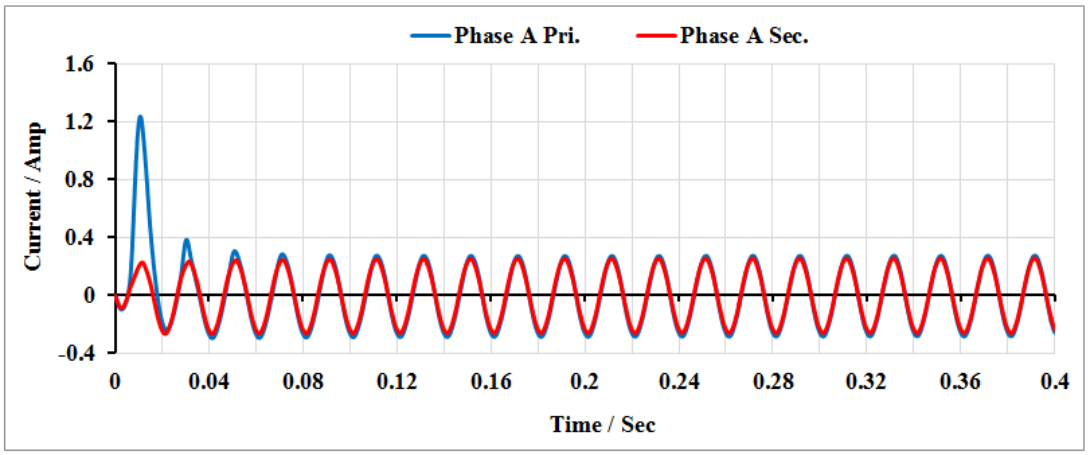

Fig 8-11 Currents in phase A when on-load transformer was energized

The simulation results for inrush current condition indicated that the PAD at first quarter of the first cycle (number 1) was 9.49 % for phase A, 16.58 % for phase B and 8.99 % for phase C. On the other hand, PAD at last quarter of the first cycle (number 2) was 22.3 % for phase A, -58.97 % for phase B and 5.71% for phase C as shown in Fig 8-12.

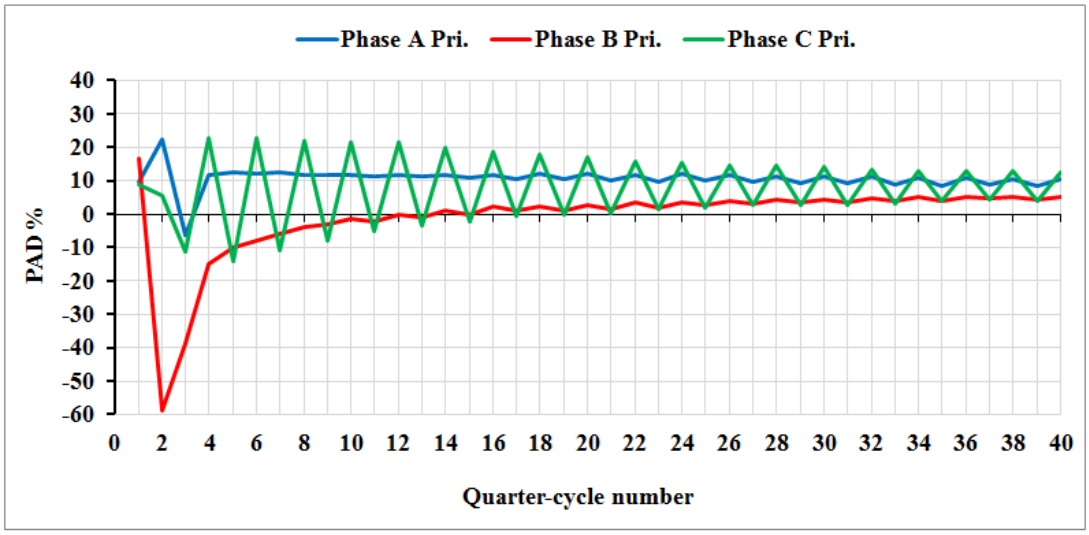

Fig 8-12 PAD when loaded transformer was energized without fault

In this figure, for each phase, the odd numbers show PAD for first quarter of each cycle while even numbers for last quarter, e.g. numbers 1 and 2 mean first and last quarter of one cycle (first cycle) respectively. The action of the algorithm can be

demonstrated as follows: At first process, the TMR was odd, PAD of first quarter of cycles (odd number 1) was less than 30% for all phases, so the program continued to half-cycle and diffmax was checked (odd numbers represent the first half of cycles). At half-cycle number 1, the values of diffmax were equal to 0.989 for phase A, 1.74 for phase B and 0.63 for phase C, i.e. they were greater than the threshold value of 0.1 as shown in Fig 8-13.

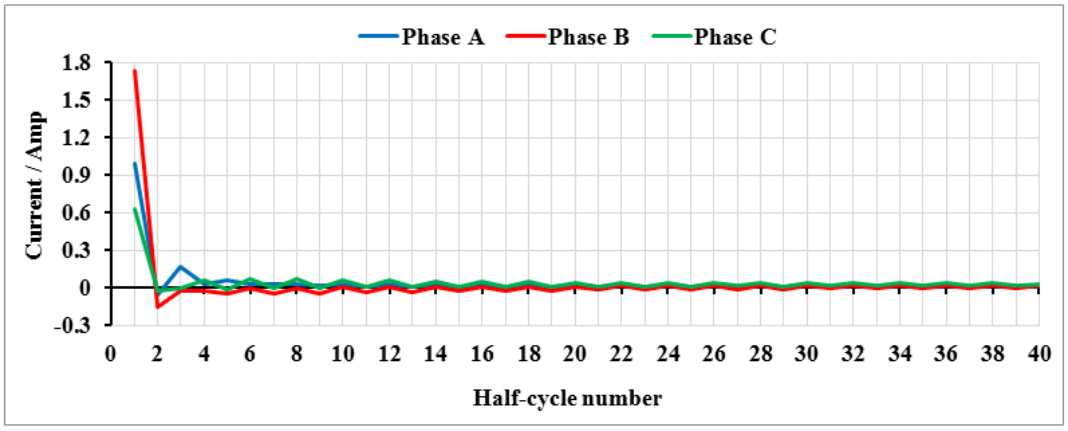

Fig 8-13 Diffmax when loaded transformer was energized without faults

The CCR was then checked. They were 0.19 for phase A, 0.14 for phase B and 0.42 for phase C as shown in Fig 8-14 i.e. they were under the threshold of 0.8 which means that it was an inrush condition at the first half-cycle current. Similarly, when TMR changed to 2 (even numbers), values of diffmax were less than 0.1 and greater than -0.1 and also CCR were less than 0.8. Since PAD was less than 30%, it was considered inrush at the second half-cycle. At the third half-cycle current when TMR was 3, the normal operation started in phase B in which the value of diffmax was -0.03 and CCR was 1.5 while small inrush shape was still detected in phases A and C which their normal operation started from half-cycle number 4 when diffmax reduced to 0.027 and 0.062 for phases A and C respectively and also CCR increased to 0.94 and 1.28 for phases A and C respectively. However, the algorithm can be followed using the flowchart that shown in Fig 4-4.

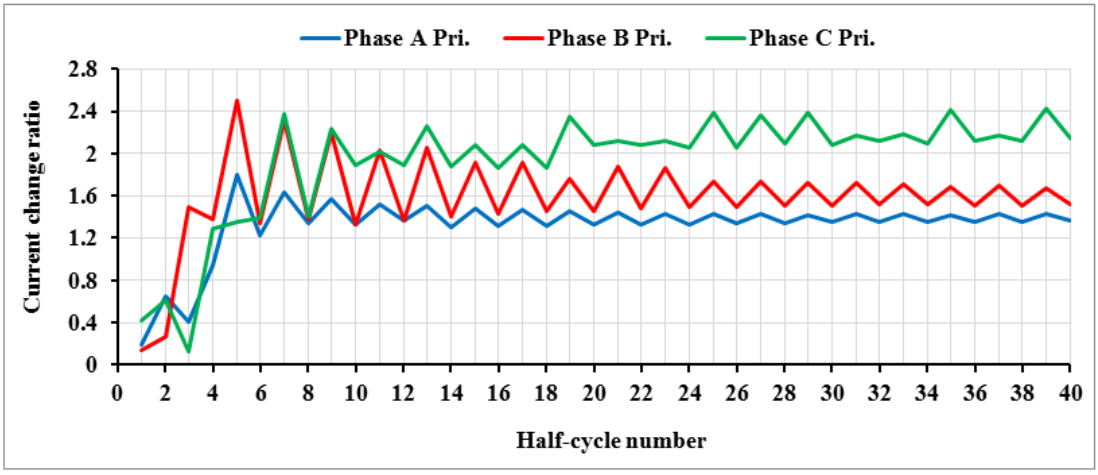

Fig 8-14 CCR when loaded transformer was energized without fault

Inrush duration and normal operation status can also be recognized and monitored using indicators, DP2P and D2PK. It was clear that inrush has completely faded out and normal operation started at cycle number 3 as shown in Figs 8-15 and 8-16 for variations of DP2P and D2PK respectively.

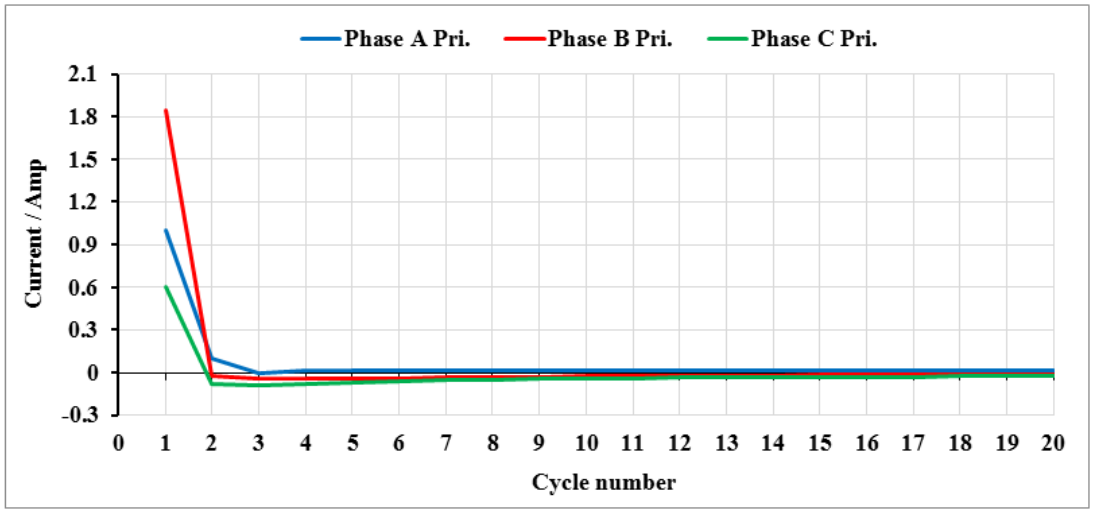

Fig 8-15 DP2P when loaded transformer was energized without fault

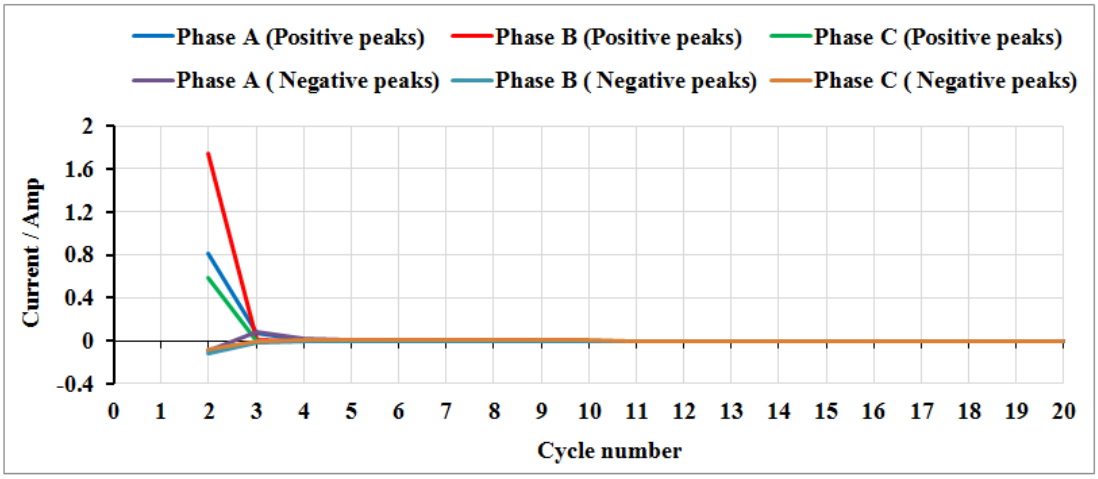

Fig 8-16 D2PK when loaded transformer was energized without fault

2. Interturn fault with inrush condition

Transformer switching on with turn-turn (interturn) fault also resulted in a clear area difference at first quarter of current cycles between primary and secondary currents. This difference increases when more turns are damaged (more turns are short-circuited). Four turns on primary side of phase A were short-circuited as an interturn fault then the transformer was switched on. Since it was a minor fault in phase A, both Phases B and C were not affected by this fault as shown in Fig 8-17.

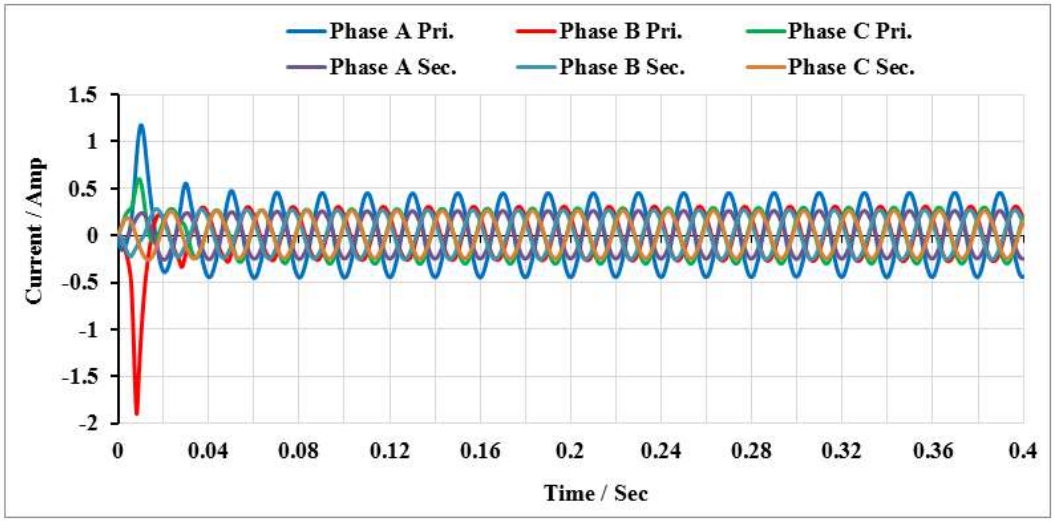

Fig 8-17 The currents when loaded transformer was energized with turn-turn fault in phase A

Obviously, the effect of inrush current was still predominant as the fault was a minor fault and submerged to the inrush particularly at the first cycle as shown in Fig 8-18. This makes a big challenge for the suggested algorithm to detect this minor fault.

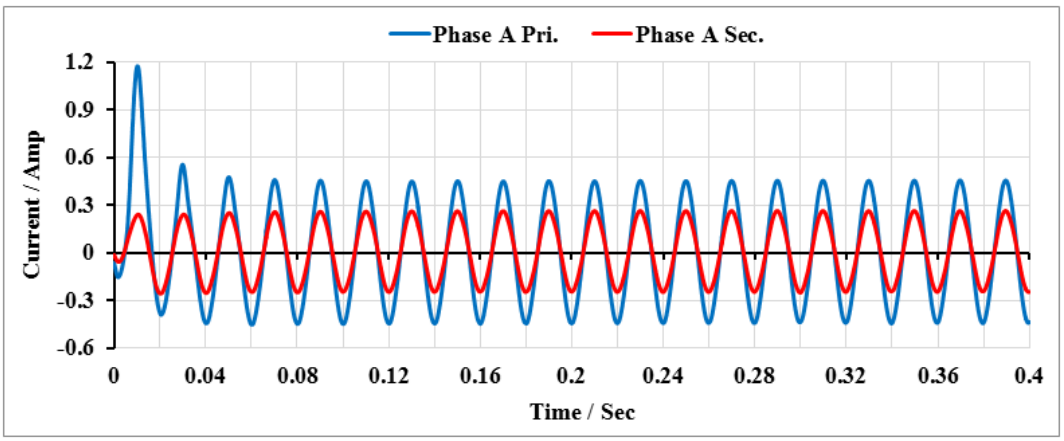

Fig 8-18 Phase A currents when loaded transformer was energized with turn-turn fault in phase A

The results that obtained from processing this case showed clearly that PAD of faulty phase A at the first and last quarter of each cycle was greater than 30% due to this fault as shown in Fig 8-19. According to the flowchart of the algorithm shown in Fig 4-4, this internal fault was detected after the first quarter of the cycle i.e. just 5 ms from the moment of transformer switch on.

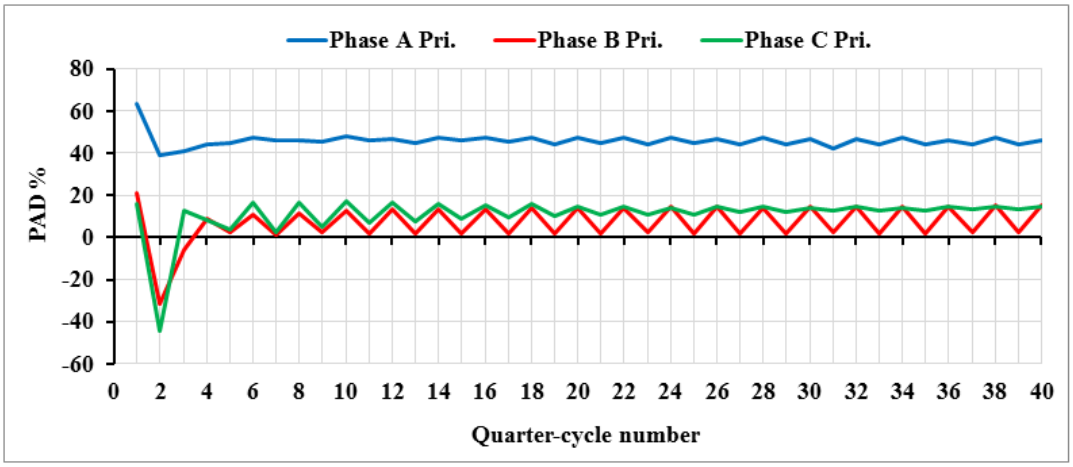

Fig 8-19 PAD when loaded transformer was energized with interturn fault in phase A

It can be noticed that at the first half-cycle of current signal in phase A, the Diffmax value was greater than 0.1 as shown in Fig 8-20 and also the current change ratio was less than 0.8 as shown in Fig 8-21 because the fault was not large enough to change the shape of the inrush current signal into sinusoid and hence the signal was still having the shape of inrush. This means, if there was no PAD, it would not be considered a fault. However, there was no need for algorithm to check the CCR as the PAD at the first quarter-cycle made the algorithm sending a trip signal not to continue to the half-cycle for checking the CCR.

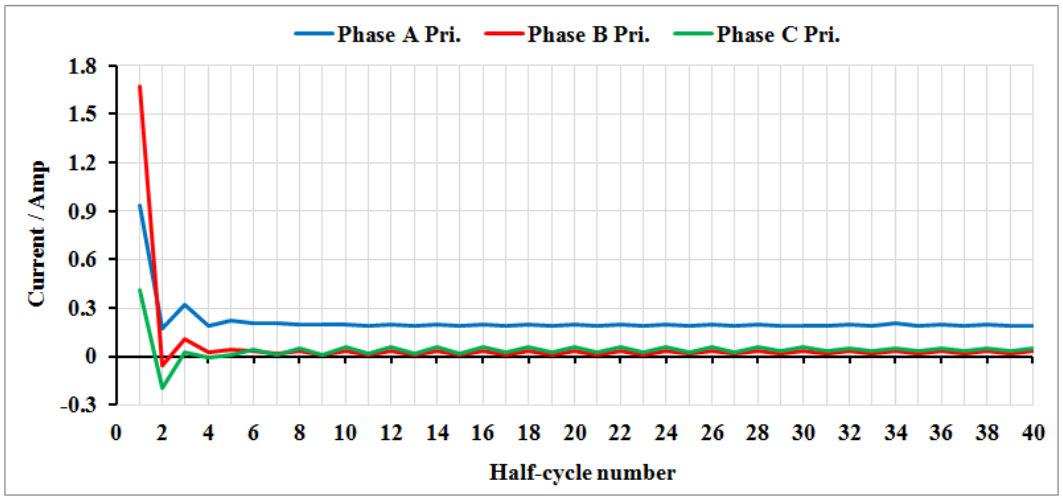

Fig 8-20 Diffmax when loaded transformer was energized with interturn fault in phase A

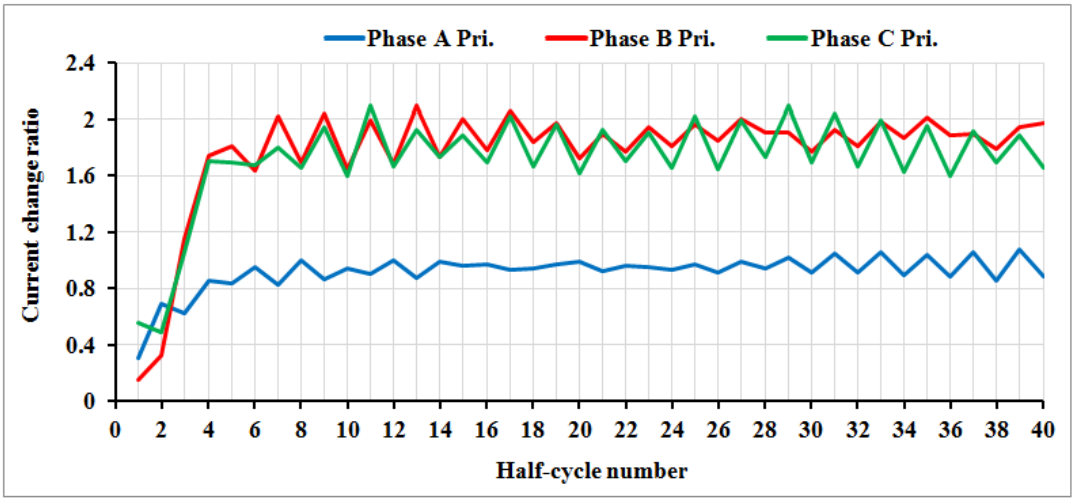

Fig 8-21 CCR when loaded transformer was energized with interturn fault in phase A

When monitoring the decrease of DP2P, the inrush can be seen clearly at the first cycle and then faded out as shown in Fig 8-22.

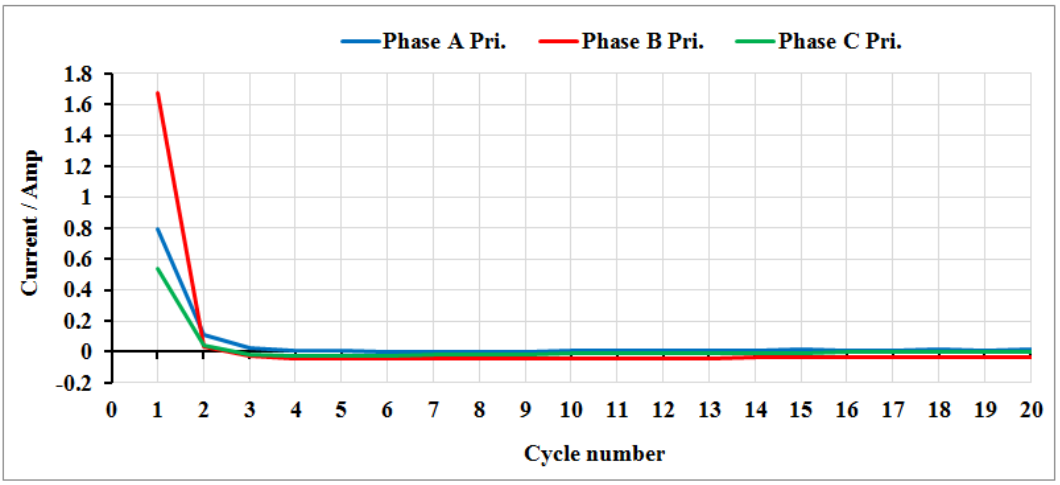

Fig 8-22 DP2P when loaded transformer was energized with interturn fault in phase A

3. Turn-ground fault with inrush condition

The loaded transformer was switched on with Turn-ground fault on primary side of phase A. At the first cycle, the inrush phenomenon also appeared in phase A as shown in Fig 8-23.

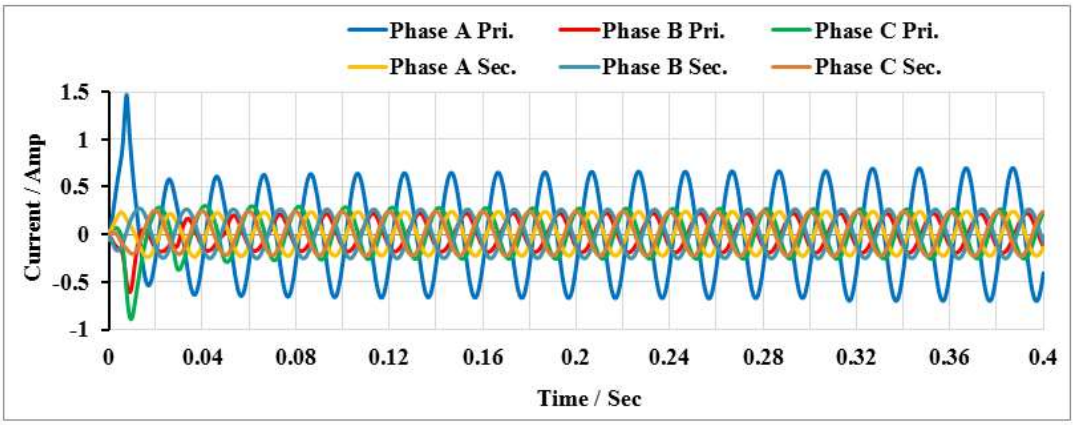

Fig 8-23 Currents when loaded transformer was energized with turn-to-ground fault in phase A

Although the inrush current was high at the first cycle, the fault was able to noticeably enforce the shape of inrush to be closer to sinusoid as shown in Fig 8-24. Since the fault had submerged to inrush which was a predominant feature at the first cycle, it was also a challenge to protection algorithms for distinguishing inrush from internal fault. Therefore, the proposed algorithm was tested for this case to see whether it is able to detect this fault or not.

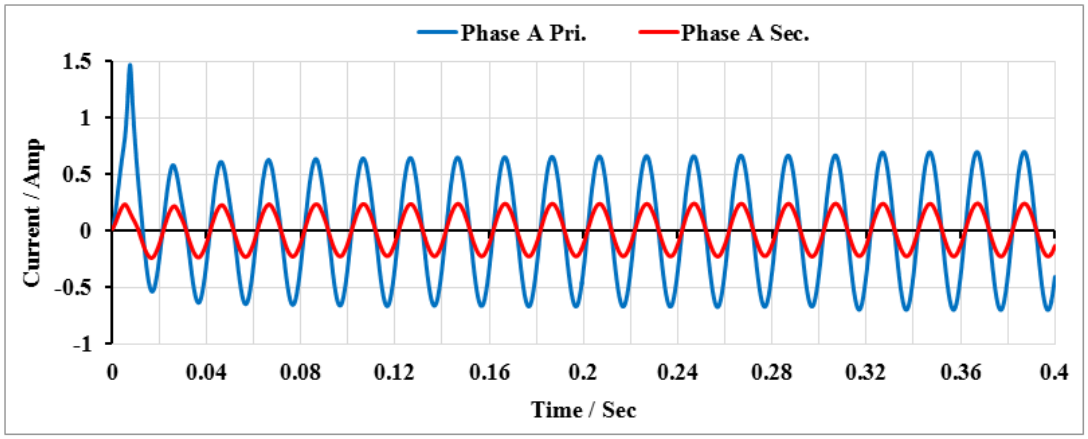

Fig 8-24 Phase A currents when loaded transformer was energized with turn-ground fault in phase A

In the zone prior to saturation point of transformer core which was selected as the first quarter of each cycle, there was a large percentage area difference (PAD) caused by this fault. It can be seen in Fig 8-25 that PAD at quarter-cycle number 1 was 64.82% for faulty phase A, so this fault was detected at the first quarter cycle.

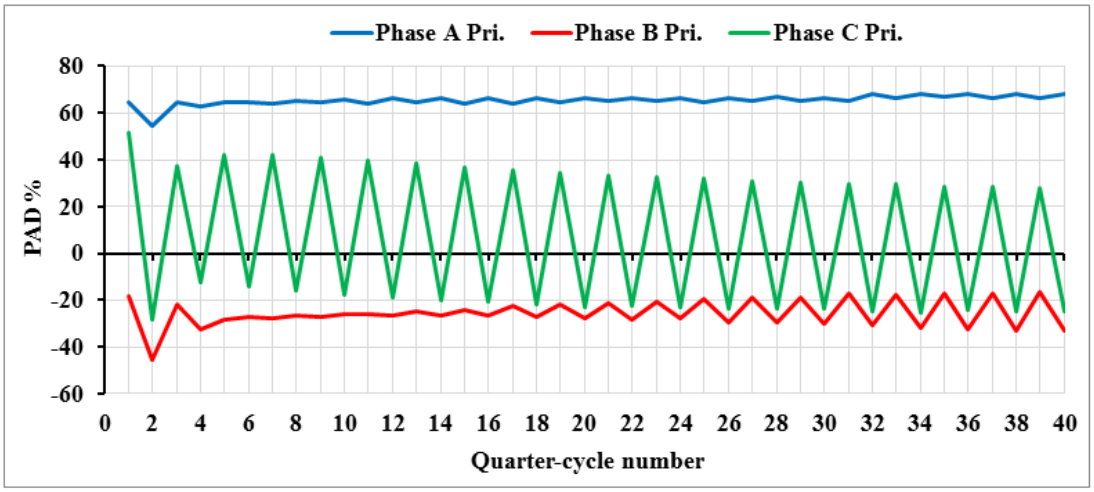

Fig 8-25 PAD when loaded transformer was energized with turn-ground fault in phase A

Since the influence of inrush was still exist in phase B which was not affected by the fault, it can be seen that its PAD was always under 30% while CCR in both phases, B and C was below 0.8 at half-cycle numbers 1, 2 and 3 as shown in Fig 8-26.

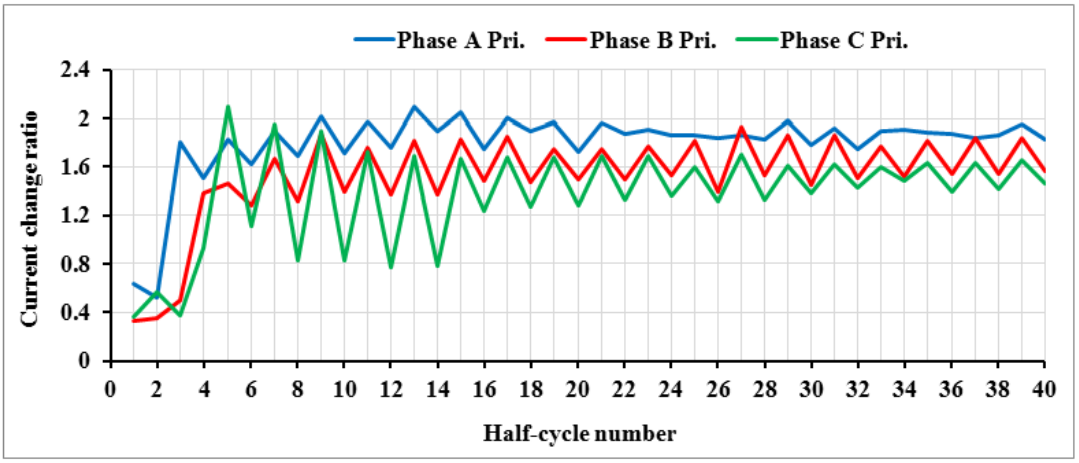

Fig 8-26 CCR when loaded transformer was energized with turn-ground fault in phase A

The DP2P for all phases dropped to less than 0.1 at cycle number 2 as shown in Fig 8-27. It means that inrush ended after one cycle and a half then normal operation resumed at second cycle or half-cycle number 4.

Since the fault occurred in phase A, diffmax did not go back to its value for normal operation and remained greater than 0.1 as shown in Fig 8-28.

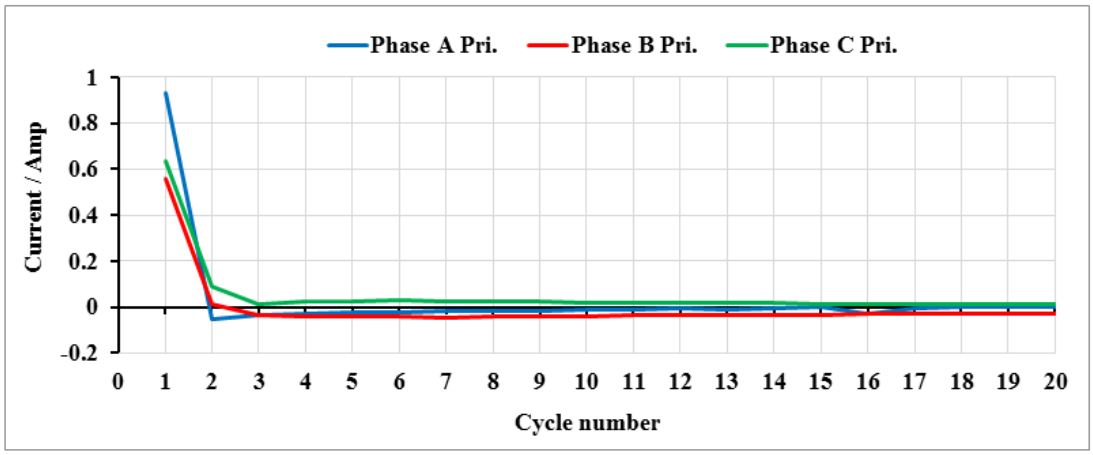

Fig 8-27 DP2P when loaded transformer was energized with turn-ground fault in phase A

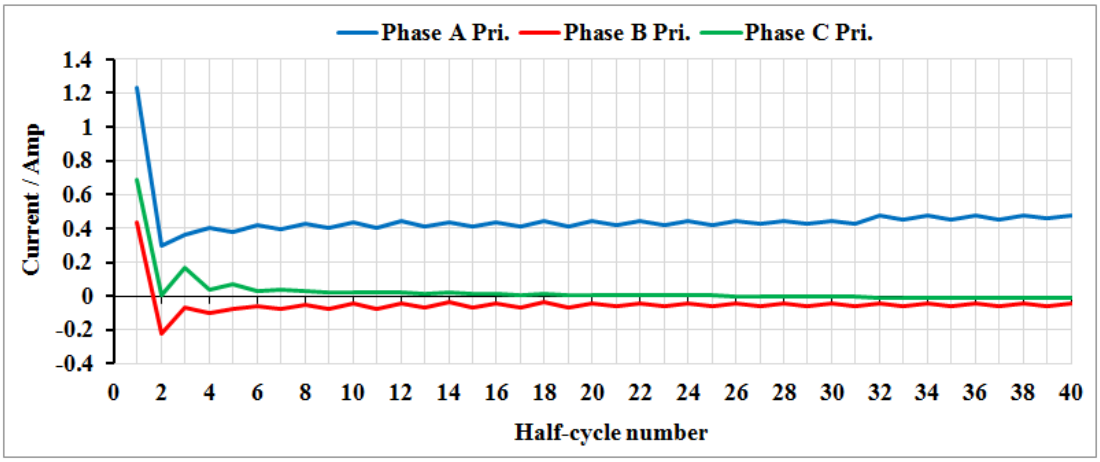

Fig 8-28 Diffmax when loaded transformer was energized with turn-ground fault in phase A

In result, five milliseconds from instant of transformers' switch on was the time taken by the algorithm to trip against this fault.

8.4. Summary

In transformer energisation case, transient inrush current could cause the mal-operation which is considered a major problem in the differential protection. The differential protective relays may mal-operate if they are not blocked in the case of inrush and must only operate in case of internal fault. Two methods CCR and PAD were proposed to solve the mal-operation problem for relays by discriminating the inrush current from real internal faults when the transformer is energized. The first method was individually used only when the transformer was on no-load condition while both methods were used when the transformer was on-load condition. The methods were concluded after observing and analyzing the behavior and shape of large number of both inrush and internal fault signals.

The methods were tested on the practical model under similar conditions of inrush and internal faults that were generated on the MATLAB/SIMULINK model. It was practically proved that the methods were fast and reliable in discrimination between inrush current and internal fault signal. Their response time speed was 10ms for CCR when transformer was on no-load and 5ms for PAD when the transformer was on-load. This response time is faster than the most popular method relying on the second harmonic, which needs at least one cycle (20ms in 50 Hz systems) to recognize the condition.

Al though only four turns were short-circuited as an interturn fault which means that it is difficult to be detected, however it was practicly proved that the proposed algorithm was able to detect it. Also, the algorithm successfully distinguished the inrush current from the minor internal faults that were submerged under the inrush current particularly at the first cycle of the current signal, which makes it difficult to be distinquishable from each other.

CHAPTER 9

Conclusion and Future Work

9.1. Conclusion

The first transformer protection device was a fuse, which was able to protect only up to certain rated voltage. In order to overcome the drawbacks of the fuse, thermal, Buchholz relay, differential and over-current protection relays were developed and they are still used for transformer protections. But due to advance in science and technology, digital signal processing based techniques and artificial intelligence (AI) approaches, which were not known before, have recently been introduced to power system protection. These techniques provide the means to enhance the classical protection principles to be faster, more secure and dependable protection for power transformers. The advanced techniques improved the relay response times from a relatively slow time of around 100 milliseconds to be faster of less than 20 milliseconds. Also it is anticipated that in the near future more measurements will be available to transformer relays owing to both substation integration and novel sensors installed on power transformers. All this will change the practice for power transformer protection.

9. Conclusion and Future Work

Transformer protection is very important and essential in the electrical power system to ensure a reliable power supply. In the recent years, rapid changes and developments are being witnessed in the transformer protection. The increased growth of power systems both in size and complexity has brought about the need for the fast and reliable relays to protect major equipment and to maintain system stability. The power transformer is major and very important equipment in a power system. It requires highly reliable protective devices to ensure a reliable power supply.

Protective relays in electric power system are one of the main factors that keep power system to work properly and maintain its steady state. Reliability, operation speed, performance and simplicity are main aspects that should be considered when protection systems are designed.

For several decades, a prime protection for most power transformers is performed by implementing differential protection systems. These systems might be maloperated due to inrush current or occurnce of external fault. Therefore, it is very necessary for the protection system to distinguish between inrush current, internal fault and external short-circuit fault conditions in order to reduce or eliminate any chance of mal-function of differential protection systems.

The second harmonic principle is still used in the differential protection although it has so many disadvantages as mentioned in the literature. But as yet, there is no satisfied method has been accepted to be an alternative to the second harmonic method.

Each method mentioned in the literature was trying to overcome disadvantages of antecedent methods. The suggested methods are also doing the same but the challenges of these methods are simplicity in algorithm design, fast response to detect internal faults and discrimination between inrush condition and the internal fault which is accompanied by transformer's energization. This makes the proposed new approach a competitive alternative to existing methods.

The objectives of the research were achieved as follows:

1. *To model transformers, faults and current transformer saturation using MATLAB/SIMULINK program*

MATLAB/SIMULINK with SIMPOWER package is a powerful program was successfully used for modelling transformers, internal and external faults and also the saturation of current transformers. The program offered possibility of changing transformer parameters, hysteresis of transformer core and control on fault duration. The suggested techniques were tested on the models that built using this program.

2. *To process the data that obtained by simulating models in the same program*

Many methods simulate the model in another program such as ATP program and data are then imported to be processed in MATLAB program. Instead of that, the data was processed during simulation of the model in the same program of MATLAB/SIMULINK. This was achieved by MATLAB function block where the MATLAB code of the proposed algorithm was stored. This block was run simultaneously with simulation of the model.

3. *To simulate all possible faults when transformer operation is in steady state and then to test the capability of the proposed technique in detecting these faults*

In steady state of the transformer operation, a new technique was proposed and then applied on a model designed by MATLAB/SIMULINK program. This technique which was based on cross-correlation coefficients analysis of current waveforms was used for detecting internal faults that occur in three phase transformer as well as to distinguish them from external faults.

The cross-correlation scheme has been developed here by combining it with additional coefficients called auto-correlation coefficients. This was to increase security in faults detection and to obtain a better discrimination than the scheme that

uses cross-correlation coefficients only and also to speed up the response to faults. The response time of the proposed scheme was so fast, ranging from 2 to 6 ms according to the type of fault and how heavy the fault was.

The new suggested technique doesn't depend on current values, but rather on the shape of the waveform, which changes during the fault, and consequently leads to change in correlation coefficients. Traditionally, the protection techniques depend on the detection of current increases when external faults occur. This current can also be detected by the proposed algorithm based on correlation coefficient method, but the difference is that the proposed algorithm takes no action (no tripping) against this fault. This shows how this algorithm is better than other protection techniques such as overcurrent protection which trip depending on the increase of the current regardless whether it is due to internal fault, overload or external fault. External faults can be considered a good example for changing currents due to load changes, i.e. if the load has changed, the change in current will be considered by the proposed technique as if it were an external fault, so the relay is still stable, and no tripping for this case.

4. *To simulate the problem of current transformer saturation and then to check how it can be overcome by the proposed technique*

All possible cases of CT saturation which is a major problem in protection schemes were simulated using a SIMULINK model that was particularly designed by MATLAB/SIMULINK program for this purpose. The proposed correlation technique was tested under those cases. It was proved that the technique could overcome this problem as it could detect the faults before the CTs driving into the saturation which caused by those faults. So the problem was solved depending on the fast response of the technique which was faster than the time which is usually taken by CTs to reach a saturation level.

5. *To simulate the inrush problem that occurs at the time of transformer's energization and then to see how the proposed technique is able to safely discriminate between inrush condition and real internal faults*

In transformer energisation case, transient inrush could cause the mal-operation which is considered a major problem in the differential protection. The differential protective relays may mal-operate if such schemes are not able to block the relay in case of inrush and only operate in case of internal fault. This is the most important thing for differential protection system to improve the security of relays. Two methods CCR and PAD were proposed to solve the mal-operation problem for relays. The methods were concluded after observing and analyzing the behavior and shape of large number of both inrush and internal fault signals. These signals had been practically obtained in the laboratory on a model transformer as well as using MATLAB/SIMULINK program in order to find out a best method for discriminating inrush current signal from internal fault signal when transformer switches on. So many simulations in MATLAB program were carried out to test the efficiency of these methods. The methods were tested under the conditions of inrush and internal faults which were generated on MATLAB/SIMULINK model. It was proved that these methods were fast and reliable in discrimination between inrush and internal fault signal. The response time speed of the methods was 10 ms for CCR when transformer was at no-load and 5 ms for PAD when the transformer was on-load. This response time is faster than the most popular method the second harmonic which needs at least one cycle (20ms in 50 Hz systems) to recognize the condition.

6. *To carry out all tests in the previous points 3, 4 and 5 in the laboratory, which means that the real data are used in these tests*

In 3, the proposed correlation coefficient algorithm was examined and tested on a practical model under different and most prevalent cases of external and internal faults. For the purpose of comparison as well as confirmation of proposed technique performance, these cases were similar to those which were simulated using MATLAB program. It was proved that the algorithm detected successfully the internal faults within a very short time, ranging from 0.8 to 2.5 ms according to the

type and severity of the fault. It also distinguished successfully between internal and external faults.

In 4, the burden of CT in practical model was replaced with higher resistance of 4Ω in order to make the CT saturated during the fault. The proposed correlation technique was tested under real cases of current transformer saturation that implemented on the practical model. These cases were similar to those that simulated in MATLAB model. The technique was fast enough to recognize the case before the CT had started to saturate. Although the time to saturation in practical test was much shorter than the time in the cases that simulated by MATLAB program, the technique succeeded in detecting this case.

In 5, the efficiency of the two methods CCR and PAD were tested using laboratory data as all the tests performed on the transformer at different fault conditions were successful. The methods were tested on the practical model under the similar conditions of inrush and internal faults that were generated on the MATLAB/SIMULINK model. It was practically proved that the methods were fast and reliable in discrimination between inrush current and internal fault signal. Their response time to the cases was the same as that when the tests were implemented on the MATLAB/SIMULINK model.

In laboratory test, the proposed methods were able to detect turn-turn faults although they were minor faults as they were generated, on a small transformer model of 20 kVA as well as with only two and four turns were short-circuited which is less than the standard that has been specified by IEEE. In addition, the faults were generated by means of the protection resistor (R_f) which reduced the value of fault current. Certainly, the methods will be more efficient if it is implemented on larger transformer or more turns are short-circuited and also the faults are generated without protection resistor, which means that there will be a significant increase in the turn-turn fault current.

In general, the research has presented new competitive methods over those mentioned in the literature particularly, the second harmonic method which is still

dependable and widely used in transformer differential protection up to now, although it has too many shortcomings. The competition was based on two factors, the response speed to the cases and the simplicity in algorithm design. At the same time, the improvement of these factors was not at the cost of lower reliability and security. The methods have shown a very high accuracy and all the tests performed on the transformer gave high repeatability levels. The efficiency and effectiveness of these methods were proved by both simulation in MATLAB/SIMULINK program and practical experiments as too many simulations were repeated as well as all the experimental work were repeated more than three times and in either way, the results were very close.

9.2. Future work

The proposed correlation technique can be evolved in order to be able to recognize the type of internal fault and on which side of the transformer it occurs. The first steps were achieved using laboratory data and the results for the three phases were arranged in flowcharts shown in appendix E.

In the proposed PAD method, the location of the pre-saturation zone was chosen simply as the first quarter-cycle of current in order to avoid any further complex calculations in finding that zone. This zone can be mathematically estimated using an analytical formula if two values are known, residual and saturation fluxes. More details about this formula can be found in [126].

The proposed methods were performed on a small scale research transformer, but the final results and conclusions could be implemented on a large scale transformer, which can be planned for future work by liaising with power distribution companies.

In almost similar way as in transformer, internal faults, turn-ground and turn-turn also occur in generators. Turn-turn fault is not usually discovered by generator protection system. The proposed correlation technique can be applied on generators to detect these internal faults as well as discriminate those faults from the external faults that occur outside the generator. On the sides of generator stator windings, the three currents for three phases I_A, I_B and I_C entering stator windings (Nuetral side) and the other three currents I_a, I_b and I_c leaving the stator windings (Load side) as

shown in Fig 9-1, are measured by CTs in order to be used for calculating the correlation coefficients in the same way that followed in the transformer.

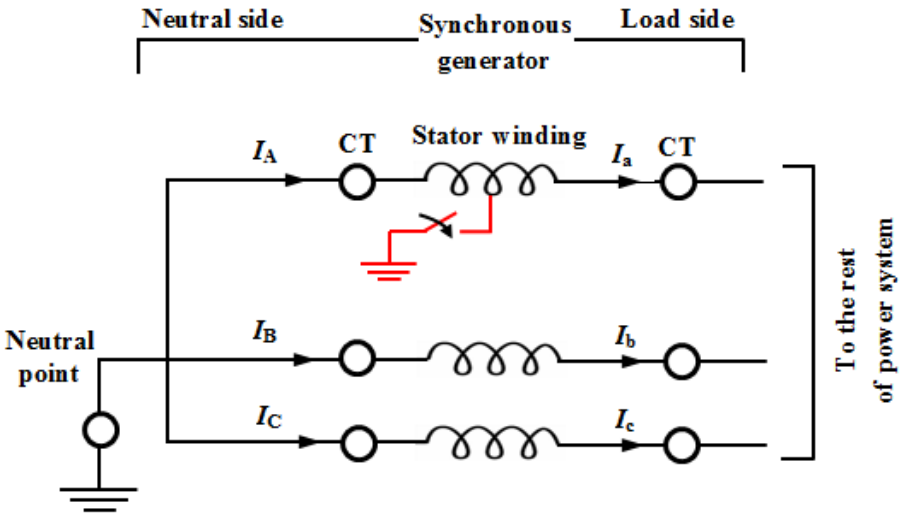

Fig 9-1 Generator's stator windings diagram

References

[1] S. H. Horowitz and A. G. Phadke, *Power system relaying*, 3rd ed. John Wiley & Sons Ltd, 2008.

[2] W. H. Tang, K. Spurgeon, Q. H. Wu, and Z. J. Richardson, "An evidential reasoning approach to transformer condition assessments," *IEEE Trans. Power Deliv.*, vol. 19, no. 4, pp. 1696–1703, 2004.

[3] *Transformer Protection Principles* (2015). GE Digital Energy. [Online]. Available: https://www.gedigitalenergy.com/smartgrid/ /Mar07/article5.pdf.

[4] M. R. Barzegaran, "Detecting the Position of Winding Short Circuit Faults in Transformer Using High Frequency Analysis," *EURO journels*, vol. 23, no. 4, pp. 644–658, 2008.

[5] W. H. Bartley, "An International Analysis of Transformer Failures," *Part 1, Locomot. Winter 2004*, vol. 78, no. 1, 2004.

[6] *Distribution Automation Handbook* (2015). ABB. [Online]. Available: https://library.e.abb.com/public/74b47888d7788642c125795f00430599/DAHandbook_Section_08p07_Protection_of_HV_Transformers_757288_ENa.pdf.

[7] J. Blackburn and T. Domin, *Protective Relaying: Principles and Applications*, 3rd ed. CRC Press Taylor & Francis Group, LLC., 2006.

[8] M. Tripathy, R. P. Maheshwari, and H. K. Verma, "Advances in Transformer Protection: A Review," *Electr. Power Components Syst.*, vol. 33, no. 11, pp. 1203–1209, 2005.

[9] Z. Wei-nan TANG Tao and Y. Yi-song, "Automation technology and application of power plant and transformation substation," *China Electr. Power Press*, 2005.

[10] S. H. Horowitz and A. G. Phadke, *Power System Relaying*. John Wiley & Sons, 1992.

[11] A. G. Phadke and J. S. Thorp, "A New Computer-Based Flux-Restrained Current-Differential Relay for Power Transformer Protection," *IEEE Trans. Power Appar. Syst.*, vol. PAS-102, no. 11, pp. 3624–3628, 1983.

[12] T. S. Sidhu and M. S. Sachdev, “On-line identification of magnetizing inrush and internal faults in three-phase transformers,” *IEEE Trans. Power Deliv.*, vol. 7, no. 4, pp. 1885–1891, 1992.

[13] R. G. Carter, *Electromagnetism for Electronic Engineers*. Richard G. Carter & Ventus Publishing ApS, 2010.

[14] *Faraday’s notebooks: Electromagnetic Induction* (2015). RIGB. [Online]. Available: http://www.rigb.org/docs/faraday_notebooks__induction_0.pdf.

[15] *Transformer Construction* (2015). Electronics-tutorials. [Online]. Available: http://www.electronics-tutorials.ws/transformer/transformer-construction.html.

[16] M. S. Sarma, *Electric Machines*, 2nd ed. Saint Paul, USA: West publishing company, 1994.

[17] S. J. Chapman, *Electric Machinery Fundamentals*, 5th ed. McGraw-Hill, Inc., 2012.

[18] R. M. Del Vecchio, B. Poulin, P. T. Feghali, D. M. Shah and R. Ahuja, *Transformer Design Principles: With Applications to Core-form Power Transformers*, 2nd ed. CRC Press, Boca Raton, FL., 2010.

[19] *Three Phase Transformers* (2015). Electronics-tutorials. [Online]. Available: http://www.electronics-tutorials.ws/transformer/three-phase-transformer.html.

[20] *Magnetic Hysteresis* (2015). Electronics-tutorials. [Online]. Available: http:// www.electronics-tutorials.ws/ electromagnetism/magnetic-hysteresis.html.

[21] *Magnetizing Inrush Current in Power Transformer* (2015). Electrical4u. [Online]. Available: http://www.electrical4u.com/magnetizing-inrush-current-in-power-transformer.

[22] W. K. Sonnemann, C. L. Wagner, and G. D. Rockefeller, “Magnetizing Inrush Phenomena in Transformer Banks,” *Trans. Am. Inst. Electr. Eng. Part III Power Appar. Syst.*, vol. 77, no. 3, pp. 884–892, 1958.

[23] J. Berdy, W. Kaufman and K. Winick, “A Dissertation on Power Transformer Excitation and Inrush Characteristics,” in *Symposium on Transformer Excitation and Inrush Characteristics and Their Relationship to Transformer Protective Relaying, Houston, TX, August 5*, 1976.

[24] L. F. Blume, *Transformer engineering*, vol. 251, no. 4. New York: Wiley & Sons, 1951.

[25] K. Karsai, D. Kerenyi and L. Kiss, *Large power transformers*. New York: Elsevier, 1987.

[26] Y. Kang, U. Lim, S. Kang and Y. Kim, "Compensating algorithm for use with measurement type current transformers for protection," *IEEE Russ. Power Tech*, 2005.

[27] L. Kojovic, "Comparison of different current transformer modeling techniques for protection system studies," *IEEE Power Eng. Soc. Summer Meet.*, 2002.

[28] C.57.13-1993 ANSI /IEEE Standard, *Requirements For Instrument Transformers*.

[29] *Transformer and Transformer-feeder Protection* (2015). FECIME. [Online]. Available: http://www.fecime.org/referencias/npag/chap16-254-279.pdf.

[30] J. J. Grainger, S. H. Lee, and A. a. El-Kib, "Design of a Real-Time Switching Control Scheme for Capacitive Compensation of Distribution Feeders," *IEEE Trans. Power Appar. Syst.*, vol. PAS-101, no. 8, pp. 2420 – 2428, 1982.

[31] IEEE Std C37.91-2000, *IEEE Guide for Protective Relay Applications to Power Transformers*. 2000.

[32] P.M. Anderson, *Power System Protection*. John Wiley & Sons, Inc., 1999.

[33] W. H. Bartley, "Analysis of Transformer Failures," *Int. Assoc. Eng. Insur. 36th Annu. Conf. Stock. Sweden*, 2003.

[34] A. R. Van. and C. Warrington, *Protective Relays: Their Theory and Practice*. London: Chapman and Hall, 1962.

[35] and S. R. H. Ding, R. Heywood, J. Lapworth, "Why Transformers Fail," *Euro TechCon 2009, Stretton, United Kingdom*, 2009.

[36] IEEE Std C37.108-2002, *IEEE Guide for the Protection of Network Transformers*. 2002.

[37] W. A. Elmore, *protective relaying theory and applications*, 2nd ed. New York: Marcel Dekker, Inc., 2000.

[38] *Transformer Protection* (2015). EWH. [Online]. Available: http://ewh.ieee.org/r1/boston/pes/Education/TransformerCourse2010/CourseResources/IEEEPESTransformerProtection.pdf.

[39] G. Rockefeller, *Transformer Protection Application Guide*. Basler Electric Company, 1999.

[40] H. P. Sleeper, “Ratio differential relay protection,” *Electr. World*, pp. 827–831, 1927.

[41] R. E. Cordray, “Percentage Differential Transformer Protection,” *Electr. Eng.*, vol. 50, pp. 361–363, 1931.

[42] R. E. Cordray, “Preventing False Operation of Differential Relays,” *Electr. World*, pp. 160–161, 1931.

[43] G. Ziegler, *Numerical differential protection*, 2nd ed. Erlangen, Germany: Publicis Pub, 2012.

[44] A. Guzman, G. Benmouyal, S. E. Zocholl, and H. Altuve, “Performance Analysis of Traditional and Improved Transformer Differential Protective Relays,” *2002 Western Protective Relaying Conference*, pp. 22–24, 2002.

[45] I. T. Monseth and P. H. Robinson, *Relay Systems: Theory and Applications*. New York: McGraw Hill Co., 1935.

[46] E. L. Harder and W. E. Marter, “Principles and Practices of Relaying in the United States,” *Trans. Am. Inst. Electr. Eng.*, vol. 67, no. 2, pp. 1005–1023, 1948.

[47] L. F. Kennedy and C. D. Hayward, “Harmonic-Current-Restrained Relays for Differential Protection,” *Trans. Am. Inst. Electr. Eng.*, vol. 57, no. 5, 1938.

[48] C. D. Hayward, “Harmonic-Current-Restrained Relays for Transformer Differential Protection,” *Trans. Am. Inst. Electr. Eng.*, vol. 60, no. 6, pp. 377–382, 1941.

[49] C. A. Mathews, “An Improved Transformer Differential Relay,” *Trans. Am. Inst. Electr. Eng. Part III Power Appar. Syst.*, vol. 73, no. 1, pp. 645–650, 1954.

[50] R. L. Sharp and W. E. Glassburn, “A Transformer Differential Relay with Second-Harmonic Restraint,” *Trans. Am. Inst. Electr. Eng. Part III Power Appar. Syst.*, vol. 77, no. 3, pp. 913–918, 1958.

[51] C. H. Einvall and J. R. Linders, “A three-phase differential relay for transformer protection,” *IEEE Trans. Power Appar. Syst.*, vol. 94, no. 6, pp. 1971–1980, 1975.

[52] A. Guzman, “Performance analysis of traditional and improved transformer differential protective relays,” *SEL Tech. Pap.*, pp. 405–412, 2000.

[53] A. Guzmán, S. Zocholl, G. Benmouyal, and H. J. Altuve, “A current-based solution for transformer differential protection - Part I: Problem statement,” *IEEE Trans. Power Deliv.*, vol. 16, no. 4, pp. 485–491, 2001.

[54] Pei Liu, O. Malik, Deshu Chen, G. Hope and Yong Guo, “Improved operation of differential protection of power transformers for internal faults,” *IEEE Trans. Power Deliv.*, vol. 7, no. 4, pp. 1912–1919, 1992.

[55] A. Kulidjian, B. Kasztenny and B. Campbell, “New Magnetizing Inrush Restraining Algorithm for Power Transformer Protection,” *IEE Int. Conf. on Developments in Power System Protection*, pp. 181–184, 2001.

[56] A. K. Al-Othman and K. M. El-Naggar, “A New Digital Dynamic Algorithm for Detection of Magnetizing Inrush Current in Transformers,” *Electr. Power Components Syst.*, vol. 37, no. 4, pp. 355–372, 2009.

[57] M. Golshan, M. Saghaian-Nejad, A. Saha, and H. Samet, “A new method for recognizing internal faults from inrush current conditions in digital differential protection of power transformers,” *Electr. Power Syst. Res.*, vol. 71, no. 1, pp. 61–71, 2004.

[58] H. K. Verma and G. C. Kakoti, “Algorithm for harmonic restraint differential relaying based on the discrete Hartley transform,” *Electr. Power Syst. Res.*, vol. 18, no. 2, pp. 125–129, 1990.

[59] J. A. Sykes and I. F. Morrison, “A Proposed Method of Harmonic Restraint Differential Protecting of Transformers by Digital Computer,” *IEEE Trans. Power Appar. Syst.*, vol. PAS-91, no. 3, pp. 1266–1 273, 1972.

[60] O. P. Malik, P. K. Dash and G. S. Hope, “Digital Protection of a Power Transformer,” *IEEE PES Winter Meeting*, p. A76 191–7, 1976.

[61] E. O. Schweitzer, R. R. Larson and A. J. Flechsig, “An Efficient Inrush Current Detection Algorithm for Digital Computer Relaying, Protection of Transformers,” *IEEE PES Summer Meeting*, p. 77 51 0–1, 1977.

[62] Hu Yufeng, D. C. Deshu, X. Y. Xianggen and Z. Zhang, “A novel theory for identifying transformer magnetizing inrush current,” *2003 IEEE PES Transm. Distrib. Conf. Expo. (IEEE Cat. No.03CH37495)*, vol. 1, pp. 274–278, 2003.

[63] E. Madzikanda and M. Negnevitsky, “A Practical Look at Harmonics in Power Transformer Differential Protection,” *IEEE Int. Conf. Power Syst. Technol. Powercon 2012*, pp. 1–6, 2012.

[64] A. M. Dmitrenko, “Semiconductor Pulse-Duration Differential Restraint Relay,” *Izv. Vyss. Uchebnykh Zaved. Elektromekhanika*, no. 3, pp. 335–339, 1970.

[65] A. Giuliante and G. Clough, “Advances in the Design of Differential Protection for Power Transformers,” *Protective Relaying Conference*, pp. 1−12, 1991.

[66] W. Zhuguang, “Transformer differential protection based on the dead angle,” *Autom. Electr. Power Syst. Chinese*, vol. 3, no. 1, pp. 18–30, 1979.

[67] X. N. Lin, P. Liu, and O. P. Malik, “Studies for identification of the inrush based on improved correlation algorithm,” *IEEE Trans. Power Deliv.*, vol. 17, no. 4, pp. 901–907, 2002.

[68] G. D. Rockefeller, “Fault Protection with a Digital Computer,” *IEEE Trans. Power Appar. Syst.*, vol. PAS-88, no. 4, 1969.

[69] A. H. Hamouda, F. Q. Al-anzi, H. K. Gad, A. Gastli, and S. Member, “Numerical Differential Protection Algorithm for Power Transformers,” pp. 440–445, 2013.

[70] B. Kasztenny, N. Fischer, and Y. Xia, “A new inrush detection algorithm for transformer differential protection,” *12th IET Int. Conf. Dev. Power Syst. Prot. (DPSP 2014)*, pp. 5.1.4–5.1.4, 2014.

[71] B. Kasztenny, S. Hodder, N. Fischer, and Y. Xia, “Low second-harmonic content in transformer inrush currents - Analysis and practical solutions for protection security,” *2014 67th Annu. Conf. Prot. Relay Eng.*, pp. 705–722, 2014.

[72] A. Hooshyar, M. Sanaye-Pasand, S. Afsharnia, M. Davarpanah, and B. M. Ebrahimi, “Time-domain analysis of differential power signal to detect magnetizing inrush in power transformers,” *IEEE Trans. Power Deliv.*, vol. 27, no. 3, pp. 1394–1404, 2012.

[73] K. Inagaki, M. Higaki, Y. Matsui, K. Kurita, M. Suzuki, K. Yoshida, and T. Maeda, “Digital protection method for power transformers based on an equivalent circuit composed of inverse inductance,” *IEEE Trans. Power Deliv.*, vol. 3, no. 4, pp. 1501–1510, 1988.

[74] T. A. Kawady, H. E. Labna, and A. E. M. I. Taalab, “A practical winding fault detector for power transformers,” *2008 12th Int. Middle East Power Syst. Conf. MEPCON 2008*, pp. 130–135, 2008.

[75] Y. C. Kang, B. E. Lee, S. H. Kang, and P. A. Crossley, “Transformer protection based on the increment of flux linkages,” *IEE Proc. Gener. Transm. Distrib.*, vol. 151, no. 4, p. 548, 2004.

[76] Y. C. Kang, B. E. Lee, T. Y. Zheng, Y. H. Kim and P. A. Crossley, “Protection, faulted phase and winding identification for the three-winding transformer using the increments of flux linkages,” *IET Gener. Transm. Distrib.*, vol. 4, no. 9, p. 1060, 2010.

[77] Y. C. Kang, B. E. Lee, and S. H. Kang, “Transformer protection relay based on the induced voltages,” *Int. J. Electr. Power Energy Syst.*, vol. 29, no. 4, pp. 281–289, 2007.

[78] M. S. Sachdev, T. S. Sidhu, and H. C. Wood, “Digital relaying algorithm for detecting transformer winding faults,” *IEEE Trans. Power Deliv.*, vol. 4, no. 3, pp. 1638–1648, 1989.

[79] H. Zhang, J. F. Wen, P. Liu, and O. P. Malik, “Discrimination between fault and magnetizing inrush current in transformers using short-time correlation transform,” *Int. J. Electr. Power Energy Syst.*, vol. 24, no. 7, pp. 557–562, 2002.

[80] D. Q. Bi, X. A. Zhang, H. H. Yang, G. W. Yu, X. H. Wang, and W. J. Wang, “Correlation analysis of waveforms in nonsaturation zone-based method to identify the magnetizing inrush in transformer,” *IEEE Trans. Power Deliv.*, vol. 22, no. 3, pp. 1380–1385, 2007.

[81] D. Y. Shi, J. Buse, Q. H. Wu, L. Jiang, and Y. S. Xue, “Fast identification of power transformer magnetizing inrush currents based on mathematical morphology and ANN,” *Power Energy Soc. Gen. Meet. 2011 IEEE*, pp. 1–6, 2011.

[82] M. Tripathy, R. P. Maheshwari, and H. K. Verma, “Radial basis probabilistic neural network for differential protection of power transformer,” *IET Gener. Transm. Distrib.*, vol. 2, no. 1, p. 43, 2008.

[83] L. Y. L. Yongli, H. J. H. Jiali, and D. Y. D. Yuqian, “Application of neural network to microprocessor-based transformer protective relaying,” *Proc. 1995 Int. Conf. Energy Manag. Power Deliv. EMPD ’95*, vol. 2, 1995.

[84] L. G. Perez, A. J. Flechsig, J. L. Meador, and Z. Obradovic, “Training an artificial neural network to discriminate between magnetizing inrush and internal faults,” *IEEE Trans. Power Deliv.*, vol. 9, no. 1, pp. 434–441, 1994.

[85] P. Bastard, “Neural network-based algorithm for power transformer differential relays,” *IEE Proc. - Gener. Transm. Distrib.*, vol. 142, no. 4, pp. 386–392, 1995.

[86] J. Pihler, B. Grcar, and D. Dolinar, “Improved operation of power transformer protection using artificial neural network,” *IEEE Trans. Power Deliv.*, vol. 12, no. 3, pp. 1128–1136, 1997.

[87] M. R. Zaman and M. a. Rahman, “Experimental testing of the artificial neural network based protection of power transformers,” *IEEE Trans. Power Deliv.*, vol. 13, no. 2, pp. 510–515, 1998.

[88] Á.́ L. Orille-Fernández, N. K. I. Ghonaim, and J. A. Valencia, “A FIRANN as a differential relay for three phase power transformer protection,” *IEEE Trans. Power Deliv.*, vol. 16, no. 2, pp. 215–218, 2001.

[89] K. Erdal, Ö. Okan, U. Ömer, and D. Thomas, “PCA based protection algorithm for transformer internal faults,” *Turkish J. Electr. Eng. Comput. Sci.*, vol. 17, no. 2, pp. 125–142, 2009.

[90] H. Khorashadi-Zadeh, “Power transformer differential protection scheme based on symmetrical component and artificial neural network,” *7th Semin. Neural Netw. Appl. Electr. Eng.*, vol. C, pp. 261–265, 2004.

[91] A. Wiszniewski and B. Kasztenny, “Multi-criteria differential transformer relay based on fuzzy logic,” *IEEE Trans. Power Deliv.*, vol. 10, no. 4, pp. 1786–1792, 1995.

[92] M. C. Shin, C. W. Park, and J. H. Kim, “Fuzzy logic-based relaying for large power transformer protection,” *IEEE Trans. Power Deliv.*, vol. 18, no. 3, pp. 718–724, 2003.

[93] A. Rahmati and M. Sanaye-Pasand, “A fast WT-based algorithm to distinguish between transformer internal faults and inrush currents,” *Eur. Trans. Electr. Power*, vol. 22, no. 4, pp. 471–490, 2011.

[94] M. H. Zendehdel and M. Sanaye-Pasand, “Development of two indices based on discrete wavelet transform for transformer differential protection,” *Eur. Trans. Electr. Power*, vol. 22, no. 8, pp. 1078–1092, 2012.

[95] A. A. H. Eldin and M. A. Refaey, “A novel algorithm for discrimination between inrush current and internal faults in power transformer differential protection based on discrete wavelet transform,” *Electric Power Systems Research*, vol. 81, no. 1. pp. 19–24, 2011.

[96] M. O. Oliveira and A. S. Bretas, “Application of Discrete Wavelet Transform for differential protection of power transformers,” *2009 IEEE Bucharest PowerTech*, pp. 1–8, 2009.

[97] L. Yang and J. Ning, “A wavelet transform based discrimination between internal faults and inrush currents in power transformers,” *2011 Int. Conf. Electr. Inf. Control Eng. ICEICE 2011 - Proc.*, pp. 1127–1129, 2011.

[98] M. M. Eissa, “A novel digital directional transformer protection technique based on wavelet packet,” *IEEE Trans. Power Deliv.*, vol. 20, no. 3, pp. 1830–1836, 2005.

[99] J. H. He, Z. J. Ou, Z. Q. Bo, B. R. J. Caunce, and A. Klimek, “Transformer protection based on fault transient detection,” *2006 Int. Conf. Power Syst. Technol. POWERCON2006*, pp. 1–3, 2007.

[100] S. Y. Hong and W. Qin, “A wavelet-based method to discriminate between inrush current and internal fault,” *PowerCon 2000. 2000 Int. Conf. Power Syst. Technol. Proc. (Cat. No.00EX409)*, vol. 2, pp. 927–931, 2000.

[101] C. Jettanasen, C. Pothisarn, J. Klomjit, and A. Ngaopitakkul, “Discriminating among Inrush Current , External Fault and Internal Fault in Power Transformer using Low Frequency Components Comparison of DWT,” *2012 15th Int. Conf. Electr. Mach. Syst.*, pp. 1–6, 2012.

[102] A. Ngaopitakkul, A. Kunakorn, and I. Ngamroo, “Discrimination between external short circuits and internal faults in transformer windings using discrete wavelet transforms,” *Conf. Rec. - IAS Annu. Meet. (IEEE Ind. Appl. Soc.*, vol. 1, pp. 448–452, 2005.

[103] O. Ozgonenel, “Wavelet based ANN approach for transformer protection,” *Int. J. Comput. Intell.*, vol. 2, no. 3, pp. 31–39, 2005.

[104] C. Jettanasen, J. Klomjit, C. Positharn, S. Bunjongjit, and a. Ngaopitakkul, “Differential protection schemes for classification of fault detection between external fault and internal winding fault in transformer using probabilistic neural network,” *2012 Int. Conf. Fuzzy Theory Its Appl. iFUZZY 2012*, pp. 150–153, 2012.

[105] A. Ngaopitakkul and A. Kunakorn, “Internal Fault Classification in Transformer Windings using Combination of Discrete Wavelet Transforms and Back-propagation Neural Networks,” *Int. J. Control. Autom. Sytsems*, vol. 4, no. no. 3, pp. 365–371, 2006.

[106] K. Yabe, “Power differential method for discrimination between fault and magnetizing inrush current in transformers,” *IEEE Trans. Power Deliv.*, vol. 12, no. 3, pp. 1109–1115, 1997.

[107] B. He, X. Zhang, and Z. Q. Bo, “A New Method to Identify Inrush Current Based on Error Estimation,” *IEEE Trans. Power Deliv.*, vol. 21, no. 3, pp. 1163–1168, 2006.

[108] A. M. Mahmoud, M. F. El-Naggar, and E. H. Shehab_Eldin, “A New Technique for Power Transformer Protection Based on Transient Components,” *Energy Procedia*, vol. 14, pp. 318–324, 2012.

[109] M. Eissa, E. Shehab-Eldin, M. Masoud and A. Abd-Elatif, "Laboratory investigation for power transformer protection technique based on positive sequence admittance approach," *Euro. Trans. Electr. Power*, vol. 22, no. 2, pp. 253–270, 2011.

[110] M. Eissa, E. Shehab-Eldin, M. Masoud and A. Abd-Elatif, "Digital technique for power transformer fault detection based on positive sequence admittance approach," *2008 12th Int. Middle East Power Syst. Conf. MEPCON 2008*, no. 3, pp. 517–522, 2008.

[111] T. S. Sidhu, H. S. Gill, and M. S. Sachdev, "A power transformer protection technique with stability during current transformer saturation and ratio-mismatch conditions," *IEEE Trans. Power Deliv.*, vol. 14, no. 3, pp. 798–804, 1999.

[112] M. Babiy, R. Gokaraju, and J. C. Garcia, "Turn-to-turn fault detection in transformers using negative sequence currents," *2011 IEEE Electr. Power Energy Conf. EPEC 2011*, pp. 158–163, 2011.

[113] W. Hauschild and W. Mosch, *Statistical Techniques for High-Voltage Engineering*. London: P. Peregrinus on behalf of the Institution of Electrical Engineers, 1992.

[114] W. H. Press, B. P. Flannery, S. A. Teukolsky and W. T. Vetterling, *Linear Correlation*. Cambridge: Cambridge University Press, 1992.

[115] A. L. Edwards, *an Introduction to Linear Regression and Correlation*. San Francisco: CA: W. H. Freeman, 1976.

[116] L. Gonick and S. Woollcott, *The Cartoon Guide to Statistics*. New York: Harper Perennial, 1993.

[117] J. F. Kenney and E. S. Keeping, *Mathematics of Statistics*. New Jersey: Princeton, N.J. : Van Nostrand, 1962.

[118] G. W. Snedecor, and W. G. Cochran, *Statistical Methods*, 7th ed. Ames: Iowa State University Press, 1980.

[119] M. R. Spiegel, *Theory and Problems of Probability and Statistics*, 2nd ed. New York: McGraw-Hill, 1992.

[120] G. Robinson and E. T. Whittaker, *The Calculus of Observations: A Treatise on Numerical Mathematics*, 4th ed. New York, 1967.

[121] M. Vitins, "A Correlation Method for Transmission Line Protection," *IEEE Trans. Power Appar. Syst.*, vol. PAS-97, no. 5, pp. 1607–1617, 1978.

[122] E. H. Shehab-Eldin and P. G. McLaren, “Travelling wave distance protection-problem areas and solutions,” *IEEE Trans. Power Deliv.*, vol. 3, no. 3, pp. 894–902, 1988.

[123] W. Wang, *Proceedings of the Second International Conference on Mechatronics and Automatic Control*. Switzerland: Springer International Publishing, 2015.

[124] X. Lin and Z. Bo, “A novel CT saturation identification scheme for differential protection of generators,” *2011 IEEE Power Energy Soc. Gen. Meet.*, pp. 1–4, 2011.

[125] E. S. Jin, T. Chen, Z. Q. Bo, a Klimek, and M. F. Yang, “A New Method to Identify CT Saturation Based on the time Difference Algorithm,” pp. 1–4, 2009.

[126] Y. Wang, S. G. Abdulsalam, and W. Xu, “Analytical Formula to Estimate the Maximum Inrush Current,” *Power Deliv. IEEE Trans.*, vol. 23, no. 2, pp. 1266–1268, 2008.

APPENDIX A – LIST OF PUBLICATIONS

Journal papers:

[1] **A. Etumi** and F. Anayi, " The Application of Correlation Technique in Detecting, Internal and External Faults in Three-phase Transformer and Saturation of Current Transformer", *IEEE Transactions on Power Delivery*, 2015

[2] **A. Etumi** and F. Anayi, " New Methods to Discriminate Internal Faults from Magnetizing Inrush Current", *IET Electric Power Applications*, 2016

Conference papers:

[1] **A. Etumi,** E. Eldukhri, F. Anayi and A. Fahmy, "New algorithm based on auto-correlation and cross-correlation scheme to detect the internal fault in single phase transformer", *12th IET International Conference on Developments in Power System Protection (DPSP 2014)*, pp. 1-5, 2014

[2] **A. Etumi,** F. Anayi, A. Fahmy and E. Eldukhri, "Auto-cross correlation coefficients used for detecting an internal fault in three phase transformer", *16th IEEE International Conference on Harmonics and Quality of Power (ICHQP)*, pp. 370-374, 2014

APPENDIX B – MODEL DESCRIPTION

The model that was simulated in steady state consists of:

1- Three-phase transformer with winding of 100 turns and nominal power of 75 MVA, winding nominal voltage of 500 kVrms, winding resistance of 0.002 pu, winding leakage inductance of 0.08 pu and magnetization resistance of 500 pu. The core of transformer was modelled using hysteresis data in table B-1.

Table B-1 Core hysteresis data

Saturation region Currents (pu)	Saturation region fluxes (pu)
0.015	1.2
0.03	1.35
0.06	1.5
0.09	1.56
0.12	1.572
$2.5*10^{12}$	10^{12}

The remnant flux is 0.85 Pu, saturation flux is 1.2 Pu, saturation current is 0.015 and coercive current is 0.003 Pu as they were appeared in red spots on the hysteresis curve shown in Fig B-1.

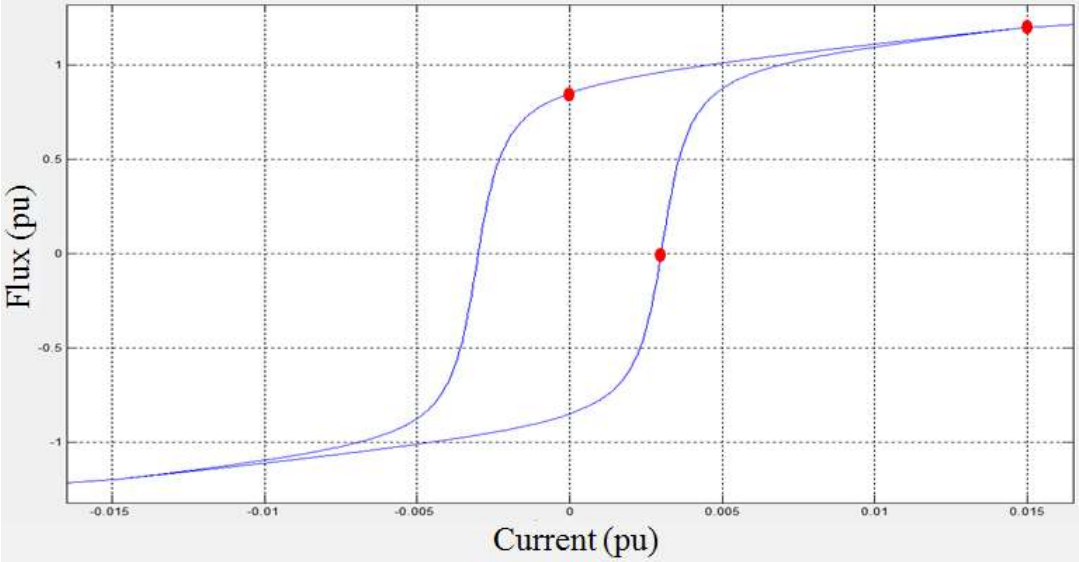

Fig B-1 Core hysteresis curve

2- Three-phase voltage source in series with RL branch and the data set are 500 kVrms is phase to phase voltage, phase angle of phase A is 0 degree, 10^9 VA is three-phase short-circuit level and X/R ratio is 2.

3- Six current transformers (CT1-CT6), three of them (CT1-CT3) were connected in the primary side between voltage source and transformer and the others (CT4-CT6) in the secondary side between transformer and the load. The current transformer (CT) was represented by saturable transformer and its data set were 25 VA is nominal power, turn ratio 1000/5, winding resistance of 0.001 pu, winding leakage inductance of 0.04 pu, magnetization resistance of 100 pu and saturation characteristics are shown in table B-2.

Table B-2 saturation characteristics of current transformer

Current (pu)	Flux (pu)
0	0
0.01	10
1	10.5

APPENDIX C – MATLAB CODE

1- MATLAB code in MATLAB function of the SIMULINK model

```
%%%%%%%%%   calculation of correlation coefficients %%%%%%%%%%%%
ia =reshape(u1,1,21);
iaa =reshape(u2,1,21);
iA =reshape(u3,1,21);
iAA =reshape(u4,1,21);
ib =reshape(x1,1,21);
ibb =reshape(x2,1,21);
iB =reshape(x3,1,21);
iBB =reshape(x4,1,21);
ic =reshape(y1,1,21);
icc =reshape(y2,1,21);
iC =reshape(y3,1,21);
iCC =reshape(y4,1,21);
j=0:1:20;
plot (j,iA,'b',j,ia,'r'),grid;
title('iA blue, ia red');
xlabel('samples');
ylabel('values');
figure;
plot (j,iB,'b',j,ib,'r'),grid;
title('iB blue, ib red');
xlabel('samples');
ylabel('values');
figure;
plot (j,iC,'b',j,ic,'r'),grid;
title('iC blue, ic red');
xlabel('samples');
```

```
ylabel('values');
%%%%%%%%%   calculation of correlation coefficients in phase A  %%%%%%%
if all(abs(ia)<0.0001)
   ia(:,:)=0;
end
if all(abs(iA)<0.0001)
   iA(:,:)=0;
end
sA1=iA.*ia;
sAa=sum(sA1);
siA=sum(iA);
sia=sum(ia);
nAa=(21*sAa)-(siA*sia);
sqiA=iA.^2;
sqia=ia.^2;
ssqA=sum(sqiA);
ssqa=sum(sqia);
lAa=((21*ssqA)-siA^2)*((21*ssqa)-sia^2);
dAa=sqrt(lAa);
if dAa==0
   ra12=0;
else
ra12=nAa/dAa;
end
if all(abs(iaa)<0.0001)
   iaa(:,:)=0;
end
sA2=iaa.*ia;
saa=sum(sA2);
siaa=sum(iaa);
naa=(21*saa)-(siaa*sia);
sqiaa=iaa.^2;
```

```
ssqaa=sum(sqiaa);
laa=((21*ssqaa)-siaa^2)*((21*ssqa)-sia^2);
daa=sqrt(laa);
if daa==0
   ra22=0;
else
ra22=naa/daa;
end
if all(abs(iAA)<0.0001)
   iAA(:,:)=0;
end
sA3=iA.*iAA;
sAA=sum(sA3);
siAA=sum(iAA);
nAA=(21*sAA)-(siA*siAA);
sqiAA=iAA.^2;
ssqAA=sum(sqiAA);
lAA=((21*ssqA)-siA^2)*((21*ssqAA)-siAA^2);
dAA=sqrt(lAA);
if dAA==0
   ra11=0;
else
ra11=nAA/dAA;
end
if ra11<0.9&&ra12<0.9||ra11<0.9&&ra22<0.9&&ra12<0.9||ra22<0.9&&ra12<0.9
     DMa=1;
     else
     DMa=0;
end
if ra11==0&&ra22==0&&ra12==0
     DMa=0;
End
```

```
%%%%%% calculation of correlation coefficients in phase B %%%%%%%%%
if all(abs(ib)<0.0001)
   ib(:,:)=0;
end
if all(abs(iB)<0.0001)
   iB(:,:)=0;
end
sB1=iB.*ib;
sBb=sum(sB1);
siB=sum(iB);
sib=sum(ib);
nBb=(21*sBb)-(siB*sib);
sqiB=iB.^2;
sqib=ib.^2;
ssqB=sum(sqiB);
ssqb=sum(sqib);
lBb=((21*ssqB)-siB^2)*((21*ssqb)-sib^2);
dBb=sqrt(lBb);
if dBb==0
   rb12=0;
else
rb12=nBb/dBb;
end
if all(abs(ibb)<0.0001)
   ibb(:,:)=0;
end
sB2=ibb.*ib;
sbb=sum(sB2);
sibb=sum(ibb);
nbb=(21*sbb)-(sibb*sib);
sqibb=ibb.^2;
ssqbb=sum(sqibb);
```

```
lbb=((21*ssqbb)-sibb^2)*((21*ssqb)-sib^2);
dbb=sqrt(lbb);
if dbb==0
   rb22=0;
else
rb22=nbb/dbb;
end
if all(abs(iBB)<0.0001)
   iBB(:,:)=0;
end
sB3=iB.*iBB;
sBB=sum(sB3);
siBB=sum(iBB);
nBB=(21*sBB)-(siB*siBB);
sqiBB=iBB.^2;
ssqBB=sum(sqiBB);
lBB=((21*ssqB)-siB^2)*((21*ssqBB)-siBB^2);
dBB=sqrt(lBB);
if dBB==0
   rb11=0;
else
rb11=nBB/dBB;
end
if rb11<0.9&&rb12<0.9||rb11<0.9&&rb22<0.9&&rb12<0.9||rb22<0.9&&rb12<0.9
   DMb=1;
else
   DMb=0;
end
if rb11==0&&rb22==0&&rb12==0
 DMb=0;
end
%%%%%% Calculation of correlation coefficients in phase C %%%%%%%%%
```

```
if all(abs(ic)<0.0001)
   ic(:,:)=0;
end
if all(abs(iC)<0.0001)
   iC(:,:)=0;
end
sC1=iC.*ic;
sCc=sum(sC1);
siC=sum(iC);
sic=sum(ic);
nCc=(21*sCc)-(siC*sic);
sqiC=iC.^2;
sqic=ic.^2;
ssqC=sum(sqiC);
ssqc=sum(sqic);
lCc=((21*ssqC)-siC^2)*((21*ssqc)-sic^2);
dCc=sqrt(lCc);
if dCc==0
   rc12=0;
else
rc12=nCc/dCc;
end
if all(abs(icc)<0.0001)
   icc(:,:)=0;
end
sC2=icc.*ic;
scc=sum(sC2);
sicc=sum(icc);
ncc=(21*scc)-(sicc*sic);
sqicc=icc.^2;
ssqcc=sum(sqicc);
lcc=((21*ssqcc)-sicc^2)*((21*ssqc)-sic^2);
```

```
dcc=sqrt(lcc);
if dcc==0
   rc22=0;
else
rc22=ncc/dcc;
end
if all(abs(iCC)<0.0001)
   iCC(:,:)=0;
end
sC3=iC.*iCC;
sCC=sum(sC3);
siCC=sum(iCC);
nCC=(21*sCC)-(siC*siCC);
sqiCC=iCC.^2;
ssqCC=sum(sqiCC);
lCC=((21*ssqC)-siC^2)*((21*ssqCC)-siCC^2);
dCC=sqrt(lCC);
if dCC==0
   rc11=0;
else
rc11=nCC/dCC;
end
 if rc11<0.9&&rc12<0.9||rc11<0.9&&rc22<0.9&&rc12<0.9||rc22<0.9&&rc12<0.9
   DMc=1;
else
   DMc=0;
end
if rc11==0&&rc22==0&&rc12==0
   DMc=0;
end
%%%%%%%% Calculation of current change ratio (CCR) %%%%%%%%%%%
a =reshape(u1,1,101);
```

```
A =reshape(u2,1,101);
b =reshape(x1,1,101);
B =reshape(x2,1,101);
c =reshape(y1,1,101);
C =reshape(y2,1,101);
nax=0;
nbx=0;
ncx=0;
namin=0;
namax=0;
nbmin=0;
nbmax=0;
ncmin=0;
ncmax=0;
AvA=0;
AvB=0;
AvC=0;
ipaCR=0;
ipbCR=0;
ipcCR=0;
iaminCR=0;
iamaxCR=0;
ibminCR=0;
ibmaxCR=0;
icminCR=0;
icmaxCR=0;
DP2Pa=0;
D2PKminA=0;
D2PKmaxA=0;
DP2Pb=0;
D2PKminB=0;
D2PKmaxB=0;
```

```
DP2Pc=0;
D2PKminC=0;
D2PKmaxC=0;
DiffpkAa=0;
DiffpkBb=0;
DiffpkCc=0;
%%%%%%%%%%%%%%%%%%%%%%%%%%%%%%%%%%%%%%%%%%%
 t1=1:101;
 stem(t1,a),grid;
 title('1/2 cycle original sequence phase A')
 figure;
 stem(t1,b),grid;
 title('1/2 cycle original sequence phase B')
 figure;
 stem(t1,c),grid;
 title('1/2 cycle original sequence phase C')
 %%%%%%%%%%%%%%%%%%%%%%%%% Phase A  %%%%%%%%%%%%
if  all(abs(A)<0.0001)
   AvA=0;
else
%%%%%%% primary %%%%%
   ha1=max(abs(A));
    ha2=max(A);
    if ha1>ha2;
    ia=-ha1;
    else ia=ha2;
    end
    nax=find(A==ia);
 %%%%% calculate difference btw lower peak & higher peak for 1 cycle
 %%%%% difference btw 2 max. and min. successive peaks.
 %%%%% this is to find when inrush and DC offset ends.
    ipaCR=ia;
```

```
    iamaxCR=max(A);
    iaminCR=min(A);
    namin=find(A==iaminCR);
    namax=find(A==iamaxCR);
%%%%%%% %%% %%%% Difference max. Peaks btwn pri. & Sec. for phase A
    if ipa01PR==0;
     if ipaCR>=0
        DiffpkAa=abs(max(A))-abs(max(a));
        else
        DiffpkAa=abs(min(A))-abs(min(a));
     end
    else
      if ipa01PR>=0
        DiffpkAa=abs(min(A))-abs(min(a));
        else
        DiffpkAa=abs(max(A))-abs(max(a));
      end
    end
    if ipa01PR>=0
        ipaCR=iaminCR;
    else
        ipaCR=iamaxCR;
    end
%%%%%%%%%%%%%%%%%%%%%%%%%%%%%%%%%%%%%%%%%%%%%%%%%%%%%%%%%%%%%%%%%
    if ipa01PR>=0
        DP2Pa=ipa01PR-abs(iaminCR);% difference btwn higher & lower peaks  of
one cycle
        D2PKminA=abs(iamin02PR)-abs(iaminCR);% difference btwn two min. peaks
of successive cycles
    else
        DP2Pa=abs(ipa01PR)-abs(iamaxCR);% difference btwn higher & lower peaks
of one cycle
```

```
        D2PKminA=abs(iamax02PR)-abs(iamaxCR);% difference btwn two min.
peaks of successive cycles
    end
        D2PKmaxA=abs(ipa02PR)-abs(ipaCR);% difference btwn two max. peaks of
successive cycles
%%%%%%%%%%%%%%%%%% Average A %%%%%%%%%%%%%%%%%
        if (nax-1)>(101-nax)
        if ipaCR>=0
            da=abs(nax-namin);
            if mod(da,2)==0
            mida=(da/2)+namin;
            else
            mida=((da-1)/2)+namin;
            end
            AvA=abs((A(mida)-iaminCR)/(A(mida)-A(nax)));
        else
            da=abs(nax-namax);
            if mod(da,2)==0
            mida=(da/2)+namax;
            else
            mida=((da-1)/2)+namax;
            end
            AvA=abs((A(mida)-iamaxCR)/(A(mida)-A(nax)));
         end
    end
 if (nax-1)<(101-nax)
         if ipaCR>=0
            da=abs(namin-nax);
            if mod(da,2)==0
            mida=(da/2)+nax;
            else
            mida=((da+1)/2)+nax;
```

```
        end
          AvA=abs((A(mida)-iaminCR)/(A(mida)-A(nax)));
        else
          da=abs(namax-nax);
          if mod(da,2)==0
          mida=(da/2)+nax;
          else
          mida=((da+1)/2)+nax;
          end
          AvA=abs((A(mida)-iamaxCR)/(A(mida)-A(nax)));
        end
    end
   if (nax-1)==(101-nax)
       mida1=25;
       AvA1=abs((A(mida1)-A(1))/(A(mida1)-A(nax)));
       mida2=77;
       AvA2=abs((A(mida2)-A(101))/(A(mida2)-A(nax)));
       if AvA1<=AvA2
       AvA=AvA1;
       else
       AvA=AvA2;
       end
    end
end
%%%%%%%%%%%%%%% Phase B %%%%%%%%%%%%%%%%%%%
 if  all(abs(B)<0.0001)
    AvB=0;
 else
    hb1=max(abs(B));
    hb2=max(B);
    if hb1>hb2;
    ib=-hb1;
```

```
    else ib=hb2;
    end
    nbx=find(B==ib);
%%%% calculate difference btw lower peak & higher peak for 1 cycle %
%%%% difference btw 2 max. and min. successive peaks.
%%%% this is to find when inrush and DC offset ends.
    ipbCR=ib;
    ibmaxCR=max(B);
    ibminCR=min(B);
    nbmin=find(B==ibminCR);
    if B(1)==0&&B(2)==0&&B(3)==0&&B(4)==0
       nbmax=1;
    else
    nbmax=find(B==ibmaxCR);
    end
 %%%%%%%%%%%%% Difference max. Peaks btwn pri. & Sec. for phase B
     if ipb01PR==0
        if ipbCR>=0
        DiffpkBb=abs(max(B))-abs(max(b));
        else
        DiffpkBb=abs(min(B))-abs(min(b));
        end
     else
        if ipb01PR>=0
          DiffpkBb=abs(min(B))-abs(min(b));
        else
          DiffpkBb=abs(max(B))-abs(max(b));
        end
     end

%%%%%%%%%%%%%%%%%%%%%%%%%%%%%%%%%%%%%%%%%%%%%%%%%%%%%%%%%%%%%%%%
    if ipb01PR>=0
```

```
    DP2Pb=ipb01PR-abs(ibminCR);% difference btwn higher & lower peaks  of
one cycle
    D2PKminB=abs(ibmin02PR)-abs(ibminCR);% difference btwn two min. peaks
of successive cycles
  else
    DP2Pb=abs(ipb01PR)-abs(ibmaxCR);% difference btwn higher & lower peaks
of one cycle
    D2PKminB=abs(ibmax02PR)-abs(ibmaxCR);% difference btwn two min.
peaks of successive cycles
  end
    D2PKmaxB=abs(ipb02PR)-abs(ipbCR);%difference btwn two max. peaks of
successive cycles
%%%%%%%%%%%%%%%%%% Average B %%%%%%%%%%%%%%%%%%
    if (nbx-1)>(101-nbx)
      if ipbCR>=0
        db=abs(nbx-nbmin);
        if mod(db,2)==0
        midb=(db/2)+nbmin;
        else
        midb=((db-1)/2)+nbmin;
        end
        AvB=abs((B(midb)-ibminCR)/(B(midb)-B(nbx)));
      else
        db=abs(nbx-nbmax);
        if mod(db,2)==0
        midb=(db/2)+nbmax;
        else
        midb=((db-1)/2)+nbmax;
        end
        AvB=abs((B(midb)-ibmaxCR)/(B(midb)-B(nbx)));
      end
   end
```

```
    if (nbx-1)<(101-nbx)
        if ipbCR>=0
          db=abs(nbmin-nbx);
          if mod(db,2)==0
          midb=(db/2)+nbx;
          else
          midb=((db+1)/2)+nbx;
          end
          AvB=abs((B(midb)-ibminCR)/(B(midb)-B(nbx)));
        else
          db=abs(nbmax-nbx);
          if mod(db,2)==0
          midb=(db/2)+nbx;
          else
          midb=((db+1)/2)+nbx;
          end
          AvB=abs((B(midb)-ibmaxCR)/(B(midb)-B(nbx)));
        end
     end
     if (nbx-1)==(101-nbx)
        midb1=25;
        AvB1=abs((B(midb1)-B(1))/(B(midb1)-B(nbx)));
        midb2=77;
        AvB2=abs((B(midb2)-B(101))/(B(midb2)-B(nbx)));
         if AvB1<=AvB2
        AvB=AvB1;
         else
        AvB=AvB2;
         end
      end
end
%%%%%%%%%%%%%% Phase C %%%%%%%%%%%%%%%%%%%
```

```
if  all(abs(C)<0.0001)
   AvC=0;
else
      hc1=max(abs(C));
      hc2=max(C);
      if hc1>hc2;
      ic=-hc1;
      else ic=hc2;
      end
      ncx=find(C==ic);
%%%%%  calculate difference btw lower peak & higher peak for 1 cycle
%%%%%  difference btw 2 max. and min. successive peaks.
%%%%%  this is to find when inrush and DC offset ends.
      ipcCR=ic;
      icmaxCR=max(C);
      icminCR=min(C);
      ncmin=find(C==icminCR);
      ncmax=find(C==icmaxCR);
%%%%%%% %%% %%%% Difference max. Peaks btwn pri. & Sec. for phase C
     if ipc01PR==0
       if ipcCR>=0
       DiffpkCc=abs(max(C))-abs(max(c));
       else
       DiffpkCc=abs(min(C))-abs(min(c));
       end
     else
       if ipc01PR>=0
          DiffpkCc=abs(min(C))-abs(min(c));
       else
          DiffpkCc=abs(max(C))-abs(max(c));
       end
     end
```

```
%%%%%%%%%%%%%%%%%%%%%%%%%%%%%%%%%%%%%%%%
    if ipc01PR>=0
     DP2Pc=ipc01PR-abs(icminCR);% difference btwn higher & lower peaks  of
one cycle
     D2PKminC=abs(icmin02PR)-abs(icminCR);% difference btwn two min. peaks
of successive cycles
    else
     DP2Pc=abs(ipc01PR)-abs(icmaxCR);% difference btwn higher & lower peaks
of one cycle
     D2PKminC=abs(icmax02PR)-abs(icmaxCR);% difference btwn two min.
peaks of successive cycles
    end
     D2PKmaxC=abs(ipc02PR)-abs(ipcCR);%difference btwn two max. peaks of
successive cycles
%%%%%%%%%%%%%%%%%%%% Average C %%%%%%%%%%%%%%%%%%
      if (ncx-1)>(101-ncx)
         if ipcCR>=0
           dc=abs(ncx-ncmin);
           if mod(dc,2)==0
           midc=(dc/2)+ncmin;
           else
           midc=((dc-1)/2)+ncmin;
           end
           AvC=abs((C(midc)-icminCR)/(C(midc)-C(ncx)));
         else
           dc=abs(ncx-ncmax);
           if mod(dc,2)==0
           midc=(dc/2)+ncmax;
           else
           midc=((dc-1)/2)+ncmax;
           end
           AvC=abs((C(midc)-icmaxCR)/(C(midc)-C(ncx)));
```

```
    end
end
if (ncx-1)<(101-ncx)
    if ipcCR>=0
      dc=abs(ncmin-ncx);
      if mod(dc,2)==0
      midc=(dc/2)+ncx;
      else
      midc=((dc+1)/2)+ncx;
      end
      AvC=abs((C(midc)-icminCR)/(C(midc)-C(ncx)));
    else
      dc=abs(ncmax-ncx);
      if mod(dc,2)==0
      midc=(dc/2)+ncx;
      else
      midc=((dc+1)/2)+ncx;
      end
      AvC=abs((C(midc)-icmaxCR)/(C(midc)-C(ncx)));
    end
end
 if (ncx-1)==(101-ncx)
    midc1=25;
    AvC1=abs((C(midc1)-C(1))/(C(midc1)-C(ncx)));
    midc2=77;
    AvC2=abs((C(midc2)-C(101))/(C(midc2)-C(ncx)));
    if AvC1<=AvC2
      AvC=AvC1;
    else
      AvC=AvC2;
    end
 end
```

```
 end
%%%%%%%%%%%%%%%%%%  Averages A, B & C %%%%%%%%%%%%
t2=1:40;
figure;
plot(t2,AvrA,t2,AvrB,t2,AvrC),grid;
title('current change ratio for phases A ,B and C')
figure;
plot(t2,AvrA),grid;
title(' current change ratio for phase A')
figure;
plot(t2,AvrB),grid;
title(' current change ratio for phase B')
figure;
plot(t2,AvrC),grid;
title(' current change ratio for phase C')
t3=1:20;
figure;
plot(t3,DP2Pa),grid;
title('difference btwn higher & lower peaks  of one cycle for phase A')
figure;
plot(t3,DP2Pb),grid;
title('difference btwn higher & lower peaks  of one cycle for phase B')
figure;
plot(t3,DP2Pc),grid;
title('difference btwn higher & lower peaks  of one cycle for phase C')
t4=2:20;
figure;
plot(t4,D2maxPKa,'r',t4,D2minPKa,'b'),grid;
title(' difference btwn two peaks of successive cycles for phase A, Red = max. peaks
& blue = min. peaks')
figure;
```

```
plot(t4,D2maxPKb,'r',t4,D2minPKb,'b'),grid;
title(' difference btwn two peaks of successive cycles for phase B, Red = max. peaks & blue = min. peaks')
figure;
plot(t4,D2maxPKc,'r',t4,D2minPKc,'b'),grid;
title(' difference btwn two peaks of successive cycles for phase C, Red = max. peaks & blue = min. peaks')
%%%%%%%% Calculation of percentage area difference (PAD) %%%%%%%%%
a =reshape(u1,1,51);
A =reshape(u2,1,51);
b =reshape(x1,1,51);
B =reshape(x2,1,51);
c =reshape(y1,1,51);
C =reshape(y2,1,51);

DiffArA=0;
DiffArB=0;
DiffArC=0;
q=0;
App=zeros(1,51);
Bpp=zeros(1,51);
Cpp=zeros(1,51);
Ass=zeros(1,51);
Bss=zeros(1,51);
Css=zeros(1,51);
    for g=2:2:50
    q=q+1;
    App(q)=A(g);
    Bpp(q)=B(g);
    Cpp(q)=C(g);
    Ass(q)=a(g);
    Bss(q)=b(g);
```

```
    Css(q)=c(g);
    end
%%%%%%%%%%%%%%%%%%%% Area difference phase A %%%%%%%%%
if  all(abs(A)<0.0001)
   DiffArA=0;
else
   sap=abs(App);
   sas=abs(Ass);
   Arap=(sum(sap))*0.0002;
   Aras=(sum(sas))*0.0002;
   if Arap==Aras
   DiffArA=0;
   elseif Arap>Aras
   DiffArA=((Arap-Aras)/Arap)*100;
   else
   DiffArA=((Arap-Aras)/Aras)*100;
   end
end
%%%%%%%%%%%%%%%%%%%% Area difference phase B %%%%%%%%%
if  all(abs(B)<0.0001)
   DiffArB=0;
else
   sbp=abs(Bpp);
   sbs=abs(Bss);
   Arbp=(sum(sbp))*0.0002;
   Arbs=(sum(sbs))*0.0002;
   if Arbp==Arbs
   DiffArB=0;
   elseif Arbp>Arbs
   DiffArB=((Arbp-Arbs)/Arbp)*100;
   else
   DiffArB=((Arbp-Arbs)/Arbs)*100;
```

```
    end
end
%%%%%%%%%%%%%%%%%%%% Area difference phase C %%%%%%%%%
if  all(abs(A)<0.0001)
    DiffArC=0;
else
    scp=abs(Cpp);
    scs=abs(Css);
    Arcp=(sum(scp))*0.0002;
    Arcs=(sum(scs))*0.0002;
    if Arcp==Arcs
    DiffArC=0;
    elseif Arcp>Arcs
    DiffArC=((Arcp-Arcs)/Arcp)*100;
    else
    DiffArC=((Arcp-Arcs)/Arcs)*100;
    end
end
```

2- MATLAB code for laboratory data

```
dataPA=data(:,2);
dataPB=data(:,3);
dataPC=data(:,4);
dataSa=data(:,5);
dataSb=data(:,6);
dataSc=data(:,7);
xA=reshape(dataPA,1,100000);
xa=reshape(dataSa,1,100000);
xB=reshape(dataPB,1,100000);
xb=reshape(dataSb,1,100000);
```

```
xC=reshape(dataPC,1,100000);
xc=reshape(dataSc,1,100000);
yA=xA/8;
ya=xa/8;
yB=xB/8;
yb=xb/8;
yC=xC/8;
yc=xc/8;
%%%%%%%%%%%  reduce no. of samples to 10000 in order to be easily drawn
k=1;
for jj=0:10:100000
   if jj==0
      j=1;
   else
      j=jj;
   end
   AA(k)=yA(j);
   aa(k)=ya(j);
   BB(k)=yB(j);
   bb(k)=yb(j);
   CC(k)=yC(j);
   cc(k)=yc(j);
   k=k+1;
end
priA=reshape(AA,10001,1);
secA=reshape(aa,10001,1);
priB=reshape(BB,10001,1);
secB=reshape(bb,10001,1);
priC=reshape(CC,10001,1);
secC=reshape(cc,10001,1);
%%%%%%%%%%%%%%%%%%%%%%%%%%%%%%%%%%%%%%%%%
n=0:99999;
```

```
n1=0:0.0001:9.9999;
plot(n1,yA,'b',n1,ya,'r',n1,yB,'m',n1,yb,'g',n1,yC,'k',n1,yc,'c','LineWidth',3),grid;
xlabel('Time, t (sec)','FontSize',30,'FontWeight','bold','FontName','Times New
Roman')
ylabel('Current, i (A)','FontSize',30,'FontWeight','bold','FontName','Times New
Roman')
set(gca, 'FontName', 'Times New Roman')
set(gca, 'FontSize', 30)
figure;
plot(n,yA,'b',n,ya,'r','LineWidth',3),grid;
title('Phase A Pri. blue, Phase A Sec.
red','FontSize',30,'FontWeight','bold','FontName','Times New Roman');
xlabel('Sample number','FontSize',30,'FontWeight','bold','FontName','Times New
Roman')
ylabel('Current/Amps.','FontSize',30,'FontWeight','bold','FontName','Times New
Roman')
set(gca, 'FontName', 'Times New Roman')
set(gca, 'FontSize', 30)
figure;
plot(n,yB,'b',n,yb,'r','LineWidth',3),grid;
title('Phase B Pri. blue, Phase B Sec.
red','FontSize',30,'FontWeight','bold','FontName','Times New Roman');
xlabel('Sample number','FontSize',30,'FontWeight','bold','FontName','Times New
Roman')
ylabel('Current/Amps.','FontSize',30,'FontWeight','bold','FontName','Times New
Roman')
set(gca, 'FontName', 'Times New Roman')
set(gca, 'FontSize', 30)
figure;
plot(n,yC,'b',n,yc,'r','LineWidth',3),grid;
title('Phase C Pri. blue, Phase C Sec.
red','FontSize',30,'FontWeight','bold','FontName','Times New Roman');
```

```
xlabel('Sample number','FontSize',30,'FontWeight','bold','FontName','Times New Roman')
ylabel('Current/Amps.','FontSize',30,'FontWeight','bold','FontName','Times New Roman')
set(gca, 'FontName', 'Times New Roman')
set(gca, 'FontSize', 30)
%%%%%%%%%   calculation of correlation coefficients  %%%%%%%%%%%%
dataPA=data(:,2);
dataPB=data(:,3);
dataPC=data(:,4);
dataSa=data(:,5);
dataSb=data(:,6);
dataSc=data(:,7);
figure;
xA=reshape(dataPA,1,2001);
xa=reshape(dataSa,1,2001);
xB=reshape(dataPB,1,2001);
xb=reshape(dataSb,1,2001);
xC=reshape(dataPC,1,2001);
xc=reshape(dataSc,1,2001);
yA=xA/8;
ya=xa/8;
yB=xB/8;
yb=xb/8;
yC=xC/8;
yc=xc/8;
n=0:2000;
n1=0:0.0001:0.2;
priA=reshape(yA,2001,1);
secA=reshape(ya,2001,1);
priB=reshape(yB,2001,1);
secB=reshape(yb,2001,1);
```

```
priC=reshape(yC,2001,1);
secC=reshape(yc,2001,1);
Tm=reshape(n1,2001,1);
plot(n1,yA,'b',n1,ya,'r',n1,yB,'m',n1,yb,'g',n1,yC,'k',n1,yc,'c','LineWidth',3),grid;
title('Phase A Pri. blue, Phase A Sec.
red','FontSize',30,'FontWeight','bold','FontName','Times New Roman');
xlabel('Time, t (sec)','FontSize',30,'FontWeight','bold','FontName','Times New
Roman')
ylabel('Current, i (A)','FontSize',30,'FontWeight','bold','FontName','Times New
Roman')
set(gca, 'FontName', 'Times New Roman')
set(gca, 'FontSize', 30)
figure;
plot(n,yA,'b',n,ya,'r','LineWidth',3),grid;
title('Phase A Pri. blue, Phase A Sec.
red','FontSize',30,'FontWeight','bold','FontName','Times New Roman');
xlabel('Sample number','FontSize',30,'FontWeight','bold','FontName','Times New
Roman')
ylabel('Current, i (A)','FontSize',30,'FontWeight','bold','FontName','Times New
Roman')
set(gca, 'FontName', 'Times New Roman')
set(gca, 'FontSize', 30)
figure;
plot(n,yB,'b',n,yb,'r','LineWidth',3),grid;
title('Phase B Pri. blue, Phase B Sec.
red','FontSize',30,'FontWeight','bold','FontName','Times New Roman');
xlabel('Sample number','FontSize',30,'FontWeight','bold','FontName','Times New
Roman')
ylabel('Current/Amps.','FontSize',30,'FontWeight','bold','FontName','Times New
Roman')
set(gca, 'FontName', 'Times New Roman')
set(gca, 'FontSize', 30)
```

```
figure;
plot(n,yC,'b',n,yc,'r','LineWidth',3),grid;
title('Phase C Pri. blue, Phase C Sec.
red','FontSize',30,'FontWeight','bold','FontName','Times New Roman');
xlabel('Sample number','FontSize',30,'FontWeight','bold','FontName','Times New
Roman')
ylabel('Current/Amps.','FontSize',30,'FontWeight','bold','FontName','Times New
Roman')
set(gca, 'FontName', 'Times New Roman')
set(gca, 'FontSize', 30)
j=0;
for i=0:20:1780
   j=j+1;
%%%%%%%%%%%%  calculation of correlation coefficients in phase A  %%%
   iA=yA(201+i:221+i);
   ia=ya(201+i:221+i);
     sA1=iA.*ia;
     sAa=sum(sA1);
     siA=sum(iA);
     sia=sum(ia);
     nAa=(21*sAa)-(siA*sia);
     sqiA=iA.^2;
     sqia=ia.^2;
     ssqA=sum(sqiA);
     ssqa=sum(sqia);
     lAa=((21*ssqA)-siA^2)*((21*ssqa)-sia^2);
     dAa=sqrt(lAa);
     ra12=nAa/dAa;
     RA12(j)=ra12;
 fprintf('\n RA12 is %.4f \n',ra12)
%%%%%%%%%%%%%%%%%%%%%%%%%%%%%%%%%%%%%%%%%%%%%%%%%%%%%%%%%%%%%%%%%%%%%%%
  iA=yA(201+i:221+i);
```

```
  iAA=yA(1+i:21+i);
    sA3=iA.*iAA;
    sAA=sum(sA3);
    siAA=sum(iAA);
    nAA=(21*sAA)-(siA*siAA);
    sqiAA=iAA.^2;
    ssqAA=sum(sqiAA);
    lAA=((21*ssqA)-siA^2)*((21*ssqAA)-siAA^2);
    dAA=sqrt(lAA);
    ra11=nAA/dAA;
    RA11(j)=ra11;
 fprintf('\n RA11 is %.4f \n',ra11)
%%%%%%%%%%%%%%%%%%%%%%%%%%%%%%%%%%%%%%%%
  ia=ya(201+i:221+i);
  iaa=ya(1+i:21+i);
   sA2=iaa.*ia;
   saa=sum(sA2);
   siaa=sum(iaa);
   naa=(21*saa)-(siaa*sia);
   sqiaa=iaa.^2;
   ssqaa=sum(sqiaa);
   laa=((21*ssqaa)-siaa^2)*((21*ssqa)-sia^2);
   daa=sqrt(laa);
   ra22=naa/daa;
   RA22(j)=ra22;
 fprintf('\n RA22 is %.4f \n',ra22)
%%%%%%%%%%%%%%%%%%%%%%%%%%%%%%  calculation of correlation coefficients in phase B  %%%
  iB=yB(201+i:221+i);
  ib=yb(201+i:221+i);
   sB1=iB.*ib;
   sBb=sum(sB1);
   siB=sum(iB);
```

```
   sib=sum(ib);
   nBb=(21*sBb)-(siB*sib);
   sqiB=iB.^2;
   sqib=ib.^2;
   ssqB=sum(sqiB);
   ssqb=sum(sqib);
   lBb=((21*ssqB)-siB^2)*((21*ssqb)-sib^2);
   dBb=sqrt(lBb);
   rb12=nBb/dBb;
   RB12(j)=rb12;
 fprintf('\n RB12 is %.4f \n',rb12)
%%%%%%%%%%%%%%%%%%%%%%%%%%%%%%%%%%%%%%%%%
 iB=yB(201+i:221+i);
 iBB=yB(1+i:21+i);
   sB3=iB.*iBB;
   sBB=sum(sB3);
   siBB=sum(iBB);
   nBB=(21*sBB)-(siB*siBB);
   sqiBB=iBB.^2;
   ssqBB=sum(sqiBB);
   lBB=((21*ssqB)-siB^2)*((21*ssqBB)-siBB^2);
   dBB=sqrt(lBB);
   rb11=nBB/dBB;
   RB11(j)=rb11;
 fprintf('\n RB11 is %.4f \n',rb11)
%%%%%%%%%%%%%%%%%%%%%%%%%%%%%%%%%%%%%%%%%
 ib=yb(201+i:221+i);
 ibb=yb(1+i:21+i);
   sB2=ibb.*ib;
   sbb=sum(sB2);
   sibb=sum(ibb);
   nbb=(21*sbb)-(sibb*sib);
```

```
    sqibb=ibb.^2;
    ssqbb=sum(sqibb);
    lbb=((21*ssqbb)-sibb^2)*((21*ssqb)-sib^2);
    dbb=sqrt(lbb);
    rb22=nbb/dbb;
    RB22(j)=rb22;
 fprintf('\n RB22 is %.4f \n',rb22)
%%%%%%%%%%%%  calculation of correlation coefficients in phase C  %%%
  iC=yC(201+i:221+i);
  ic=yc(201+i:221+i);
    sC1=iC.*ic;
    sCc=sum(sC1);
    siC=sum(iC);
    sic=sum(ic);
    nCc=(21*sCc)-(siC*sic);
    sqiC=iC.^2;
    sqic=ic.^2;
    ssqC=sum(sqiC);
    ssqc=sum(sqic);
    lCc=((21*ssqC)-siC^2)*((21*ssqc)-sic^2);
    dCc=sqrt(lCc);
    rc12=nCc/dCc;
    RC12(j)=rc12;
 fprintf('\n RC12 is %.4f \n',rc12)
%%%%%%%%%%%%%%%%%%%%%%%%%%%%%%%%%%%%%%%%%%%%%%%%%%%%%%%%%%%%%%%%%%%%
 iC=yC(201+i:221+i);
 iCC=yC(1+i:21+i);
    sC3=iC.*iCC;
    sCC=sum(sC3);
    siCC=sum(iCC);
    nCC=(21*sCC)-(siC*siCC);
    sqiCC=iCC.^2;
```

```
    ssqCC=sum(sqiCC);
    lCC=((21*ssqC)-siC^2)*((21*ssqCC)-siCC^2);
    dCC=sqrt(lCC);
    rc11=nCC/dCC;
    RC11(j)=rc11;
 fprintf('\n RC11 is %.4f \n',rc11)
%%%%%%%%%%%%%%%%%%%%%%%%%%%%%%%%%%%%%%%%%%%%%%%%%%%%%%%%
 ic=yc(201+i:221+i);
 icc=yc(1+i:21+i);
    sC2=icc.*ic;
    scc=sum(sC2);
    sicc=sum(icc);
    ncc=(21*scc)-(sicc*sic);
    sqicc=icc.^2;
    ssqcc=sum(sqicc);
    lcc=((21*ssqcc)-sicc^2)*((21*ssqc)-sic^2);
    dcc=sqrt(lcc);
    rc22=ncc/dcc;
    RC22(j)=rc22;
 fprintf('\n RC22 is %.4f \n',rc22)
end
t=1:90;
plot(t,RA12,'b.-',t,RA11,'r.-',t, RA22,'g.-','MarkerSize',30),grid;
title('RA12 blue, RA11 red, RA22
green','FontSize',30,'FontWeight','bold','FontName','Times New Roman');
xlabel('Window number','FontSize',30,'FontWeight','bold','FontName','Times New
Roman')
ylabel('Correlation coefficient
value','FontSize',30,'FontWeight','bold','FontName','Times New Roman')
set(gca, 'FontName', 'Times New Roman')
set(gca, 'FontSize', 30)
figure;
```

```
plot(t,RB12,'b.-',t,RB11,'r.-',t, RB22,'g.-','MarkerSize',30),grid;
title('RB12 blue, RB11 red, RB22
green','FontSize',30,'FontWeight','bold','FontName','Times New Roman');
xlabel('Window number','FontSize',30,'FontWeight','bold','FontName','Times New
Roman')
ylabel('Correlation coefficient
value','FontSize',30,'FontWeight','bold','FontName','Times New Roman')
set(gca, 'FontName', 'Times New Roman')
set(gca, 'FontSize', 30)
figure;
plot(t,RC12,'b.-',t,RC11,'r.-',t, RC22,'g.-','MarkerSize',30),grid;
title('RC12 blue, RC11 red, RC22
green','FontSize',30,'FontWeight','bold','FontName','Times New Roman');
xlabel('Window number','FontSize',30,'FontWeight','bold','FontName','Times New
Roman')
ylabel('Correlation coefficient
value','FontSize',30,'FontWeight','bold','FontName','Times New Roman')
set(gca, 'FontName', 'Times New Roman')
set(gca, 'FontSize', 30)
%%%%%%%%%%%%%%%%  Calculation of PAD and CCR   %%%%%%%%
dataPA=data(:,2);
dataPB=data(:,3);
dataPC=data(:,4);
dataPa=data(:,5);
dataPb=data(:,6);
dataPc=data(:,7);
xA=reshape(dataPA,1,4001);
xB=reshape(dataPB,1,4001);
xC=reshape(dataPC,1,4001);
xa=reshape(dataPa,1,4001);
xb=reshape(dataPb,1,4001);
xc=reshape(dataPc,1,4001);
```

```
yA=xA/8;
yB=xB/8;
yC=xC/8;
ya=xa/8;
yb=xb/8;
yc=xc/8;
n1=0:.0001:0.4;
plot(n1,yA,'b',n1,ya,'r',n1,yB,'m',n1,yb,'g',n1,yC,'k',n1,yc,'c','LineWidth',3),grid;
xlabel('Time, t (sec)','FontSize',30,'FontWeight','bold','FontName','Times New
Roman')
ylabel('Current, i (A)','FontSize',30,'FontWeight','bold','FontName','Times New
Roman')
set(gca, 'FontName', 'Times New Roman')
set(gca, 'FontSize', 30)
%%%%%%%%%%%%%%%%%%%%%%%%%%%%%%%%%%%%%%%%%%%%%%%%%%%%%%%%%%%%%%%%%%%%%%%%%%%%%%%%
yyA=reshape(yA,4001,1);
yya=reshape(ya,4001,1);
 yyB=reshape(yB,4001,1);
yyb=reshape(yb,4001,1);
yyC=reshape(yC,4001,1);
yyc=reshape(yc,4001,1);
%%%%%%%%%%%%%%%%%%%%%%%%%%%%%%%%%%%%%%%%%%%%%%%%%%%%%%%%%%%%%%%%%%%%%%%%%%%%%%%%
t=1:4001;
figure;
 plot(t,yA),grid;
 title('original waveform for phase A Pri.')
 figure;
 plot(t,yB),grid;
 title('original waveform for phase B Pri.')
 figure;
 plot(t,yC),grid;
 title('original waveform for phase C Pri.')
```

```
 figure;
 plot(t,ya),grid;
 title('original waveform for phase A Sec.')
 figure;
 plot(t,yb),grid;
 title('original waveform for phase B Sec.')
 figure;
 plot(t,yc),grid;
 title('original waveform for phase C Sec.')
j=0;
k=0;
ga1=0;
ga2=0;
ga3=0;
gb1=0;
gb2=0;
gb3=0;
gc1=0;
gc2=0;
gc3=0;
for n=1:40
    k=k+1;
j=j+101;
h=j-101;
h=h+1;
ap=yA(1,h:j);
bp=yB(1,h:j);
cp=yC(1,h:j);
as=ya(1,h:j);
bs=yb(1,h:j);
cs=yc(1,h:j);
t1=1:101;
```

```
figure;
stem(t1,a),grid;
title('1/2 cycle original sequence phase A')
figure;
stem(t1,b),grid;
title('1/2 cycle original sequence phase B')
figure;
stem(t1,c),grid;
title('1/2 cycle original sequence phase C')
%%%%% calculating Percentage Area Difference for first and last quarter of cycle
if mod(n,2)==0
    q=0;
    for g=52:2:100
    q=q+1;
    App(q)=ap(g);
    Bpp(q)=bp(g);
    Cpp(q)=cp(g);
    Ass(q)=as(g);
    Bss(q)=bs(g);
    Css(q)=cs(g);
    end
else
    q=0;
    for g=2:2:50
    q=q+1;
    App(q)=ap(g);
    Bpp(q)=bp(g);
    Cpp(q)=cp(g);
    Ass(q)=as(g);
    Bss(q)=bs(g);
    Css(q)=cs(g);
    end
```

```
end
%%%%%%%%%%%%%%%%%%%%  PAD for phase A  %%%%%%%%%%%
sap=abs(App);
sas=abs(Ass);
Arap=(sum(sap))*0.0002;
Aras=(sum(sas))*0.0002;
if Arap==Aras
    DAa=0;
elseif Arap>Aras
   DAa=((Arap-Aras)/Arap)*100;
else
   DAa=((Arap-Aras)/Aras)*100;
end
DiffArA(k)=DAa;
%%%%%%%%%%%%%%%%%%%%  PAD for phase B  %%%%%%%%%%%
sbp=abs(Bpp);
sbs=abs(Bss);
Arbp=(sum(sbp))*0.0002;
Arbs=(sum(sbs))*0.0002;
if Arbp==Arbs
    DAb=0;
elseif Arbp>Arbs
   DAb=((Arbp-Arbs)/Arbp)*100;
else
   DAb=((Arbp-Arbs)/Arbs)*100;
end
DiffArB(k)=DAb;
%%%%%%%%%%%%%%%%%%%%  PAD for phase C  %%%%%%%%%%%
scp=abs(Cpp);
scs=abs(Css);
Arcp=(sum(scp))*0.0002;
Arcs=(sum(scs))*0.0002;
```

```
if Arcp==Arcs
   DAc=0;
elseif Arcp>Arcs
  DAc=((Arcp-Arcs)/Arcp)*100;
else
  DAc=((Arcp-Arcs)/Arcs)*100;
end
DiffArC(k)=DAc;
%%%%%%%%%%%%%%%%%%% Phase A Secondary %%%%%%%%%%
    has1=max(abs(as));
    has2=max(as);
    if has1>has2;
      ias=-has1;
    else ias=has2;
    end
    naxs=find(as==ias);
    ipas(k)=ias;
%%%%%%%%%%%%%%%%%%% Phase B Secondary %%%%%%%%%%
    hbs1=max(abs(bs));
    hbs2=max(bs);
    if hbs1>hbs2;
      ibs=-hbs1;
    else ibs=hbs2;
    end
    nbxs=find(bs==ibs);
    ipbs(k)=ibs;
%%%%%%%%%%%%%%%%%%% Phase C Secondary %%%%%%%%%%
    hcs1=max(abs(cs));
    hcs2=max(cs);
    if hcs1>hcs2;
      ics=-hcs1;
    else ics=hcs2;
```

```
    end
    ncxs=find(cs==ics);
    ipcs(k)=ics;
%%%%%%%%%%%%%%%%%%%%  Phase A Primary  %%%%%%%%%%
 hap1=max(abs(ap));
 hap2=max(ap);
 if hap1>hap2;
   iap=-hap1;
 else iap=hap2;
 end
 naxp=find(ap==iap);
%%%%%  calculate difference btw lower peak & higher peak for 1 cycle %
%%%%% difference btw 2 max. and min. successive peaks.
%%%%%  this is to find when inrush and DC offset ends.
 ipap(k)=iap;
 iamaxp(k)=max(ap);
 iaminp(k)=min(ap);
 namaxp=find(ap==max(ap));
 naminp=find(ap==min(ap));
 [rw cl]=size(ipap);
%%%%%%%%%% Difference max. peaks btwn pri.&Sec. for phase A
if mod(cl,2)==0
    if ipap(1)>=0
    DiffpkAa=abs(min(ap))-abs(min(as));
    else
    DiffpkAa=abs(max(ap))-abs(max(as));
    end
 else
    if ipap(1)>=0
    DiffpkAa=abs(max(ap))-abs(max(as));
    else
    DiffpkAa=abs(min(ap))-abs(min(as));
```

```
    end
 end
 DiffmaxAa(k)=DiffpkAa;
 %%%%%%%%%%%%%%%%%%%%%%%%%%%%%%%%%%%%%%%%%%
 if cl==2
    ga1=ga1+1;
    if ipap(1)>=0
       DPKap=ipap(1)-abs(iaminp(2));
    else
       DPKap=abs(ipap(1))-abs(iamaxp(2));
    end
    DP2Pap(ga1)=DPKap;% difference btwn higher & lower peaks  of one cycle
 end
 if cl>2
if mod(cl,2)==0
   ga1=ga1+1;
   ga2=ga2+1;
   if ipap(cl-1)>=0
   D2PKminAp=abs(iaminp(cl-2))-abs(iaminp(cl));
   DPKap=ipap(cl-1)-abs(iaminp(cl));
  else
   D2PKminAp=abs(iamaxp(cl-2))-abs(iamaxp(cl));
   DPKap=abs(ipap(cl-1))-abs(iamaxp(cl));
   end
   DP2Pap(ga1)=DPKap; % difference btwn higher & lower peaks  of one cycle
   D2minPKap(ga2)=D2PKminAp; %difference btwn two min. peaks of successive
cycles
   else
    ga3=ga3+1;
    D2PKmaxAp=abs(ipap(cl-2))-abs(ipap(cl));
    D2maxPKap(ga3)=D2PKmaxAp; %difference btwn two max. peaks of
successive cycles
```

```
            end
 end
%%%%%%%%%%%%%%%%%%%%  Phase B Primary  %%%%%%%%%%
hbp1=max(abs(bp));
 hbp2=max(bp);
 if hbp1>hbp2;
   ibp=-hbp1;
 else ibp=hbp2;
 end
 nbxp=find(bp==ibp);
%%%%% calculate difference btw lower peak & higher peak for 1 cycle
%%%%% difference btw 2 max. and min. successive peaks.
%%%%% this is to find when inrush and DC offset ends.
 ipbp(k)=ibp;
 ibmaxp(k)=max(bp);
 ibminp(k)=min(bp);
 nbmaxp=find(bp==max(bp));
 nbminp=find(bp==min(bp));
 [rw cl]=size(ipbp);
%%%%%%%%%% Difference max. peaks btwn pri.&Sec. for phase B
 if mod(cl,2)==0
    if ipbp(1)>=0
    DiffpkBb=abs(min(bp))-abs(min(bs));
    else
    DiffpkBb=abs(max(bp))-abs(max(bs));
    end
 else
    if ipbp(1)>=0
    DiffpkBb=abs(max(bp))-abs(max(bs));
    else
    DiffpkBb=abs(min(bp))-abs(min(bs));
    end
```

```
 end
DiffmaxBb(k)=DiffpkBb;
%%%%%%%%%%%%%%%%%%%%%%%%%%%%%%%%%%%%%%%%%%%%%%%%%%%%%%%%%%%%%%%%%%%%%%%%%%%%%%%%%%%%%%%
 if cl==2
    gb1=gb1+1;
    if ipbp(1)>=0
       DPKbp=ipbp(1)-abs(ibminp(2));
    else
       DPKbp=abs(ipbp(1))-abs(ibmaxp(2));
    end
    DP2Pbp(gb1)=DPKbp;% difference btwn higher & lower peaks  of one cycle
 end
 if cl>2
        if mod(cl,2)==0
           gb1=gb1+1;
           gb2=gb2+1;
           if ipbp(cl-1)>=0
           D2PKminBp=abs(ibminp(cl-2))-abs(ibminp(cl));
           DPKbp=ipbp(cl-1)-abs(ibminp(cl));
           else
           D2PKminBp=abs(ibmaxp(cl-2))-abs(ibmaxp(cl));
           DPKbp=abs(ipbp(cl-1))-abs(ibmaxp(cl));
           end
           DP2Pbp(gb1)=DPKbp;% difference btwn higher & lower peaks  of one cycle
           D2minPKbp(gb2)=D2PKminBp; %difference btwn two min. peaks of
successive cycles
        else
           gb3=gb3+1;
           D2PKmaxBp=abs(ipbp(cl-2))-abs(ipbp(cl));
           D2maxPKbp(gb3)=D2PKmaxBp; %difference btwn two max. peaks of
successive cycles
```

```
        end
 end
%%%%%%%%%%%%%%%%%%%%  Phase C Primary  %%%%%%%%%%%
hcp1=max(abs(cp));
 hcp2=max(cp);
 if hcp1>hcp2;
    icp=-hcp1;
 else icp=hcp2;
 end
 ncxp=find(cp==icp);
%%%%% calculate difference btw lower peak & higher peak for 1 cycle
%%%%% difference btw 2 max. and min. successive peaks.
%%%%% this is to find when inrush and DC offset ends.
 ipcp(k)=icp;
 icmaxp(k)=max(cp);
 icminp(k)=min(cp);
 ncmaxp=find(cp==max(cp));
 ncminp=find(cp==min(cp));
 [rw cl]=size(ipcp);
 %%%%%%%%%% Difference max. peaks btwn pri.&Sec. for phase C
 if mod(cl,2)==0
    if ipcp(1)>=0
    DiffpkCc=abs(min(cp))-abs(min(cs));
    else
    DiffpkCc=abs(max(cp))-abs(max(cs));
    end
 else
    if ipcp(1)>=0
    DiffpkCc=abs(max(cp))-abs(max(cs));
    else
    DiffpkCc=abs(min(cp))-abs(min(cs));
    end
```

```
end
DiffmaxCc(k)=DiffpkCc;
%%%%%%%%%%%%%%%%%%%%%%%%%%%%%%%%%%%%%%%%%%%%%
if cl==2
    gc1=gc1+1;
    if ipcp(1)>=0
        DPKcp=ipcp(1)-abs(icminp(2));
    else
        DPKcp=abs(ipcp(1))-abs(icmaxp(2));
    end
    DP2Pcp(gc1)=DPKcp;% difference btwn higher & lower peaks  of one cycle
end
if cl>2
       if mod(cl,2)==0
           gc1=gc1+1;
           gc2=gc2+1;
           if ipcp(cl-1)>=0
           D2PKminCp=abs(icminp(cl-2))-abs(icminp(cl));
           DPKcp=ipcp(cl-1)-abs(icminp(cl));
           else
           D2PKminCp=abs(icmaxp(cl-2))-abs(icmaxp(cl));
           DPKcp=abs(ipcp(cl-1))-abs(icmaxp(cl));
           end
           DP2Pcp(gc1)=DPKcp;% difference btwn higher & lower peaks  of one cycle
           D2minPKcp(gc2)=D2PKminCp; %difference btwn two min. peaks of
successive cycles
       else
           gc3=gc3+1;
           D2PKmaxCp=abs(ipcp(cl-2))-abs(ipcp(cl));
           D2maxPKcp(gc3)=D2PKmaxCp; %difference btwn two max. peaks of
successive cycles
       end
```

```
 end
%%%%%%%%%%%%%%%%%%  Calculation of CCR  %%%%%%%%%%%%
%%%%%%%%%%%%%%%%%%  Average for phase A  %%%%%%%%%%%%
if (naxp-1)>(101-naxp)
        if iap>=0
          Dfap=abs(naxp-naminp);
          if mod(Dfap,2)==0
          midap=(Dfap/2)+naminp;
          else
          midap=((Dfap-1)/2)+naminp;
          end
          AvAp=abs((ap(midap)-ap(naminp))/(ap(midap)-ap(naxp)));
       else
          Dfap=abs(naxp-namaxp);
          if mod(Dfap,2)==0
          midap=(Dfap/2)+namaxp;
          else
          midap=((Dfap-1)/2)+namaxp;
          end
          AvAp=abs((ap(midap)-ap(namaxp))/(ap(midap)-ap(naxp)));
        end
 end
 if (naxp-1)<(101-naxp)
       if iap>=0
         Dfap=abs(naminp-naxp);
         if mod(Dfap,2)==0
          midap=(Dfap/2)+naxp;
         else
          midap=((Dfap+1)/2)+naxp;
         end
         AvAp=abs((ap(midap)-ap(naminp))/(ap(midap)-ap(naxp)));
       else
```

```
        Dfap=abs(namaxp-naxp);
        if mod(Dfap,2)==0
         midap=(Dfap/2)+naxp;
        else
         midap=((Dfap+1)/2)+naxp;
        end
        AvAp=abs((ap(midap)-ap(namaxp))/(ap(midap)-ap(naxp)));
      end
end
if (naxp-1)==(101-naxp)
   midap1=25;
   AvAp1=abs((ap(midap1)-ap(1))/(ap(midap1)-ap(naxp)));
   midap2=77;
   AvAp2=abs((ap(midap2)-ap(101))/(ap(midap2)-ap(naxp)));
   if AvAp1<=AvAp2
      AvAp=AvAp1;
   else
      AvAp=AvAp2;
   end
end
%%%%%%%%%%%%%%%%  Average for phase B  %%%%%%%%%%%%
if (nbxp-1)>(101-nbxp)
       if ibp>=0
         Dfbp=abs(nbxp-nbminp);
         if mod(Dfbp,2)==0
         midbp=(Dfbp/2)+nbminp;
         else
         midbp=((Dfbp-1)/2)+nbminp;
         end
         AvBp=abs((bp(midbp)-bp(nbminp))/(bp(midbp)-bp(nbxp)));
      else
         Dfbp=abs(nbxp-nbmaxp);
```

```
        if mod(Dfbp,2)==0
        midbp=(Dfbp/2)+nbmaxp;
        else
        midbp=((Dfbp-1)/2)+nbmaxp;
        end
        AvBp=abs((bp(midbp)-bp(nbmaxp))/(bp(midbp)-bp(nbxp)));
      end
end
if (nbxp-1)<(101-nbxp)
     if ibp>=0
       Dfbp=abs(nbminp-nbxp);
       if mod(Dfbp,2)==0
        midbp=(Dfbp/2)+nbxp;
       else
        midbp=((Dfbp+1)/2)+nbxp;
       end
       AvBp=abs((bp(midbp)-bp(nbminp))/(bp(midbp)-bp(nbxp)));
     else
       Dfbp=abs(nbmaxp-nbxp);
       if mod(Dfbp,2)==0
        midbp=(Dfbp/2)+nbxp;
       else
        midbp=((Dfbp+1)/2)+nbxp;
       end
       AvBp=abs((bp(midbp)-bp(nbmaxp))/(bp(midbp)-bp(nbxp)));
     end
end

if (nbxp-1)==(101-nbxp)
   midbp1=25;
   AvBp1=abs((bp(midbp1)-bp(1))/(bp(midbp1)-bp(nbxp)));
   midbp2=77;
```

```
    AvBp2=abs((bp(midbp2)-bp(101))/(bp(midbp2)-bp(nbxp)));
    if AvBp1<=AvBp2
       AvBp=AvBp1;
    else
       AvBp=AvBp2;
    end
 end
%%%%%%%%%%%%%%%%  Average for phase C  %%%%%%%%%%%
 if (ncxp-1)>(101-ncxp)
        if icp>=0
          Dfcp=abs(ncxp-ncminp);
          if mod(Dfcp,2)==0
          midcp=(Dfcp/2)+ncminp;
          else
          midcp=((Dfcp-1)/2)+ncminp;
          end
          AvCp=abs((cp(midcp)-cp(ncminp))/(cp(midcp)-cp(ncxp)));
       else
          Dfcp=abs(ncxp-ncmaxp);
          if mod(Dfcp,2)==0
          midcp=(Dfcp/2)+ncmaxp;
          else
          midcp=((Dfcp-1)/2)+ncmaxp;
          end
          AvCp=abs((cp(midcp)-cp(ncmaxp))/(cp(midcp)-cp(ncxp)));
        end
 end
 if (ncxp-1)<(101-ncxp)
       if icp>=0
         Dfcp=abs(ncminp-ncxp);
         if mod(Dfcp,2)==0
          midcp=(Dfcp/2)+ncxp;
```

```
        else
         midcp=((Dfcp+1)/2)+ncxp;
        end
        AvCp=abs((cp(midcp)-cp(ncminp))/(cp(midcp)-cp(ncxp)));
      else
        Dfcp=abs(ncmaxp-ncxp);
        if mod(Dfcp,2)==0
         midcp=(Dfcp/2)+ncxp;
        else
         midcp=((Dfcp+1)/2)+ncxp;
        end
        AvCp=abs((cp(midcp)-cp(ncmaxp))/(cp(midcp)-cp(ncxp)));
      end
 end
if (ncxp-1)==(101-ncxp)
    midcp1=25;
    AvCp1=abs((cp(midcp1)-cp(1))/(cp(midcp1)-cp(ncxp)));
    midcp2=77;
    AvCp2=abs((cp(midcp2)-cp(101))/(cp(midcp2)-cp(ncxp)));
    if AvCp1<=AvCp2
       AvCp=AvCp1;
    else
       AvCp=AvCp2;
    end
 end
%%%%%%%%%%%%%  Averages for phases A, B & C  %%%%%%%%%
 AvrAp(k)=AvAp;
 AvrBp(k)=AvBp;
 AvrCp(k)=AvCp;
 j=j-1;
end
%%%%%%%%%%%%%%%%%%%%%%%%%%%%%%%%%%%%%%%%%%%%%%%%%%%%%%
```

```
t2=1:40;
figure;
    plot(t2,DiffArA,'b',t2,DiffArB,'r',t2,DiffArC,'g','LineWidth',3),grid;
    title('Percentage area difference  for phases A blue, phase B red, phase c
green','FontSize',30,'FontWeight','bold','FontName','Times New Roman');
    xlabel('Quarter cycle
number','FontSize',30,'FontWeight','bold','FontName','Times New Roman')
    ylabel('Percentage area difference
%','FontSize',30,'FontWeight','bold','FontName','Times New Roman')
    set(gca, 'FontName', 'Times New Roman')
    set(gca, 'FontSize',30,'FontWeight','bold')
%%%%%%%%%%%%%%%%%%%%%%%%%%%%%%%%%%%%%%%%%%%%%%%%%%%%%%%%%%%%%%%%%%%%%%%%%%%%
figure;
plot(t2,AvrAp,'b',t2,AvrBp,'r',t2,AvrCp,'g','LineWidth',3),grid;
title('current change ratio for phases A (blue) ,B (red) and C (green)
Primary','FontSize',30,'FontWeight','bold','FontName','Times New Roman');
    xlabel('Half-cycle number','FontSize',30,'FontWeight','bold','FontName','Times
New Roman')
    ylabel('Rate of change','FontSize',30,'FontWeight','bold','FontName','Times New
Roman')
    set(gca, 'FontName', 'Times New Roman')
    set(gca, 'FontSize',30,'FontWeight','bold')
%%%%%%%%%%%%%%%%%%%%%%%%%%%%%%%%%%%%%%%%%%%%%%%%%%%%%%%%%%%%%%%%%%%%%%%%%%%%
figure;
plot(t2,DiffmaxAa,'b',t2,DiffmaxBb,'r',t2,DiffmaxCc,'g','LineWidth',3),grid;
title('Difference btwn Pri.& Sec. max. peaks for phase A = Blue, phase B = Red and
phase C = Green')
xlabel('Half-cycle number','FontSize',30,'FontWeight','bold','FontName','Times New
Roman')
ylabel('Difference current values /
Amps.','FontSize',30,'FontWeight','bold','FontName','Times New Roman')
set(gca, 'FontName', 'Times New Roman')
```

```
set(gca, 'FontSize',30,'FontWeight','bold')
t3=1:20;
figure;
plot(t3,DP2Pap,'b',t3,DP2Pbp,'r',t3,DP2Pcp,'g','LineWidth',3),grid;
title('difference btwn higher & lower peaks  of one cycle, phase A (blue) ,B (red) and C (green) Primary')
xlabel('Cycle number','FontSize',30,'FontWeight','bold','FontName','Times New Roman')
    ylabel('Difference current values','FontSize',30,'FontWeight','bold','FontName','Times New Roman')
    set(gca, 'FontName', 'Times New Roman')
    set(gca, 'FontSize',30,'FontWeight','bold')
    %%%%%%%%
t4=2:20;
figure;
plot(t4,D2maxPKap,'r',t4,D2minPKap,'b','LineWidth',3),grid;
title(' difference btwn two peaks of successive cycles for phase A Pri., Red = max. peaks & blue = min. peaks')
xlabel('Cycle number','FontSize',30,'FontWeight','bold','FontName','Times New Roman')
    ylabel('Difference current values','FontSize',30,'FontWeight','bold','FontName','Times New Roman')
    set(gca, 'FontName', 'Times New Roman')
    set(gca, 'FontSize',30,'FontWeight','bold')
    %%%%%%%%%%
figure;
plot(t4,D2maxPKbp,'r',t4,D2minPKbp,'b','LineWidth',3),grid;
title(' difference btwn two peaks of successive cycles for phase B Pri., Red = max. peaks & blue = min. peaks')
    xlabel('Cycle number','FontSize',30,'FontWeight','bold','FontName','Times New Roman')
```

```
      ylabel('Difference current
values','FontSize',30,'FontWeight','bold','FontName','Times New Roman')
      set(gca, 'FontName', 'Times New Roman')
      set(gca, 'FontSize',30,'FontWeight','bold')
%%%%%%%%%%%%%%%%%%%%%%%%%%
figure;
plot(t4,D2maxPKcp,'r',t4,D2minPKcp,'b','LineWidth',3),grid;
title(' difference btwn two peaks of successive cycles for phase C Pri., Red = max.
peaks & blue = min. peaks')
     xlabel('Cycle number','FontSize',30,'FontWeight','bold','FontName','Times New
Roman')
     ylabel('Difference current
values','FontSize',30,'FontWeight','bold','FontName','Times New Roman')
     set(gca, 'FontName', 'Times New Roman')
     set(gca, 'FontSize',30,'FontWeight','bold')
```

APPENDIX D – LABVIEW MODEL

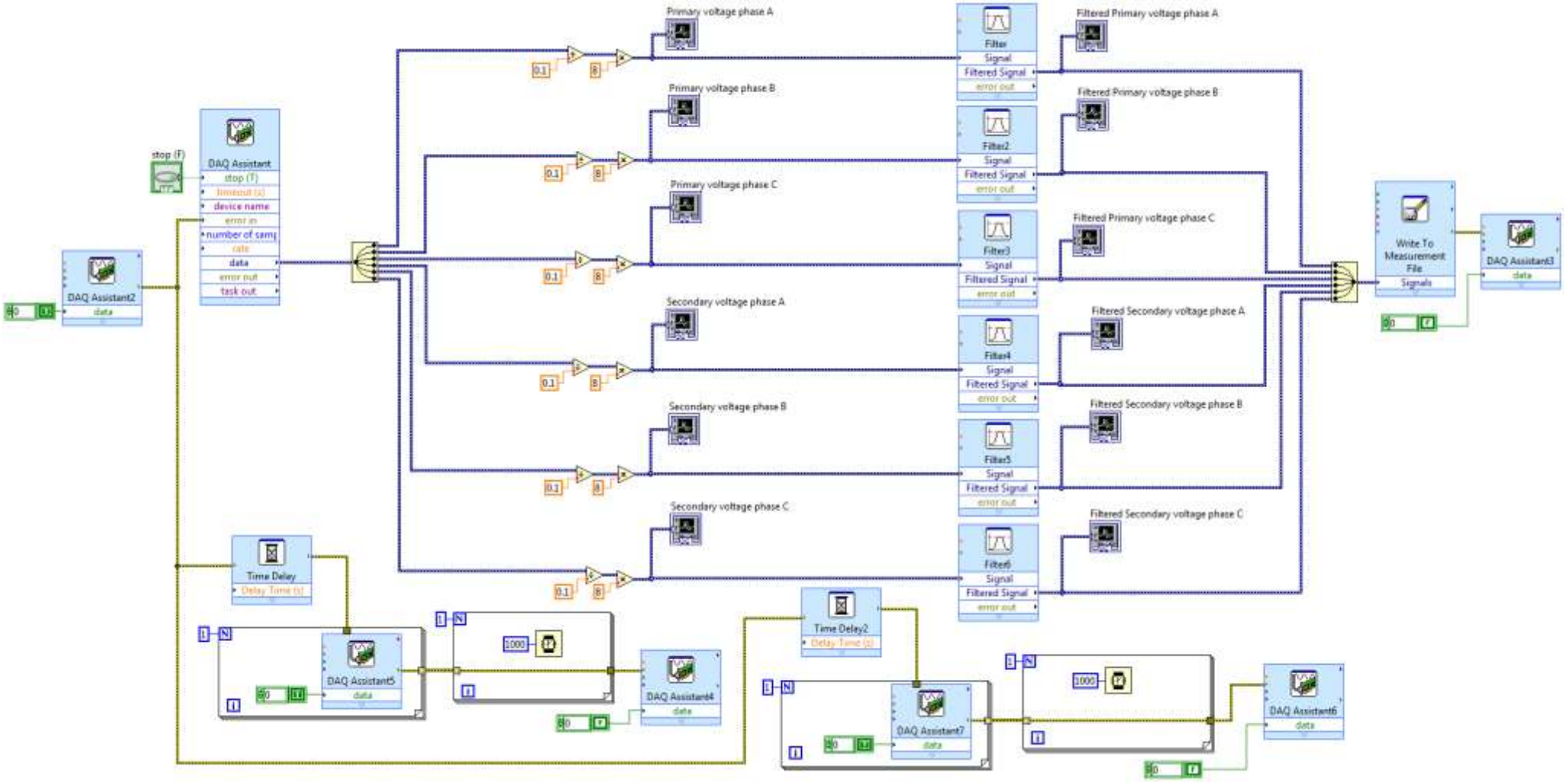

APPENDIX E – FAULT TYPE AND LOCATION

Figs C-1, C-2 and C-3 show the range of changes in correlation coefficient values according to the type and location of the internal fault that occurred in phases A, B and C respectively.

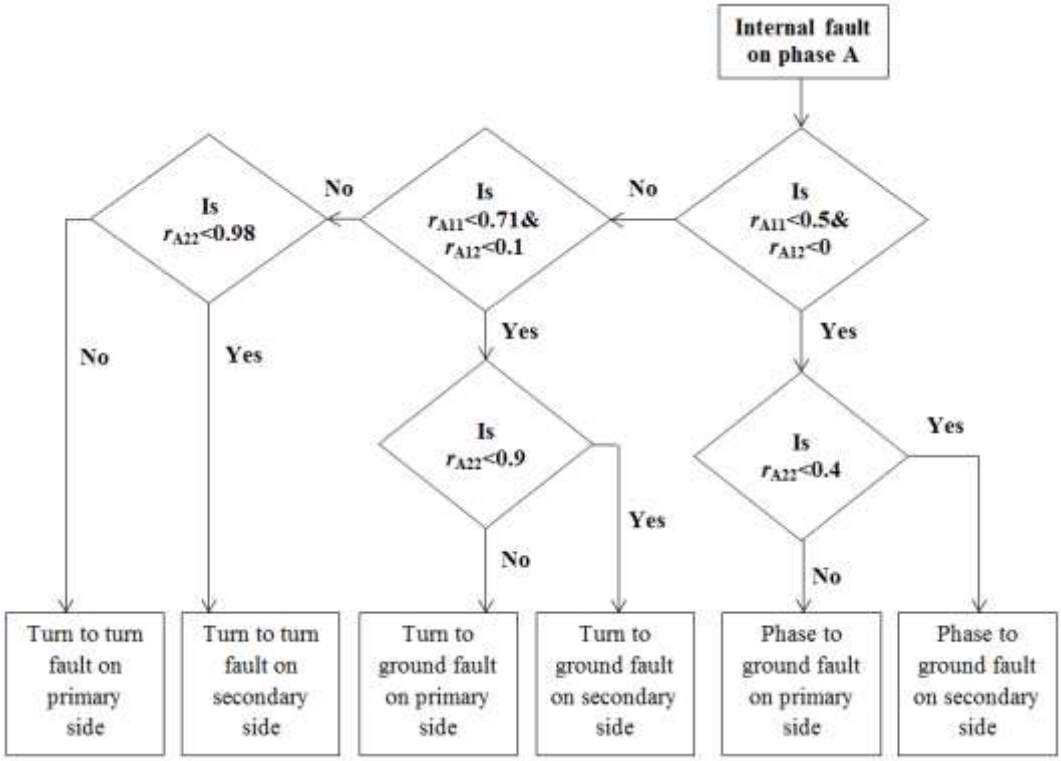

Fig C-1 Change in correlation coefficients due to internal faults in phase A

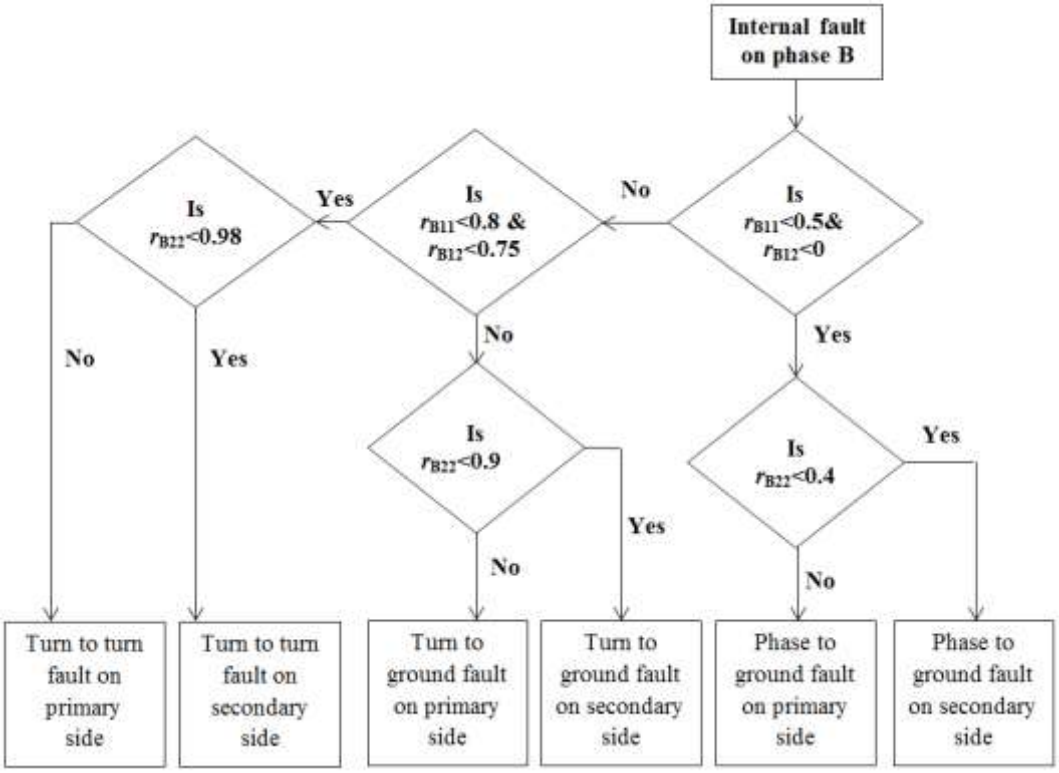

Fig C-2 Change in correlation coefficients due to internal faults in phase B

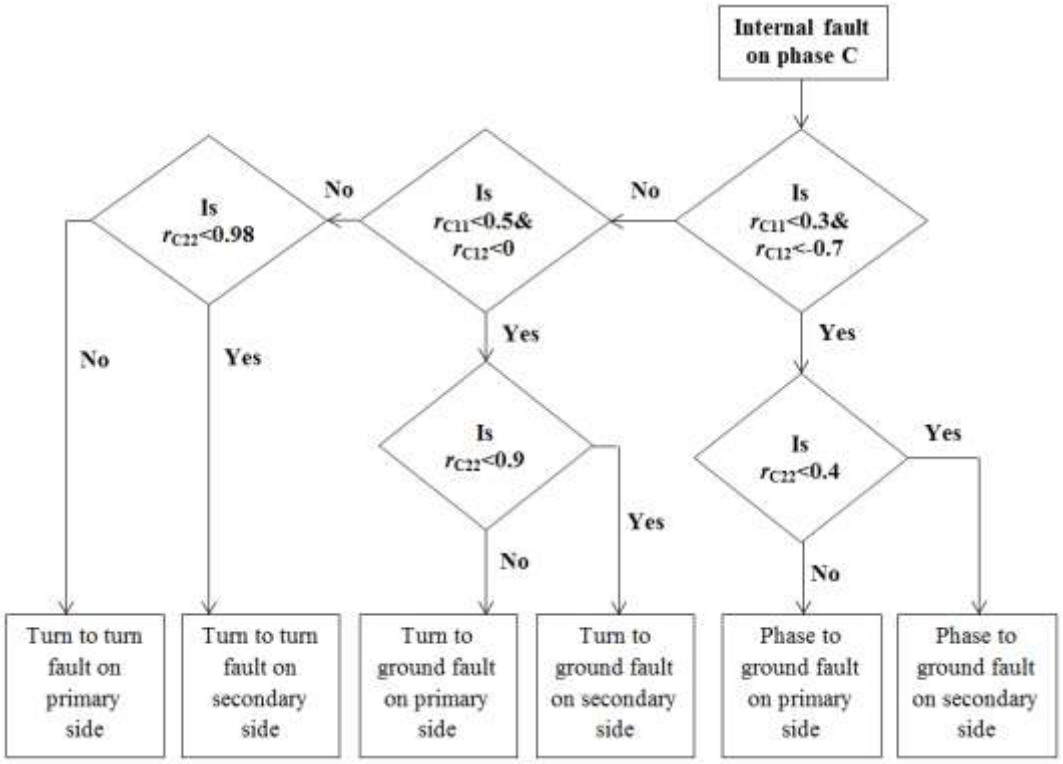

Fig C-3 Change in correlation coefficients due to internal faults in phase C

APPENDIX F – CORRELATION COEFFICIENTS

Here are the changes in correlation coefficients for all types of faults on all three phases A, B and C. and both sides of the transformer.

Interturn fault in phase A primary									
	Phase A			Phase B			Phase C		
Window No.	r_{A11}	r_{A12}	r_{A22}	r_{B11}	r_{B12}	r_{B22}	r_{C11}	r_{C12}	r_{C22}
1	1.0000	1.0000	1.0000	0.9999	0.9999	1.0000	1.0000	1.0000	1.0000
2	1.0000	0.9999	1.0000	1.0000	0.9999	0.9998	1.0000	0.9998	1.0000
3	0.9899	0.9478	0.9862	0.9805	0.9922	0.9634	0.9960	0.8965	0.9972
4	1.0000	0.9999	0.9999	0.9999	1.0000	0.9999	1.0000	1.0000	1.0000
5	1.0000	0.9999	1.0000	1.0000	0.9999	1.0000	1.0000	1.0000	1.0000
6	1.0000	1.0000	1.0000	1.0000	0.9999	0.9999	1.0000	1.0000	1.0000
7	1.0000	0.9999	1.0000	1.0000	0.9999	0.9999	1.0000	0.9999	1.0000
8	0.9953	0.9588	0.9982	0.9923	0.9792	0.9939	0.9867	0.9198	0.9973
9	1.0000	0.9999	1.0000	0.9999	1.0000	1.0000	1.0000	1.0000	1.0000
10	1.0000	1.0000	1.0000	0.9998	0.9997	0.9999	1.0000	1.0000	1.0000
11	1.0000	1.0000	1.0000	1.0000	0.9999	1.0000	0.9999	0.9999	1.0000
12	1.0000	1.0000	1.0000	0.9996	0.9996	1.0000	0.9998	0.9992	1.0000
13	0.7887	0.4862	0.9953	0.8505	0.6715	0.9847	0.8489	0.3929	0.9876
14	0.9995	0.9990	0.9999	0.9994	0.9994	0.9999	0.9998	0.9998	1.0000
15	1.0000	1.0000	1.0000	1.0000	0.9999	1.0000	0.9999	0.9999	1.0000
16	1.0000	1.0000	1.0000	0.9999	0.9999	0.9999	1.0000	0.9999	1.0000
17	0.9999	1.0000	1.0000	0.9998	0.9998	0.9998	0.9993	0.9985	1.0000
18	0.8253	0.9250	0.9961	0.8324	0.7799	0.9932	0.6623	0.2436	0.9971
19	1.0000	1.0000	1.0000	0.9997	0.9995	1.0000	0.9997	0.9997	1.0000
20	1.0000	1.0000	1.0000	1.0000	0.9999	1.0000	0.9999	0.9998	1.0000
21	1.0000	1.0000	1.0000	1.0000	0.9999	1.0000	0.9997	0.9998	1.0000
22	0.9999	1.0000	1.0000	0.9999	0.9986	0.9998	1.0000	0.9989	1.0000
23	0.4347	0.9380	0.9568	0.9960	0.8231	0.9531	0.9816	0.2223	0.9997
24	0.9995	1.0000	0.9999	0.9999	0.9993	1.0000	1.0000	0.9998	1.0000
25	1.0000	1.0000	1.0000	1.0000	0.9999	1.0000	1.0000	0.9999	1.0000
26	1.0000	1.0000	1.0000	1.0000	0.9999	1.0000	1.0000	0.9999	1.0000
27	1.0000	1.0000	1.0000	1.0000	0.9996	0.9999	1.0000	0.9990	1.0000
28	0.9771	0.9604	0.9936	0.9997	0.8026	0.9981	0.9999	0.2163	0.9982
29	1.0000	1.0000	1.0000	1.0000	0.9992	1.0000	1.0000	0.9996	1.0000
30	1.0000	0.9999	1.0000	1.0000	0.9996	0.9999	1.0000	0.9999	1.0000
31	1.0000	1.0000	1.0000	1.0000	0.9999	1.0000	1.0000	0.9999	1.0000
32	1.0000	1.0000	1.0000	0.9999	0.9992	0.9998	1.0000	0.9986	1.0000

33	0.9984	0.9487	0.9993	0.9995	0.8466	0.9957	0.9986	0.1051	0.9851
34	1.0000	0.9999	0.9998	1.0000	0.9996	1.0000	1.0000	0.9997	0.9999
35	1.0000	1.0000	1.0000	1.0000	0.9999	1.0000	1.0000	0.9998	1.0000
36	1.0000	1.0000	1.0000	1.0000	0.9999	1.0000	1.0000	0.9999	1.0000
37	1.0000	1.0000	1.0000	1.0000	0.9996	1.0000	1.0000	0.9987	1.0000
38	0.9974	0.9289	0.9864	0.9998	0.8523	0.9952	0.9985	0.1415	0.9914
39	1.0000	1.0000	1.0000	1.0000	0.9997	0.9999	1.0000	0.9997	1.0000
40	1.0000	1.0000	1.0000	1.0000	0.9999	0.9999	1.0000	0.9999	1.0000
41	1.0000	1.0000	1.0000	0.9999	0.9999	1.0000	1.0000	0.9998	1.0000
42	1.0000	1.0000	1.0000	0.9999	0.9998	0.9999	1.0000	0.9991	1.0000
43	0.9977	0.9504	0.9981	0.9976	0.7754	0.9944	0.9993	0.0466	0.9954
44	1.0000	1.0000	1.0000	1.0000	0.9995	1.0000	1.0000	0.9997	1.0000
45	1.0000	1.0000	1.0000	1.0000	0.9998	1.0000	1.0000	0.9999	1.0000
46	1.0000	1.0000	1.0000	1.0000	0.9999	0.9999	1.0000	0.9998	1.0000
47	1.0000	1.0000	1.0000	1.0000	0.9998	0.9999	1.0000	0.9985	1.0000
48	0.9929	0.9821	0.9961	0.9981	0.8739	0.9944	0.9999	0.0465	0.9951
49	1.0000	1.0000	0.9999	1.0000	0.9996	1.0000	1.0000	0.9995	1.0000
50	1.0000	0.9999	1.0000	1.0000	1.0000	1.0000	1.0000	0.9999	1.0000
51	1.0000	1.0000	1.0000	1.0000	0.9999	1.0000	1.0000	0.9999	1.0000
52	1.0000	1.0000	1.0000	1.0000	0.9998	1.0000	1.0000	0.9986	1.0000
53	0.9955	0.9578	0.9976	0.9982	0.8305	0.9876	0.9997	0.1147	0.9956
54	1.0000	0.9999	0.9999	0.9998	0.9996	0.9999	1.0000	0.9997	1.0000
55	1.0000	1.0000	1.0000	1.0000	0.9998	1.0000	1.0000	0.9998	1.0000
56	1.0000	1.0000	1.0000	1.0000	0.9998	1.0000	1.0000	0.9999	1.0000
57	1.0000	1.0000	1.0000	1.0000	0.9998	1.0000	1.0000	0.9987	1.0000
58	0.9967	0.9776	0.9939	0.9984	0.8431	0.9994	0.9996	0.0485	0.9996
59	1.0000	1.0000	1.0000	1.0000	0.9997	1.0000	1.0000	0.9997	1.0000
60	1.0000	0.9999	1.0000	0.9999	0.9997	1.0000	1.0000	0.9998	1.0000
61	1.0000	1.0000	1.0000	0.9999	0.9997	0.9999	1.0000	0.9999	1.0000
62	1.0000	1.0000	1.0000	0.9999	0.9994	0.9999	1.0000	0.9991	1.0000
63	0.9957	0.9675	0.9985	0.9988	0.9101	0.9775	0.9989	0.1001	0.9975
64	1.0000	1.0000	0.9999	0.9998	0.9995	0.9999	1.0000	0.9996	1.0000
65	1.0000	0.9999	1.0000	1.0000	0.9998	1.0000	1.0000	0.9998	1.0000
66	1.0000	1.0000	1.0000	1.0000	0.9999	1.0000	1.0000	0.9999	1.0000
67	1.0000	1.0000	1.0000	1.0000	0.9998	1.0000	1.0000	0.9990	1.0000
68	0.9979	0.9778	0.9975	0.9999	0.8747	0.9964	0.9984	0.0342	0.9977
69	1.0000	1.0000	1.0000	0.9999	0.9994	1.0000	1.0000	0.9995	1.0000
70	1.0000	1.0000	1.0000	0.9999	0.9999	1.0000	1.0000	0.9998	1.0000
71	1.0000	1.0000	1.0000	1.0000	1.0000	0.9999	1.0000	0.9999	1.0000
72	1.0000	1.0000	1.0000	1.0000	0.9995	1.0000	1.0000	0.9993	1.0000
73	0.9964	0.9696	0.9971	0.9992	0.8976	0.9982	0.9994	0.0441	0.9956
74	1.0000	1.0000	0.9999	1.0000	0.9992	0.9998	1.0000	0.9997	1.0000

75	1.0000	0.9998	1.0000	1.0000	1.0000	0.9999	1.0000	0.9999	1.0000
76	1.0000	1.0000	1.0000	1.0000	1.0000	1.0000	1.0000	0.9999	1.0000
77	1.0000	1.0000	1.0000	1.0000	0.9996	1.0000	1.0000	0.9988	1.0000
78	0.9989	0.9663	0.9950	0.9990	0.9153	0.9978	0.9994	0.0280	0.9995
79	1.0000	1.0000	1.0000	1.0000	0.9992	1.0000	1.0000	0.9996	1.0000
80	1.0000	0.9999	1.0000	1.0000	1.0000	0.9999	1.0000	0.9999	1.0000
81	1.0000	1.0000	1.0000	1.0000	1.0000	1.0000	1.0000	0.9998	1.0000
82	1.0000	1.0000	1.0000	1.0000	0.9995	0.9999	1.0000	0.9989	1.0000
83	0.9989	0.9655	0.9981	0.9995	0.8814	0.9991	0.9979	0.0717	0.9993
84	1.0000	1.0000	1.0000	0.9999	0.9994	0.9998	1.0000	0.9993	0.9999
85	1.0000	0.9999	1.0000	1.0000	0.9998	0.9999	1.0000	0.9999	1.0000
86	1.0000	1.0000	1.0000	1.0000	0.9999	1.0000	1.0000	0.9999	1.0000
87	1.0000	1.0000	1.0000	1.0000	0.9993	0.9999	1.0000	0.9987	1.0000
88	0.9976	0.9759	0.9996	0.9991	0.9137	0.9987	0.9986	0.0177	0.9978
89	1.0000	1.0000	0.9999	0.9999	0.9997	1.0000	1.0000	0.9995	1.0000
90	1.0000	0.9999	1.0000	0.9999	0.9999	0.9999	1.0000	0.9998	1.0000

Interturn fault in phase A Secondary									
	Phase A			**Phase B**			**Phase C**		
Window No.	r_{A11}	r_{A12}	r_{A22}	r_{B11}	r_{B12}	r_{B22}	r_{C11}	r_{C12}	r_{C22}
1	1.0000	1.0000	1.0000	1.0000	1.0000	0.9999	1.0000	1.0000	1.0000
2	1.0000	0.9998	1.0000	0.9999	0.9993	0.9996	1.0000	1.0000	1.0000
3	0.9983	0.9120	0.9963	0.9647	0.8757	0.9612	0.9997	0.9997	0.9981
4	1.0000	0.9999	1.0000	1.0000	0.9999	1.0000	1.0000	0.9999	1.0000
5	1.0000	1.0000	1.0000	1.0000	1.0000	1.0000	1.0000	1.0000	1.0000
6	1.0000	1.0000	1.0000	0.9999	0.9997	0.9996	1.0000	1.0000	1.0000
7	1.0000	0.9998	1.0000	0.9999	0.9999	0.9995	1.0000	1.0000	1.0000
8	0.9960	0.9142	0.9993	0.9964	0.9170	0.9901	0.9997	0.9995	0.9931
9	1.0000	0.9999	1.0000	0.9999	0.9999	0.9999	1.0000	0.9999	1.0000
10	1.0000	1.0000	1.0000	0.9999	0.9999	0.9999	1.0000	1.0000	1.0000
11	1.0000	1.0000	1.0000	1.0000	1.0000	1.0000	1.0000	1.0000	1.0000
12	1.0000	0.9998	1.0000	0.9997	0.9994	0.9998	1.0000	1.0000	1.0000
13	0.9994	0.8935	0.9967	0.9922	0.9588	0.9812	0.9927	0.9990	0.9952
14	1.0000	0.9999	1.0000	1.0000	0.9999	1.0000	1.0000	0.9999	1.0000
15	1.0000	1.0000	1.0000	1.0000	0.9998	1.0000	1.0000	1.0000	1.0000
16	1.0000	1.0000	1.0000	1.0000	0.9997	0.9999	1.0000	0.9998	1.0000
17	1.0000	0.9999	1.0000	0.9998	0.9991	0.9999	0.9996	0.9995	1.0000
18	0.7066	0.1052	0.9627	0.7782	0.4689	0.9993	0.8436	0.8301	0.9991
19	0.9994	0.9989	1.0000	0.9999	0.9997	1.0000	0.9999	1.0000	1.0000
20	1.0000	1.0000	1.0000	1.0000	0.9999	0.9999	1.0000	0.9999	1.0000
21	1.0000	1.0000	1.0000	0.9999	0.9999	0.9999	0.9999	0.9999	1.0000

22	0.9998	1.0000	1.0000	0.9998	0.9993	0.9997	0.9988	0.9987	1.0000
23	0.8584	0.9837	0.9926	0.7034	0.3505	0.9843	0.7729	0.6859	0.9953
24	1.0000	1.0000	0.9999	0.9996	0.9989	0.9999	0.9998	1.0000	1.0000
25	1.0000	1.0000	1.0000	1.0000	0.9999	1.0000	0.9999	0.9999	1.0000
26	1.0000	1.0000	1.0000	1.0000	0.9995	0.9999	0.9998	0.9999	1.0000
27	0.9999	1.0000	1.0000	1.0000	0.9993	0.9999	0.9999	0.9988	1.0000
28	0.2389	0.9958	0.9745	0.9974	0.3350	0.9947	0.9795	0.7361	0.9982
29	0.9991	1.0000	1.0000	0.9999	0.9992	0.9999	1.0000	0.9999	1.0000
30	1.0000	0.9999	1.0000	1.0000	0.9998	1.0000	1.0000	0.9999	1.0000
31	1.0000	1.0000	1.0000	1.0000	0.9999	0.9999	1.0000	0.9999	1.0000
32	1.0000	1.0000	1.0000	0.9996	0.9989	0.9991	1.0000	0.9990	0.9999
33	0.9998	0.9983	0.9892	0.9987	0.4991	0.9880	0.9996	0.7207	0.9968
34	1.0000	1.0000	0.9999	0.9998	0.9997	0.9999	1.0000	1.0000	1.0000
35	1.0000	1.0000	1.0000	1.0000	0.9997	1.0000	1.0000	0.9999	1.0000
36	1.0000	1.0000	1.0000	0.9999	0.9995	0.9998	1.0000	0.9999	1.0000
37	1.0000	1.0000	1.0000	1.0000	0.9990	1.0000	1.0000	0.9991	1.0000
38	0.9983	0.9952	0.9985	0.9985	0.4202	0.9946	1.0000	0.7270	0.9994
39	1.0000	1.0000	1.0000	1.0000	0.9990	1.0000	1.0000	1.0000	1.0000
40	1.0000	0.9999	1.0000	0.9999	0.9998	1.0000	1.0000	0.9999	1.0000
41	1.0000	1.0000	1.0000	1.0000	0.9999	0.9999	1.0000	0.9999	1.0000
42	1.0000	1.0000	1.0000	0.9999	0.9972	0.9997	0.9997	0.9997	1.0000
43	0.9996	0.9953	0.9989	0.9996	0.4599	0.9989	0.9995	0.7388	0.9981
44	1.0000	1.0000	1.0000	0.9999	0.9997	0.9999	1.0000	1.0000	1.0000
45	1.0000	1.0000	1.0000	1.0000	0.9999	1.0000	1.0000	0.9999	1.0000
46	1.0000	1.0000	1.0000	1.0000	0.9998	0.9998	1.0000	0.9999	1.0000
47	1.0000	1.0000	1.0000	0.9999	0.9987	1.0000	1.0000	0.9987	1.0000
48	0.9998	0.9951	0.9994	0.9978	0.2977	0.9804	0.9997	0.7867	0.9927
49	1.0000	1.0000	0.9999	0.9999	0.9995	1.0000	1.0000	1.0000	1.0000
50	1.0000	1.0000	1.0000	0.9999	0.9999	1.0000	1.0000	0.9998	1.0000
51	1.0000	1.0000	1.0000	1.0000	0.9999	1.0000	1.0000	0.9999	1.0000
52	1.0000	1.0000	1.0000	1.0000	0.9993	0.9991	0.9997	0.9988	1.0000
53	0.9969	0.9844	0.9995	0.9993	0.4739	0.9994	0.9998	0.7998	0.9962
54	1.0000	1.0000	1.0000	0.9999	0.9996	0.9999	1.0000	1.0000	1.0000
55	1.0000	1.0000	1.0000	1.0000	0.9999	1.0000	1.0000	0.9999	1.0000
56	1.0000	1.0000	1.0000	1.0000	0.9999	1.0000	1.0000	0.9999	1.0000
57	1.0000	1.0000	1.0000	1.0000	0.9975	0.9997	1.0000	0.9991	1.0000
58	0.9979	0.9978	0.9954	0.9975	0.3245	0.9990	0.9992	0.7749	0.9995
59	1.0000	1.0000	1.0000	1.0000	0.9991	0.9999	1.0000	1.0000	1.0000
60	1.0000	0.9999	1.0000	0.9999	1.0000	1.0000	1.0000	0.9999	1.0000
61	1.0000	1.0000	1.0000	1.0000	0.9999	1.0000	1.0000	0.9999	1.0000
62	1.0000	1.0000	1.0000	0.9999	0.9999	0.9995	0.9999	0.9987	1.0000
63	0.9989	0.9959	0.9914	0.9945	0.5046	0.9946	0.9996	0.8122	0.9986

64	1.0000	1.0000	1.0000	0.9998	0.9992	0.9999	1.0000	1.0000	1.0000
65	1.0000	0.9999	1.0000	1.0000	0.9999	1.0000	1.0000	0.9999	1.0000
66	1.0000	1.0000	1.0000	1.0000	0.9998	1.0000	1.0000	0.9999	1.0000
67	1.0000	1.0000	0.9999	0.9999	0.9995	0.9994	1.0000	0.9986	1.0000
68	0.9985	0.9933	0.9997	0.9956	0.3181	0.9949	0.9996	0.8449	0.9941
69	1.0000	1.0000	1.0000	0.9999	0.9992	1.0000	1.0000	1.0000	1.0000
70	1.0000	0.9999	1.0000	0.9997	0.9997	1.0000	1.0000	0.9999	1.0000
71	1.0000	1.0000	1.0000	0.9999	0.9999	0.9998	1.0000	0.9999	1.0000
72	1.0000	1.0000	1.0000	0.9999	0.9994	0.9992	0.9999	0.9990	1.0000
73	0.9981	0.9918	0.9992	0.9933	0.1384	0.9598	0.9998	0.8119	0.9996
74	1.0000	1.0000	1.0000	0.9999	0.9993	1.0000	1.0000	1.0000	1.0000
75	1.0000	1.0000	1.0000	1.0000	0.9999	1.0000	1.0000	0.9999	1.0000
76	1.0000	1.0000	1.0000	1.0000	0.9999	1.0000	1.0000	0.9999	1.0000
77	1.0000	1.0000	1.0000	1.0000	0.9996	0.9999	1.0000	0.9990	1.0000
78	0.9987	0.9967	0.9965	0.9980	0.2379	0.9885	0.9989	0.8325	0.9992
79	1.0000	1.0000	1.0000	1.0000	0.9992	1.0000	1.0000	0.9999	1.0000
80	1.0000	0.9999	1.0000	0.9999	0.9999	1.0000	1.0000	0.9999	1.0000
81	1.0000	1.0000	1.0000	1.0000	0.9999	1.0000	1.0000	0.9999	1.0000
82	1.0000	1.0000	1.0000	0.9999	0.9984	0.9996	1.0000	0.9992	1.0000
83	0.9992	0.9935	0.9976	0.9921	0.3441	0.9945	0.9998	0.8571	0.9950
84	1.0000	1.0000	1.0000	1.0000	0.9995	1.0000	1.0000	0.9999	1.0000
85	1.0000	1.0000	1.0000	1.0000	0.9998	1.0000	1.0000	0.9999	1.0000
86	1.0000	1.0000	1.0000	1.0000	0.9998	1.0000	1.0000	0.9999	1.0000
87	1.0000	1.0000	1.0000	0.9999	0.9992	0.9998	1.0000	0.9988	1.0000
88	0.9991	0.9975	0.9983	0.9978	0.3479	0.9940	0.9996	0.8384	0.9995
89	1.0000	1.0000	1.0000	0.9999	0.9996	1.0000	1.0000	1.0000	1.0000
90	1.0000	0.9999	1.0000	1.0000	0.9999	1.0000	1.0000	0.9999	1.0000

Interturn fault in phase B primary									
	Phase A			**Phase B**			**Phase C**		
Window No.	r_{A11}	r_{A12}	r_{A22}	r_{B11}	r_{B12}	r_{B22}	r_{C11}	r_{C12}	r_{C22}
1	1.0000	1.0000	1.0000	1.0000	0.9999	1.0000	1.0000	1.0000	1.0000
2	1.0000	0.9999	1.0000	1.0000	0.9999	0.9999	1.0000	1.0000	1.0000
3	0.9964	0.8980	0.9966	0.9873	0.9577	0.9941	0.9969	0.9988	0.9972
4	1.0000	0.9998	1.0000	0.9999	1.0000	1.0000	1.0000	0.9998	1.0000
5	1.0000	1.0000	1.0000	1.0000	0.9999	1.0000	1.0000	1.0000	1.0000
6	1.0000	1.0000	1.0000	1.0000	1.0000	1.0000	1.0000	1.0000	1.0000
7	1.0000	0.9999	1.0000	1.0000	0.9998	1.0000	1.0000	1.0000	1.0000
8	0.9908	0.8912	0.9979	0.6764	0.1467	0.9814	0.9920	0.9994	0.9961
9	1.0000	0.9999	1.0000	0.9996	0.9994	1.0000	0.9997	0.9999	1.0000
10	1.0000	1.0000	1.0000	1.0000	1.0000	1.0000	0.9998	0.9998	1.0000

11	0.9996	0.9994	1.0000	0.9999	1.0000	1.0000	1.0000	0.9999	1.0000
12	0.9995	0.9998	1.0000	0.9998	0.9999	1.0000	0.9998	0.9999	0.9999
13	0.6410	0.9300	0.9983	0.7968	0.9839	0.9769	0.7958	0.7322	0.9985
14	0.9994	0.9998	1.0000	0.9999	1.0000	1.0000	0.9999	0.9994	1.0000
15	1.0000	0.9998	1.0000	1.0000	1.0000	0.9999	1.0000	1.0000	1.0000
16	0.9999	1.0000	1.0000	1.0000	1.0000	1.0000	1.0000	0.9999	1.0000
17	0.9993	0.9999	1.0000	0.9996	0.9999	0.9999	0.9998	0.9997	1.0000
18	0.5186	0.8638	0.9991	0.0457	0.9666	0.9871	0.6963	0.6641	0.9994
19	0.9996	0.9999	1.0000	0.9995	1.0000	1.0000	0.9989	0.9992	1.0000
20	0.9999	0.9999	1.0000	0.9999	1.0000	1.0000	0.9999	1.0000	1.0000
21	0.9992	1.0000	1.0000	1.0000	0.9999	0.9999	1.0000	0.9999	1.0000
22	1.0000	0.9998	1.0000	1.0000	0.9999	0.9999	1.0000	0.9998	1.0000
23	0.9746	0.8780	0.9943	0.9987	0.9787	0.9931	0.9962	0.6241	0.9978
24	1.0000	0.9999	1.0000	1.0000	1.0000	1.0000	1.0000	0.9993	1.0000
25	1.0000	0.9999	1.0000	1.0000	1.0000	1.0000	1.0000	1.0000	1.0000
26	1.0000	0.9999	1.0000	1.0000	1.0000	1.0000	1.0000	0.9999	1.0000
27	1.0000	0.9998	1.0000	0.9999	1.0000	1.0000	1.0000	0.9996	1.0000
28	0.9993	0.8932	0.9953	0.9993	0.9780	0.9974	0.9951	0.7062	0.9992
29	1.0000	1.0000	1.0000	1.0000	1.0000	1.0000	1.0000	0.9993	1.0000
30	1.0000	0.9999	1.0000	1.0000	1.0000	1.0000	1.0000	1.0000	1.0000
31	1.0000	1.0000	1.0000	0.9999	1.0000	1.0000	1.0000	1.0000	1.0000
32	0.9999	0.9997	1.0000	0.9999	0.9999	0.9998	1.0000	0.9997	1.0000
33	0.9990	0.8894	0.9979	0.9991	0.9892	0.9990	0.9964	0.6682	0.9996
34	1.0000	1.0000	1.0000	1.0000	0.9999	1.0000	1.0000	0.9993	1.0000
35	1.0000	0.9998	1.0000	1.0000	1.0000	1.0000	1.0000	1.0000	1.0000
36	1.0000	0.9999	1.0000	1.0000	1.0000	1.0000	1.0000	0.9999	1.0000
37	1.0000	0.9996	1.0000	1.0000	0.9999	0.9999	1.0000	0.9996	1.0000
38	0.9995	0.9085	0.9979	0.9905	0.9844	0.9853	0.9983	0.7082	0.9984
39	1.0000	1.0000	1.0000	1.0000	1.0000	1.0000	1.0000	0.9992	1.0000
40	1.0000	0.9998	1.0000	1.0000	1.0000	1.0000	1.0000	1.0000	1.0000
41	1.0000	1.0000	1.0000	1.0000	1.0000	1.0000	1.0000	0.9999	1.0000
42	1.0000	0.9997	1.0000	0.9999	1.0000	0.9999	1.0000	0.9998	0.9999
43	0.9993	0.8999	0.9981	0.9957	0.9979	0.9805	0.9931	0.6855	0.9956
44	1.0000	0.9999	1.0000	1.0000	1.0000	1.0000	1.0000	0.9993	1.0000
45	1.0000	0.9998	1.0000	1.0000	1.0000	1.0000	1.0000	1.0000	1.0000
46	1.0000	1.0000	1.0000	1.0000	1.0000	1.0000	1.0000	0.9999	1.0000
47	1.0000	0.9998	1.0000	0.9999	0.9999	0.9999	1.0000	0.9997	0.9999
48	0.9998	0.9239	0.9981	0.9985	0.9694	0.9990	0.9900	0.7426	0.9957
49	1.0000	1.0000	1.0000	1.0000	1.0000	1.0000	1.0000	0.9994	1.0000
50	1.0000	0.9998	1.0000	1.0000	1.0000	0.9999	1.0000	1.0000	1.0000
51	1.0000	1.0000	1.0000	0.9999	0.9999	1.0000	1.0000	0.9999	1.0000
52	1.0000	0.9996	1.0000	0.9997	0.9999	0.9999	1.0000	0.9998	1.0000

53	1.0000	0.9235	0.9980	0.9991	0.9879	0.9955	0.9971	0.7322	0.9998
54	1.0000	1.0000	1.0000	1.0000	1.0000	1.0000	1.0000	0.9991	1.0000
55	1.0000	0.9997	1.0000	1.0000	1.0000	1.0000	1.0000	0.9999	1.0000
56	1.0000	1.0000	1.0000	1.0000	1.0000	1.0000	1.0000	0.9999	1.0000
57	1.0000	0.9996	1.0000	1.0000	1.0000	0.9999	1.0000	0.9997	1.0000
58	0.9999	0.9356	0.9991	0.9997	0.9902	0.9920	0.9990	0.7448	0.9993
59	1.0000	1.0000	1.0000	1.0000	1.0000	1.0000	1.0000	0.9992	1.0000
60	1.0000	0.9999	1.0000	1.0000	1.0000	0.9999	1.0000	1.0000	1.0000
61	1.0000	1.0000	1.0000	0.9999	1.0000	1.0000	1.0000	0.9999	1.0000
62	1.0000	0.9997	1.0000	0.9999	1.0000	0.9999	1.0000	0.9997	0.9999
63	0.9991	0.9357	0.9972	0.9969	0.9844	0.9975	0.9985	0.7389	0.9992
64	1.0000	1.0000	1.0000	1.0000	1.0000	1.0000	1.0000	0.9993	1.0000
65	1.0000	0.9999	1.0000	1.0000	1.0000	1.0000	1.0000	0.9999	1.0000
66	1.0000	0.9999	1.0000	1.0000	1.0000	1.0000	1.0000	1.0000	1.0000
67	1.0000	0.9997	1.0000	0.9999	1.0000	1.0000	1.0000	0.9998	1.0000
68	0.9995	0.9595	0.9941	0.9996	0.9895	0.9994	0.9955	0.7911	0.9997
69	1.0000	0.9999	0.9999	1.0000	1.0000	1.0000	1.0000	0.9993	1.0000
70	1.0000	0.9999	1.0000	1.0000	1.0000	0.9999	1.0000	1.0000	1.0000
71	1.0000	1.0000	1.0000	1.0000	1.0000	1.0000	1.0000	0.9999	1.0000
72	1.0000	0.9995	1.0000	0.9999	1.0000	0.9999	1.0000	0.9997	1.0000
73	0.9999	0.9574	0.9966	0.9989	0.9845	0.9995	0.9872	0.8002	0.9983
74	1.0000	1.0000	1.0000	1.0000	1.0000	1.0000	1.0000	0.9992	1.0000
75	1.0000	0.9998	1.0000	1.0000	1.0000	1.0000	1.0000	1.0000	1.0000
76	1.0000	1.0000	1.0000	1.0000	1.0000	1.0000	1.0000	0.9999	1.0000
77	1.0000	0.9996	1.0000	0.9999	0.9999	1.0000	1.0000	0.9997	1.0000
78	0.9996	0.9623	0.9992	0.9986	0.9938	0.9959	0.9912	0.8281	0.9977
79	1.0000	0.9999	1.0000	1.0000	1.0000	1.0000	1.0000	0.9994	1.0000
80	1.0000	0.9999	1.0000	1.0000	1.0000	1.0000	1.0000	1.0000	1.0000
81	1.0000	1.0000	1.0000	1.0000	1.0000	1.0000	1.0000	1.0000	1.0000
82	1.0000	0.9997	1.0000	0.9999	0.9997	0.9999	1.0000	0.9996	1.0000
83	0.9998	0.9524	0.9993	0.9961	0.9913	0.9920	0.9942	0.8387	0.9992
84	1.0000	0.9999	1.0000	1.0000	1.0000	1.0000	1.0000	0.9992	1.0000
85	1.0000	0.9999	1.0000	1.0000	0.9999	1.0000	1.0000	1.0000	1.0000
86	1.0000	1.0000	1.0000	1.0000	1.0000	0.9999	1.0000	0.9999	1.0000
87	1.0000	0.9998	1.0000	1.0000	0.9998	0.9999	1.0000	0.9998	1.0000
88	0.9997	0.9581	0.9999	0.9995	0.9964	0.9980	0.9978	0.8534	0.9998
89	1.0000	0.9999	1.0000	1.0000	1.0000	1.0000	1.0000	0.9993	1.0000
90	1.0000	0.9999	1.0000	1.0000	1.0000	1.0000	1.0000	1.0000	1.0000

Interturn fault in phase B secondary									
	Phase A			Phase B			Phase C		
Window No.	r_{A11}	r_{A12}	r_{A22}	r_{B11}	r_{B12}	r_{B22}	r_{C11}	r_{C12}	r_{C22}
1	1.0000	1.0000	1.0000	0.9999	0.9999	1.0000	1.0000	1.0000	1.0000
2	1.0000	1.0000	1.0000	0.9999	0.9998	0.9994	1.0000	1.0000	0.9999
3	0.9976	0.9963	0.9944	0.9982	0.9248	0.9790	0.9800	0.9971	0.9971
4	1.0000	0.9999	1.0000	0.9999	0.9999	0.9999	1.0000	0.9998	1.0000
5	1.0000	0.9999	1.0000	0.9999	0.9999	0.9999	1.0000	1.0000	1.0000
6	1.0000	1.0000	1.0000	0.9999	0.9999	0.9999	1.0000	1.0000	1.0000
7	1.0000	0.9999	1.0000	0.9998	0.9997	0.9999	1.0000	0.9999	1.0000
8	0.9968	0.9960	0.9923	0.9764	0.9602	0.9790	0.9908	0.9983	0.9944
9	1.0000	1.0000	1.0000	1.0000	0.9999	1.0000	0.9999	0.9998	1.0000
10	1.0000	0.9999	1.0000	1.0000	0.9999	0.9999	1.0000	1.0000	1.0000
11	1.0000	1.0000	1.0000	1.0000	0.9998	0.9996	1.0000	1.0000	1.0000
12	1.0000	1.0000	1.0000	0.9959	0.9958	0.9994	1.0000	0.9999	1.0000
13	0.9967	0.9958	0.9963	0.7799	0.7405	0.9439	0.9976	0.9990	0.9955
14	1.0000	1.0000	0.9999	0.9998	0.9998	0.9999	0.9984	0.9965	0.9999
15	0.9998	0.9999	1.0000	1.0000	0.9999	0.9999	0.9998	0.9999	1.0000
16	0.9998	0.9998	1.0000	1.0000	1.0000	0.9999	1.0000	0.9999	1.0000
17	0.9996	0.9997	1.0000	0.9996	0.9998	0.9998	0.9997	0.9999	0.9999
18	0.6664	0.5228	0.9947	0.9173	0.9824	0.9979	0.6032	0.6901	0.9978
19	0.9998	0.9997	0.9999	0.9999	1.0000	1.0000	0.9998	0.9994	1.0000
20	1.0000	0.9995	0.9999	0.9999	1.0000	1.0000	1.0000	1.0000	1.0000
21	1.0000	0.9999	1.0000	1.0000	0.9999	0.9999	1.0000	1.0000	1.0000
22	0.9994	0.9996	1.0000	0.9945	0.9999	0.9988	0.9997	0.9997	1.0000
23	0.4693	0.3378	0.9984	0.6934	0.9495	0.9729	0.6108	0.7062	0.9875
24	0.9997	0.9997	1.0000	0.9997	1.0000	1.0000	0.9996	0.9989	0.9999
25	0.9997	0.9997	1.0000	1.0000	0.9999	0.9999	1.0000	1.0000	1.0000
26	1.0000	0.9998	0.9999	0.9999	0.9999	1.0000	1.0000	1.0000	1.0000
27	1.0000	0.9999	1.0000	0.9999	1.0000	0.9998	1.0000	0.9997	0.9999
28	0.9983	0.4320	0.9984	0.9815	0.9355	0.9372	0.9897	0.6776	0.9916
29	1.0000	0.9994	0.9999	1.0000	1.0000	0.9999	1.0000	0.9991	1.0000
30	1.0000	0.9999	1.0000	1.0000	0.9999	0.9999	1.0000	1.0000	1.0000
31	1.0000	1.0000	1.0000	0.9999	0.9998	0.9999	1.0000	1.0000	1.0000
32	1.0000	0.9995	1.0000	0.9999	0.9998	0.9996	0.9999	0.9998	0.9999
33	0.9907	0.3777	0.9956	0.9909	0.9565	0.9889	0.9967	0.7390	0.9919
34	1.0000	0.9997	1.0000	1.0000	0.9999	1.0000	1.0000	0.9995	0.9999
35	1.0000	0.9997	1.0000	1.0000	1.0000	0.9999	1.0000	0.9999	1.0000
36	1.0000	0.9998	1.0000	1.0000	0.9998	0.9998	1.0000	0.9999	1.0000
37	1.0000	0.9998	0.9999	0.9998	0.9999	0.9999	1.0000	0.9998	0.9999
38	0.9904	0.5345	0.9996	0.9852	0.9300	0.9825	0.9991	0.7726	0.9942
39	1.0000	0.9998	0.9999	1.0000	1.0000	1.0000	1.0000	0.9994	1.0000

40	1.0000	0.9997	1.0000	1.0000	1.0000	1.0000	1.0000	1.0000	1.0000
41	1.0000	0.9998	1.0000	0.9999	1.0000	0.9998	1.0000	0.9999	1.0000
42	1.0000	0.9997	1.0000	0.9998	0.9998	0.9993	1.0000	0.9997	1.0000
43	0.9947	0.4339	0.9991	0.9968	0.9225	0.9852	0.9987	0.7965	0.9878
44	0.9999	0.9993	0.9997	0.9999	1.0000	0.9999	0.9999	0.9992	1.0000
45	1.0000	0.9998	1.0000	1.0000	1.0000	1.0000	1.0000	1.0000	1.0000
46	1.0000	0.9999	1.0000	1.0000	1.0000	0.9998	1.0000	1.0000	1.0000
47	1.0000	0.9998	1.0000	0.9999	0.9997	0.9999	1.0000	0.9998	0.9999
48	0.9929	0.6004	0.9992	0.9974	0.9445	0.9970	0.9943	0.8054	0.9866
49	0.9999	0.9997	0.9999	1.0000	1.0000	1.0000	1.0000	0.9991	1.0000
50	1.0000	0.9998	1.0000	0.9999	0.9999	1.0000	1.0000	0.9999	1.0000
51	1.0000	0.9999	1.0000	0.9999	0.9999	0.9999	1.0000	1.0000	1.0000
52	1.0000	0.9995	1.0000	0.9999	0.9999	0.9997	1.0000	0.9999	0.9999
53	0.9913	0.5132	0.9992	0.9854	0.9432	0.9936	0.9990	0.7694	0.9972
54	1.0000	0.9996	0.9999	0.9999	0.9999	1.0000	1.0000	0.9991	1.0000
55	1.0000	0.9997	1.0000	0.9999	1.0000	0.9999	1.0000	0.9999	1.0000
56	1.0000	0.9999	1.0000	1.0000	0.9999	0.9999	1.0000	0.9999	1.0000
57	1.0000	0.9998	1.0000	1.0000	1.0000	0.9998	1.0000	0.9999	1.0000
58	0.9929	0.6459	0.9982	0.9900	0.9667	0.9975	0.9988	0.7993	0.9988
59	1.0000	0.9992	0.9999	1.0000	0.9999	1.0000	0.9999	0.9992	0.9999
60	1.0000	0.9997	1.0000	1.0000	0.9999	0.9999	1.0000	1.0000	1.0000
61	1.0000	0.9999	1.0000	0.9998	1.0000	1.0000	1.0000	1.0000	1.0000
62	1.0000	0.9996	1.0000	0.9999	0.9996	0.9994	1.0000	0.9999	1.0000
63	0.9908	0.5975	0.9993	0.9688	0.9799	0.9962	0.9984	0.8251	0.9887
64	0.9999	0.9997	0.9999	1.0000	0.9999	0.9999	1.0000	0.9992	1.0000
65	1.0000	0.9998	0.9999	1.0000	0.9999	0.9999	1.0000	1.0000	1.0000
66	1.0000	0.9999	1.0000	1.0000	0.9998	0.9999	1.0000	1.0000	1.0000
67	1.0000	0.9997	1.0000	1.0000	0.9999	1.0000	1.0000	0.9999	1.0000
68	0.9937	0.7070	0.9996	0.9994	0.9640	0.9986	0.9965	0.8619	0.9811
69	0.9999	0.9995	1.0000	1.0000	0.9999	1.0000	1.0000	0.9990	1.0000
70	1.0000	0.9999	1.0000	1.0000	0.9999	0.9999	1.0000	0.9999	1.0000
71	1.0000	0.9999	1.0000	0.9999	0.9998	0.9999	1.0000	1.0000	1.0000
72	1.0000	0.9996	1.0000	0.9998	0.9998	0.9998	1.0000	0.9999	1.0000
73	0.9951	0.6424	0.9991	0.9931	0.9818	0.9952	0.9981	0.8693	0.9886
74	1.0000	0.9996	0.9999	0.9999	1.0000	0.9999	1.0000	0.9992	1.0000
75	1.0000	0.9998	1.0000	1.0000	1.0000	1.0000	1.0000	1.0000	1.0000
76	1.0000	0.9998	1.0000	0.9999	0.9999	0.9997	1.0000	1.0000	1.0000
77	1.0000	0.9998	1.0000	0.9999	0.9998	0.9999	1.0000	0.9998	1.0000
78	0.9953	0.7362	0.9987	0.9790	0.9770	0.9899	0.9995	0.9177	0.9886
79	0.9999	0.9995	0.9999	1.0000	1.0000	1.0000	1.0000	0.9992	1.0000
80	1.0000	0.9998	0.9999	1.0000	1.0000	0.9999	1.0000	0.9999	1.0000
81	1.0000	0.9999	1.0000	1.0000	1.0000	0.9999	1.0000	0.9999	1.0000

82	1.0000	0.9996	1.0000	0.9992	0.9999	0.9995	1.0000	0.9999	1.0000
83	0.9952	0.6967	0.9997	0.9898	0.9984	0.9977	0.9996	0.8973	0.9963
84	0.9999	0.9992	0.9997	0.9999	0.9999	0.9997	0.9999	0.9991	1.0000
85	1.0000	0.9998	1.0000	1.0000	1.0000	1.0000	1.0000	1.0000	1.0000
86	1.0000	0.9999	1.0000	1.0000	1.0000	0.9999	1.0000	0.9999	1.0000
87	1.0000	0.9998	1.0000	1.0000	0.9998	0.9999	1.0000	0.9998	1.0000
88	0.9960	0.7577	0.9985	0.9961	0.9745	0.9944	0.9995	0.9174	0.9988
89	1.0000	0.9996	0.9999	1.0000	1.0000	1.0000	0.9999	0.9989	1.0000
90	0.9999	0.9996	1.0000	1.0000	0.9999	0.9998	1.0000	0.9999	1.0000

Interturn fault in phase C primary									
	Phase A			**Phase B**			**Phase C**		
Window No.	r_{A11}	r_{A12}	r_{A22}	r_{B11}	r_{B12}	r_{B22}	r_{C11}	r_{C12}	r_{C22}
1	1.0000	1.0000	1.0000	0.9999	1.0000	0.9999	1.0000	1.0000	1.0000
2	1.0000	1.0000	1.0000	0.9999	0.9998	1.0000	1.0000	1.0000	1.0000
3	0.9996	0.9964	0.9966	0.9972	0.9958	0.9955	0.9990	0.9920	0.9983
4	0.9999	0.9998	0.9999	1.0000	1.0000	0.9999	1.0000	0.9998	1.0000
5	1.0000	0.9999	1.0000	1.0000	1.0000	1.0000	1.0000	1.0000	1.0000
6	1.0000	1.0000	1.0000	1.0000	1.0000	1.0000	1.0000	1.0000	1.0000
7	1.0000	1.0000	1.0000	1.0000	1.0000	1.0000	1.0000	1.0000	1.0000
8	0.9994	0.9995	0.9994	0.9965	0.9975	0.9993	0.9986	0.9986	0.9955
9	1.0000	1.0000	0.9999	0.9999	1.0000	1.0000	1.0000	0.9999	1.0000
10	1.0000	1.0000	1.0000	1.0000	1.0000	1.0000	1.0000	1.0000	1.0000
11	1.0000	1.0000	1.0000	1.0000	1.0000	1.0000	1.0000	1.0000	1.0000
12	1.0000	1.0000	1.0000	0.9995	0.9998	1.0000	1.0000	1.0000	0.9999
13	0.9991	0.9997	0.9990	0.9976	0.9992	0.9903	0.9970	0.9993	0.9978
14	0.9999	1.0000	0.9999	1.0000	1.0000	0.9999	1.0000	0.9999	1.0000
15	1.0000	1.0000	1.0000	1.0000	1.0000	1.0000	1.0000	1.0000	1.0000
16	1.0000	1.0000	1.0000	1.0000	1.0000	1.0000	1.0000	1.0000	1.0000
17	1.0000	1.0000	1.0000	0.9998	0.9997	1.0000	0.9946	0.9936	0.9998
18	0.9995	0.9993	0.9963	0.6746	0.6958	0.9952	0.7582	0.6665	0.9850
19	0.9994	0.9996	1.0000	0.9998	0.9998	1.0000	0.9999	0.9998	1.0000
20	0.9999	1.0000	1.0000	0.9999	1.0000	1.0000	1.0000	1.0000	1.0000
21	1.0000	1.0000	1.0000	1.0000	1.0000	1.0000	1.0000	1.0000	1.0000
22	0.9999	0.9999	1.0000	0.9990	0.9994	0.9998	0.9999	0.9999	0.9999
23	0.9193	0.9175	0.9997	0.5634	0.4716	0.9923	0.9365	0.9207	0.9988
24	0.9999	0.9998	1.0000	0.9998	0.9999	1.0000	1.0000	1.0000	1.0000
25	1.0000	1.0000	1.0000	0.9999	1.0000	1.0000	1.0000	1.0000	1.0000
26	0.9999	1.0000	1.0000	1.0000	1.0000	0.9999	1.0000	1.0000	1.0000
27	0.9999	0.9996	1.0000	0.9996	0.9987	0.9999	0.9931	0.9999	0.9999
28	0.8852	0.8501	0.9988	0.9793	0.5378	0.9998	0.3863	0.9195	0.9973

29	0.9987	0.9997	1.0000	1.0000	0.9996	1.0000	0.9998	1.0000	1.0000
30	1.0000	1.0000	1.0000	1.0000	0.9998	0.9999	1.0000	1.0000	1.0000
31	1.0000	1.0000	1.0000	1.0000	0.9999	1.0000	1.0000	1.0000	1.0000
32	1.0000	0.9997	1.0000	0.9997	0.9995	0.9997	1.0000	0.9997	0.9999
33	0.9992	0.9074	0.9996	0.9992	0.5185	0.9995	0.9995	0.9572	0.9945
34	1.0000	0.9997	1.0000	1.0000	0.9997	1.0000	1.0000	1.0000	1.0000
35	1.0000	1.0000	1.0000	1.0000	1.0000	1.0000	1.0000	1.0000	1.0000
36	1.0000	1.0000	1.0000	1.0000	0.9999	1.0000	1.0000	1.0000	1.0000
37	1.0000	0.9998	1.0000	0.9998	0.9995	0.9999	1.0000	0.9998	1.0000
38	0.9997	0.8484	0.9996	0.9996	0.5166	0.9990	0.9988	0.9595	0.9964
39	1.0000	0.9996	1.0000	1.0000	0.9994	1.0000	1.0000	1.0000	1.0000
40	1.0000	1.0000	1.0000	1.0000	0.9999	1.0000	1.0000	1.0000	1.0000
41	1.0000	1.0000	1.0000	1.0000	0.9999	0.9999	1.0000	1.0000	1.0000
42	1.0000	0.9998	1.0000	1.0000	0.9996	1.0000	1.0000	0.9998	0.9999
43	0.9999	0.8593	0.9940	0.9921	0.4732	0.9971	0.9997	0.9577	0.9994
44	1.0000	0.9997	1.0000	1.0000	0.9996	1.0000	1.0000	1.0000	1.0000
45	1.0000	1.0000	1.0000	1.0000	1.0000	0.9999	1.0000	1.0000	1.0000
46	1.0000	1.0000	1.0000	1.0000	0.9999	1.0000	1.0000	1.0000	1.0000
47	1.0000	0.9996	1.0000	0.9999	0.9998	1.0000	1.0000	0.9998	1.0000
48	0.9997	0.8421	0.9991	0.9996	0.5497	0.9975	0.9999	0.9655	0.9997
49	1.0000	0.9995	0.9999	1.0000	0.9997	1.0000	1.0000	1.0000	1.0000
50	1.0000	1.0000	1.0000	1.0000	0.9999	1.0000	1.0000	1.0000	1.0000
51	1.0000	1.0000	1.0000	1.0000	0.9999	0.9999	1.0000	1.0000	1.0000
52	1.0000	0.9998	1.0000	1.0000	0.9996	1.0000	1.0000	0.9999	0.9999
53	0.9992	0.8395	0.9961	0.9981	0.6269	0.9903	0.9998	0.9701	0.9988
54	1.0000	0.9997	0.9999	1.0000	0.9995	1.0000	1.0000	1.0000	1.0000
55	1.0000	1.0000	1.0000	0.9999	0.9998	1.0000	1.0000	1.0000	1.0000
56	1.0000	1.0000	1.0000	0.9999	0.9999	1.0000	1.0000	1.0000	1.0000
57	1.0000	0.9997	1.0000	0.9999	0.9990	0.9999	1.0000	0.9998	1.0000
58	0.9997	0.8360	0.9993	0.9984	0.5363	0.9994	0.9995	0.9514	0.9996
59	1.0000	0.9997	1.0000	1.0000	0.9997	1.0000	1.0000	1.0000	1.0000
60	1.0000	1.0000	1.0000	1.0000	0.9999	1.0000	1.0000	1.0000	1.0000
61	1.0000	1.0000	1.0000	1.0000	1.0000	1.0000	1.0000	1.0000	1.0000
62	1.0000	0.9997	1.0000	0.9999	0.9997	0.9999	1.0000	0.9998	1.0000
63	0.9998	0.8583	0.9997	0.9966	0.5638	0.9956	0.9996	0.9601	0.9994
64	1.0000	0.9998	1.0000	1.0000	0.9997	0.9999	1.0000	0.9999	1.0000
65	1.0000	1.0000	1.0000	1.0000	0.9999	1.0000	1.0000	1.0000	1.0000
66	1.0000	1.0000	1.0000	0.9999	1.0000	1.0000	1.0000	1.0000	1.0000
67	1.0000	0.9995	1.0000	0.9999	0.9997	0.9996	1.0000	0.9998	1.0000
68	0.9995	0.8115	0.9972	0.9995	0.5822	0.9974	0.9993	0.9688	0.9951
69	1.0000	0.9996	1.0000	1.0000	0.9997	1.0000	1.0000	1.0000	1.0000
70	1.0000	1.0000	1.0000	0.9999	0.9998	0.9999	1.0000	1.0000	1.0000

71	1.0000	1.0000	1.0000	1.0000	1.0000	1.0000	1.0000	1.0000	1.0000
72	1.0000	0.9997	1.0000	0.9997	0.9995	0.9999	1.0000	0.9998	1.0000
73	0.9998	0.8551	0.9997	0.9991	0.6140	0.9982	0.9978	0.9689	0.9941
74	1.0000	0.9999	1.0000	1.0000	0.9998	1.0000	1.0000	1.0000	1.0000
75	1.0000	1.0000	1.0000	1.0000	1.0000	1.0000	1.0000	1.0000	1.0000
76	1.0000	0.9999	1.0000	1.0000	0.9999	0.9999	1.0000	1.0000	1.0000
77	0.9999	0.9998	1.0000	0.9998	0.9996	0.9999	1.0000	0.9997	1.0000
78	0.9999	0.8364	0.9989	0.9995	0.5128	0.9961	0.9999	0.9699	0.9997
79	1.0000	0.9997	0.9999	1.0000	0.9998	1.0000	1.0000	0.9999	1.0000
80	1.0000	1.0000	1.0000	0.9999	0.9999	1.0000	1.0000	1.0000	1.0000
81	1.0000	1.0000	1.0000	1.0000	0.9999	1.0000	1.0000	1.0000	1.0000
82	1.0000	0.9997	1.0000	0.9998	0.9994	1.0000	1.0000	0.9998	0.9999
83	0.9999	0.8483	0.9996	0.9973	0.6379	0.9926	0.9999	0.9686	0.9996
84	1.0000	0.9997	1.0000	1.0000	0.9997	1.0000	1.0000	0.9999	1.0000
85	1.0000	1.0000	1.0000	1.0000	0.9999	1.0000	1.0000	1.0000	1.0000
86	1.0000	1.0000	1.0000	1.0000	1.0000	1.0000	1.0000	1.0000	1.0000
87	1.0000	0.9997	1.0000	0.9999	0.9989	0.9997	1.0000	0.9999	1.0000
88	0.9999	0.7609	0.9906	0.9990	0.6573	0.9878	1.0000	0.9796	0.9991
89	1.0000	0.9997	1.0000	1.0000	0.9999	0.9998	1.0000	1.0000	1.0000
90	1.0000	1.0000	1.0000	1.0000	0.9999	1.0000	1.0000	1.0000	1.0000

Interturn fault in phase C secondary									
	Phase A			**Phase B**			**Phase C**		
Window No.	r_{A11}	r_{A12}	r_{A22}	r_{B11}	r_{B12}	r_{B22}	r_{C11}	r_{C12}	r_{C22}
1	1.0000	1.0000	1.0000	1.0000	1.0000	0.9999	1.0000	1.0000	1.0000
2	1.0000	0.9999	1.0000	0.9992	0.9999	0.9995	1.0000	1.0000	0.9999
3	0.9985	0.9622	0.9885	0.9951	0.9574	0.9821	0.9995	0.9988	0.9979
4	1.0000	1.0000	1.0000	0.9999	0.9999	1.0000	0.9999	0.9997	1.0000
5	1.0000	0.9999	1.0000	1.0000	0.9999	1.0000	1.0000	1.0000	0.9999
6	1.0000	1.0000	1.0000	1.0000	1.0000	1.0000	1.0000	1.0000	1.0000
7	1.0000	1.0000	1.0000	0.9999	0.9999	0.9999	1.0000	1.0000	1.0000
8	0.9988	0.9354	0.9960	0.9988	0.8933	0.9986	0.9936	0.9976	0.9993
9	1.0000	0.9998	1.0000	1.0000	0.9999	1.0000	1.0000	0.9998	1.0000
10	0.9999	0.9998	1.0000	1.0000	0.9999	0.9999	1.0000	1.0000	1.0000
11	1.0000	1.0000	1.0000	0.9996	0.9989	0.9999	1.0000	1.0000	1.0000
12	1.0000	0.9998	1.0000	0.9997	0.9999	0.9999	1.0000	1.0000	1.0000
13	0.9974	0.9627	0.9971	0.7843	0.8896	0.9944	0.2776	0.3103	0.9528
14	0.9999	0.9998	1.0000	0.9996	0.9999	1.0000	0.9999	0.9992	1.0000
15	0.9998	0.9999	1.0000	1.0000	0.9999	0.9999	1.0000	1.0000	1.0000
16	0.9999	0.9998	1.0000	0.9999	0.9999	1.0000	1.0000	1.0000	1.0000
17	0.9997	0.9990	0.9999	0.9994	0.9998	0.9998	0.9999	0.9997	1.0000

18	0.8980	0.6545	0.9986	0.5455	0.8035	0.9930	0.9269	0.8902	0.9877
19	0.9998	0.9994	1.0000	0.9997	0.9999	1.0000	1.0000	1.0000	1.0000
20	0.9997	1.0000	1.0000	0.9998	0.9999	0.9998	1.0000	1.0000	1.0000
21	1.0000	0.9999	1.0000	0.9993	1.0000	1.0000	1.0000	1.0000	1.0000
22	0.9998	0.9994	1.0000	0.9998	0.9998	0.9999	0.9999	0.9998	0.9999
23	0.8919	0.6990	0.9982	0.9428	0.5606	0.9816	0.0740	0.9165	0.9257
24	0.9993	0.9994	0.9999	0.9999	1.0000	0.9999	0.9997	1.0000	1.0000
25	1.0000	1.0000	1.0000	1.0000	1.0000	0.9999	1.0000	1.0000	1.0000
26	1.0000	0.9999	1.0000	1.0000	0.9999	0.9999	1.0000	1.0000	1.0000
27	1.0000	0.9996	0.9999	0.9997	0.9999	0.9999	1.0000	0.9998	1.0000
28	0.9985	0.6956	0.9939	0.9997	0.7648	0.9977	0.9919	0.9226	0.9983
29	1.0000	0.9992	1.0000	1.0000	0.9999	1.0000	1.0000	1.0000	1.0000
30	1.0000	1.0000	1.0000	1.0000	1.0000	0.9998	1.0000	1.0000	1.0000
31	1.0000	0.9999	1.0000	0.9999	0.9997	0.9998	1.0000	1.0000	1.0000
32	1.0000	0.9994	1.0000	0.9996	0.9997	0.9997	1.0000	0.9999	0.9999
33	0.9995	0.7118	0.9988	0.9981	0.5757	0.9968	0.9990	0.9257	0.9989
34	0.9999	0.9992	0.9999	1.0000	0.9999	1.0000	1.0000	1.0000	1.0000
35	1.0000	1.0000	1.0000	1.0000	0.9999	1.0000	1.0000	1.0000	1.0000
36	1.0000	0.9999	1.0000	1.0000	0.9999	1.0000	1.0000	1.0000	1.0000
37	1.0000	0.9996	1.0000	0.9999	0.9998	1.0000	1.0000	0.9998	1.0000
38	0.9999	0.6759	0.9995	0.9996	0.7414	0.9981	0.9993	0.9154	0.9992
39	1.0000	0.9991	1.0000	1.0000	0.9999	1.0000	1.0000	1.0000	1.0000
40	1.0000	1.0000	1.0000	1.0000	0.9999	0.9999	1.0000	1.0000	1.0000
41	1.0000	0.9999	1.0000	0.9998	1.0000	1.0000	1.0000	1.0000	1.0000
42	1.0000	0.9995	1.0000	0.9999	0.9996	0.9998	1.0000	0.9997	1.0000
43	0.9995	0.7345	0.9976	0.9967	0.6486	0.9889	0.9994	0.9060	0.9989
44	1.0000	0.9993	0.9999	1.0000	0.9998	1.0000	1.0000	0.9999	1.0000
45	1.0000	0.9999	1.0000	1.0000	0.9999	1.0000	1.0000	1.0000	1.0000
46	1.0000	0.9998	0.9999	1.0000	1.0000	0.9999	1.0000	1.0000	1.0000
47	1.0000	0.9994	1.0000	0.9999	0.9998	0.9999	1.0000	0.9998	1.0000
48	1.0000	0.6860	0.9997	0.9962	0.7084	0.9906	0.9977	0.8698	0.9985
49	1.0000	0.9993	1.0000	1.0000	1.0000	1.0000	1.0000	1.0000	1.0000
50	1.0000	1.0000	1.0000	1.0000	1.0000	0.9999	1.0000	1.0000	1.0000
51	1.0000	1.0000	1.0000	0.9999	1.0000	0.9999	1.0000	1.0000	1.0000
52	1.0000	0.9994	1.0000	0.9996	0.9981	0.9997	1.0000	0.9998	1.0000
53	0.9992	0.7499	0.9978	0.9831	0.8352	0.9886	0.9982	0.9018	0.9976
54	1.0000	0.9992	1.0000	0.9999	0.9999	0.9999	1.0000	1.0000	1.0000
55	1.0000	1.0000	1.0000	1.0000	0.9999	1.0000	1.0000	1.0000	1.0000
56	1.0000	1.0000	0.9999	1.0000	1.0000	0.9999	1.0000	1.0000	1.0000
57	1.0000	0.9995	1.0000	0.9999	0.9994	0.9999	1.0000	0.9999	1.0000
58	0.9994	0.7110	0.9975	0.9942	0.6412	0.9991	0.9957	0.9064	0.9993
59	1.0000	0.9990	1.0000	1.0000	0.9999	1.0000	1.0000	1.0000	1.0000

60	1.0000	1.0000	1.0000	1.0000	1.0000	0.9999	1.0000	1.0000	1.0000
61	1.0000	1.0000	1.0000	0.9999	0.9999	0.9999	1.0000	1.0000	1.0000
62	1.0000	0.9997	1.0000	0.9998	0.9998	0.9991	1.0000	0.9999	1.0000
63	0.9998	0.7528	0.9995	0.9966	0.7071	0.9874	0.9989	0.9002	0.9988
64	1.0000	0.9989	1.0000	1.0000	0.9999	1.0000	1.0000	1.0000	1.0000
65	1.0000	1.0000	1.0000	1.0000	1.0000	1.0000	1.0000	1.0000	1.0000
66	1.0000	0.9999	1.0000	1.0000	1.0000	0.9999	1.0000	1.0000	1.0000
67	1.0000	0.9994	1.0000	1.0000	0.9995	0.9999	1.0000	0.9999	1.0000
68	0.9999	0.7499	0.9988	0.9937	0.7241	0.9980	0.9992	0.8885	0.9979
69	1.0000	0.9992	1.0000	1.0000	1.0000	1.0000	1.0000	1.0000	1.0000
70	1.0000	1.0000	1.0000	1.0000	0.9999	1.0000	1.0000	1.0000	1.0000
71	1.0000	1.0000	1.0000	1.0000	0.9999	0.9997	1.0000	1.0000	1.0000
72	1.0000	0.9996	1.0000	0.9999	0.9992	0.9997	1.0000	0.9999	1.0000
73	0.9996	0.7310	0.9988	0.9947	0.6823	0.9908	0.9997	0.9060	0.9988
74	1.0000	0.9991	1.0000	1.0000	0.9998	0.9999	1.0000	1.0000	1.0000
75	1.0000	1.0000	1.0000	1.0000	1.0000	1.0000	1.0000	1.0000	1.0000
76	1.0000	1.0000	1.0000	1.0000	0.9999	0.9999	1.0000	1.0000	1.0000
77	1.0000	0.9996	1.0000	0.9999	0.9994	0.9999	1.0000	0.9997	1.0000
78	0.9998	0.7817	0.9978	0.9971	0.7544	0.9985	0.9987	0.8808	0.9977
79	1.0000	0.9993	1.0000	1.0000	0.9999	1.0000	1.0000	1.0000	1.0000
80	1.0000	1.0000	1.0000	0.9999	0.9999	1.0000	1.0000	1.0000	1.0000
81	1.0000	1.0000	1.0000	1.0000	1.0000	0.9999	1.0000	1.0000	1.0000
82	1.0000	0.9995	1.0000	0.9997	0.9999	0.9998	1.0000	0.9999	1.0000
83	0.9993	0.7793	0.9934	0.9926	0.7307	0.9965	0.9994	0.8807	0.9976
84	1.0000	0.9987	1.0000	1.0000	0.9999	1.0000	1.0000	1.0000	1.0000
85	1.0000	1.0000	1.0000	0.9999	0.9999	1.0000	1.0000	1.0000	1.0000
86	1.0000	0.9999	1.0000	1.0000	1.0000	1.0000	1.0000	1.0000	1.0000
87	1.0000	0.9994	0.9999	1.0000	0.9997	0.9999	1.0000	0.9999	1.0000
88	0.9999	0.7616	0.9992	0.9992	0.7582	0.9983	0.9988	0.8835	0.9988
89	1.0000	0.9992	1.0000	0.9999	0.9999	1.0000	1.0000	1.0000	1.0000
90	1.0000	1.0000	1.0000	0.9999	1.0000	1.0000	1.0000	1.0000	1.0000

Turn to ground fault in phase A primary									
	Phase A			**Phase B**			**Phase C**		
Window No.	r_{A11}	r_{A12}	r_{A22}	r_{B11}	r_{B12}	r_{B22}	r_{C11}	r_{C12}	r_{C22}
1	1.0000	1.0000	1.0000	0.9999	0.9997	0.9999	1.0000	1.0000	1.0000
2	1.0000	0.9999	1.0000	0.9999	0.9999	0.9999	1.0000	1.0000	1.0000
3	0.9820	0.8268	0.9964	0.9883	0.9522	0.9980	0.9951	0.9927	0.9984
4	1.0000	0.9999	1.0000	1.0000	1.0000	0.9999	1.0000	1.0000	1.0000
5	1.0000	1.0000	1.0000	1.0000	1.0000	1.0000	1.0000	1.0000	1.0000
6	1.0000	1.0000	1.0000	1.0000	0.9998	0.9999	1.0000	1.0000	1.0000

7	1.0000	0.9998	1.0000	0.9999	0.9999	1.0000	1.0000	1.0000	1.0000
8	0.9972	0.8801	0.9939	0.9981	0.9382	0.9988	0.9792	0.9829	0.9856
9	1.0000	0.9998	1.0000	0.9962	0.9960	0.9999	1.0000	0.9999	1.0000
10	1.0000	1.0000	1.0000	0.9979	0.9990	0.9999	1.0000	1.0000	1.0000
11	1.0000	1.0000	1.0000	0.9991	0.9995	0.9999	0.9973	0.9973	1.0000
12	0.9994	0.9988	1.0000	0.9956	0.9975	0.9998	0.9974	0.9982	1.0000
13	0.6392	0.0948	0.9978	0.3907	0.5109	0.9793	0.1139	0.4801	0.9631
14	0.9956	0.9944	1.0000	0.9987	0.9988	1.0000	0.9942	0.9939	1.0000
15	1.0000	1.0000	1.0000	0.9996	0.9998	1.0000	0.9994	0.9995	1.0000
16	0.9999	1.0000	1.0000	0.9993	0.9994	0.9999	0.9997	0.9998	1.0000
17	0.9993	0.9995	0.9999	0.9920	0.9934	1.0000	0.9982	0.9985	1.0000
18	0.4583	0.5816	0.9392	0.2836	0.4663	0.9868	0.1289	0.4825	0.9814
19	0.9999	1.0000	1.0000	0.9891	0.9989	0.9999	0.9871	0.9861	1.0000
20	0.9999	0.9998	1.0000	0.9992	0.9999	0.9999	0.9991	0.9992	1.0000
21	1.0000	1.0000	1.0000	1.0000	0.9995	0.9999	0.9953	0.9996	1.0000
22	0.9982	0.9996	0.9999	0.9985	0.9933	0.9998	0.9999	0.9987	1.0000
23	-0.2691	0.6217	0.8609	0.9997	0.4412	0.9954	0.9979	0.5607	0.9868
24	0.9946	0.9999	0.9999	1.0000	0.9990	1.0000	0.9975	0.9836	1.0000
25	0.9999	0.9998	1.0000	1.0000	0.9997	1.0000	0.9999	0.9992	1.0000
26	1.0000	1.0000	1.0000	0.9999	0.9993	1.0000	1.0000	0.9997	1.0000
27	1.0000	0.9997	1.0000	0.9998	0.9945	1.0000	1.0000	0.9990	1.0000
28	0.9819	0.6361	0.9923	0.9993	0.4382	0.9982	0.9999	0.5419	0.9968
29	1.0000	0.9999	1.0000	1.0000	0.9989	1.0000	0.9999	0.9859	1.0000
30	1.0000	0.9997	1.0000	1.0000	0.9996	0.9999	1.0000	0.9992	1.0000
31	1.0000	1.0000	1.0000	0.9999	0.9999	1.0000	1.0000	0.9996	1.0000
32	1.0000	0.9997	1.0000	0.9995	0.9948	0.9999	1.0000	0.9985	1.0000
33	0.9969	0.6498	0.9987	0.9997	0.3771	0.9950	0.9997	0.6043	0.9956
34	1.0000	1.0000	0.9999	0.9999	0.9983	0.9999	1.0000	0.9840	1.0000
35	1.0000	0.9998	1.0000	1.0000	0.9996	1.0000	1.0000	0.9994	1.0000
36	1.0000	1.0000	1.0000	0.9999	0.9996	1.0000	1.0000	0.9997	1.0000
37	1.0000	0.9997	1.0000	0.9997	0.9964	1.0000	1.0000	0.9987	1.0000
38	0.9974	0.6782	0.9996	0.9996	0.3703	0.9945	0.9999	0.6189	0.9940
39	1.0000	0.9999	1.0000	1.0000	0.9986	1.0000	0.9997	0.9815	1.0000
40	1.0000	0.9998	0.9999	1.0000	0.9998	0.9999	1.0000	0.9992	1.0000
41	1.0000	1.0000	1.0000	0.9999	0.9993	0.9999	1.0000	0.9996	1.0000
42	1.0000	0.9998	1.0000	0.9998	0.9944	0.9998	1.0000	0.9990	1.0000
43	0.9962	0.6423	0.9953	0.9988	0.4982	0.9718	1.0000	0.6355	0.9969
44	1.0000	0.9999	1.0000	1.0000	0.9980	1.0000	0.9999	0.9835	1.0000
45	1.0000	0.9998	1.0000	1.0000	0.9998	1.0000	1.0000	0.9992	1.0000
46	1.0000	1.0000	1.0000	1.0000	0.9996	1.0000	1.0000	0.9997	1.0000
47	1.0000	0.9996	1.0000	0.9999	0.9964	1.0000	1.0000	0.9991	1.0000
48	0.9980	0.6485	0.9945	0.9994	0.2858	0.9979	1.0000	0.6843	0.9958

49	1.0000	0.9999	1.0000	1.0000	0.9987	0.9999	0.9999	0.9798	1.0000
50	1.0000	0.9997	0.9999	1.0000	0.9999	1.0000	1.0000	0.9990	1.0000
51	1.0000	1.0000	1.0000	1.0000	0.9994	0.9999	1.0000	0.9996	1.0000
52	1.0000	0.9998	1.0000	0.9999	0.9952	1.0000	1.0000	0.9986	1.0000
53	0.9970	0.6677	0.9988	0.9986	0.2125	0.9176	1.0000	0.7010	0.9955
54	1.0000	1.0000	1.0000	1.0000	0.9984	1.0000	0.9999	0.9828	1.0000
55	1.0000	0.9999	1.0000	1.0000	0.9998	1.0000	1.0000	0.9993	1.0000
56	1.0000	1.0000	1.0000	1.0000	0.9997	1.0000	1.0000	0.9997	1.0000
57	1.0000	0.9998	1.0000	0.9999	0.9944	1.0000	1.0000	0.9989	1.0000
58	0.9949	0.6476	0.9946	0.9986	0.1291	0.9759	0.9999	0.7362	0.9961
59	1.0000	0.9999	1.0000	1.0000	0.9989	1.0000	0.9997	0.9845	1.0000
60	1.0000	0.9998	1.0000	1.0000	0.9998	1.0000	1.0000	0.9991	1.0000
61	1.0000	1.0000	1.0000	0.9999	0.9997	1.0000	1.0000	0.9996	1.0000
62	1.0000	0.9998	1.0000	0.9997	0.9972	1.0000	1.0000	0.9989	1.0000
63	0.9969	0.6544	0.9955	1.0000	0.1241	0.9948	0.9999	0.7332	0.9982
64	1.0000	1.0000	1.0000	1.0000	0.9980	1.0000	0.9999	0.9828	1.0000
65	1.0000	0.9998	1.0000	1.0000	0.9997	1.0000	1.0000	0.9990	1.0000
66	1.0000	0.9999	1.0000	1.0000	0.9998	1.0000	1.0000	0.9996	1.0000
67	1.0000	0.9997	1.0000	0.9998	0.9966	0.9999	1.0000	0.9990	1.0000
68	0.9935	0.6453	0.9928	0.9999	0.0195	0.9930	0.9999	0.7974	0.9940
69	1.0000	0.9999	1.0000	1.0000	0.9986	0.9999	0.9995	0.9795	1.0000
70	1.0000	0.9999	1.0000	1.0000	0.9998	1.0000	1.0000	0.9992	1.0000
71	1.0000	1.0000	1.0000	1.0000	0.9996	1.0000	1.0000	0.9996	1.0000
72	1.0000	0.9998	1.0000	0.9996	0.9952	1.0000	1.0000	0.9990	1.0000
73	0.9916	0.6869	0.9961	0.9998	0.1895	0.9937	0.9997	0.7764	0.9960
74	1.0000	0.9999	1.0000	1.0000	0.9980	1.0000	0.9998	0.9793	1.0000
75	1.0000	0.9998	1.0000	1.0000	0.9995	1.0000	1.0000	0.9988	1.0000
76	1.0000	1.0000	1.0000	0.9999	0.9997	1.0000	1.0000	0.9996	1.0000
77	1.0000	0.9998	1.0000	0.9998	0.9949	1.0000	1.0000	0.9990	1.0000
78	0.9965	0.6754	0.9989	0.9998	-0.0460	0.9965	1.0000	0.8154	0.9993
79	1.0000	1.0000	1.0000	1.0000	0.9983	1.0000	0.9999	0.9780	1.0000
80	1.0000	0.9998	1.0000	1.0000	0.9998	1.0000	1.0000	0.9989	1.0000
81	1.0000	1.0000	1.0000	0.9998	0.9992	0.9999	1.0000	0.9997	1.0000
82	1.0000	0.9998	1.0000	0.9997	0.9961	1.0000	1.0000	0.9988	1.0000
83	0.9951	0.7230	0.9988	0.9994	0.0888	0.9879	1.0000	0.8222	0.9971
84	1.0000	1.0000	1.0000	1.0000	0.9985	1.0000	0.9997	0.9749	1.0000
85	1.0000	0.9998	1.0000	0.9999	0.9998	1.0000	1.0000	0.9991	1.0000
86	1.0000	1.0000	1.0000	1.0000	0.9995	0.9999	1.0000	0.9997	1.0000
87	1.0000	0.9998	1.0000	0.9999	0.9956	0.9999	1.0000	0.9990	1.0000
88	0.9940	0.7152	0.9985	0.9993	-0.0181	0.9997	1.0000	0.8364	0.9994
89	1.0000	0.9999	1.0000	1.0000	0.9983	1.0000	0.9999	0.9777	1.0000
90	1.0000	0.9999	1.0000	1.0000	0.9999	1.0000	1.0000	0.9987	1.0000

Turn to ground fault in phase A secondary									
	Phase A			**Phase B**			**Phase C**		
Window No.	r_{A11}	r_{A12}	r_{A22}	r_{B11}	r_{B12}	r_{B22}	r_{C11}	r_{C12}	r_{C22}
1	1.0000	1.0000	1.0000	1.0000	0.9999	0.9999	1.0000	1.0000	1.0000
2	1.0000	0.9999	1.0000	0.9999	0.9998	0.9999	1.0000	1.0000	1.0000
3	0.9992	0.9702	0.9970	0.9885	0.9704	0.9974	0.9976	0.9987	0.9935
4	0.9999	0.9998	1.0000	1.0000	1.0000	1.0000	1.0000	1.0000	1.0000
5	1.0000	1.0000	1.0000	1.0000	0.9999	1.0000	1.0000	1.0000	1.0000
6	1.0000	1.0000	1.0000	1.0000	1.0000	0.9999	1.0000	1.0000	1.0000
7	1.0000	0.9999	1.0000	1.0000	0.9998	0.9998	1.0000	1.0000	1.0000
8	0.9994	0.9699	0.9992	0.9943	0.9566	0.9949	0.9993	0.9953	0.9969
9	1.0000	0.9999	1.0000	0.9997	0.9987	0.9982	1.0000	0.9999	1.0000
10	1.0000	1.0000	1.0000	0.9997	0.9998	0.9991	1.0000	1.0000	1.0000
11	1.0000	1.0000	1.0000	0.9998	1.0000	0.9994	0.9999	1.0000	0.9999
12	0.9995	0.9823	0.9900	0.9998	0.9999	0.9992	0.9995	0.9992	0.9970
13	0.7050	-0.7383	0.1997	0.6166	0.9419	0.0923	0.7658	0.9705	0.5571
14	0.9986	0.9951	0.9996	0.9998	1.0000	0.9994	1.0000	0.9997	0.9999
15	1.0000	1.0000	1.0000	1.0000	0.9999	0.9996	1.0000	0.9999	0.9998
16	1.0000	1.0000	0.9999	0.9999	0.9999	0.9996	0.9999	0.9999	0.9998
17	0.9999	1.0000	0.9999	0.9998	0.9999	0.9988	0.9989	0.9972	0.9917
18	0.9919	0.9822	0.8482	0.7063	0.9295	0.1132	0.6641	0.9764	0.4046
19	0.9997	0.9998	0.9998	0.9994	0.9999	0.9956	0.9999	0.9996	0.9999
20	0.9999	0.9997	1.0000	0.9999	0.9999	0.9995	1.0000	0.9999	0.9999
21	1.0000	0.9999	0.9997	1.0000	1.0000	1.0000	0.9998	0.9999	0.9998
22	0.9992	1.0000	0.9888	0.9999	1.0000	1.0000	0.9998	0.9975	0.9988
23	0.8815	0.9947	-0.2381	0.9906	0.9504	0.9956	0.9897	0.9814	0.9959
24	0.9994	0.9989	0.9998	1.0000	0.9998	0.9999	1.0000	0.9996	0.9999
25	1.0000	0.9996	0.9999	1.0000	1.0000	1.0000	1.0000	0.9999	1.0000
26	1.0000	1.0000	1.0000	0.9999	1.0000	1.0000	1.0000	0.9999	1.0000
27	1.0000	1.0000	1.0000	1.0000	1.0000	0.9999	1.0000	0.9976	1.0000
28	0.9872	0.9954	0.9939	0.9995	0.9333	0.9997	0.9999	0.9786	0.9998
29	1.0000	0.9999	1.0000	1.0000	0.9998	0.9999	1.0000	0.9996	1.0000
30	1.0000	0.9998	1.0000	1.0000	1.0000	0.9999	1.0000	1.0000	1.0000
31	1.0000	0.9999	1.0000	1.0000	0.9999	1.0000	1.0000	0.9999	1.0000
32	1.0000	1.0000	1.0000	1.0000	1.0000	1.0000	0.9999	0.9972	0.9999
33	0.9979	0.9937	0.9982	0.9977	0.9533	0.9997	0.9996	0.9778	0.9998
34	1.0000	0.9996	0.9996	1.0000	0.9999	1.0000	1.0000	0.9994	1.0000
35	1.0000	0.9997	1.0000	1.0000	1.0000	1.0000	1.0000	1.0000	1.0000
36	1.0000	1.0000	1.0000	0.9999	1.0000	1.0000	1.0000	0.9999	1.0000
37	1.0000	1.0000	1.0000	1.0000	1.0000	1.0000	1.0000	0.9968	0.9999
38	0.9986	0.9974	0.9950	0.9979	0.9456	0.9997	0.9998	0.9767	0.9999
39	1.0000	0.9997	1.0000	1.0000	0.9997	0.9999	1.0000	0.9996	1.0000

40	1.0000	0.9998	1.0000	1.0000	1.0000	1.0000	1.0000	0.9999	1.0000
41	1.0000	1.0000	1.0000	0.9999	1.0000	0.9999	1.0000	0.9999	1.0000
42	1.0000	1.0000	0.9999	1.0000	1.0000	1.0000	0.9999	0.9976	1.0000
43	0.9999	0.9995	0.9921	0.9981	0.9369	0.9952	0.9996	0.9770	0.9997
44	1.0000	0.9996	1.0000	1.0000	0.9999	1.0000	1.0000	0.9996	1.0000
45	1.0000	0.9996	1.0000	1.0000	0.9999	1.0000	1.0000	0.9999	1.0000
46	1.0000	1.0000	0.9999	1.0000	0.9999	0.9999	1.0000	1.0000	1.0000
47	1.0000	1.0000	0.9999	1.0000	1.0000	1.0000	1.0000	0.9973	0.9999
48	0.9997	0.9985	0.9993	0.9991	0.9270	0.9976	0.9998	0.9800	1.0000
49	1.0000	0.9995	1.0000	1.0000	1.0000	0.9999	1.0000	0.9995	1.0000
50	1.0000	0.9998	1.0000	1.0000	0.9999	1.0000	1.0000	0.9999	1.0000
51	1.0000	1.0000	1.0000	0.9999	1.0000	1.0000	1.0000	1.0000	1.0000
52	1.0000	1.0000	1.0000	0.9999	1.0000	0.9999	1.0000	0.9979	1.0000
53	0.9990	0.9988	0.9961	0.9982	0.9591	0.9928	0.9999	0.9777	0.9999
54	1.0000	0.9994	1.0000	1.0000	0.9999	1.0000	1.0000	0.9995	1.0000
55	1.0000	0.9995	1.0000	1.0000	0.9999	1.0000	1.0000	1.0000	1.0000
56	1.0000	0.9999	1.0000	1.0000	1.0000	1.0000	1.0000	1.0000	1.0000
57	1.0000	0.9999	0.9999	0.9999	0.9999	1.0000	1.0000	0.9979	0.9999
58	0.9998	0.9992	0.9995	0.9993	0.9204	0.9998	0.9997	0.9737	0.9997
59	1.0000	0.9999	0.9999	1.0000	0.9999	0.9999	1.0000	0.9996	1.0000
60	1.0000	0.9998	1.0000	1.0000	1.0000	1.0000	1.0000	0.9999	1.0000
61	1.0000	1.0000	1.0000	1.0000	0.9999	0.9999	1.0000	0.9999	1.0000
62	1.0000	1.0000	1.0000	0.9999	1.0000	0.9999	1.0000	0.9982	0.9999
63	0.9978	0.9976	0.9987	0.9996	0.9484	0.9986	0.9993	0.9718	1.0000
64	1.0000	0.9998	0.9999	0.9999	0.9999	1.0000	1.0000	0.9995	1.0000
65	1.0000	0.9997	1.0000	1.0000	1.0000	1.0000	1.0000	0.9999	1.0000
66	1.0000	1.0000	1.0000	1.0000	1.0000	1.0000	1.0000	0.9999	1.0000
67	1.0000	1.0000	0.9999	0.9999	0.9999	1.0000	1.0000	0.9975	1.0000
68	0.9955	0.9967	0.9990	0.9976	0.9494	0.9996	0.9994	0.9710	0.9997
69	1.0000	0.9998	0.9999	1.0000	0.9997	0.9999	1.0000	0.9997	1.0000
70	1.0000	0.9998	1.0000	1.0000	0.9999	1.0000	1.0000	0.9999	1.0000
71	1.0000	1.0000	1.0000	0.9999	1.0000	1.0000	1.0000	1.0000	1.0000
72	1.0000	1.0000	1.0000	0.9999	0.9999	1.0000	1.0000	0.9980	0.9999
73	0.9987	0.9963	0.9986	0.9938	0.9710	0.9994	0.9998	0.9720	0.9999
74	1.0000	0.9995	0.9999	0.9999	0.9999	0.9999	1.0000	0.9995	1.0000
75	1.0000	0.9997	0.9999	1.0000	1.0000	1.0000	1.0000	0.9999	1.0000
76	1.0000	1.0000	1.0000	1.0000	1.0000	1.0000	1.0000	1.0000	1.0000
77	1.0000	1.0000	0.9999	0.9998	0.9999	0.9999	1.0000	0.9977	0.9999
78	0.9995	0.9993	0.9976	0.9995	0.9592	0.9994	0.9999	0.9694	1.0000
79	1.0000	0.9997	1.0000	1.0000	0.9999	0.9999	1.0000	0.9997	1.0000
80	1.0000	0.9998	1.0000	1.0000	1.0000	1.0000	1.0000	0.9999	1.0000
81	1.0000	0.9999	1.0000	0.9999	0.9999	1.0000	1.0000	1.0000	1.0000

82	1.0000	1.0000	1.0000	0.9999	1.0000	1.0000	1.0000	0.9988	0.9998
83	0.9998	0.9851	0.9953	0.9989	0.9560	0.9969	0.9995	0.9770	0.9999
84	1.0000	0.9997	1.0000	1.0000	0.9998	0.9999	1.0000	0.9993	1.0000
85	1.0000	0.9996	1.0000	1.0000	0.9999	1.0000	1.0000	0.9999	1.0000
86	1.0000	0.9999	1.0000	1.0000	1.0000	1.0000	1.0000	1.0000	1.0000
87	1.0000	1.0000	1.0000	0.9999	1.0000	1.0000	1.0000	0.9979	1.0000
88	0.9999	0.9946	0.9968	0.9987	0.9558	0.9981	0.9998	0.9693	1.0000
89	1.0000	0.9997	0.9999	0.9999	0.9997	1.0000	1.0000	0.9996	1.0000
90	1.0000	0.9998	1.0000	1.0000	1.0000	1.0000	1.0000	0.9999	1.0000

Turn to ground fault in phase B primary									
	Phase A			**Phase B**			**Phase C**		
Window No.	r_{A11}	r_{A12}	r_{A22}	r_{B11}	r_{B12}	r_{B22}	r_{C11}	r_{C12}	r_{C22}
1	1.0000	1.0000	1.0000	0.9999	1.0000	1.0000	1.0000	1.0000	1.0000
2	1.0000	0.9999	1.0000	0.9999	0.9999	1.0000	1.0000	1.0000	1.0000
3	0.9963	0.9969	0.9965	0.9963	0.9938	0.9900	0.9955	0.9962	0.9943
4	1.0000	0.9999	0.9999	1.0000	0.9998	0.9999	1.0000	0.9999	1.0000
5	1.0000	0.9998	1.0000	1.0000	0.9999	1.0000	1.0000	1.0000	1.0000
6	1.0000	1.0000	1.0000	1.0000	1.0000	1.0000	1.0000	1.0000	1.0000
7	1.0000	1.0000	1.0000	0.9662	0.9576	0.9997	1.0000	1.0000	1.0000
8	0.9979	0.9998	0.9974	0.6821	0.7628	0.9799	0.9900	0.9937	0.9933
9	1.0000	0.9999	0.9999	0.9989	0.9988	0.9999	0.9972	0.9985	1.0000
10	0.9971	0.9971	0.9999	1.0000	1.0000	0.9998	0.9993	0.9993	1.0000
11	0.9986	0.9988	1.0000	1.0000	0.9999	0.9998	0.9994	0.9994	1.0000
12	0.9980	0.9976	1.0000	0.9992	0.9993	0.9999	0.9890	0.9884	1.0000
13	0.6919	0.7534	0.9870	0.5586	0.5044	0.9862	0.5812	0.6158	0.9985
14	0.9912	0.9911	0.9999	1.0000	0.9996	1.0000	0.9986	0.9988	0.9999
15	0.9990	0.9996	1.0000	1.0000	0.9999	1.0000	0.9997	0.9996	1.0000
16	0.9995	0.9996	1.0000	1.0000	0.9999	0.9999	0.9993	0.9995	1.0000
17	0.9987	0.9984	1.0000	0.9611	0.9998	0.9994	0.9845	0.9843	1.0000
18	0.6619	0.7576	0.9920	0.0975	0.6596	0.9964	0.5920	0.6041	0.9995
19	0.9850	0.9863	1.0000	0.9987	1.0000	1.0000	0.9997	0.9994	1.0000
20	0.9931	0.9995	0.9999	1.0000	1.0000	1.0000	0.9999	0.9996	1.0000
21	0.9997	0.9996	1.0000	1.0000	1.0000	0.9998	1.0000	0.9996	1.0000
22	1.0000	0.9982	1.0000	1.0000	0.9995	0.9998	0.9993	0.9829	1.0000
23	0.9998	0.8206	0.9917	0.9818	0.6030	0.9955	0.9997	0.5673	0.9983
24	0.9991	0.9854	1.0000	1.0000	1.0000	0.9998	1.0000	0.9992	1.0000
25	1.0000	0.9996	1.0000	1.0000	0.9999	1.0000	1.0000	0.9997	1.0000
26	1.0000	0.9996	1.0000	1.0000	1.0000	0.9999	1.0000	0.9994	1.0000
27	1.0000	0.9984	1.0000	1.0000	0.9999	1.0000	0.9999	0.9865	1.0000
28	0.9999	0.7738	0.9989	0.9943	0.7100	0.9988	0.9992	0.5474	0.9937

29	0.9999	0.9848	1.0000	1.0000	1.0000	1.0000	1.0000	0.9993	1.0000
30	1.0000	0.9996	1.0000	1.0000	1.0000	1.0000	1.0000	0.9997	1.0000
31	1.0000	0.9995	1.0000	1.0000	1.0000	1.0000	1.0000	0.9993	1.0000
32	1.0000	0.9984	1.0000	1.0000	0.9998	0.9999	0.9995	0.9859	1.0000
33	0.9999	0.8035	0.9997	0.9947	0.5779	0.9900	0.9999	0.5527	0.9982
34	0.9999	0.9841	0.9999	1.0000	0.9999	1.0000	1.0000	0.9991	1.0000
35	1.0000	0.9994	1.0000	1.0000	1.0000	1.0000	1.0000	0.9996	1.0000
36	1.0000	0.9996	1.0000	1.0000	1.0000	1.0000	1.0000	0.9995	1.0000
37	1.0000	0.9984	1.0000	1.0000	0.9999	1.0000	0.9999	0.9844	1.0000
38	1.0000	0.8328	0.9952	0.9992	0.6786	0.9962	0.9996	0.5086	0.9994
39	1.0000	0.9844	1.0000	1.0000	1.0000	1.0000	1.0000	0.9991	1.0000
40	1.0000	0.9995	1.0000	1.0000	0.9999	0.9999	1.0000	0.9997	1.0000
41	1.0000	0.9997	1.0000	1.0000	1.0000	0.9998	1.0000	0.9994	1.0000
42	1.0000	0.9984	1.0000	1.0000	0.9999	1.0000	0.9999	0.9830	0.9999
43	1.0000	0.8298	0.9988	0.9986	0.6135	0.9982	0.9999	0.4978	0.9978
44	0.9989	0.9772	1.0000	1.0000	1.0000	1.0000	1.0000	0.9991	1.0000
45	1.0000	0.9993	1.0000	1.0000	0.9999	1.0000	1.0000	0.9997	1.0000
46	1.0000	0.9995	1.0000	1.0000	1.0000	1.0000	1.0000	0.9996	1.0000
47	1.0000	0.9985	1.0000	1.0000	0.9998	1.0000	0.9998	0.9864	1.0000
48	1.0000	0.8296	0.9995	0.9972	0.7184	0.9985	0.9999	0.4056	0.9935
49	0.9999	0.9848	1.0000	1.0000	1.0000	1.0000	1.0000	0.9986	1.0000
50	1.0000	0.9995	1.0000	1.0000	1.0000	0.9999	1.0000	0.9997	1.0000
51	1.0000	0.9997	1.0000	1.0000	0.9998	0.9999	1.0000	0.9993	1.0000
52	1.0000	0.9984	1.0000	1.0000	0.9999	1.0000	0.9999	0.9845	1.0000
53	1.0000	0.8282	0.9999	0.9997	0.6192	0.9990	0.9998	0.4277	0.9954
54	0.9999	0.9807	0.9999	1.0000	0.9998	0.9998	1.0000	0.9994	1.0000
55	1.0000	0.9996	0.9999	1.0000	1.0000	1.0000	1.0000	0.9997	1.0000
56	1.0000	0.9997	1.0000	1.0000	1.0000	1.0000	1.0000	0.9996	1.0000
57	1.0000	0.9985	1.0000	1.0000	0.9999	1.0000	1.0000	0.9866	1.0000
58	0.9999	0.8414	0.9993	0.9968	0.7440	0.9988	0.9998	0.4171	0.9997
59	0.9999	0.9827	1.0000	1.0000	0.9999	1.0000	1.0000	0.9991	1.0000
60	1.0000	0.9994	1.0000	1.0000	0.9998	0.9999	1.0000	0.9996	1.0000
61	1.0000	0.9997	1.0000	1.0000	1.0000	0.9998	1.0000	0.9994	1.0000
62	1.0000	0.9984	1.0000	1.0000	0.9996	0.9996	0.9998	0.9881	1.0000
63	0.9999	0.8709	0.9963	0.9952	0.6825	0.9973	1.0000	0.3732	0.9980
64	0.9997	0.9754	1.0000	1.0000	0.9998	1.0000	1.0000	0.9991	0.9999
65	1.0000	0.9991	1.0000	1.0000	1.0000	1.0000	1.0000	0.9997	1.0000
66	1.0000	0.9995	1.0000	1.0000	1.0000	0.9999	1.0000	0.9995	1.0000
67	1.0000	0.9985	1.0000	1.0000	0.9999	0.9999	0.9999	0.9871	1.0000
68	1.0000	0.8521	0.9996	0.9965	0.7835	0.9994	0.9998	0.3442	0.9976
69	0.9998	0.9803	1.0000	1.0000	0.9999	1.0000	1.0000	0.9991	1.0000
70	1.0000	0.9995	1.0000	1.0000	1.0000	0.9999	1.0000	0.9996	1.0000

71	1.0000	0.9996	1.0000	1.0000	1.0000	1.0000	1.0000	0.9995	1.0000
72	1.0000	0.9982	1.0000	1.0000	0.9996	0.9998	0.9999	0.9875	1.0000
73	0.9999	0.8738	0.9998	0.9928	0.6796	0.9903	0.9999	0.3845	0.9991
74	0.9997	0.9799	1.0000	1.0000	0.9999	0.9999	1.0000	0.9991	1.0000
75	1.0000	0.9994	1.0000	1.0000	0.9999	1.0000	1.0000	0.9997	1.0000
76	1.0000	0.9997	1.0000	1.0000	1.0000	0.9999	1.0000	0.9994	1.0000
77	1.0000	0.9983	1.0000	1.0000	1.0000	0.9999	0.9999	0.9884	1.0000
78	1.0000	0.8648	0.9996	0.9996	0.7678	0.9987	0.9998	0.3282	0.9987
79	0.9999	0.9805	1.0000	1.0000	0.9999	1.0000	1.0000	0.9990	1.0000
80	1.0000	0.9993	1.0000	1.0000	1.0000	1.0000	1.0000	0.9997	1.0000
81	1.0000	0.9995	1.0000	1.0000	0.9999	0.9999	1.0000	0.9995	1.0000
82	1.0000	0.9982	1.0000	1.0000	0.9996	0.9999	0.9998	0.9861	1.0000
83	1.0000	0.8723	0.9998	0.9973	0.6926	0.9980	0.9999	0.2681	0.9913
84	0.9995	0.9748	1.0000	1.0000	1.0000	1.0000	1.0000	0.9990	1.0000
85	1.0000	0.9994	1.0000	1.0000	0.9999	1.0000	1.0000	0.9996	1.0000
86	1.0000	0.9996	1.0000	1.0000	1.0000	1.0000	1.0000	0.9996	1.0000
87	1.0000	0.9982	1.0000	1.0000	0.9999	1.0000	1.0000	0.9883	1.0000
88	1.0000	0.8902	0.9982	0.9963	0.8050	0.9996	1.0000	0.2860	0.9981
89	0.9993	0.9768	0.9999	1.0000	1.0000	1.0000	1.0000	0.9992	1.0000
90	1.0000	0.9994	1.0000	1.0000	1.0000	1.0000	1.0000	0.9997	1.0000

Turn to ground fault in phase B secondary									
	Phase A			**Phase B**			**Phase C**		
Window No.	r_{A11}	r_{A12}	r_{A22}	r_{B11}	r_{B12}	r_{B22}	r_{C11}	r_{C12}	r_{C22}
1	1.0000	1.0000	1.0000	1.0000	1.0000	1.0000	1.0000	1.0000	1.0000
2	1.0000	1.0000	1.0000	1.0000	0.9999	1.0000	1.0000	1.0000	1.0000
3	0.9998	0.9954	0.9982	0.9979	0.9954	0.9757	0.9993	0.9992	0.9996
4	1.0000	1.0000	1.0000	1.0000	0.9999	0.9999	0.9999	0.9999	1.0000
5	1.0000	1.0000	1.0000	1.0000	0.9999	1.0000	1.0000	1.0000	1.0000
6	1.0000	1.0000	1.0000	1.0000	1.0000	0.9999	1.0000	1.0000	1.0000
7	1.0000	1.0000	1.0000	0.9999	0.9999	0.9998	1.0000	1.0000	1.0000
8	0.9995	0.9997	0.9999	0.8628	0.1793	0.7670	0.9982	0.9890	0.9994
9	1.0000	1.0000	0.9999	0.9981	0.9934	0.9990	1.0000	0.9999	1.0000
10	1.0000	1.0000	1.0000	1.0000	0.9998	0.9999	1.0000	0.9999	0.9999
11	1.0000	1.0000	1.0000	1.0000	1.0000	1.0000	0.9999	0.9998	0.9993
12	0.9999	0.9995	0.9991	0.9998	0.9999	0.9997	0.9999	0.9998	0.9991
13	0.7040	0.8256	0.2705	0.9544	0.9855	0.8587	0.7472	0.8697	0.2939
14	0.9999	0.9997	0.9997	0.9998	0.9999	0.9999	0.9999	1.0000	0.9997
15	1.0000	1.0000	0.9999	0.9998	0.9998	1.0000	1.0000	0.9999	0.9998
16	0.9999	1.0000	0.9998	0.9999	1.0000	0.9998	0.9999	0.9999	0.9996
17	0.9994	0.9979	0.9954	1.0000	0.9999	0.9998	0.9996	0.9999	0.9993

18	0.2333	0.9223	-0.1654	0.9759	0.9929	0.4604	0.7136	0.8808	0.1560
19	0.9998	0.9997	0.9994	0.9995	0.9997	0.9981	0.9998	1.0000	0.9992
20	1.0000	1.0000	0.9999	0.9999	0.9999	0.9998	0.9999	0.9999	0.9998
21	0.9999	1.0000	0.9997	1.0000	0.9999	0.9997	1.0000	1.0000	1.0000
22	0.9997	0.9983	0.9985	0.9999	0.9999	0.9995	1.0000	0.9998	1.0000
23	0.8537	0.9095	0.9299	0.9967	0.9731	0.9523	0.9796	0.8903	0.9871
24	1.0000	0.9996	0.9999	0.9999	0.9997	1.0000	1.0000	0.9998	0.9997
25	1.0000	1.0000	1.0000	1.0000	0.9998	1.0000	1.0000	0.9999	1.0000
26	1.0000	1.0000	1.0000	1.0000	0.9999	0.9999	1.0000	1.0000	1.0000
27	1.0000	0.9983	1.0000	1.0000	0.9999	0.9998	1.0000	0.9999	1.0000
28	0.9995	0.9186	0.9999	0.9998	0.9970	0.9976	0.9981	0.9071	0.9999
29	1.0000	0.9996	1.0000	1.0000	0.9999	0.9999	1.0000	1.0000	1.0000
30	1.0000	1.0000	1.0000	1.0000	0.9999	1.0000	1.0000	0.9999	1.0000
31	1.0000	1.0000	1.0000	1.0000	1.0000	0.9999	1.0000	1.0000	1.0000
32	1.0000	0.9977	1.0000	0.9999	0.9999	0.9998	1.0000	0.9999	1.0000
33	0.9994	0.9018	0.9999	0.9993	0.9844	0.9963	0.9974	0.9061	0.9994
34	1.0000	0.9997	1.0000	1.0000	0.9995	1.0000	1.0000	0.9999	1.0000
35	1.0000	1.0000	1.0000	1.0000	0.9999	1.0000	1.0000	0.9999	1.0000
36	1.0000	1.0000	1.0000	1.0000	1.0000	0.9999	1.0000	0.9999	1.0000
37	1.0000	0.9986	1.0000	1.0000	0.9998	0.9996	1.0000	0.9999	1.0000
38	0.9994	0.9152	0.9999	0.9989	0.9642	0.9858	0.9994	0.9080	0.9998
39	1.0000	0.9999	1.0000	1.0000	0.9998	0.9999	1.0000	0.9999	1.0000
40	0.9999	1.0000	1.0000	1.0000	0.9998	1.0000	1.0000	0.9999	1.0000
41	1.0000	1.0000	1.0000	1.0000	1.0000	0.9999	1.0000	1.0000	1.0000
42	1.0000	0.9979	1.0000	0.9999	0.9998	0.9999	1.0000	0.9999	1.0000
43	0.9997	0.9058	0.9999	0.9935	0.9946	0.9811	0.9997	0.9138	0.9999
44	1.0000	0.9998	1.0000	0.9999	0.9993	1.0000	1.0000	0.9999	1.0000
45	1.0000	1.0000	1.0000	1.0000	0.9999	1.0000	1.0000	0.9999	1.0000
46	1.0000	1.0000	1.0000	1.0000	1.0000	0.9999	1.0000	0.9999	1.0000
47	1.0000	0.9985	1.0000	0.9999	0.9999	0.9998	1.0000	0.9999	1.0000
48	0.9986	0.9312	0.9998	0.9997	0.9879	0.9897	0.9990	0.9150	0.9998
49	1.0000	0.9997	1.0000	1.0000	0.9999	0.9999	1.0000	0.9999	1.0000
50	1.0000	1.0000	1.0000	0.9999	0.9998	0.9998	1.0000	0.9999	1.0000
51	1.0000	1.0000	1.0000	1.0000	1.0000	0.9999	1.0000	0.9999	1.0000
52	1.0000	0.9984	1.0000	1.0000	0.9998	0.9993	1.0000	1.0000	1.0000
53	0.9996	0.9073	1.0000	0.9990	0.9959	0.9978	0.9990	0.9161	0.9997
54	1.0000	0.9997	1.0000	1.0000	0.9996	1.0000	1.0000	1.0000	1.0000
55	1.0000	1.0000	1.0000	1.0000	0.9999	1.0000	1.0000	0.9999	1.0000
56	1.0000	1.0000	1.0000	1.0000	1.0000	0.9999	1.0000	1.0000	1.0000
57	1.0000	0.9987	0.9999	0.9999	0.9999	0.9999	1.0000	0.9999	1.0000
58	0.9992	0.9252	0.9997	0.9955	0.9772	0.9982	0.9997	0.9177	0.9999
59	1.0000	0.9998	1.0000	1.0000	0.9999	0.9999	1.0000	0.9999	1.0000

60	1.0000	1.0000	1.0000	1.0000	0.9999	0.9999	1.0000	0.9999	1.0000
61	1.0000	0.9999	1.0000	1.0000	0.9999	0.9998	1.0000	0.9999	1.0000
62	1.0000	0.9978	1.0000	0.9999	1.0000	0.9993	1.0000	0.9999	1.0000
63	0.9963	0.8744	0.9999	0.9981	0.9965	0.9991	0.9990	0.9197	0.9998
64	1.0000	0.9997	1.0000	1.0000	0.9993	0.9999	1.0000	0.9999	0.9999
65	1.0000	1.0000	1.0000	1.0000	0.9999	1.0000	1.0000	0.9999	1.0000
66	1.0000	1.0000	1.0000	1.0000	0.9999	0.9999	1.0000	1.0000	1.0000
67	1.0000	0.9984	1.0000	0.9999	0.9999	0.9999	1.0000	0.9999	1.0000
68	0.9983	0.9018	0.9999	0.9980	0.9909	0.9988	0.9995	0.9276	1.0000
69	1.0000	0.9998	1.0000	1.0000	0.9997	0.9998	1.0000	1.0000	1.0000
70	1.0000	1.0000	1.0000	1.0000	0.9999	1.0000	1.0000	0.9999	1.0000
71	1.0000	1.0000	1.0000	1.0000	0.9999	0.9999	1.0000	0.9999	1.0000
72	0.9999	0.9988	1.0000	0.9999	0.9998	0.9999	1.0000	0.9999	1.0000
73	0.9991	0.8601	0.9998	0.9971	0.9944	0.9977	0.9991	0.9285	0.9999
74	0.9999	0.9999	1.0000	1.0000	0.9996	0.9998	1.0000	0.9999	1.0000
75	1.0000	1.0000	1.0000	1.0000	0.9999	1.0000	1.0000	0.9999	1.0000
76	1.0000	1.0000	1.0000	1.0000	0.9999	0.9997	1.0000	1.0000	1.0000
77	1.0000	0.9986	1.0000	0.9998	0.9999	0.9999	1.0000	0.9999	1.0000
78	0.9998	0.9111	0.9997	0.9962	0.9732	0.9967	0.9993	0.9335	0.9997
79	1.0000	0.9996	1.0000	1.0000	0.9999	0.9999	1.0000	0.9999	1.0000
80	1.0000	1.0000	1.0000	1.0000	0.9998	0.9999	1.0000	0.9999	1.0000
81	1.0000	1.0000	1.0000	1.0000	1.0000	0.9999	1.0000	0.9999	1.0000
82	1.0000	0.9982	1.0000	0.9999	0.9998	0.9999	1.0000	0.9999	1.0000
83	0.9994	0.8563	0.9998	0.9990	0.9935	0.9948	0.9993	0.9364	0.9999
84	0.9999	0.9996	1.0000	1.0000	0.9997	0.9999	1.0000	0.9998	1.0000
85	1.0000	1.0000	1.0000	1.0000	1.0000	0.9999	1.0000	0.9999	1.0000
86	1.0000	1.0000	1.0000	1.0000	1.0000	0.9999	1.0000	1.0000	1.0000
87	1.0000	0.9988	1.0000	1.0000	1.0000	0.9999	1.0000	0.9999	1.0000
88	0.9979	0.8791	0.9999	0.9979	0.9876	0.9913	0.9998	0.9291	0.9997
89	1.0000	0.9997	1.0000	1.0000	0.9997	0.9999	1.0000	0.9999	1.0000
90	1.0000	1.0000	1.0000	1.0000	0.9998	0.9998	1.0000	0.9999	1.0000

Turn to ground fault in phase C primary									
	Phase A			**Phase B**			**Phase C**		
Window No.	r_{A11}	r_{A12}	r_{A22}	r_{B11}	r_{B12}	r_{B22}	r_{C11}	r_{C12}	r_{C22}
1	1.0000	1.0000	1.0000	1.0000	0.9999	0.9999	1.0000	1.0000	1.0000
2	1.0000	0.9999	1.0000	0.9994	0.9999	0.9999	1.0000	1.0000	1.0000
3	0.9976	0.9805	0.9982	0.9969	0.9719	0.9881	0.9956	0.9994	0.9982
4	1.0000	0.9998	1.0000	0.9999	0.9999	0.9999	1.0000	0.9999	1.0000
5	1.0000	1.0000	1.0000	1.0000	1.0000	1.0000	1.0000	1.0000	1.0000
6	1.0000	1.0000	1.0000	0.9983	0.9987	1.0000	1.0000	1.0000	1.0000

7	1.0000	0.9999	1.0000	0.9975	0.9975	0.9997	1.0000	1.0000	1.0000
8	0.9993	0.9797	0.9967	0.3835	0.1487	0.9964	-0.3808	-0.5247	0.9671
9	1.0000	0.9998	1.0000	0.9941	0.9943	1.0000	0.9939	0.9930	1.0000
10	0.9993	0.9993	0.9999	0.9994	0.9990	0.9999	0.9999	0.9999	1.0000
11	0.9994	0.9995	1.0000	0.9996	0.9993	1.0000	1.0000	1.0000	1.0000
12	0.9953	0.9969	1.0000	0.9974	0.9986	0.9998	0.9994	0.9991	1.0000
13	-0.0231	0.1573	0.9995	0.2172	0.0124	0.9951	0.8010	0.5716	0.9403
14	0.9982	0.9993	1.0000	0.9818	0.9813	1.0000	0.9998	0.9999	1.0000
15	0.9997	0.9995	1.0000	0.9989	0.9987	1.0000	0.9999	0.9999	1.0000
16	0.9995	0.9997	1.0000	0.9969	0.9997	1.0000	1.0000	1.0000	1.0000
17	0.9926	0.9942	0.9999	0.9999	0.9971	0.9997	0.9997	0.9993	1.0000
18	-0.1878	0.0747	0.9977	0.9950	0.1232	0.9971	-0.7750	0.6718	0.8839
19	0.9977	0.9986	0.9999	0.9977	0.9848	1.0000	0.9923	1.0000	1.0000
20	0.9999	0.9994	1.0000	1.0000	0.9988	0.9999	0.9997	0.9999	1.0000
21	1.0000	0.9998	1.0000	1.0000	0.9991	1.0000	1.0000	1.0000	1.0000
22	0.9991	0.9922	1.0000	0.9999	0.9976	1.0000	1.0000	0.9991	1.0000
23	0.9970	0.0291	0.9981	0.9998	0.1606	0.9852	0.9911	0.6714	0.9997
24	1.0000	0.9991	1.0000	0.9993	0.9869	1.0000	1.0000	0.9999	1.0000
25	1.0000	0.9996	1.0000	1.0000	0.9989	1.0000	1.0000	1.0000	1.0000
26	1.0000	0.9995	1.0000	1.0000	0.9994	1.0000	1.0000	1.0000	1.0000
27	1.0000	0.9933	1.0000	1.0000	0.9978	0.9999	1.0000	0.9994	1.0000
28	0.9999	0.0628	0.9999	0.9999	0.1492	0.9988	0.9999	0.6669	0.9997
29	1.0000	0.9992	1.0000	0.9998	0.9847	0.9999	1.0000	1.0000	1.0000
30	1.0000	0.9993	1.0000	1.0000	0.9989	0.9999	1.0000	0.9999	1.0000
31	1.0000	0.9996	1.0000	1.0000	0.9998	0.9998	1.0000	1.0000	1.0000
32	0.9999	0.9941	1.0000	0.9999	0.9987	0.9999	1.0000	0.9990	1.0000
33	0.9998	0.0276	0.9997	0.9998	0.1262	0.9946	0.9999	0.7014	0.9982
34	1.0000	0.9985	0.9999	0.9999	0.9869	1.0000	1.0000	0.9999	1.0000
35	1.0000	0.9996	1.0000	0.9999	0.9988	1.0000	1.0000	0.9999	1.0000
36	1.0000	0.9997	1.0000	1.0000	0.9991	1.0000	1.0000	1.0000	1.0000
37	0.9999	0.9933	1.0000	0.9999	0.9975	0.9999	1.0000	0.9991	1.0000
38	0.9999	0.0632	0.9995	0.9997	0.1455	0.9995	0.9999	0.7468	0.9931
39	1.0000	0.9990	1.0000	0.9998	0.9845	1.0000	1.0000	0.9999	1.0000
40	1.0000	0.9994	1.0000	0.9999	0.9993	1.0000	1.0000	1.0000	1.0000
41	1.0000	0.9996	1.0000	1.0000	0.9994	0.9999	1.0000	1.0000	1.0000
42	0.9999	0.9937	1.0000	0.9999	0.9982	0.9999	1.0000	0.9992	1.0000
43	0.9997	-0.0011	0.9986	0.9997	0.1254	0.9973	0.9998	0.7070	0.9989
44	1.0000	0.9988	0.9999	0.9998	0.9868	1.0000	1.0000	0.9998	1.0000
45	1.0000	0.9995	1.0000	1.0000	0.9987	1.0000	1.0000	0.9999	1.0000
46	0.9999	0.9993	1.0000	1.0000	0.9993	1.0000	1.0000	1.0000	1.0000
47	0.9999	0.9938	1.0000	1.0000	0.9971	0.9999	1.0000	0.9994	1.0000
48	1.0000	0.0030	0.9978	0.9999	0.0962	0.9983	0.9997	0.7021	0.9957

49	1.0000	0.9985	1.0000	0.9999	0.9866	0.9999	1.0000	0.9999	1.0000
50	1.0000	0.9993	1.0000	0.9999	0.9987	1.0000	1.0000	1.0000	1.0000
51	1.0000	0.9993	1.0000	1.0000	0.9994	1.0000	1.0000	1.0000	1.0000
52	0.9999	0.9938	1.0000	1.0000	0.9978	0.9999	1.0000	0.9989	0.9999
53	0.9998	0.0808	0.9974	0.9984	0.1383	0.9979	0.9996	0.6237	0.9899
54	1.0000	0.9989	1.0000	0.9998	0.9847	1.0000	1.0000	0.9999	1.0000
55	1.0000	0.9994	1.0000	1.0000	0.9990	1.0000	1.0000	1.0000	1.0000
56	0.9999	0.9996	1.0000	1.0000	0.9989	0.9999	1.0000	1.0000	1.0000
57	0.9999	0.9931	1.0000	1.0000	0.9976	0.9999	1.0000	0.9995	1.0000
58	1.0000	0.0799	0.9965	0.9999	0.1670	0.9963	0.9999	0.5894	0.9892
59	1.0000	0.9989	1.0000	1.0000	0.9852	1.0000	1.0000	0.9999	1.0000
60	1.0000	0.9995	1.0000	0.9999	0.9989	1.0000	1.0000	1.0000	1.0000
61	1.0000	0.9996	1.0000	1.0000	0.9998	0.9999	1.0000	1.0000	1.0000
62	1.0000	0.9932	1.0000	1.0000	0.9981	0.9999	1.0000	0.9993	0.9999
63	0.9999	0.0307	0.9984	0.9986	0.2321	0.9890	0.9999	0.6727	0.9983
64	1.0000	0.9987	1.0000	0.9998	0.9871	1.0000	1.0000	0.9999	1.0000
65	1.0000	0.9996	1.0000	1.0000	0.9990	1.0000	1.0000	0.9999	1.0000
66	1.0000	0.9997	1.0000	1.0000	0.9994	0.9999	1.0000	1.0000	1.0000
67	1.0000	0.9925	1.0000	1.0000	0.9978	0.9999	1.0000	0.9993	1.0000
68	0.9999	0.0199	0.9976	1.0000	0.1514	0.9989	0.9999	0.6146	0.9995
69	1.0000	0.9986	1.0000	0.9998	0.9874	1.0000	1.0000	1.0000	1.0000
70	1.0000	0.9995	1.0000	0.9999	0.9994	0.9999	1.0000	0.9999	1.0000
71	1.0000	0.9997	1.0000	0.9999	0.9993	1.0000	1.0000	1.0000	1.0000
72	1.0000	0.9940	1.0000	1.0000	0.9964	0.9997	1.0000	0.9993	1.0000
73	0.9998	-0.0014	0.9992	0.9998	0.0103	0.9707	0.9998	0.6419	0.9993
74	1.0000	0.9989	1.0000	0.9999	0.9880	1.0000	1.0000	1.0000	1.0000
75	1.0000	0.9995	1.0000	1.0000	0.9985	0.9999	1.0000	0.9999	1.0000
76	1.0000	0.9998	1.0000	1.0000	0.9992	1.0000	1.0000	1.0000	1.0000
77	0.9999	0.9923	1.0000	1.0000	0.9976	1.0000	1.0000	0.9994	1.0000
78	1.0000	-0.0404	0.9967	0.9999	0.2291	0.9965	0.9999	0.6105	0.9996
79	1.0000	0.9984	1.0000	0.9999	0.9863	1.0000	1.0000	0.9999	1.0000
80	1.0000	0.9997	1.0000	1.0000	0.9989	1.0000	1.0000	1.0000	1.0000
81	1.0000	0.9996	1.0000	0.9999	0.9996	0.9999	1.0000	1.0000	1.0000
82	0.9999	0.9946	1.0000	0.9999	0.9980	0.9998	1.0000	0.9996	1.0000
83	0.9998	0.0364	0.9991	0.9997	0.3026	0.9578	0.9999	0.6072	0.9984
84	1.0000	0.9988	1.0000	0.9995	0.9826	1.0000	1.0000	1.0000	1.0000
85	1.0000	0.9995	1.0000	0.9999	0.9984	0.9999	1.0000	0.9999	1.0000
86	1.0000	0.9995	1.0000	1.0000	0.9994	1.0000	1.0000	1.0000	1.0000
87	0.9999	0.9921	0.9999	0.9999	0.9980	0.9999	1.0000	0.9994	1.0000
88	0.9998	0.0152	0.9981	0.9997	0.2686	0.9960	0.9998	0.6048	0.9993
89	1.0000	0.9988	1.0000	0.9999	0.9854	1.0000	1.0000	1.0000	1.0000
90	1.0000	0.9994	1.0000	1.0000	0.9990	1.0000	1.0000	1.0000	1.0000

Turn to ground fault in phase C secondary									
	Phase A			**Phase B**			**Phase C**		
Window No.	r_{A11}	r_{A12}	r_{A22}	r_{B11}	r_{B12}	r_{B22}	r_{C11}	r_{C12}	r_{C22}
1	1.0000	1.0000	1.0000	0.9999	0.9999	0.9997	1.0000	1.0000	1.0000
2	1.0000	0.9999	1.0000	0.9993	0.9993	0.9997	0.9999	0.9999	1.0000
3	0.9989	0.9253	0.9971	0.9975	0.9015	0.9950	0.9990	0.9965	0.9974
4	0.9999	0.9999	0.9998	0.9999	0.9997	1.0000	1.0000	1.0000	1.0000
5	1.0000	1.0000	1.0000	0.9999	0.9999	0.9997	1.0000	1.0000	1.0000
6	1.0000	1.0000	1.0000	0.9999	0.9998	0.9998	1.0000	1.0000	1.0000
7	1.0000	0.9998	1.0000	0.9994	0.9999	0.9998	1.0000	0.9999	1.0000
8	0.9987	0.9144	0.9942	0.9945	0.9620	0.9970	0.9971	0.9779	0.9935
9	0.9999	0.9997	0.9998	1.0000	1.0000	0.9999	1.0000	0.9996	0.9999
10	1.0000	0.9999	0.9999	0.9999	0.9999	0.9999	1.0000	1.0000	1.0000
11	1.0000	1.0000	1.0000	0.9998	0.9998	0.9995	1.0000	1.0000	1.0000
12	1.0000	0.9999	1.0000	0.9985	0.9970	0.9959	0.9999	0.9997	0.9997
13	0.9994	0.8991	0.9984	0.5797	0.9744	0.7374	0.3017	-0.6167	0.4977
14	0.9996	0.9988	0.9977	0.9998	0.9993	0.9997	0.9988	0.9968	0.9997
15	0.9999	0.9992	0.9989	0.9999	0.9997	0.9997	1.0000	1.0000	1.0000
16	0.9997	1.0000	0.9994	0.9999	0.9999	0.9996	1.0000	1.0000	1.0000
17	0.9998	1.0000	0.9991	0.9971	0.9939	0.9851	1.0000	0.9999	1.0000
18	0.8393	0.9787	0.3757	0.5572	0.9682	0.5735	0.9976	0.7712	0.8701
19	1.0000	0.9999	0.9992	1.0000	0.9996	0.9997	0.9999	0.9997	0.9998
20	1.0000	0.9996	0.9996	1.0000	0.9997	0.9997	0.9999	0.9998	1.0000
21	0.9999	1.0000	0.9997	0.9995	0.9994	0.9972	1.0000	1.0000	1.0000
22	0.9998	1.0000	0.9994	0.9993	0.9942	0.9981	1.0000	0.9999	0.9998
23	0.9141	0.9441	0.3581	0.9786	0.9873	0.9908	0.3762	0.9266	0.1372
24	0.9995	0.9995	0.9950	0.9998	0.9994	0.9998	0.9996	0.9996	0.9995
25	1.0000	0.9998	0.9997	0.9999	0.9996	0.9999	1.0000	0.9997	0.9999
26	1.0000	1.0000	0.9999	0.9999	0.9995	0.9999	1.0000	0.9999	0.9999
27	1.0000	1.0000	1.0000	0.9998	0.9966	0.9989	1.0000	0.9997	1.0000
28	0.9961	0.9478	0.9978	0.9980	0.9791	0.9998	0.9951	0.9775	0.9227
29	1.0000	0.9997	0.9999	1.0000	0.9994	1.0000	1.0000	0.9994	0.9999
30	1.0000	0.9998	1.0000	0.9999	0.9999	0.9998	1.0000	0.9997	1.0000
31	1.0000	1.0000	1.0000	0.9999	0.9999	0.9997	1.0000	0.9999	1.0000
32	1.0000	1.0000	1.0000	0.9995	0.9915	0.9995	0.9999	0.9998	0.9999
33	0.9995	0.9583	0.9996	0.9991	0.9809	0.9995	0.9954	0.9480	0.9904
34	0.9999	0.9999	0.9999	0.9999	0.9994	0.9999	1.0000	0.9999	0.9998
35	1.0000	0.9998	1.0000	0.9999	0.9993	0.9999	1.0000	0.9998	0.9999
36	1.0000	0.9999	1.0000	0.9997	0.9995	0.9997	1.0000	0.9999	1.0000
37	1.0000	1.0000	1.0000	0.9990	0.9951	0.9996	1.0000	0.9999	0.9996
38	0.9990	0.9580	0.9977	0.9981	0.9689	0.9998	0.9998	0.9570	0.9937

39	0.9999	0.9998	0.9999	1.0000	0.9997	1.0000	1.0000	0.9995	1.0000
40	1.0000	0.9997	1.0000	1.0000	1.0000	1.0000	1.0000	0.9996	1.0000
41	1.0000	1.0000	1.0000	0.9999	0.9996	0.9999	1.0000	1.0000	1.0000
42	1.0000	1.0000	1.0000	0.9995	0.9915	0.9994	1.0000	0.9998	1.0000
43	0.9933	0.9361	0.9987	0.9997	0.9799	0.9995	0.9988	0.9738	0.9948
44	0.9999	0.9999	0.9999	1.0000	0.9995	0.9999	1.0000	0.9998	0.9998
45	1.0000	0.9999	0.9999	0.9998	1.0000	0.9998	1.0000	0.9995	0.9999
46	1.0000	1.0000	1.0000	0.9994	0.9998	0.9997	1.0000	1.0000	1.0000
47	1.0000	1.0000	1.0000	0.9999	0.9953	0.9995	1.0000	0.9996	0.9996
48	0.9933	0.9409	0.9981	0.9981	0.9756	0.9995	0.9905	0.9893	0.9591
49	1.0000	0.9999	0.9999	1.0000	0.9997	1.0000	1.0000	0.9993	0.9999
50	1.0000	0.9997	1.0000	0.9999	0.9998	0.9999	1.0000	0.9997	1.0000
51	1.0000	1.0000	1.0000	0.9998	0.9995	0.9997	1.0000	0.9999	1.0000
52	1.0000	1.0000	1.0000	0.9997	0.9907	0.9995	1.0000	1.0000	0.9999
53	0.9991	0.9378	0.9992	0.9980	0.9852	0.9997	0.9889	0.9574	0.9941
54	0.9999	1.0000	1.0000	0.9999	0.9990	0.9999	1.0000	0.9997	0.9999
55	1.0000	0.9998	1.0000	0.9999	0.9999	0.9999	1.0000	0.9995	1.0000
56	1.0000	0.9999	1.0000	0.9999	0.9997	1.0000	1.0000	1.0000	1.0000
57	1.0000	1.0000	1.0000	0.9996	0.9911	0.9976	1.0000	0.9997	1.0000
58	0.9985	0.9148	0.9992	0.9991	0.9694	0.9999	0.9997	0.9812	0.9975
59	0.9999	1.0000	1.0000	1.0000	0.9999	1.0000	1.0000	0.9998	0.9999
60	1.0000	0.9998	1.0000	0.9999	1.0000	1.0000	1.0000	0.9997	1.0000
61	1.0000	0.9999	1.0000	0.9999	0.9998	0.9999	1.0000	0.9999	1.0000
62	1.0000	1.0000	1.0000	0.9998	0.9924	0.9990	1.0000	0.9997	0.9998
63	0.9981	0.9337	0.9992	0.9988	0.9888	0.9997	0.9979	0.9606	0.9958
64	0.9999	0.9996	0.9999	0.9999	0.9996	0.9999	1.0000	0.9998	0.9999
65	1.0000	0.9997	1.0000	0.9999	0.9999	1.0000	1.0000	0.9999	0.9999
66	1.0000	1.0000	1.0000	0.9999	0.9999	0.9998	1.0000	0.9999	1.0000
67	1.0000	1.0000	1.0000	0.9999	0.9918	0.9995	1.0000	0.9999	1.0000
68	0.9982	0.9400	0.9960	0.9951	0.9886	0.9998	0.9804	0.9707	0.9868
69	1.0000	0.9998	0.9999	1.0000	0.9997	1.0000	0.9999	0.9996	0.9999
70	1.0000	0.9998	1.0000	0.9999	1.0000	1.0000	1.0000	0.9996	1.0000
71	1.0000	1.0000	1.0000	0.9999	0.9995	0.9999	1.0000	0.9999	1.0000
72	1.0000	1.0000	1.0000	0.9997	0.9921	0.9993	1.0000	0.9999	0.9996
73	0.9990	0.9256	0.9999	0.9982	0.9816	0.9997	0.9968	0.9824	0.9829
74	1.0000	0.9999	0.9998	0.9999	0.9998	0.9999	1.0000	0.9998	0.9999
75	1.0000	0.9998	1.0000	0.9999	0.9997	1.0000	1.0000	0.9997	1.0000
76	1.0000	1.0000	1.0000	0.9999	0.9999	1.0000	1.0000	1.0000	1.0000
77	1.0000	1.0000	1.0000	0.9996	0.9967	0.9983	1.0000	0.9999	0.9999
78	0.9989	0.9235	0.9973	0.9999	0.9878	1.0000	0.9997	0.9841	0.9958
79	1.0000	0.9999	0.9999	1.0000	0.9996	1.0000	1.0000	0.9998	1.0000
80	1.0000	0.9998	1.0000	0.9998	0.9999	0.9998	1.0000	0.9998	1.0000

81	1.0000	1.0000	1.0000	0.9998	0.9998	0.9998	1.0000	1.0000	1.0000
82	1.0000	1.0000	1.0000	0.9997	0.9952	0.9987	1.0000	0.9999	0.9998
83	0.9988	0.9404	0.9992	0.9995	0.9824	0.9998	0.9980	0.9819	0.9979
84	1.0000	0.9997	1.0000	0.9999	0.9997	0.9999	1.0000	0.9998	1.0000
85	1.0000	0.9998	1.0000	1.0000	0.9998	0.9999	1.0000	0.9997	1.0000
86	1.0000	0.9999	1.0000	0.9999	0.9996	0.9996	1.0000	1.0000	1.0000
87	0.9999	1.0000	1.0000	0.9995	0.9922	0.9980	1.0000	0.9996	0.9998
88	0.9971	0.9201	0.9979	0.9998	0.9854	0.9998	0.9990	0.9531	0.9903
89	0.9999	1.0000	0.9998	1.0000	0.9997	1.0000	1.0000	0.9998	0.9999
90	1.0000	0.9998	1.0000	0.9997	0.9997	0.9999	1.0000	0.9997	1.0000

Single phase to ground fault in phase A Primary									
	Phase A			**Phase B**			**Phase C**		
Window No.	r_{A11}	r_{A12}	r_{A22}	r_{B11}	r_{B12}	r_{B22}	r_{C11}	r_{C12}	r_{C22}
1	1.0000	1.0000	1.0000	1.0000	1.0000	1.0000	1.0000	1.0000	1.0000
2	1.0000	0.9999	1.0000	1.0000	0.9998	0.9999	1.0000	1.0000	1.0000
3	0.9825	0.9179	0.9912	0.9682	0.9541	0.9664	0.9979	0.9978	0.9978
4	1.0000	0.9999	1.0000	1.0000	1.0000	0.9999	1.0000	0.9997	0.9997
5	1.0000	1.0000	1.0000	1.0000	1.0000	1.0000	1.0000	1.0000	1.0000
6	1.0000	1.0000	1.0000	1.0000	0.9999	0.9997	1.0000	1.0000	1.0000
7	1.0000	0.9999	1.0000	0.9999	0.9997	0.9998	1.0000	1.0000	1.0000
8	0.9910	0.9080	0.9945	0.9947	0.9170	0.9846	0.9893	0.9997	0.9997
9	1.0000	0.9998	0.9999	1.0000	0.9999	1.0000	1.0000	0.9999	0.9999
10	1.0000	1.0000	1.0000	1.0000	0.9999	0.9999	1.0000	1.0000	1.0000
11	1.0000	1.0000	1.0000	1.0000	0.9999	0.9999	1.0000	1.0000	1.0000
12	1.0000	0.9997	1.0000	1.0000	0.9995	0.9999	1.0000	1.0000	1.0000
13	0.9952	0.9030	0.9909	0.9937	0.9066	0.9969	0.9935	0.9989	0.9989
14	1.0000	0.9999	1.0000	0.9998	0.9999	0.9996	1.0000	0.9999	0.9999
15	1.0000	1.0000	1.0000	0.9999	1.0000	0.9999	0.9999	1.0000	1.0000
16	1.0000	1.0000	1.0000	0.9999	0.9999	0.9996	0.9999	1.0000	1.0000
17	0.8920	0.8137	0.9892	1.0000	0.9996	0.9999	1.0000	1.0000	1.0000
18	0.4101	-0.1229	0.9918	0.9514	0.9609	0.9834	0.8759	0.9870	0.9870
19	0.9965	0.9958	0.9999	1.0000	0.9999	1.0000	0.9999	0.9997	0.9997
20	1.0000	1.0000	1.0000	1.0000	1.0000	1.0000	1.0000	1.0000	1.0000
21	1.0000	1.0000	1.0000	1.0000	0.9999	1.0000	1.0000	1.0000	1.0000
22	0.9990	0.9989	0.9997	0.9996	0.9996	0.9995	1.0000	1.0000	1.0000
23	0.5529	0.3027	0.7496	0.9249	0.9726	0.9830	0.8982	0.9826	0.9826
24	0.9998	0.9999	0.9999	0.9998	0.9999	0.9997	1.0000	0.9999	0.9999
25	1.0000	0.9998	1.0000	0.9999	0.9999	1.0000	0.9997	1.0000	1.0000
26	1.0000	0.9999	0.9999	0.9999	0.9999	0.9999	0.9998	1.0000	1.0000
27	0.8727	0.9989	0.9869	0.9999	0.9995	1.0000	1.0000	1.0000	1.0000

28	-0.5295	0.4544	0.7848	0.9963	0.9568	0.9948	0.9915	0.9887	0.9887
29	0.9951	0.9999	1.0000	1.0000	1.0000	1.0000	0.9999	0.9998	0.9998
30	0.9998	0.9998	1.0000	1.0000	1.0000	0.9999	1.0000	1.0000	1.0000
31	1.0000	1.0000	1.0000	0.9999	1.0000	0.9999	1.0000	1.0000	1.0000
32	1.0000	0.9989	1.0000	0.9999	0.9992	0.9992	1.0000	1.0000	1.0000
33	0.9993	0.5272	0.9770	0.9952	0.9926	0.9991	0.9907	0.9886	0.9886
34	1.0000	0.9998	0.9999	1.0000	0.9999	1.0000	0.9999	0.9998	0.9998
35	1.0000	0.9998	1.0000	1.0000	1.0000	1.0000	1.0000	1.0000	1.0000
36	1.0000	1.0000	0.9999	1.0000	0.9999	1.0000	1.0000	1.0000	1.0000
37	1.0000	0.9988	1.0000	1.0000	0.9997	1.0000	0.9999	1.0000	1.0000
38	0.9986	0.5869	0.9783	0.9980	0.9596	0.9987	0.9898	0.9948	0.9948
39	1.0000	0.9999	1.0000	1.0000	1.0000	1.0000	1.0000	0.9998	0.9998
40	1.0000	0.9998	1.0000	1.0000	1.0000	0.9999	1.0000	1.0000	1.0000
41	1.0000	1.0000	1.0000	1.0000	0.9999	0.9998	1.0000	1.0000	1.0000
42	1.0000	0.9987	1.0000	0.9999	0.9995	0.9996	1.0000	1.0000	1.0000
43	0.9990	0.5812	0.9935	0.9943	0.9598	0.9942	0.9878	0.9846	0.9846
44	1.0000	0.9999	1.0000	1.0000	0.9999	1.0000	1.0000	0.9997	0.9997
45	1.0000	0.9999	1.0000	1.0000	1.0000	1.0000	1.0000	1.0000	1.0000
46	1.0000	1.0000	1.0000	1.0000	0.9999	1.0000	1.0000	1.0000	1.0000
47	1.0000	0.9989	1.0000	0.9998	0.9997	0.9999	1.0000	1.0000	1.0000
48	0.9991	0.5853	0.9988	0.9912	0.9906	0.9991	0.9982	0.9846	0.9846
49	1.0000	1.0000	1.0000	1.0000	1.0000	1.0000	1.0000	0.9998	0.9998
50	1.0000	0.9998	1.0000	1.0000	0.9999	1.0000	1.0000	1.0000	1.0000
51	1.0000	1.0000	1.0000	1.0000	0.9999	0.9997	1.0000	1.0000	1.0000
52	1.0000	0.9986	1.0000	1.0000	0.9998	0.9998	1.0000	1.0000	1.0000
53	0.9991	0.6236	0.9952	0.9829	0.9888	0.9987	0.9954	0.9966	0.9966
54	1.0000	0.9999	1.0000	0.9999	1.0000	1.0000	1.0000	0.9998	0.9998
55	1.0000	0.9998	1.0000	1.0000	1.0000	1.0000	1.0000	1.0000	1.0000
56	1.0000	1.0000	1.0000	1.0000	0.9999	1.0000	1.0000	1.0000	1.0000
57	1.0000	0.9986	1.0000	0.9999	0.9996	0.9998	1.0000	1.0000	1.0000
58	0.9992	0.7112	0.9787	0.9979	0.9907	0.9974	0.9820	0.9958	0.9958
59	1.0000	0.9999	1.0000	1.0000	0.9999	1.0000	1.0000	0.9997	0.9997
60	1.0000	0.9998	1.0000	0.9999	1.0000	1.0000	1.0000	1.0000	1.0000
61	1.0000	1.0000	1.0000	1.0000	0.9998	0.9999	1.0000	1.0000	1.0000
62	1.0000	0.9986	1.0000	0.9999	0.9998	0.9997	1.0000	0.9999	0.9999
63	0.9992	0.7142	0.9866	0.9997	0.9896	0.9997	0.9951	0.9910	0.9910
64	1.0000	0.9997	0.9999	1.0000	1.0000	1.0000	1.0000	0.9998	0.9998
65	1.0000	0.9997	1.0000	1.0000	1.0000	1.0000	1.0000	1.0000	1.0000
66	1.0000	1.0000	1.0000	1.0000	1.0000	1.0000	1.0000	1.0000	1.0000
67	1.0000	0.9985	1.0000	0.9999	0.9996	0.9999	1.0000	1.0000	1.0000
68	0.9992	0.7809	0.9891	0.9985	0.9863	0.9971	0.9961	0.9978	0.9978
69	1.0000	0.9999	1.0000	1.0000	1.0000	1.0000	1.0000	0.9997	0.9997

70	1.0000	0.9999	1.0000	1.0000	1.0000	0.9999	1.0000	1.0000	1.0000
71	1.0000	1.0000	1.0000	0.9999	1.0000	0.9998	1.0000	1.0000	1.0000
72	1.0000	0.9984	1.0000	0.9989	0.9987	0.9999	1.0000	0.9999	0.9999
73	0.9994	0.7817	0.9904	0.9956	0.9956	0.9992	0.9897	0.9986	0.9986
74	1.0000	0.9999	0.9998	1.0000	1.0000	1.0000	1.0000	0.9998	0.9998
75	1.0000	0.9998	1.0000	1.0000	1.0000	1.0000	1.0000	1.0000	1.0000
76	1.0000	0.9999	1.0000	1.0000	1.0000	0.9999	1.0000	1.0000	1.0000
77	1.0000	0.9984	1.0000	0.9998	0.9999	1.0000	0.9999	1.0000	1.0000
78	0.9995	0.8031	0.9972	0.9973	0.9962	0.9996	0.9957	0.9970	0.9970
79	1.0000	0.9999	1.0000	1.0000	1.0000	1.0000	1.0000	0.9997	0.9997
80	1.0000	0.9999	1.0000	0.9999	1.0000	1.0000	1.0000	1.0000	1.0000
81	1.0000	0.9999	1.0000	1.0000	0.9998	0.9999	1.0000	1.0000	1.0000
82	1.0000	0.9983	1.0000	0.9986	0.9996	0.9996	1.0000	1.0000	1.0000
83	0.9997	0.8217	0.9958	0.9974	0.9963	0.9982	0.9972	0.9991	0.9991
84	1.0000	0.9999	1.0000	1.0000	0.9998	0.9999	1.0000	0.9998	0.9998
85	1.0000	0.9999	1.0000	1.0000	0.9999	1.0000	1.0000	1.0000	1.0000
86	1.0000	1.0000	1.0000	0.9999	0.9999	1.0000	1.0000	1.0000	1.0000
87	1.0000	0.9984	1.0000	1.0000	1.0000	1.0000	1.0000	1.0000	1.0000
88	0.9996	0.8698	0.9879	0.9994	0.9904	0.9967	0.9959	0.9993	0.9993
89	1.0000	1.0000	1.0000	1.0000	1.0000	1.0000	1.0000	0.9998	0.9998
90	1.0000	0.9998	1.0000	1.0000	1.0000	1.0000	1.0000	1.0000	1.0000

Single phase to ground fault in phase A Secondary									
	Phase A			**Phase B**			**Phase C**		
Window No.	r_{A11}	r_{A12}	r_{A22}	r_{B11}	r_{B12}	r_{B22}	r_{C11}	r_{C12}	r_{C22}
1	1.0000	1.0000	1.0000	1.0000	1.0000	0.9999	1.0000	1.0000	1.0000
2	1.0000	0.9999	1.0000	0.9997	0.9998	0.9997	0.9999	1.0000	1.0000
3	0.9991	0.9660	0.9924	0.9934	0.9991	0.9787	0.9988	0.9989	0.9989
4	1.0000	1.0000	0.9999	1.0000	1.0000	1.0000	0.9999	1.0000	1.0000
5	1.0000	1.0000	1.0000	1.0000	1.0000	1.0000	1.0000	1.0000	1.0000
6	1.0000	1.0000	1.0000	1.0000	0.9999	1.0000	1.0000	1.0000	1.0000
7	1.0000	0.9999	1.0000	1.0000	0.9999	0.9999	1.0000	1.0000	1.0000
8	0.9906	0.9629	0.9766	0.9844	0.9946	0.9922	0.9982	0.9986	0.9986
9	1.0000	0.9999	0.9999	1.0000	1.0000	1.0000	1.0000	0.9998	0.9998
10	1.0000	0.9999	1.0000	0.9997	1.0000	0.9996	1.0000	1.0000	1.0000
11	1.0000	1.0000	1.0000	0.9990	1.0000	0.9988	0.9985	0.9999	0.9999
12	1.0000	0.9999	1.0000	0.9976	1.0000	0.9974	0.9964	1.0000	1.0000
13	0.3206	-0.9061	0.3426	0.0867	0.9989	0.0260	0.6723	0.9998	0.9998
14	0.9830	0.9619	0.9954	0.9958	0.9998	0.9944	1.0000	0.9999	0.9999
15	0.9999	0.9990	0.9992	0.9997	1.0000	0.9996	0.9998	1.0000	1.0000
16	1.0000	1.0000	1.0000	0.9992	1.0000	0.9992	0.9990	1.0000	1.0000

17	0.9998	0.9989	0.9993	0.9989	1.0000	0.9983	0.9565	0.9964	0.9964
18	0.9452	0.2213	0.2830	0.0306	0.9993	0.0899	0.6036	0.9999	0.9999
19	0.9998	0.9944	0.9909	0.9929	0.9999	0.9909	0.9994	1.0000	1.0000
20	0.9998	0.9999	0.9999	0.9999	1.0000	0.9999	0.9996	1.0000	1.0000
21	1.0000	0.9999	0.9998	0.9999	1.0000	0.9999	0.9947	1.0000	1.0000
22	1.0000	0.9990	0.9989	1.0000	0.9999	0.9999	0.9803	0.9983	0.9983
23	0.3870	0.7734	-0.6050	0.9985	0.9994	0.9990	0.9881	1.0000	1.0000
24	0.9893	0.9996	0.9879	0.9998	0.9997	0.9997	0.9998	0.9999	0.9999
25	0.9997	0.9999	0.9994	1.0000	1.0000	1.0000	1.0000	1.0000	1.0000
26	1.0000	0.9997	0.9998	1.0000	1.0000	1.0000	1.0000	1.0000	1.0000
27	1.0000	0.9994	0.9999	1.0000	1.0000	1.0000	1.0000	0.9971	0.9971
28	0.9539	0.6675	0.9782	1.0000	0.9995	0.9999	1.0000	1.0000	1.0000
29	1.0000	0.9984	0.9989	1.0000	0.9999	0.9999	1.0000	0.9999	0.9999
30	1.0000	1.0000	0.9999	1.0000	1.0000	1.0000	1.0000	1.0000	1.0000
31	1.0000	0.9998	1.0000	1.0000	0.9999	1.0000	1.0000	1.0000	1.0000
32	1.0000	0.9991	0.9999	0.9999	1.0000	1.0000	0.9999	0.9960	0.9960
33	0.9984	0.6999	0.9981	0.9999	0.9998	0.9999	0.9999	1.0000	1.0000
34	1.0000	0.9997	0.9998	1.0000	0.9999	0.9999	1.0000	0.9999	0.9999
35	1.0000	0.9997	0.9999	1.0000	1.0000	1.0000	1.0000	1.0000	1.0000
36	1.0000	0.9997	1.0000	1.0000	1.0000	1.0000	1.0000	1.0000	1.0000
37	1.0000	0.9994	1.0000	1.0000	1.0000	1.0000	0.9997	0.9975	0.9975
38	0.9994	0.6299	0.9985	1.0000	0.9996	0.9999	1.0000	1.0000	1.0000
39	1.0000	0.9990	0.9995	0.9999	1.0000	1.0000	1.0000	1.0000	1.0000
40	1.0000	0.9999	0.9999	1.0000	1.0000	1.0000	1.0000	1.0000	1.0000
41	1.0000	0.9999	1.0000	0.9999	1.0000	1.0000	1.0000	1.0000	1.0000
42	1.0000	0.9993	1.0000	0.9999	0.9999	1.0000	0.9996	0.9968	0.9968
43	0.9958	0.6757	0.9979	0.9998	0.9997	0.9998	1.0000	1.0000	1.0000
44	1.0000	0.9994	0.9998	0.9999	0.9999	1.0000	1.0000	1.0000	1.0000
45	1.0000	0.9989	0.9996	0.9999	0.9999	1.0000	1.0000	1.0000	1.0000
46	1.0000	0.9998	1.0000	1.0000	1.0000	1.0000	1.0000	1.0000	1.0000
47	1.0000	0.9995	0.9999	1.0000	1.0000	0.9999	0.9994	0.9969	0.9969
48	0.9942	0.5287	0.9981	0.9999	1.0000	0.9992	1.0000	0.9999	0.9999
49	1.0000	0.9991	0.9999	1.0000	0.9999	1.0000	1.0000	1.0000	1.0000
50	1.0000	0.9999	1.0000	1.0000	1.0000	1.0000	1.0000	1.0000	1.0000
51	1.0000	0.9997	0.9999	0.9999	1.0000	0.9999	1.0000	1.0000	1.0000
52	1.0000	0.9996	0.9999	0.9999	0.9999	1.0000	0.9998	0.9958	0.9958
53	0.9979	0.6759	0.9975	0.9996	0.9987	0.9999	1.0000	0.9999	0.9999
54	1.0000	0.9992	0.9998	0.9999	1.0000	0.9998	1.0000	0.9999	0.9999
55	1.0000	0.9999	0.9989	1.0000	1.0000	1.0000	1.0000	1.0000	1.0000
56	1.0000	0.9999	0.9999	1.0000	1.0000	1.0000	1.0000	1.0000	1.0000
57	1.0000	0.9993	0.9999	1.0000	1.0000	0.9999	1.0000	0.9948	0.9948
58	0.9984	0.4798	0.9994	0.9999	0.9996	0.9999	0.9999	1.0000	1.0000

59	1.0000	0.9992	0.9999	1.0000	1.0000	0.9999	1.0000	0.9999	0.9999
60	1.0000	0.9999	0.9999	1.0000	1.0000	1.0000	1.0000	1.0000	1.0000
61	1.0000	0.9998	1.0000	0.9999	1.0000	0.9999	1.0000	1.0000	1.0000
62	1.0000	0.9991	0.9999	1.0000	1.0000	1.0000	0.9997	0.9957	0.9957
63	0.9989	0.6217	0.9990	0.9998	0.9995	0.9997	0.9999	1.0000	1.0000
64	1.0000	0.9988	0.9998	0.9999	1.0000	0.9999	1.0000	0.9999	0.9999
65	1.0000	0.9998	0.9998	1.0000	1.0000	1.0000	1.0000	1.0000	1.0000
66	1.0000	0.9997	0.9999	1.0000	1.0000	1.0000	1.0000	1.0000	1.0000
67	1.0000	0.9991	1.0000	1.0000	1.0000	1.0000	0.9998	0.9930	0.9930
68	0.9980	0.4515	0.9990	0.9999	0.9999	0.9994	1.0000	1.0000	1.0000
69	1.0000	0.9999	0.9995	1.0000	1.0000	1.0000	1.0000	1.0000	1.0000
70	1.0000	0.9998	0.9998	1.0000	1.0000	1.0000	1.0000	1.0000	1.0000
71	1.0000	0.9998	1.0000	1.0000	1.0000	1.0000	1.0000	1.0000	1.0000
72	1.0000	0.9991	1.0000	1.0000	1.0000	1.0000	0.9999	0.9960	0.9960
73	0.9915	0.5533	0.9955	0.9994	0.9989	0.9997	1.0000	0.9999	0.9999
74	1.0000	0.9997	0.9997	1.0000	0.9999	1.0000	1.0000	0.9999	0.9999
75	1.0000	0.9999	0.9998	1.0000	1.0000	1.0000	1.0000	1.0000	1.0000
76	1.0000	0.9994	0.9999	1.0000	1.0000	1.0000	1.0000	1.0000	1.0000
77	1.0000	0.9991	0.9999	1.0000	1.0000	0.9999	0.9994	0.9950	0.9950
78	0.9981	0.4686	0.9951	0.9997	0.9994	0.9999	1.0000	1.0000	1.0000
79	1.0000	0.9994	0.9996	0.9999	1.0000	1.0000	1.0000	1.0000	1.0000
80	1.0000	1.0000	0.9997	1.0000	1.0000	1.0000	1.0000	1.0000	1.0000
81	1.0000	0.9998	0.9999	1.0000	1.0000	1.0000	1.0000	1.0000	1.0000
82	1.0000	0.9994	0.9999	1.0000	1.0000	1.0000	0.9997	0.9936	0.9936
83	0.9949	0.5073	0.9979	0.9998	0.9995	0.9995	1.0000	0.9999	0.9999
84	1.0000	0.9996	0.9994	0.9999	1.0000	0.9999	1.0000	0.9999	0.9999
85	1.0000	1.0000	0.9999	1.0000	1.0000	1.0000	1.0000	1.0000	1.0000
86	1.0000	0.9998	0.9998	1.0000	0.9999	1.0000	1.0000	1.0000	1.0000
87	1.0000	0.9993	0.9998	1.0000	1.0000	1.0000	0.9999	0.9943	0.9943
88	0.9929	0.3725	0.9979	0.9998	0.9993	1.0000	0.9999	1.0000	1.0000
89	1.0000	0.9996	0.9998	1.0000	1.0000	1.0000	1.0000	0.9999	0.9999
90	1.0000	0.9999	0.9999	1.0000	1.0000	1.0000	1.0000	1.0000	1.0000

Single phase to ground fault in phase B Primary									
	Phase A			**Phase B**			**Phase C**		
Window No.	r_{A11}	r_{A12}	r_{A22}	r_{B11}	r_{B12}	r_{B22}	r_{C11}	r_{C12}	r_{C22}
1	1.0000	1.0000	1.0000	0.9999	1.0000	0.9999	1.0000	1.0000	1.0000
2	1.0000	0.9999	1.0000	1.0000	0.9998	0.9999	0.9999	1.0000	1.0000
3	0.9915	0.9013	0.9963	0.9983	0.9516	0.9902	0.9996	0.9963	0.9958
4	1.0000	0.9999	1.0000	0.9999	0.9999	0.9999	1.0000	0.9998	1.0000
5	1.0000	0.9999	1.0000	1.0000	1.0000	1.0000	1.0000	1.0000	1.0000

6	1.0000	1.0000	1.0000	1.0000	0.9999	1.0000	1.0000	1.0000	1.0000
7	1.0000	0.9998	1.0000	0.9998	0.9995	0.9999	1.0000	1.0000	0.9999
8	0.9924	0.9081	0.9972	0.1980	-0.8310	0.6660	0.9995	0.9986	0.9989
9	1.0000	0.9998	1.0000	0.9819	0.9808	1.0000	0.9996	0.9998	0.9998
10	1.0000	1.0000	1.0000	1.0000	1.0000	1.0000	0.9999	1.0000	0.9999
11	0.9998	1.0000	0.9998	0.9999	1.0000	0.9999	1.0000	1.0000	1.0000
12	0.9999	0.9998	1.0000	0.9990	0.9986	0.9997	1.0000	1.0000	0.9999
13	0.8983	0.9093	0.8895	0.5505	0.1802	0.7573	0.9648	0.9994	0.9778
14	0.9998	0.9998	0.9999	0.9998	0.9997	0.9999	0.9999	1.0000	1.0000
15	1.0000	1.0000	1.0000	0.9999	1.0000	1.0000	1.0000	1.0000	1.0000
16	1.0000	1.0000	1.0000	1.0000	1.0000	1.0000	1.0000	1.0000	1.0000
17	1.0000	0.9999	1.0000	0.9988	0.9994	0.9999	1.0000	1.0000	1.0000
18	0.8915	0.9368	0.8542	-0.4284	0.4745	-0.0500	0.9696	0.9998	0.9758
19	1.0000	0.9999	0.9999	0.9816	0.9999	0.9999	0.9995	0.9999	0.9997
20	1.0000	1.0000	1.0000	0.9996	0.9998	1.0000	1.0000	1.0000	1.0000
21	0.9998	1.0000	0.9998	1.0000	1.0000	0.9999	1.0000	1.0000	1.0000
22	1.0000	0.9998	1.0000	1.0000	0.9993	0.9998	1.0000	1.0000	0.9999
23	0.9958	0.9186	0.9973	0.9910	0.4474	0.9873	0.9993	0.9994	0.9996
24	1.0000	0.9998	0.9999	1.0000	0.9997	0.9999	1.0000	1.0000	1.0000
25	1.0000	1.0000	1.0000	1.0000	0.9999	1.0000	1.0000	1.0000	1.0000
26	1.0000	1.0000	1.0000	1.0000	1.0000	1.0000	1.0000	1.0000	1.0000
27	1.0000	0.9999	1.0000	1.0000	0.9994	0.9999	1.0000	1.0000	1.0000
28	0.9921	0.9211	0.9857	0.9975	0.6059	0.9736	0.9980	0.9979	0.9997
29	1.0000	0.9999	1.0000	1.0000	0.9999	1.0000	1.0000	0.9999	1.0000
30	1.0000	1.0000	1.0000	1.0000	0.9999	1.0000	1.0000	1.0000	1.0000
31	1.0000	1.0000	1.0000	1.0000	0.9997	0.9996	1.0000	1.0000	1.0000
32	0.9999	1.0000	1.0000	1.0000	0.9991	1.0000	1.0000	1.0000	1.0000
33	0.9991	0.8905	0.9975	0.9990	0.3848	0.9984	0.9936	0.9995	0.9980
34	1.0000	0.9998	1.0000	1.0000	0.9998	1.0000	1.0000	1.0000	1.0000
35	1.0000	1.0000	1.0000	1.0000	1.0000	1.0000	1.0000	1.0000	1.0000
36	1.0000	1.0000	1.0000	1.0000	1.0000	1.0000	1.0000	1.0000	1.0000
37	1.0000	0.9999	1.0000	1.0000	0.9996	0.9999	1.0000	0.9999	1.0000
38	0.9992	0.8990	0.9961	0.9985	0.5494	0.9993	0.9996	0.9987	0.9995
39	1.0000	0.9999	1.0000	1.0000	1.0000	0.9999	1.0000	0.9999	1.0000
40	1.0000	1.0000	1.0000	1.0000	1.0000	1.0000	1.0000	1.0000	1.0000
41	1.0000	1.0000	1.0000	1.0000	0.9999	0.9998	1.0000	1.0000	1.0000
42	1.0000	0.9998	1.0000	1.0000	0.9987	1.0000	1.0000	1.0000	1.0000
43	0.9945	0.9027	0.9968	0.9996	0.4482	0.9942	0.9996	0.9999	0.9998
44	1.0000	0.9998	1.0000	1.0000	0.9997	1.0000	1.0000	1.0000	1.0000
45	1.0000	1.0000	1.0000	1.0000	1.0000	1.0000	1.0000	1.0000	1.0000
46	1.0000	1.0000	1.0000	1.0000	1.0000	1.0000	1.0000	1.0000	1.0000
47	1.0000	0.9998	1.0000	1.0000	0.9993	0.9998	1.0000	1.0000	0.9999

48	0.9974	0.8764	0.9927	0.9990	0.6238	0.9904	0.9993	0.9997	0.9977
49	1.0000	0.9998	0.9999	1.0000	1.0000	1.0000	1.0000	0.9999	1.0000
50	1.0000	1.0000	1.0000	1.0000	0.9999	1.0000	1.0000	1.0000	1.0000
51	1.0000	1.0000	1.0000	1.0000	1.0000	0.9998	1.0000	1.0000	1.0000
52	1.0000	0.9999	1.0000	1.0000	0.9987	0.9999	0.9999	1.0000	0.9998
53	0.9958	0.8943	0.9940	0.9995	0.6229	0.9606	0.9995	0.9999	0.9989
54	1.0000	0.9997	1.0000	1.0000	0.9997	1.0000	1.0000	0.9999	0.9999
55	1.0000	1.0000	1.0000	1.0000	0.9999	0.9999	1.0000	1.0000	1.0000
56	1.0000	1.0000	1.0000	1.0000	1.0000	1.0000	1.0000	1.0000	1.0000
57	1.0000	0.9999	1.0000	1.0000	0.9991	0.9999	1.0000	1.0000	1.0000
58	0.9962	0.8811	0.9968	0.9984	0.6708	0.9928	0.9998	0.9999	0.9995
59	1.0000	0.9999	1.0000	1.0000	1.0000	1.0000	1.0000	0.9999	1.0000
60	1.0000	1.0000	1.0000	1.0000	0.9999	1.0000	1.0000	1.0000	1.0000
61	1.0000	1.0000	1.0000	1.0000	1.0000	1.0000	1.0000	1.0000	1.0000
62	1.0000	0.9999	1.0000	1.0000	0.9983	0.9997	1.0000	1.0000	0.9999
63	0.9974	0.8364	0.9821	0.9997	0.6131	0.9964	0.9988	0.9997	0.9978
64	1.0000	0.9998	1.0000	1.0000	0.9998	1.0000	1.0000	0.9999	1.0000
65	1.0000	1.0000	1.0000	1.0000	1.0000	0.9999	1.0000	1.0000	1.0000
66	1.0000	1.0000	1.0000	1.0000	1.0000	1.0000	1.0000	1.0000	1.0000
67	1.0000	0.9999	1.0000	1.0000	0.9995	0.9999	1.0000	1.0000	1.0000
68	0.9954	0.8969	0.9981	0.9995	0.6294	0.9982	0.9987	0.9998	0.9993
69	1.0000	0.9999	1.0000	1.0000	1.0000	1.0000	1.0000	0.9999	1.0000
70	1.0000	1.0000	1.0000	1.0000	0.9999	1.0000	1.0000	1.0000	1.0000
71	1.0000	1.0000	1.0000	1.0000	1.0000	0.9999	1.0000	1.0000	1.0000
72	1.0000	0.9998	1.0000	1.0000	0.9988	0.9999	1.0000	1.0000	1.0000
73	0.9878	0.9171	0.9983	0.9992	0.7300	0.9772	0.9998	0.9994	0.9996
74	1.0000	0.9998	1.0000	1.0000	0.9997	1.0000	1.0000	1.0000	1.0000
75	1.0000	1.0000	1.0000	1.0000	0.9998	0.9999	1.0000	1.0000	1.0000
76	1.0000	1.0000	1.0000	1.0000	1.0000	1.0000	1.0000	1.0000	1.0000
77	1.0000	0.9997	0.9999	1.0000	0.9992	0.9999	1.0000	1.0000	1.0000
78	0.9988	0.8563	0.9920	0.9995	0.7110	0.9890	0.9991	0.9992	0.9995
79	1.0000	0.9998	1.0000	1.0000	1.0000	1.0000	1.0000	0.9999	1.0000
80	1.0000	1.0000	1.0000	1.0000	0.9999	1.0000	1.0000	1.0000	1.0000
81	1.0000	1.0000	1.0000	1.0000	1.0000	1.0000	1.0000	1.0000	1.0000
82	1.0000	0.9999	1.0000	1.0000	0.9987	1.0000	1.0000	0.9999	1.0000
83	0.9994	0.8950	0.9964	0.9999	0.7974	0.9917	0.9996	0.9998	0.9999
84	1.0000	0.9997	1.0000	1.0000	0.9999	0.9999	1.0000	1.0000	1.0000
85	1.0000	1.0000	1.0000	1.0000	0.9999	1.0000	1.0000	1.0000	1.0000
86	1.0000	1.0000	1.0000	1.0000	1.0000	1.0000	1.0000	1.0000	1.0000
87	1.0000	0.9999	1.0000	1.0000	0.9996	0.9997	1.0000	1.0000	0.9999
88	0.9855	0.9145	0.9984	0.9991	0.7358	0.9967	0.9997	0.9998	0.9984
89	1.0000	0.9998	1.0000	1.0000	1.0000	1.0000	1.0000	1.0000	1.0000

90	1.0000	1.0000	1.0000	1.0000	0.9999	1.0000	1.0000	1.0000	1.0000

Single phase to ground fault in phase B Secondary									
	Phase A			**Phase B**			**Phase C**		
Window No.	r_{A11}	r_{A12}	r_{A22}	r_{B11}	r_{B12}	r_{B22}	r_{C11}	r_{C12}	r_{C22}
1	1.0000	1.0000	1.0000	1.0000	0.9999	1.0000	1.0000	1.0000	1.0000
2	1.0000	1.0000	1.0000	0.9999	0.9998	0.9994	1.0000	1.0000	1.0000
3	0.9888	0.9963	0.9982	0.9778	0.9166	0.9858	0.9946	0.9956	0.9894
4	1.0000	0.9997	0.9998	0.9999	1.0000	0.9999	1.0000	0.9999	0.9999
5	1.0000	0.9999	1.0000	1.0000	1.0000	0.9999	1.0000	1.0000	1.0000
6	1.0000	1.0000	1.0000	1.0000	1.0000	0.9999	1.0000	1.0000	1.0000
7	0.9999	1.0000	0.9998	0.9842	0.7837	0.8880	1.0000	1.0000	1.0000
8	0.9965	0.9991	0.9923	0.2877	-0.9673	0.3183	0.9928	0.9976	0.9936
9	1.0000	1.0000	1.0000	0.9926	0.9857	0.9993	0.9925	0.9998	0.9906
10	1.0000	1.0000	1.0000	1.0000	0.9996	0.9998	0.9980	0.9999	0.9972
11	0.9995	1.0000	0.9995	0.9999	0.9998	1.0000	0.9988	1.0000	0.9985
12	0.9951	0.9999	0.9942	0.9999	0.9997	0.9998	0.9979	1.0000	0.9978
13	-0.0528	0.9997	-0.0049	0.9218	0.7911	0.1255	0.0422	0.9999	0.1263
14	0.9995	1.0000	1.0000	0.9993	0.9985	0.9954	0.9953	1.0000	0.9943
15	0.9998	1.0000	0.9996	0.9998	1.0000	0.9998	0.9996	1.0000	0.9994
16	0.9994	1.0000	0.9992	1.0000	0.9996	0.9997	0.9993	1.0000	0.9993
17	0.9816	0.9998	0.9788	0.9817	0.9985	0.8604	0.9984	1.0000	0.9986
18	-0.2177	0.9998	-0.2565	0.7840	0.8720	-0.9129	0.0667	0.9999	0.1146
19	0.9994	1.0000	0.9994	0.9964	0.9999	0.9963	0.9708	1.0000	0.9662
20	0.9997	1.0000	0.9997	0.9998	0.9999	0.9997	0.9995	1.0000	0.9992
21	0.9983	1.0000	0.9982	1.0000	0.9999	0.9996	0.9999	1.0000	0.9999
22	0.9960	0.9999	0.9959	1.0000	0.9988	0.9991	1.0000	1.0000	1.0000
23	0.9922	0.9999	0.9932	0.9953	0.8647	0.9978	0.9994	0.9999	0.9993
24	1.0000	1.0000	0.9999	1.0000	0.9992	0.9976	0.9996	1.0000	0.9996
25	1.0000	1.0000	1.0000	1.0000	0.9999	0.9999	1.0000	1.0000	1.0000
26	1.0000	1.0000	1.0000	1.0000	0.9998	0.9999	1.0000	1.0000	1.0000
27	0.9997	0.9993	0.9999	1.0000	0.9997	0.9993	1.0000	1.0000	1.0000
28	0.9998	0.9995	0.9999	0.9984	0.8746	0.9970	0.9999	0.9999	0.9999
29	1.0000	1.0000	1.0000	1.0000	0.9993	0.9994	1.0000	1.0000	0.9999
30	1.0000	1.0000	1.0000	1.0000	0.9993	0.9995	1.0000	1.0000	1.0000
31	1.0000	1.0000	1.0000	1.0000	0.9994	0.9998	1.0000	1.0000	1.0000
32	0.9997	0.9997	0.9999	1.0000	0.9997	0.9994	1.0000	1.0000	1.0000
33	0.9999	0.9997	1.0000	0.9946	0.9169	0.9987	1.0000	0.9998	0.9999
34	1.0000	1.0000	1.0000	1.0000	0.9993	0.9984	0.9999	1.0000	0.9999
35	1.0000	1.0000	1.0000	1.0000	0.9998	0.9996	1.0000	1.0000	1.0000
36	1.0000	1.0000	1.0000	1.0000	0.9999	0.9999	1.0000	1.0000	1.0000

37	1.0000	0.9994	0.9999	1.0000	0.9997	0.9997	1.0000	1.0000	1.0000
38	1.0000	0.9994	1.0000	0.9947	0.9004	0.9976	0.9999	0.9999	1.0000
39	1.0000	1.0000	1.0000	1.0000	0.9996	0.9999	1.0000	0.9999	1.0000
40	1.0000	1.0000	1.0000	1.0000	0.9997	0.9996	1.0000	1.0000	1.0000
41	1.0000	1.0000	1.0000	1.0000	0.9998	0.9997	1.0000	1.0000	1.0000
42	1.0000	0.9999	1.0000	1.0000	0.9991	0.9992	1.0000	1.0000	1.0000
43	0.9999	0.9996	0.9999	0.9990	0.8946	0.9943	0.9999	0.9997	1.0000
44	1.0000	1.0000	1.0000	1.0000	0.9981	0.9951	1.0000	1.0000	1.0000
45	1.0000	1.0000	1.0000	1.0000	0.9999	0.9995	1.0000	1.0000	1.0000
46	1.0000	1.0000	1.0000	1.0000	0.9998	0.9999	1.0000	1.0000	1.0000
47	1.0000	0.9996	0.9999	1.0000	0.9974	0.9979	1.0000	1.0000	1.0000
48	0.9999	0.9996	0.9999	0.9997	0.9145	0.9989	0.9999	0.9999	1.0000
49	1.0000	1.0000	1.0000	1.0000	0.9997	0.9995	1.0000	1.0000	0.9998
50	1.0000	1.0000	1.0000	1.0000	1.0000	0.9997	1.0000	1.0000	1.0000
51	1.0000	1.0000	1.0000	1.0000	0.9997	0.9999	1.0000	1.0000	1.0000
52	0.9998	0.9997	1.0000	1.0000	0.9992	0.9992	1.0000	1.0000	1.0000
53	1.0000	0.9998	0.9999	0.9988	0.9597	0.9842	1.0000	0.9998	1.0000
54	1.0000	1.0000	1.0000	1.0000	0.9982	0.9996	1.0000	1.0000	0.9999
55	1.0000	1.0000	1.0000	1.0000	0.9996	0.9998	1.0000	1.0000	1.0000
56	1.0000	1.0000	1.0000	1.0000	0.9998	0.9997	1.0000	1.0000	1.0000
57	0.9999	0.9997	0.9998	1.0000	0.9993	0.9986	1.0000	1.0000	1.0000
58	1.0000	0.9994	1.0000	0.9994	0.9299	0.9996	1.0000	0.9999	1.0000
59	1.0000	1.0000	1.0000	1.0000	0.9998	0.9998	0.9999	0.9999	1.0000
60	1.0000	1.0000	1.0000	1.0000	0.9999	0.9999	1.0000	1.0000	1.0000
61	1.0000	1.0000	1.0000	1.0000	0.9995	0.9999	1.0000	1.0000	1.0000
62	1.0000	0.9996	1.0000	1.0000	0.9998	0.9998	1.0000	1.0000	1.0000
63	1.0000	0.9997	1.0000	0.9958	0.9564	0.9883	1.0000	0.9998	1.0000
64	1.0000	1.0000	1.0000	1.0000	0.9978	1.0000	0.9998	0.9999	1.0000
65	1.0000	1.0000	1.0000	1.0000	0.9998	0.9999	1.0000	1.0000	1.0000
66	1.0000	1.0000	1.0000	1.0000	0.9998	0.9995	1.0000	1.0000	1.0000
67	1.0000	0.9997	1.0000	1.0000	0.9999	0.9994	1.0000	1.0000	1.0000
68	0.9998	0.9993	0.9999	0.9993	0.9487	0.9988	1.0000	0.9999	1.0000
69	1.0000	1.0000	1.0000	1.0000	0.9986	0.9986	0.9999	0.9999	0.9999
70	1.0000	1.0000	1.0000	1.0000	1.0000	0.9998	1.0000	1.0000	1.0000
71	1.0000	1.0000	1.0000	1.0000	0.9991	0.9997	1.0000	1.0000	1.0000
72	1.0000	0.9999	0.9998	1.0000	0.9980	0.9992	1.0000	1.0000	1.0000
73	0.9999	0.9996	0.9999	0.9990	0.9316	0.9926	0.9999	0.9999	1.0000
74	1.0000	1.0000	1.0000	1.0000	0.9998	0.9987	1.0000	1.0000	0.9998
75	1.0000	1.0000	1.0000	1.0000	0.9999	0.9999	1.0000	1.0000	1.0000
76	1.0000	1.0000	1.0000	1.0000	0.9999	0.9996	1.0000	1.0000	1.0000
77	1.0000	0.9999	0.9999	1.0000	0.9995	0.9995	1.0000	1.0000	1.0000
78	1.0000	0.9997	0.9999	0.9949	0.9794	0.9975	1.0000	0.9998	0.9999

79	1.0000	1.0000	1.0000	1.0000	0.9990	0.9994	0.9999	1.0000	0.9998
80	1.0000	1.0000	1.0000	1.0000	0.9999	0.9999	1.0000	1.0000	1.0000
81	1.0000	1.0000	1.0000	1.0000	0.9997	0.9994	1.0000	1.0000	1.0000
82	0.9999	0.9997	1.0000	1.0000	0.9996	0.9979	1.0000	1.0000	1.0000
83	1.0000	0.9996	0.9999	0.9988	0.9828	0.9875	1.0000	0.9998	1.0000
84	1.0000	1.0000	1.0000	1.0000	0.9993	0.9994	0.9998	0.9999	1.0000
85	1.0000	1.0000	1.0000	1.0000	0.9999	0.9999	1.0000	1.0000	1.0000
86	1.0000	1.0000	1.0000	1.0000	0.9998	0.9998	1.0000	1.0000	1.0000
87	0.9998	0.9997	0.9999	1.0000	0.9993	0.9999	1.0000	1.0000	1.0000
88	0.9999	0.9994	1.0000	0.9998	0.9632	0.9906	1.0000	0.9998	1.0000
89	1.0000	1.0000	1.0000	0.9999	0.9990	0.9997	1.0000	1.0000	1.0000
90	1.0000	1.0000	1.0000	1.0000	1.0000	0.9999	1.0000	1.0000	1.0000

Single phase to ground fault in phase C Primary									
	Phase A			**Phase B**			**Phase C**		
Window No.	r_{A11}	r_{A12}	r_{A22}	r_{B11}	r_{B12}	r_{B22}	r_{C11}	r_{C12}	r_{C22}
1	1.0000	1.0000	1.0000	1.0000	1.0000	1.0000	1.0000	1.0000	1.0000
2	1.0000	0.9998	1.0000	1.0000	0.9999	1.0000	1.0000	1.0000	1.0000
3	0.9995	0.8623	0.9995	0.9977	0.9441	0.9997	0.9986	0.9943	0.9995
4	1.0000	0.9997	1.0000	1.0000	1.0000	1.0000	1.0000	0.9998	1.0000
5	1.0000	1.0000	1.0000	1.0000	1.0000	1.0000	1.0000	1.0000	1.0000
6	1.0000	1.0000	1.0000	1.0000	1.0000	1.0000	1.0000	1.0000	1.0000
7	1.0000	0.9999	1.0000	1.0000	0.9999	1.0000	1.0000	1.0000	1.0000
8	0.9997	0.8581	0.9996	0.9994	0.9738	0.9991	0.9995	0.9962	0.9998
9	1.0000	0.9999	1.0000	1.0000	1.0000	1.0000	1.0000	1.0000	1.0000
10	1.0000	1.0000	1.0000	1.0000	1.0000	1.0000	1.0000	1.0000	1.0000
11	1.0000	1.0000	1.0000	0.9997	1.0000	0.9997	1.0000	1.0000	1.0000
12	1.0000	0.9999	1.0000	0.9998	0.9999	0.9998	0.9940	0.9932	0.9999
13	0.9995	0.8543	0.9996	0.8638	0.9407	0.8693	-0.2098	-0.7887	0.6874
14	0.9996	0.9997	0.9996	0.9998	0.9998	0.9999	0.9877	0.9857	1.0000
15	0.9999	1.0000	0.9999	1.0000	1.0000	1.0000	0.9998	0.9999	1.0000
16	1.0000	1.0000	1.0000	1.0000	1.0000	1.0000	1.0000	1.0000	1.0000
17	1.0000	0.9998	0.9999	1.0000	1.0000	1.0000	0.9990	0.9976	0.9998
18	0.9759	0.8501	0.9727	0.8380	0.9671	0.8524	0.7073	-0.1049	0.6926
19	1.0000	0.9999	1.0000	0.9999	1.0000	0.9999	0.9954	0.9937	0.9997
20	1.0000	1.0000	1.0000	0.9999	0.9999	1.0000	0.9999	1.0000	1.0000
21	0.9999	1.0000	1.0000	0.9996	1.0000	0.9997	1.0000	1.0000	1.0000
22	1.0000	0.9996	0.9997	1.0000	0.9999	1.0000	0.9925	0.9991	0.9997
23	0.9791	0.8727	0.9856	0.9999	0.9798	0.9877	-0.5537	0.2534	-0.0722
24	0.9996	0.9998	0.9997	1.0000	0.9998	1.0000	0.9862	0.9999	0.9998
25	0.9999	1.0000	0.9999	1.0000	1.0000	1.0000	0.9996	0.9999	1.0000

26	1.0000	1.0000	1.0000	1.0000	1.0000	1.0000	1.0000	1.0000	1.0000
27	1.0000	0.9998	1.0000	1.0000	1.0000	1.0000	0.9998	0.9984	1.0000
28	0.9994	0.8671	0.9991	0.9992	0.9733	0.9976	0.9739	0.0752	0.9986
29	1.0000	0.9999	1.0000	1.0000	1.0000	1.0000	0.9979	0.9991	1.0000
30	1.0000	1.0000	1.0000	1.0000	1.0000	1.0000	1.0000	1.0000	1.0000
31	1.0000	1.0000	1.0000	1.0000	1.0000	1.0000	1.0000	0.9999	1.0000
32	1.0000	0.9997	1.0000	1.0000	0.9999	1.0000	1.0000	0.9990	1.0000
33	0.9990	0.8327	0.9933	0.9900	0.9560	0.9984	0.9884	0.3417	0.9976
34	1.0000	0.9999	1.0000	1.0000	1.0000	1.0000	1.0000	0.9999	1.0000
35	1.0000	1.0000	1.0000	1.0000	1.0000	1.0000	1.0000	0.9998	1.0000
36	1.0000	1.0000	1.0000	1.0000	1.0000	1.0000	1.0000	1.0000	1.0000
37	1.0000	0.9996	1.0000	1.0000	0.9999	1.0000	1.0000	0.9987	1.0000
38	0.9992	0.8410	0.9995	0.9991	0.9765	0.9970	0.9922	0.1319	0.9975
39	1.0000	0.9999	1.0000	0.9999	0.9999	1.0000	0.9999	0.9995	1.0000
40	1.0000	1.0000	1.0000	1.0000	1.0000	1.0000	1.0000	0.9999	1.0000
41	1.0000	1.0000	1.0000	1.0000	1.0000	1.0000	0.9999	1.0000	1.0000
42	1.0000	0.9998	1.0000	1.0000	1.0000	1.0000	1.0000	0.9991	1.0000
43	0.9997	0.8582	0.9978	0.9997	0.9607	0.9990	1.0000	0.3184	0.9993
44	1.0000	0.9998	1.0000	1.0000	0.9999	1.0000	1.0000	0.9999	1.0000
45	1.0000	1.0000	1.0000	1.0000	1.0000	1.0000	1.0000	0.9999	1.0000
46	1.0000	1.0000	1.0000	1.0000	1.0000	1.0000	1.0000	1.0000	1.0000
47	1.0000	0.9997	1.0000	1.0000	0.9999	1.0000	1.0000	0.9986	1.0000
48	0.9995	0.8326	0.9995	0.9994	0.9604	0.9984	0.9988	0.1520	0.9993
49	1.0000	0.9999	1.0000	1.0000	1.0000	1.0000	1.0000	0.9996	1.0000
50	1.0000	1.0000	1.0000	1.0000	1.0000	1.0000	1.0000	0.9999	1.0000
51	1.0000	1.0000	1.0000	1.0000	1.0000	1.0000	1.0000	1.0000	1.0000
52	1.0000	0.9997	1.0000	1.0000	0.9999	1.0000	1.0000	0.9993	1.0000
53	0.9904	0.8084	0.9984	0.9995	0.9771	0.9985	1.0000	0.3176	0.9998
54	1.0000	0.9999	1.0000	0.9999	0.9999	0.9999	1.0000	0.9999	1.0000
55	1.0000	1.0000	1.0000	1.0000	0.9999	1.0000	1.0000	0.9999	1.0000
56	1.0000	1.0000	1.0000	1.0000	1.0000	1.0000	1.0000	1.0000	1.0000
57	1.0000	0.9996	1.0000	1.0000	0.9999	1.0000	1.0000	0.9988	1.0000
58	0.9996	0.8632	0.9968	0.9997	0.9879	0.9893	0.9996	0.1638	0.9998
59	1.0000	0.9999	1.0000	1.0000	0.9999	0.9999	1.0000	0.9997	1.0000
60	1.0000	1.0000	1.0000	1.0000	0.9999	1.0000	1.0000	0.9999	1.0000
61	1.0000	1.0000	1.0000	1.0000	1.0000	1.0000	1.0000	1.0000	1.0000
62	1.0000	0.9997	1.0000	1.0000	0.9999	1.0000	1.0000	0.9990	0.9999
63	0.9984	0.8379	0.9996	0.9992	0.9695	0.9998	0.9999	0.3144	0.9997
64	1.0000	0.9998	1.0000	1.0000	0.9999	0.9999	1.0000	0.9999	1.0000
65	1.0000	1.0000	1.0000	1.0000	1.0000	1.0000	1.0000	0.9998	1.0000
66	1.0000	1.0000	1.0000	1.0000	1.0000	1.0000	1.0000	1.0000	1.0000
67	1.0000	0.9997	1.0000	1.0000	1.0000	1.0000	1.0000	0.9990	1.0000

68	0.9996	0.8427	0.9997	0.9959	0.9408	0.9931	0.9998	0.1862	0.9998
69	1.0000	1.0000	1.0000	0.9999	0.9999	0.9999	1.0000	0.9999	1.0000
70	1.0000	1.0000	1.0000	1.0000	1.0000	0.9999	1.0000	0.9999	1.0000
71	1.0000	1.0000	1.0000	1.0000	1.0000	1.0000	1.0000	1.0000	1.0000
72	1.0000	0.9998	1.0000	1.0000	0.9999	1.0000	1.0000	0.9991	1.0000
73	0.9987	0.8207	0.9997	0.9992	0.9853	0.9933	0.9995	0.2771	0.9972
74	1.0000	0.9999	1.0000	1.0000	0.9999	0.9999	1.0000	0.9998	1.0000
75	1.0000	1.0000	1.0000	1.0000	1.0000	1.0000	1.0000	0.9998	1.0000
76	1.0000	1.0000	1.0000	1.0000	1.0000	1.0000	1.0000	1.0000	1.0000
77	1.0000	0.9996	1.0000	1.0000	0.9999	1.0000	1.0000	0.9987	1.0000
78	0.9997	0.8700	0.9980	0.9999	0.9806	0.9880	0.9963	0.2319	0.9989
79	1.0000	0.9999	1.0000	1.0000	0.9999	1.0000	1.0000	0.9996	0.9999
80	1.0000	1.0000	1.0000	1.0000	0.9999	0.9999	1.0000	0.9999	1.0000
81	1.0000	1.0000	1.0000	1.0000	1.0000	1.0000	1.0000	1.0000	1.0000
82	1.0000	0.9999	1.0000	1.0000	1.0000	0.9999	1.0000	0.9991	1.0000
83	0.9998	0.8127	0.9994	0.9998	0.9857	0.9998	0.9991	0.3139	0.9999
84	1.0000	0.9999	1.0000	0.9999	0.9999	0.9999	1.0000	0.9999	1.0000
85	1.0000	1.0000	1.0000	1.0000	1.0000	1.0000	1.0000	0.9999	1.0000
86	1.0000	1.0000	1.0000	1.0000	1.0000	1.0000	1.0000	1.0000	1.0000
87	1.0000	0.9998	1.0000	1.0000	1.0000	1.0000	1.0000	0.9992	0.9999
88	0.9999	0.8459	0.9990	0.9994	0.9736	0.9980	0.9997	0.2090	0.9987
89	1.0000	0.9999	1.0000	1.0000	0.9998	1.0000	1.0000	0.9997	1.0000
90	1.0000	1.0000	1.0000	1.0000	1.0000	1.0000	1.0000	0.9999	1.0000

Single phase to ground fault in phase C Secondary									
	Phase A			**Phase B**			**Phase C**		
Window No.	r_{A11}	r_{A12}	r_{A22}	r_{B11}	r_{B12}	r_{B22}	r_{C11}	r_{C12}	r_{C22}
1	1.0000	1.0000	1.0000	1.0000	0.9999	1.0000	1.0000	1.0000	1.0000
2	1.0000	1.0000	1.0000	0.9998	0.9997	0.9997	1.0000	1.0000	1.0000
3	1.0000	0.9996	0.9991	0.9900	0.9519	0.9789	0.9986	0.9994	0.9997
4	1.0000	0.9999	0.9999	0.9999	1.0000	1.0000	1.0000	0.9997	1.0000
5	1.0000	1.0000	1.0000	1.0000	1.0000	1.0000	1.0000	1.0000	1.0000
6	1.0000	1.0000	1.0000	1.0000	1.0000	0.9999	1.0000	1.0000	1.0000
7	1.0000	0.9999	1.0000	1.0000	0.9999	0.9999	1.0000	1.0000	1.0000
8	0.9996	0.9949	0.9996	0.9907	0.9566	0.9892	0.9990	0.9979	0.9970
9	1.0000	1.0000	1.0000	1.0000	1.0000	1.0000	1.0000	0.9998	1.0000
10	1.0000	0.9999	1.0000	1.0000	1.0000	0.9999	1.0000	1.0000	1.0000
11	1.0000	1.0000	1.0000	1.0000	1.0000	1.0000	1.0000	1.0000	1.0000
12	1.0000	1.0000	1.0000	0.9999	0.9998	0.9999	1.0000	0.9999	1.0000
13	0.9997	0.9986	0.9999	0.9965	0.9498	0.9936	0.9996	0.9993	0.9996
14	1.0000	1.0000	0.9999	1.0000	1.0000	0.9999	1.0000	0.9998	1.0000

15	1.0000	0.9999	1.0000	0.9976	1.0000	0.9975	1.0000	1.0000	1.0000
16	1.0000	1.0000	1.0000	0.9998	1.0000	0.9996	1.0000	1.0000	1.0000
17	1.0000	1.0000	1.0000	0.9902	0.9991	0.9864	0.9774	-0.3578	-0.1665
18	0.9991	0.9948	0.9990	0.3974	0.9986	0.5985	0.1343	-0.8988	0.3470
19	0.9802	0.9924	0.9478	0.9998	1.0000	0.9998	0.9973	0.9931	0.9997
20	0.9990	0.9997	0.9983	0.9998	1.0000	0.9996	1.0000	1.0000	0.9999
21	0.9987	1.0000	0.9986	0.9991	1.0000	0.9993	1.0000	1.0000	0.9999
22	0.9985	1.0000	0.9979	0.9662	0.9959	0.9466	1.0000	0.9993	0.9997
23	0.7699	0.9999	0.7288	0.2594	0.9995	0.5067	0.9447	0.4015	0.0548
24	0.9905	0.9998	0.9878	0.9997	1.0000	0.9998	0.9997	0.9984	0.9950
25	0.9996	0.9999	0.9997	0.9955	1.0000	0.9953	0.9999	1.0000	0.9999
26	0.9993	1.0000	0.9993	0.9998	1.0000	0.9997	1.0000	0.9998	0.9995
27	0.9984	1.0000	0.9983	0.9965	0.9956	0.9909	0.9772	0.9990	-0.1992
28	0.6629	0.9996	0.7114	0.9964	0.9998	0.9986	0.4664	0.5481	-0.8530
29	0.9894	0.9996	0.9760	1.0000	1.0000	1.0000	0.9989	0.9994	0.9946
30	0.9998	0.9999	0.9995	1.0000	1.0000	1.0000	0.9999	0.9999	1.0000
31	1.0000	1.0000	0.9999	1.0000	1.0000	0.9999	1.0000	0.9997	0.9999
32	1.0000	1.0000	1.0000	0.9997	0.9935	0.9996	1.0000	0.9997	0.9998
33	0.9999	0.9999	1.0000	0.9999	0.9999	0.9998	0.9974	0.6221	0.9824
34	1.0000	0.9996	0.9998	1.0000	0.9999	1.0000	1.0000	0.9983	0.9999
35	1.0000	0.9999	1.0000	1.0000	1.0000	1.0000	1.0000	1.0000	1.0000
36	1.0000	1.0000	1.0000	1.0000	0.9999	1.0000	1.0000	0.9997	1.0000
37	1.0000	1.0000	1.0000	0.9997	0.9961	0.9998	1.0000	0.9991	1.0000
38	1.0000	0.9997	1.0000	0.9999	0.9995	1.0000	0.9999	0.5619	0.9995
39	1.0000	0.9997	1.0000	1.0000	1.0000	1.0000	1.0000	0.9994	0.9999
40	1.0000	0.9998	1.0000	1.0000	1.0000	1.0000	1.0000	0.9999	1.0000
41	1.0000	1.0000	1.0000	1.0000	1.0000	1.0000	1.0000	0.9997	1.0000
42	1.0000	1.0000	1.0000	0.9997	0.9947	0.9997	1.0000	0.9993	0.9998
43	0.9999	0.9996	1.0000	0.9996	0.9991	0.9997	1.0000	0.5592	0.9964
44	1.0000	0.9999	0.9999	1.0000	1.0000	0.9999	1.0000	0.9997	0.9992
45	1.0000	1.0000	1.0000	1.0000	1.0000	1.0000	1.0000	1.0000	0.9999
46	1.0000	1.0000	1.0000	1.0000	1.0000	1.0000	1.0000	0.9997	0.9999
47	1.0000	1.0000	1.0000	0.9999	0.9954	0.9999	1.0000	0.9991	0.9999
48	1.0000	0.9998	1.0000	0.9999	0.9994	1.0000	0.9995	0.5473	0.9990
49	1.0000	0.9996	1.0000	1.0000	1.0000	1.0000	1.0000	0.9996	0.9998
50	1.0000	0.9998	1.0000	1.0000	1.0000	1.0000	1.0000	0.9999	1.0000
51	1.0000	1.0000	1.0000	1.0000	1.0000	1.0000	1.0000	0.9997	0.9999
52	1.0000	1.0000	1.0000	0.9996	0.9931	0.9996	1.0000	0.9993	0.9998
53	1.0000	0.9999	0.9999	0.9997	0.9997	1.0000	0.9978	0.4908	0.9992
54	1.0000	0.9998	1.0000	1.0000	1.0000	1.0000	1.0000	0.9993	0.9997
55	1.0000	0.9999	1.0000	1.0000	1.0000	1.0000	1.0000	1.0000	0.9999
56	1.0000	1.0000	1.0000	1.0000	1.0000	1.0000	1.0000	0.9998	1.0000

57	1.0000	1.0000	1.0000	0.9997	0.9944	0.9996	1.0000	0.9994	1.0000
58	1.0000	0.9998	1.0000	1.0000	0.9993	1.0000	0.9999	0.5802	0.9991
59	1.0000	0.9995	1.0000	1.0000	1.0000	1.0000	1.0000	0.9996	0.9999
60	1.0000	0.9999	1.0000	0.9999	1.0000	1.0000	1.0000	0.9998	0.9999
61	1.0000	1.0000	1.0000	1.0000	1.0000	1.0000	1.0000	0.9997	1.0000
62	1.0000	1.0000	1.0000	0.9993	0.9966	0.9996	1.0000	0.9992	1.0000
63	1.0000	0.9999	1.0000	0.9999	0.9995	1.0000	0.9998	0.5211	0.9984
64	1.0000	0.9999	0.9999	1.0000	1.0000	1.0000	1.0000	0.9990	0.9998
65	1.0000	0.9999	1.0000	1.0000	1.0000	1.0000	1.0000	1.0000	0.9999
66	1.0000	1.0000	1.0000	1.0000	1.0000	1.0000	1.0000	0.9997	0.9999
67	1.0000	1.0000	1.0000	0.9999	0.9939	0.9994	1.0000	0.9988	0.9999
68	1.0000	0.9997	1.0000	0.9997	0.9999	0.9999	0.9975	0.5080	0.9995
69	1.0000	0.9998	0.9999	1.0000	1.0000	1.0000	1.0000	0.9996	0.9998
70	1.0000	0.9999	1.0000	1.0000	1.0000	1.0000	1.0000	0.9999	1.0000
71	1.0000	1.0000	1.0000	1.0000	0.9999	1.0000	1.0000	0.9998	1.0000
72	1.0000	1.0000	1.0000	0.9990	0.9870	0.9989	1.0000	0.9991	1.0000
73	1.0000	0.9998	1.0000	0.9999	0.9994	0.9999	0.9998	0.4799	0.9991
74	0.9999	0.9999	1.0000	1.0000	1.0000	1.0000	1.0000	0.9991	0.9997
75	1.0000	0.9998	0.9999	1.0000	1.0000	1.0000	1.0000	1.0000	1.0000
76	1.0000	1.0000	1.0000	1.0000	0.9999	1.0000	1.0000	0.9997	1.0000
77	1.0000	1.0000	1.0000	1.0000	0.9949	0.9996	1.0000	0.9992	0.9999
78	1.0000	0.9997	1.0000	0.9999	0.9993	0.9998	0.9998	0.4754	0.9992
79	1.0000	0.9998	1.0000	1.0000	1.0000	1.0000	1.0000	0.9998	0.9998
80	1.0000	0.9999	1.0000	1.0000	1.0000	1.0000	1.0000	0.9999	1.0000
81	1.0000	1.0000	1.0000	1.0000	0.9999	1.0000	1.0000	0.9998	1.0000
82	1.0000	1.0000	1.0000	0.9991	0.9947	0.9995	1.0000	0.9993	0.9999
83	1.0000	0.9999	1.0000	0.9999	0.9996	0.9999	0.9992	0.4912	0.9971
84	1.0000	0.9998	1.0000	1.0000	0.9999	1.0000	1.0000	0.9997	0.9996
85	1.0000	1.0000	1.0000	1.0000	1.0000	1.0000	1.0000	0.9999	1.0000
86	1.0000	1.0000	1.0000	1.0000	0.9999	1.0000	1.0000	0.9999	0.9999
87	1.0000	1.0000	1.0000	0.9999	0.9935	0.9996	1.0000	0.9993	1.0000
88	1.0000	0.9998	1.0000	0.9999	0.9995	0.9998	0.9997	0.4405	0.9992
89	1.0000	0.9999	0.9999	1.0000	1.0000	1.0000	1.0000	0.9994	0.9996
90	1.0000	0.9999	1.0000	1.0000	0.9999	1.0000	1.0000	1.0000	0.9999

External fault in phase A									
	Phase A			**Phase B**			**Phase C**		
Window No.	r_{A11}	r_{A12}	r_{A22}	r_{B11}	r_{B12}	r_{B22}	r_{C11}	r_{C12}	r_{C22}
1	1.0000	1.0000	1.0000	1.0000	0.9999	1.0000	1.0000	1.0000	1.0000
2	1.0000	1.0000	1.0000	1.0000	0.9999	1.0000	1.0000	1.0000	1.0000
3	0.9992	0.9818	0.9992	0.9986	0.9549	0.9996	0.9983	0.9971	0.9969

4	1.0000	0.9999	1.0000	1.0000	0.9999	1.0000	1.0000	0.9999	1.0000
5	1.0000	1.0000	1.0000	1.0000	1.0000	1.0000	1.0000	1.0000	1.0000
6	1.0000	1.0000	1.0000	1.0000	0.9999	1.0000	1.0000	1.0000	1.0000
7	1.0000	0.9999	1.0000	1.0000	0.9999	1.0000	1.0000	1.0000	1.0000
8	0.9999	0.9698	0.9990	0.9974	0.9849	0.9993	0.9995	0.9983	0.9998
9	1.0000	0.9999	1.0000	1.0000	1.0000	1.0000	1.0000	0.9998	1.0000
10	1.0000	1.0000	1.0000	1.0000	1.0000	1.0000	1.0000	1.0000	1.0000
11	1.0000	1.0000	1.0000	1.0000	1.0000	1.0000	1.0000	1.0000	1.0000
12	1.0000	0.9999	1.0000	0.9922	0.9999	0.9900	1.0000	1.0000	1.0000
13	0.9997	0.9819	0.9996	0.0581	0.9999	-0.2431	0.9997	0.9993	0.9994
14	1.0000	1.0000	1.0000	0.9894	0.9999	0.9902	0.9964	1.0000	0.9957
15	1.0000	1.0000	1.0000	0.9994	1.0000	0.9993	0.9998	1.0000	0.9997
16	0.9985	1.0000	0.9984	0.9992	1.0000	0.9989	0.9993	1.0000	0.9993
17	1.0000	1.0000	1.0000	0.9982	1.0000	0.9975	0.9822	0.9993	0.9742
18	0.7892	0.9767	0.7706	0.0459	1.0000	-0.1343	-0.0145	0.9998	0.0115
19	0.9993	1.0000	0.9991	0.9932	1.0000	0.9934	0.9995	1.0000	0.9998
20	1.0000	1.0000	0.9999	0.9997	1.0000	0.9996	0.9996	1.0000	0.9995
21	1.0000	1.0000	1.0000	0.9992	1.0000	0.9990	0.9994	1.0000	0.9993
22	0.9999	1.0000	1.0000	0.9970	1.0000	0.9955	0.9803	0.9988	0.9700
23	0.9658	0.9959	0.9358	0.9992	1.0000	0.9990	0.0179	0.9999	-0.0146
24	0.9995	1.0000	0.9993	0.9996	1.0000	0.9999	0.9929	1.0000	0.9927
25	0.9999	1.0000	0.9998	1.0000	1.0000	1.0000	1.0000	1.0000	1.0000
26	0.9987	1.0000	0.9988	1.0000	1.0000	1.0000	1.0000	1.0000	1.0000
27	1.0000	0.9999	1.0000	1.0000	1.0000	1.0000	0.9999	0.9994	0.9999
28	0.9701	0.9777	0.9713	0.9999	0.9999	0.9999	0.9999	0.9999	1.0000
29	1.0000	1.0000	1.0000	1.0000	1.0000	1.0000	1.0000	1.0000	1.0000
30	1.0000	1.0000	1.0000	1.0000	1.0000	1.0000	1.0000	1.0000	1.0000
31	1.0000	1.0000	1.0000	1.0000	1.0000	1.0000	1.0000	1.0000	1.0000
32	1.0000	1.0000	1.0000	1.0000	1.0000	1.0000	1.0000	0.9989	1.0000
33	0.9983	0.9964	0.9979	1.0000	1.0000	1.0000	1.0000	1.0000	1.0000
34	1.0000	1.0000	1.0000	1.0000	1.0000	1.0000	1.0000	1.0000	1.0000
35	1.0000	1.0000	1.0000	1.0000	1.0000	1.0000	1.0000	1.0000	1.0000
36	1.0000	1.0000	1.0000	1.0000	1.0000	1.0000	1.0000	1.0000	1.0000
37	1.0000	1.0000	1.0000	1.0000	1.0000	1.0000	1.0000	0.9994	1.0000
38	0.9996	0.9740	0.9999	1.0000	1.0000	1.0000	1.0000	0.9999	1.0000
39	1.0000	1.0000	1.0000	1.0000	1.0000	1.0000	1.0000	1.0000	1.0000
40	1.0000	1.0000	1.0000	1.0000	1.0000	1.0000	1.0000	1.0000	1.0000
41	1.0000	1.0000	1.0000	1.0000	1.0000	1.0000	1.0000	1.0000	1.0000
42	1.0000	1.0000	1.0000	1.0000	1.0000	1.0000	1.0000	0.9995	0.9999
43	0.9994	0.9934	0.9999	1.0000	1.0000	1.0000	1.0000	0.9999	1.0000
44	1.0000	1.0000	1.0000	1.0000	1.0000	1.0000	1.0000	1.0000	1.0000
45	1.0000	1.0000	1.0000	1.0000	1.0000	1.0000	1.0000	1.0000	1.0000

46	1.0000	1.0000	1.0000	1.0000	1.0000	1.0000	1.0000	1.0000	1.0000
47	1.0000	1.0000	1.0000	1.0000	1.0000	1.0000	1.0000	0.9994	1.0000
48	0.9999	0.9757	0.9997	1.0000	0.9999	1.0000	1.0000	0.9999	1.0000
49	1.0000	1.0000	1.0000	1.0000	0.9999	1.0000	1.0000	1.0000	1.0000
50	1.0000	1.0000	1.0000	1.0000	1.0000	1.0000	1.0000	1.0000	1.0000
51	1.0000	1.0000	1.0000	1.0000	1.0000	1.0000	1.0000	1.0000	1.0000
52	1.0000	1.0000	1.0000	1.0000	1.0000	1.0000	1.0000	0.9992	1.0000
53	0.9985	0.9896	0.9996	0.9999	1.0000	1.0000	1.0000	0.9999	1.0000
54	1.0000	1.0000	1.0000	1.0000	1.0000	1.0000	1.0000	1.0000	1.0000
55	1.0000	1.0000	1.0000	1.0000	1.0000	1.0000	1.0000	1.0000	1.0000
56	1.0000	1.0000	1.0000	1.0000	1.0000	1.0000	1.0000	1.0000	1.0000
57	1.0000	1.0000	1.0000	1.0000	1.0000	1.0000	1.0000	0.9995	1.0000
58	0.9996	0.9728	0.9999	1.0000	1.0000	1.0000	1.0000	0.9998	1.0000
59	1.0000	1.0000	1.0000	1.0000	0.9999	1.0000	1.0000	1.0000	1.0000
60	1.0000	1.0000	1.0000	1.0000	1.0000	1.0000	1.0000	1.0000	1.0000
61	1.0000	1.0000	1.0000	1.0000	1.0000	1.0000	1.0000	1.0000	1.0000
62	1.0000	1.0000	1.0000	1.0000	1.0000	1.0000	0.9999	0.9991	0.9999
63	0.9998	0.9891	0.9998	1.0000	1.0000	1.0000	1.0000	0.9997	1.0000
64	1.0000	1.0000	1.0000	0.9999	0.9999	1.0000	1.0000	1.0000	1.0000
65	1.0000	1.0000	1.0000	1.0000	1.0000	1.0000	1.0000	1.0000	1.0000
66	1.0000	1.0000	1.0000	1.0000	1.0000	1.0000	1.0000	1.0000	1.0000
67	1.0000	1.0000	1.0000	1.0000	1.0000	1.0000	1.0000	0.9992	1.0000
68	1.0000	0.9824	0.9986	1.0000	1.0000	1.0000	1.0000	0.9998	1.0000
69	1.0000	1.0000	1.0000	1.0000	0.9999	1.0000	1.0000	1.0000	1.0000
70	1.0000	1.0000	1.0000	1.0000	1.0000	1.0000	1.0000	1.0000	1.0000
71	1.0000	1.0000	1.0000	1.0000	1.0000	1.0000	1.0000	1.0000	1.0000
72	1.0000	1.0000	1.0000	1.0000	1.0000	1.0000	1.0000	0.9992	1.0000
73	0.9982	0.9860	0.9992	1.0000	1.0000	1.0000	1.0000	0.9997	1.0000
74	1.0000	1.0000	1.0000	1.0000	0.9999	1.0000	1.0000	1.0000	1.0000
75	1.0000	1.0000	1.0000	1.0000	1.0000	1.0000	1.0000	1.0000	1.0000
76	1.0000	1.0000	1.0000	1.0000	1.0000	1.0000	1.0000	1.0000	1.0000
77	1.0000	0.9999	1.0000	1.0000	1.0000	1.0000	1.0000	0.9994	1.0000
78	0.9990	0.9809	0.9992	1.0000	0.9999	0.9999	1.0000	0.9998	1.0000
79	1.0000	1.0000	1.0000	1.0000	0.9999	1.0000	1.0000	1.0000	1.0000
80	1.0000	1.0000	1.0000	1.0000	1.0000	1.0000	1.0000	1.0000	1.0000
81	1.0000	1.0000	1.0000	1.0000	1.0000	1.0000	1.0000	1.0000	1.0000
82	1.0000	1.0000	1.0000	1.0000	1.0000	1.0000	1.0000	0.9992	1.0000
83	0.9995	0.9904	0.9999	1.0000	1.0000	1.0000	1.0000	0.9999	1.0000
84	1.0000	1.0000	1.0000	1.0000	1.0000	1.0000	1.0000	1.0000	1.0000
85	1.0000	1.0000	1.0000	1.0000	1.0000	1.0000	1.0000	1.0000	1.0000
86	1.0000	1.0000	1.0000	1.0000	1.0000	1.0000	1.0000	1.0000	1.0000
87	1.0000	1.0000	1.0000	1.0000	1.0000	1.0000	1.0000	0.9992	0.9999

88	1.0000	0.9806	1.0000	1.0000	1.0000	0.9999	1.0000	0.9999	1.0000
89	1.0000	1.0000	1.0000	1.0000	1.0000	1.0000	1.0000	1.0000	1.0000
90	1.0000	1.0000	1.0000	1.0000	1.0000	1.0000	1.0000	1.0000	1.0000

External fault in phase B									
	Phase A			**Phase B**			**Phase C**		
Window No.	r_{A11}	r_{A12}	r_{A22}	r_{B11}	r_{B12}	r_{B22}	r_{C11}	r_{C12}	r_{C22}
1	1.0000	1.0000	1.0000	1.0000	0.9999	1.0000	1.0000	1.0000	1.0000
2	1.0000	1.0000	1.0000	0.9999	0.9998	0.9999	1.0000	1.0000	1.0000
3	0.9946	0.9447	0.9996	0.9947	0.9467	0.9946	0.9987	0.9987	0.9911
4	0.9999	1.0000	1.0000	0.9999	1.0000	1.0000	1.0000	0.9999	1.0000
5	1.0000	1.0000	1.0000	1.0000	1.0000	1.0000	1.0000	1.0000	1.0000
6	1.0000	1.0000	1.0000	0.9999	1.0000	1.0000	1.0000	1.0000	1.0000
7	1.0000	0.9999	1.0000	0.9999	0.9999	1.0000	1.0000	0.9999	1.0000
8	0.9986	0.9552	0.9969	0.9983	0.9566	0.9991	0.9885	0.9927	0.9995
9	1.0000	0.9999	1.0000	0.9999	1.0000	1.0000	1.0000	0.9999	1.0000
10	1.0000	1.0000	1.0000	1.0000	1.0000	1.0000	1.0000	1.0000	1.0000
11	1.0000	1.0000	1.0000	1.0000	1.0000	0.9999	1.0000	1.0000	1.0000
12	1.0000	0.9999	1.0000	0.9999	0.9998	0.9999	1.0000	1.0000	1.0000
13	0.9990	0.9469	0.9991	0.9949	0.9224	0.9972	0.9960	0.9978	0.9992
14	1.0000	0.9999	1.0000	0.9999	1.0000	1.0000	1.0000	0.9998	1.0000
15	1.0000	1.0000	1.0000	0.9943	1.0000	0.9941	1.0000	1.0000	1.0000
16	1.0000	1.0000	1.0000	0.9998	1.0000	0.9998	1.0000	1.0000	1.0000
17	1.0000	0.9998	1.0000	0.9999	1.0000	1.0000	0.9904	1.0000	0.9910
18	0.9985	0.9527	0.9959	0.9912	0.9996	0.9208	0.1577	0.9997	0.0176
19	0.9999	1.0000	1.0000	0.9995	1.0000	0.9994	0.9950	1.0000	0.9935
20	0.9998	1.0000	0.9997	0.9998	1.0000	0.9998	0.9996	1.0000	0.9995
21	0.9992	1.0000	0.9993	0.9999	1.0000	0.9999	0.9993	1.0000	0.9992
22	0.9820	0.9981	0.9711	1.0000	0.9998	0.9999	0.9985	1.0000	0.9983
23	-0.1282	0.9994	0.1623	0.8503	0.9954	0.6563	0.1048	0.9997	0.0195
24	0.9995	1.0000	0.9995	0.9991	1.0000	0.9990	0.9941	1.0000	0.9930
25	0.9997	1.0000	0.9995	0.9928	1.0000	0.9919	0.9996	1.0000	0.9995
26	0.9993	1.0000	0.9992	0.9999	1.0000	0.9999	0.9992	1.0000	0.9993
27	0.9807	0.9986	0.9732	1.0000	1.0000	1.0000	0.9971	1.0000	0.9967
28	-0.1114	0.9996	0.1640	0.9701	0.9946	0.9864	0.9997	0.9997	0.9996
29	0.9996	1.0000	0.9997	1.0000	1.0000	1.0000	0.9998	1.0000	0.9999
30	1.0000	1.0000	1.0000	1.0000	1.0000	1.0000	1.0000	1.0000	1.0000
31	1.0000	1.0000	1.0000	1.0000	1.0000	1.0000	1.0000	1.0000	1.0000
32	1.0000	0.9985	1.0000	1.0000	0.9999	0.9999	1.0000	1.0000	1.0000
33	1.0000	0.9997	1.0000	0.9971	0.9844	0.9998	0.9999	0.9998	1.0000
34	1.0000	1.0000	1.0000	1.0000	1.0000	1.0000	1.0000	1.0000	1.0000

35	1.0000	1.0000	1.0000	1.0000	1.0000	1.0000	1.0000	1.0000	1.0000
36	1.0000	1.0000	1.0000	1.0000	1.0000	1.0000	1.0000	1.0000	1.0000
37	0.9999	0.9982	1.0000	1.0000	1.0000	1.0000	1.0000	1.0000	1.0000
38	1.0000	0.9994	1.0000	0.9960	0.9951	0.9957	1.0000	0.9997	1.0000
39	1.0000	1.0000	1.0000	1.0000	1.0000	1.0000	1.0000	0.9999	1.0000
40	1.0000	1.0000	1.0000	1.0000	1.0000	1.0000	1.0000	1.0000	1.0000
41	1.0000	1.0000	1.0000	1.0000	1.0000	1.0000	1.0000	1.0000	1.0000
42	1.0000	0.9988	1.0000	1.0000	0.9999	1.0000	1.0000	1.0000	1.0000
43	1.0000	0.9997	1.0000	0.9994	0.9895	0.9980	0.9999	0.9999	1.0000
44	1.0000	1.0000	1.0000	1.0000	1.0000	1.0000	1.0000	0.9999	1.0000
45	1.0000	1.0000	1.0000	1.0000	1.0000	1.0000	1.0000	1.0000	1.0000
46	1.0000	1.0000	1.0000	1.0000	1.0000	1.0000	1.0000	1.0000	1.0000
47	1.0000	0.9989	0.9998	1.0000	1.0000	0.9999	1.0000	1.0000	1.0000
48	1.0000	0.9994	1.0000	0.9990	0.9959	0.9985	0.9999	0.9999	1.0000
49	1.0000	1.0000	1.0000	1.0000	1.0000	1.0000	1.0000	1.0000	0.9999
50	1.0000	1.0000	1.0000	1.0000	1.0000	1.0000	1.0000	1.0000	1.0000
51	1.0000	1.0000	1.0000	1.0000	1.0000	1.0000	1.0000	1.0000	1.0000
52	1.0000	0.9987	1.0000	1.0000	1.0000	1.0000	1.0000	1.0000	1.0000
53	0.9998	0.9993	1.0000	0.9999	0.9900	0.9997	0.9999	0.9998	0.9998
54	1.0000	1.0000	1.0000	1.0000	1.0000	1.0000	1.0000	0.9999	0.9999
55	1.0000	1.0000	1.0000	1.0000	1.0000	1.0000	1.0000	1.0000	1.0000
56	1.0000	1.0000	1.0000	1.0000	1.0000	1.0000	1.0000	1.0000	1.0000
57	1.0000	0.9987	1.0000	1.0000	1.0000	1.0000	1.0000	1.0000	1.0000
58	1.0000	0.9996	1.0000	0.9997	0.9934	0.9997	1.0000	0.9997	0.9999
59	1.0000	1.0000	1.0000	1.0000	1.0000	1.0000	1.0000	1.0000	1.0000
60	1.0000	1.0000	1.0000	1.0000	1.0000	1.0000	1.0000	1.0000	1.0000
61	1.0000	1.0000	1.0000	1.0000	1.0000	1.0000	1.0000	1.0000	1.0000
62	1.0000	0.9988	0.9999	1.0000	1.0000	1.0000	1.0000	1.0000	1.0000
63	1.0000	0.9993	1.0000	0.9996	0.9909	0.9995	1.0000	1.0000	0.9999
64	1.0000	1.0000	1.0000	1.0000	1.0000	1.0000	1.0000	1.0000	0.9999
65	1.0000	1.0000	1.0000	1.0000	1.0000	1.0000	1.0000	1.0000	1.0000
66	1.0000	1.0000	1.0000	1.0000	1.0000	1.0000	1.0000	1.0000	1.0000
67	1.0000	0.9985	0.9999	1.0000	1.0000	1.0000	1.0000	1.0000	1.0000
68	0.9999	0.9993	1.0000	0.9985	0.9950	0.9981	0.9999	0.9998	1.0000
69	1.0000	1.0000	1.0000	1.0000	1.0000	1.0000	1.0000	1.0000	1.0000
70	1.0000	1.0000	1.0000	1.0000	1.0000	1.0000	1.0000	1.0000	1.0000
71	1.0000	1.0000	1.0000	1.0000	1.0000	1.0000	1.0000	1.0000	1.0000
72	1.0000	0.9988	0.9999	1.0000	1.0000	1.0000	1.0000	1.0000	1.0000
73	1.0000	0.9995	1.0000	0.9992	0.9881	0.9999	1.0000	0.9999	1.0000
74	1.0000	0.9999	1.0000	1.0000	1.0000	1.0000	0.9999	0.9999	1.0000
75	1.0000	1.0000	1.0000	1.0000	1.0000	1.0000	1.0000	1.0000	1.0000
76	1.0000	0.9999	1.0000	1.0000	1.0000	1.0000	1.0000	1.0000	1.0000

77	1.0000	0.9991	1.0000	1.0000	1.0000	1.0000	1.0000	1.0000	1.0000
78	1.0000	0.9995	1.0000	0.9998	0.9951	0.9998	0.9999	0.9999	1.0000
79	1.0000	1.0000	1.0000	1.0000	1.0000	1.0000	1.0000	0.9999	1.0000
80	1.0000	1.0000	1.0000	1.0000	1.0000	1.0000	1.0000	1.0000	1.0000
81	1.0000	1.0000	1.0000	1.0000	1.0000	1.0000	1.0000	1.0000	1.0000
82	1.0000	0.9988	1.0000	1.0000	1.0000	1.0000	1.0000	1.0000	1.0000
83	1.0000	0.9994	1.0000	0.9983	0.9868	0.9993	0.9999	0.9999	1.0000
84	1.0000	1.0000	1.0000	1.0000	1.0000	1.0000	1.0000	1.0000	1.0000
85	1.0000	1.0000	1.0000	1.0000	0.9999	1.0000	1.0000	1.0000	1.0000
86	1.0000	0.9999	1.0000	1.0000	1.0000	1.0000	1.0000	1.0000	1.0000
87	1.0000	0.9987	1.0000	1.0000	1.0000	1.0000	1.0000	1.0000	1.0000
88	1.0000	0.9995	1.0000	0.9994	0.9982	0.9970	1.0000	0.9997	1.0000
89	1.0000	1.0000	1.0000	1.0000	1.0000	1.0000	1.0000	1.0000	1.0000
90	1.0000	1.0000	1.0000	1.0000	1.0000	1.0000	1.0000	1.0000	1.0000

External fault in phase C									
	Phase A			**Phase B**			**Phase C**		
Window No.	r_{A11}	r_{A12}	r_{A22}	r_{B11}	r_{B12}	r_{B22}	r_{C11}	r_{C12}	r_{C22}
1	1.0000	1.0000	1.0000	1.0000	1.0000	0.9999	1.0000	1.0000	1.0000
2	1.0000	0.9999	1.0000	1.0000	0.9996	0.9998	0.9999	1.0000	1.0000
3	0.9981	0.9950	0.9903	0.9938	0.9914	0.9934	0.9966	0.9984	0.9988
4	1.0000	0.9999	0.9999	0.9998	1.0000	0.9999	0.9999	0.9998	1.0000
5	1.0000	0.9999	1.0000	0.9999	1.0000	0.9999	1.0000	1.0000	1.0000
6	1.0000	1.0000	1.0000	0.9999	0.9999	1.0000	1.0000	1.0000	1.0000
7	1.0000	1.0000	1.0000	0.9998	0.9992	0.9996	1.0000	1.0000	0.9999
8	0.9997	0.9914	0.9997	0.9888	0.9195	0.9879	0.9987	0.9863	0.9989
9	0.9999	0.9999	0.9999	1.0000	0.9999	1.0000	1.0000	0.9999	1.0000
10	1.0000	0.9999	1.0000	0.9999	1.0000	0.9999	1.0000	1.0000	1.0000
11	1.0000	1.0000	1.0000	0.9999	0.9998	0.9996	1.0000	1.0000	1.0000
12	1.0000	1.0000	1.0000	0.9996	0.9998	0.9995	1.0000	1.0000	1.0000
13	0.9997	0.9953	0.9995	0.9397	0.9976	0.9559	0.9992	0.9991	0.9942
14	1.0000	1.0000	0.9999	0.9998	0.9998	0.9997	1.0000	0.9998	1.0000
15	1.0000	0.9999	1.0000	0.9996	0.9999	0.9995	0.9963	1.0000	0.9957
16	1.0000	1.0000	1.0000	0.9993	1.0000	0.9992	0.9999	1.0000	0.9999
17	0.9965	1.0000	0.9960	0.9747	0.9955	0.9610	1.0000	1.0000	1.0000
18	0.6486	0.9999	0.5369	0.1149	0.9995	0.4666	0.8943	0.9765	0.9958
19	0.9928	0.9999	0.9905	0.9994	1.0000	0.9996	0.9996	1.0000	0.9993
20	0.9996	1.0000	0.9998	0.9995	1.0000	0.9996	0.9999	1.0000	0.9999
21	0.9995	1.0000	0.9993	0.9995	1.0000	0.9997	1.0000	1.0000	1.0000
22	0.9986	1.0000	0.9986	0.9830	0.9960	0.9666	1.0000	1.0000	1.0000
23	0.5519	1.0000	0.6144	0.5836	0.9995	0.5992	0.8592	0.9997	0.8672

24	0.9895	0.9997	0.9863	0.9997	0.9999	0.9998	0.9995	0.9999	0.9991
25	0.9998	0.9999	0.9997	0.9999	1.0000	0.9999	0.9949	1.0000	0.9941
26	0.9993	1.0000	0.9993	0.9999	0.9997	0.9999	1.0000	1.0000	1.0000
27	0.9996	1.0000	0.9995	0.9995	0.9971	0.9991	1.0000	1.0000	1.0000
28	0.9996	0.9999	0.9997	0.9999	0.9999	1.0000	0.9761	0.9969	0.9379
29	0.9994	0.9996	0.9987	1.0000	1.0000	1.0000	0.9999	1.0000	1.0000
30	1.0000	1.0000	1.0000	0.9998	0.9999	0.9998	1.0000	1.0000	1.0000
31	1.0000	1.0000	1.0000	1.0000	0.9998	0.9999	1.0000	1.0000	1.0000
32	1.0000	1.0000	1.0000	0.9993	0.9981	0.9994	1.0000	1.0000	1.0000
33	0.9998	0.9998	0.9999	0.9994	0.9992	0.9995	0.9996	0.9990	0.9994
34	0.9999	0.9999	0.9999	0.9997	1.0000	0.9999	1.0000	1.0000	1.0000
35	1.0000	0.9999	1.0000	0.9999	0.9999	0.9999	1.0000	1.0000	1.0000
36	1.0000	1.0000	1.0000	0.9999	1.0000	0.9999	1.0000	1.0000	1.0000
37	1.0000	1.0000	1.0000	0.9998	0.9991	0.9990	1.0000	1.0000	1.0000
38	0.9998	0.9999	0.9998	0.9996	0.9991	1.0000	0.9996	0.9995	0.9969
39	0.9998	0.9999	0.9997	1.0000	1.0000	1.0000	1.0000	1.0000	1.0000
40	1.0000	1.0000	1.0000	0.9999	0.9999	0.9999	1.0000	1.0000	1.0000
41	1.0000	1.0000	1.0000	1.0000	1.0000	0.9998	1.0000	1.0000	1.0000
42	1.0000	1.0000	1.0000	0.9997	0.9962	0.9997	1.0000	1.0000	1.0000
43	0.9998	0.9999	0.9999	0.9993	0.9996	0.9998	0.9986	0.9998	0.9991
44	0.9999	0.9996	0.9997	0.9999	0.9999	1.0000	1.0000	1.0000	1.0000
45	1.0000	0.9998	0.9999	0.9999	0.9999	0.9999	1.0000	1.0000	1.0000
46	1.0000	1.0000	1.0000	1.0000	1.0000	1.0000	1.0000	1.0000	1.0000
47	1.0000	1.0000	1.0000	0.9997	0.9986	0.9997	1.0000	1.0000	1.0000
48	0.9998	0.9999	0.9998	0.9996	1.0000	0.9999	0.9970	0.9998	0.9975
49	0.9999	0.9996	0.9998	1.0000	1.0000	1.0000	1.0000	1.0000	1.0000
50	1.0000	0.9999	1.0000	1.0000	0.9999	1.0000	1.0000	1.0000	1.0000
51	1.0000	1.0000	1.0000	0.9999	0.9999	0.9999	1.0000	1.0000	1.0000
52	1.0000	1.0000	1.0000	0.9997	0.9970	0.9995	1.0000	1.0000	1.0000
53	1.0000	0.9999	0.9999	0.9994	0.9986	0.9994	0.9979	0.9987	0.9997
54	1.0000	0.9996	0.9999	1.0000	1.0000	1.0000	1.0000	1.0000	1.0000
55	1.0000	0.9999	1.0000	1.0000	0.9999	1.0000	1.0000	1.0000	1.0000
56	1.0000	1.0000	1.0000	1.0000	0.9998	0.9999	1.0000	1.0000	1.0000
57	1.0000	1.0000	1.0000	0.9992	0.9997	0.9995	1.0000	1.0000	1.0000
58	1.0000	0.9999	1.0000	0.9996	0.9991	0.9999	0.9993	0.9994	0.9998
59	0.9998	0.9999	0.9999	1.0000	1.0000	1.0000	1.0000	1.0000	1.0000
60	1.0000	0.9999	1.0000	0.9999	1.0000	1.0000	1.0000	1.0000	1.0000
61	1.0000	1.0000	1.0000	0.9999	1.0000	1.0000	1.0000	1.0000	1.0000
62	1.0000	1.0000	1.0000	0.9995	0.9988	0.9990	1.0000	1.0000	1.0000
63	1.0000	0.9998	1.0000	0.9999	0.9994	0.9998	0.9991	0.9998	0.9957
64	0.9999	0.9994	0.9998	1.0000	1.0000	1.0000	1.0000	1.0000	1.0000
65	1.0000	0.9999	1.0000	1.0000	0.9999	1.0000	1.0000	1.0000	1.0000

66	1.0000	1.0000	1.0000	0.9999	0.9998	1.0000	1.0000	1.0000	1.0000
67	1.0000	1.0000	1.0000	0.9988	0.9977	0.9990	1.0000	1.0000	1.0000
68	1.0000	0.9999	1.0000	0.9999	0.9998	0.9998	0.9995	0.9996	0.9991
69	0.9999	0.9995	0.9996	1.0000	1.0000	1.0000	1.0000	1.0000	1.0000
70	1.0000	1.0000	1.0000	1.0000	1.0000	1.0000	1.0000	1.0000	1.0000
71	1.0000	1.0000	1.0000	1.0000	0.9999	1.0000	1.0000	1.0000	1.0000
72	1.0000	1.0000	1.0000	0.9982	0.9987	0.9987	1.0000	1.0000	1.0000
73	1.0000	0.9997	0.9999	0.9999	0.9989	0.9999	0.9993	0.9992	0.9998
74	0.9997	0.9996	0.9998	1.0000	0.9999	1.0000	1.0000	1.0000	1.0000
75	1.0000	1.0000	1.0000	1.0000	1.0000	1.0000	1.0000	1.0000	1.0000
76	1.0000	1.0000	1.0000	0.9999	0.9998	1.0000	1.0000	1.0000	1.0000
77	1.0000	1.0000	1.0000	0.9999	0.9957	0.9994	1.0000	1.0000	1.0000
78	0.9999	0.9999	1.0000	0.9999	0.9992	0.9998	0.9980	0.9999	0.9974
79	1.0000	0.9999	0.9997	1.0000	1.0000	1.0000	1.0000	1.0000	1.0000
80	1.0000	0.9999	0.9999	1.0000	1.0000	1.0000	1.0000	1.0000	1.0000
81	1.0000	1.0000	1.0000	1.0000	1.0000	0.9999	1.0000	1.0000	1.0000
82	1.0000	1.0000	1.0000	0.9994	0.9975	0.9991	1.0000	1.0000	1.0000
83	1.0000	0.9999	0.9999	0.9999	0.9985	0.9996	0.9978	0.9989	0.9982
84	0.9999	0.9996	0.9999	1.0000	1.0000	1.0000	1.0000	1.0000	1.0000
85	1.0000	0.9999	1.0000	1.0000	1.0000	1.0000	1.0000	1.0000	1.0000
86	1.0000	1.0000	1.0000	1.0000	0.9999	0.9999	1.0000	1.0000	1.0000
87	1.0000	1.0000	1.0000	0.9998	0.9983	0.9992	1.0000	1.0000	1.0000
88	1.0000	0.9999	0.9999	0.9998	0.9995	0.9998	0.9991	0.9995	0.9999
89	0.9999	0.9999	1.0000	1.0000	1.0000	1.0000	1.0000	1.0000	1.0000
90	1.0000	0.9999	1.0000	1.0000	1.0000	1.0000	1.0000	1.0000	1.0000